
# Evaluating Mechanical Properties of Earth Material During Intelligent Compaction (2020)



## DETAILS

146 pages | 8.5 x 11 | PAPERBACK
ISBN 978-0-309-67660-1 | DOI 10.17226/25777

## CONTRIBUTORS

Soheil Nazarian, Aria Fathi, Cesar Tirado, Vladik Kreinovich, Sergio Rocha, The University of Texas at El Paso and California State University Mehran Mazari; National Cooperative Highway Research Program; Transportation Research Board; National Academies of Sciences, Engineering, and Medicine

## SUGGESTED CITATION

National Academies of Sciences, Engineering, and Medicine 2020. *Evaluating Mechanical Properties of Earth Material During Intelligent Compaction*. Washington, DC: The National Academies Press. https://doi.org/10.17226/25777.

NATIONAL COOPERATIVE HIGHWAY RESEARCH PROGRAM

NCHRP RESEARCH REPORT 933

# Evaluating Mechanical Properties of Earth Material During Intelligent Compaction

**Soheil Nazarian**
**Aria Fathi**
**Cesar Tirado**
**Vladik Kreinovich**
**Sergio Rocha**
CENTER FOR TRANSPORTATION INFRASTRUCTURE SYSTEMS
THE UNIVERSITY OF TEXAS AT EL PASO
El Paso, TX

**Mehran Mazari**
DEPARTMENT OF CIVIL ENGINEERING
CALIFORNIA STATE UNIVERSITY
Los Angeles, CA

*Subscriber Categories*
Construction • Geotechnology • Materials

Research sponsored by the American Association of State Highway and Transportation Officials
in cooperation with the Federal Highway Administration

The National Academies of
SCIENCES • ENGINEERING • MEDICINE
TRB
TRANSPORTATION RESEARCH BOARD

2020

## NATIONAL COOPERATIVE HIGHWAY RESEARCH PROGRAM

Systematic, well-designed, and implementable research is the most effective way to solve many problems facing state departments of transportation (DOTs) administrators and engineers. Often, highway problems are of local or regional interest and can best be studied by state DOTs individually or in cooperation with their state universities and others. However, the accelerating growth of highway transportation results in increasingly complex problems of wide interest to highway authorities. These problems are best studied through a coordinated program of cooperative research.

Recognizing this need, the leadership of the American Association of State Highway and Transportation Officials (AASHTO) in 1962 initiated an objective national highway research program using modern scientific techniques—the National Cooperative Highway Research Program (NCHRP). NCHRP is supported on a continuing basis by funds from participating member states of AASHTO and receives the full cooperation and support of the Federal Highway Administration (FHWA), United States Department of Transportation, under Agreement No. 693JJ31950003.

The Transportation Research Board (TRB) of the National Academies of Sciences, Engineering, and Medicine was requested by AASHTO to administer the research program because of TRB's recognized objectivity and understanding of modern research practices. TRB is uniquely suited for this purpose for many reasons: TRB maintains an extensive committee structure from which authorities on any highway transportation subject may be drawn; TRB possesses avenues of communications and cooperation with federal, state, and local governmental agencies, universities, and industry; TRB's relationship to the National Academies is an insurance of objectivity; and TRB maintains a full-time staff of specialists in highway transportation matters to bring the findings of research directly to those in a position to use them.

The program is developed on the basis of research needs identified by chief administrators and other staff of the highway and transportation departments, by committees of AASHTO, and by the FHWA. Topics of the highest merit are selected by the AASHTO Special Committee on Research and Innovation (R&I), and each year R&I's recommendations are proposed to the AASHTO Board of Directors and the National Academies. Research projects to address these topics are defined by NCHRP, and qualified research agencies are selected from submitted proposals. Administration and surveillance of research contracts are the responsibilities of the National Academies and TRB.

The needs for highway research are many, and NCHRP can make significant contributions to solving highway transportation problems of mutual concern to many responsible groups. The program, however, is intended to complement, rather than to substitute for or duplicate, other highway research programs.

## NCHRP RESEARCH REPORT 933

Project 24-45
ISSN 2572-3766 (Print)
ISSN 2572-3774 (Online)
ISBN 978-0-309-67339-6
Library of Congress Control Number 2020944292



### COPYRIGHT INFORMATION



### NOTICE

The research report was reviewed by the technical panel and accepted for publication according to procedures established and overseen by the Transportation Research Board and approved by the National Academies of Sciences, Engineering, and Medicine.

The opinions and conclusions expressed or implied in this report are those of the researchers who performed the research and are not necessarily those of the Transportation Research Board; the National Academies of Sciences, Engineering, and Medicine; the FHWA; or the program sponsors.

The Transportation Research Board; the National Academies of Sciences, Engineering, and Medicine; and the sponsors of the National Cooperative Highway Research Program do not endorse products or manufacturers. Trade or manufacturers' names appear herein solely because they are considered essential to the object of the report.

*Published research reports of the*

**NATIONAL COOPERATIVE HIGHWAY RESEARCH PROGRAM**

*are available from*

Transportation Research Board
Business Office
500 Fifth Street, NW
Washington, DC 20001

*and can be ordered through the Internet by going to*

https://www.nationalacademies.org

and then searching for TRB

Printed in the United States of America

*The National Academies of*
SCIENCES • ENGINEERING • MEDICINE

The **National Academy of Sciences** was established in 1863 by an Act of Congress, signed by President Lincoln, as a private, non-governmental institution to advise the nation on issues related to science and technology. Members are elected by their peers for outstanding contributions to research. Dr. Marcia McNutt is president.

The **National Academy of Engineering** was established in 1964 under the charter of the National Academy of Sciences to bring the practices of engineering to advising the nation. Members are elected by their peers for extraordinary contributions to engineering. Dr. John L. Anderson is president.

The **National Academy of Medicine** (formerly the Institute of Medicine) was established in 1970 under the charter of the National Academy of Sciences to advise the nation on medical and health issues. Members are elected by their peers for distinguished contributions to medicine and health. Dr. Victor J. Dzau is president.

The three Academies work together as the **National Academies of Sciences, Engineering, and Medicine** to provide independent, objective analysis and advice to the nation and conduct other activities to solve complex problems and inform public policy decisions. The National Academies also encourage education and research, recognize outstanding contributions to knowledge, and increase public understanding in matters of science, engineering, and medicine.

Learn more about the National Academies of Sciences, Engineering, and Medicine at **www.nationalacademies.org**.

---

The **Transportation Research Board** is one of seven major programs of the National Academies of Sciences, Engineering, and Medicine. The mission of the Transportation Research Board is to provide leadership in transportation improvements and innovation through trusted, timely, impartial, and evidence-based information exchange, research, and advice regarding all modes of transportation. The Board's varied activities annually engage about 8,000 engineers, scientists, and other transportation researchers and practitioners from the public and private sectors and academia, all of whom contribute their expertise in the public interest. The program is supported by state transportation departments, federal agencies including the component administrations of the U.S. Department of Transportation, and other organizations and individuals interested in the development of transportation.

Learn more about the Transportation Research Board at **www.TRB.org**.

# COOPERATIVE RESEARCH PROGRAMS

## CRP STAFF FOR NCHRP RESEARCH REPORT 933

**Christopher J. Hedges,** *Director, Cooperative Research Programs*
**Lori L. Sundstrom,** *Deputy Director, Cooperative Research Programs*
**Camille Crichton-Sumners,** *Senior Program Officer*
**Tyler Smith,** *Senior Program Assistant*
**Eileen P. Delaney,** *Director of Publications*
**Natalie Barnes,** *Associate Director of Publications*
**Sharon Lamberton,** *Editor*

## NCHRP PROJECT 24-45 PANEL
### Field of Soils and Geology—Area of Testing and Evaluation of Soils

**Bryan K. Dias,** *Washington State DOT, Olympia, WA* (Chair)
**Murad Y. Abu-Farsakh,** *Louisiana State University, Baton Rouge, LA*
**John McCartney,** *University of California - San Diego, La Jolla, CA*
**Ve'Niecy Pearman-Green,** *Illinois DOT, Collinsville, IL*
**Robert Leonard Schmitt,** *University of Wisconsin - Platteville, Platteville, WI*
**Xiaochao Tang,** *Widener University, Chester, PA*
**Michael Adams,** *FHWA Liaison*

## AUTHOR ACKNOWLEDGMENTS

The authors wish to thank a number of individuals who provided invaluable assistance throughout the project, including Nick Oetken and Bryan Downing of Caterpillar for providing rollers used for the testing activities and for sharing documentation about the specifications of the rollers used in this research project which helped improve the quality of the obtained results.

The authors are grateful for the assistance and cooperation of the state departments of transportation/highway authorities and project contractors at the five field sites where testing was conducted:

- John Siekmeier of the Minnesota Department of Transportation (Mn/DOT);
- Jim Lathrop, Ames Construction, Inc.;
- Stephen Slomski, Michelle Porr, Philip Painter, Andrew M. Jalbrzikowski, and Jordan Binkley of the Ohio Department of Transportation (ODOT);
- Josh Nichols of John R. Jurgensen Company; and
- Adrian Gonzalez, Tim Leafe, Chris Phelps, and Francisco Ruiz of Jordan Foster Construction.

The authors also acknowledge the consultants on the project including Dr. George Chang of Transtec Group, Antonio Gomes Correia of the University of Minho Portugal, and Dr. Michael Mooney of the Colorado School of Mines.

# FOREWORD

By Camille Crichton-Sumners
Staff Officer
Transportation Research Board

*NCHRP Report 933*, *Evaluating Mechanical Properties of Earth Material During Intelligent Compaction* provides finite element models used to simulate geomaterial compaction response, laboratory and field tests to validate the models, and development of two proposed generic specifications for the application of intelligent compaction in quality management. The report should be of immediate use to state department of transportation staff who are responsible for the quality management of geomaterial compaction for roadway construction projects.

---

Geomaterial compaction is necessary for the preparation of embankment, subgrade, subbase, and base for highway construction. If these earth materials are not compacted properly, it could lead to destabilization and structural failure. Although state transportation agencies require contractors to build uniform earth material layers, there is a need for a dependable means to continuously quantify and verify the degree of compaction. Current intelligent compaction (IC) technology uses vibratory rollers to help improve compaction. It has the potential to provide continuous, real-time measurements for quality control and quality acceptance of compaction. Prior studies revealed the following gaps: (1) the need to relate design parameters to construction quality control parameters and the on-site moisture content, and (2) the absence of rational means of relating different proprietary IC measurement values reported by different roller vendors.

Under NCHRP Project 24-45, the University of Texas at El Paso was asked to investigate methods to evaluate mechanical properties of geomaterials using IC technology and to develop generic specifications for the application of IC in quality management of geomaterials. The research entailed a literature review, development of finite element models to be used for geomaterial compaction response simulation, laboratory and field tests for model validation, and development of two proposed specifications. The first method entails a stiffness-based acceptance entitled "Proposed Standard Specification for Quality Management of Earthwork and Unbound Aggregates Using Intelligent Compaction (IC)," and the second is for extraction of modulus of compacted layers and is entitled "Proposed Standard Specification for Extracting Modulus of Compacted Geomaterials Using Intelligent Compaction (IC)." To manage site variability and variation in geomaterials and procedures, protocols for site-specific calibration are provided in the proposed specifications, included in Appendix A of *NCHRP Report 933*. This report should be useful to transportation agency staff who are responsible for roadway construction geomaterial compaction and related quality management.

# CONTENTS

SUMMARY

# Evaluating Mechanical Properties of Earth Material During Intelligent Compaction

Satisfactory pavement performance can only be assured with an appropriate process control to ensure that compacted materials meet proper density and stiffness requirements. The primary tool currently used for quality management of earthwork and unbound aggregates is the nuclear density gauge (NDG) to ensure appropriate density and moisture content. Measurement of moisture content and dry density, even though quite practical and straightforward, does not directly tie the construction quality with the mechanistic-empirical design processes where stress and modulus are employed. With the recent popularity of the mechanistic pavement design procedures, research efforts have been undertaken to understand and develop procedures for implementing modulus-based quality control procedures of compacted geomaterials. These procedures involve the use of in-situ nondestructive testing (NDT) devices that estimate the stiffness parameters of a constructed pavement structure. A shortcoming of NDT spot testing is that weak areas may be missed. If implemented properly, intelligent compaction (IC) can provide quality control over 100% of compacted materials. Furthermore, the uniformity of compacted earthwork can be realistically assessed with accelerometer-based IC measurement values (ICMV). Another possible benefit of using IC is the instant identification of weak areas that need to be reworked.

IC technology consists of a vibratory roller equipped with accelerometers mounted on the drum's axle, a global positioning system (GPS), and an onboard computer reporting system that displays IC measurements in real time. Despite the tremendous efforts that have been made to investigate the application of IC technology in construction quality control, knowledge gaps still prevent the use of IC technology for construction acceptance of geomaterials. These knowledge gaps include (1) the need to relate the design parameters to the construction quality control parameters and the in situ moisture content, and (2) the absence of rational means of relating different proprietary ICMVs reported by different roller vendors. To address these issues, field-calibrated numerical models are needed that can be used for the proper evaluation and acceptance of the compacted geomaterials. A realistic numerical model for a roller-soil system can be combined with a state-of-the-art inverse or backcalculation algorithm to provide reliable layer-specific ICMV for construction quality control and potential acceptance. This process must be robust and practice-ready, however, so that departments of transportation (DOTs) can readily incorporate it in their IC specifications.

This report details the findings of NCHRP Project 24-45, "Evaluating Mechanical Properties of Earth Material During Intelligent Compaction," which was undertaken to investigate methods to evaluate mechanical properties of geomaterials using IC technology and to develop generic specifications for the application of IC in quality management of soil and aggregates base materials.

## Objective

The main objective of this research was to develop procedures to estimate the mechanical properties of the geomaterials using IC technology in a robust manner so that DOTs can incorporate it in their specifications.

## Summary of Activities

The research process emphasized practicality and sought to establish field processes and analysis algorithms suitable for considering the attributes of a diverse range of geomaterials. The research team started by documenting, synthesizing, prioritizing, and conducting gap analyses on the following topics:

- National and international state of the practice and implementation of quality control/quality assurance (QC/QA) with IC technology;
- Different approaches to incorporate the unsaturated soil mechanics concepts in the process;
- Numerical models that simulate the IC roller compaction process during proof-mapping;
- Available backcalculation algorithms, including those that make use of artificial neural networks (ANNs) and genetic algorithms (GAs) to extract the mechanical properties (stiffness and/or modulus) of compacted materials; and
- Means of rapidly and robustly measuring and reporting the mechanical properties of layers.

Based on this information, the research team drafted a systematic process for implementing roller IC technology (illustrated in Figure S-1) that would allow the team to focus on:

- The most relevant parameters that should be considered and researched,
- Their practical and desirable tolerances,
- Means of rapidly measuring output parameters, and
- Means of analyzing the field results in a rapid and robust manner that balances the risks of highway agencies and the contractors.

Numerical models with different levels of complexity were developed to simulate realistically and efficiently the geomaterials' response under vibratory roller compaction with a focus on modeling the mapping operations for quality management. The proposed numerical models were evaluated in terms of execution time and results accuracy with respect to the field-measured responses. Those models were used to develop and evaluate different backcalculation techniques to extract the mechanical properties from IC roller measurements during the mapping process. To implement this step, the research team developed an extensive database comprising a wide range of layer properties and thicknesses. A sensitivity analysis and a parametric study were conducted to select the structural and stiffness parameters that significantly influence the pavement responses. These parameters were used to develop and evaluate inverse algorithms that would be robust enough to extract the layer mechanical properties from the IC measurements, in conjunction with additional spot testing using NDT devices.

The recommended specifications for the extraction of the mechanical properties were developed and pilot tested through field testing of seven active earthwork construction projects in Minnesota, Ohio, and Texas on granular soils, fine-grained soils, cement-stabilized soils, and unbound aggregate base materials commonly used in subgrade, subbase, and base course construction. Data from rollers manufactured by different manufacturers

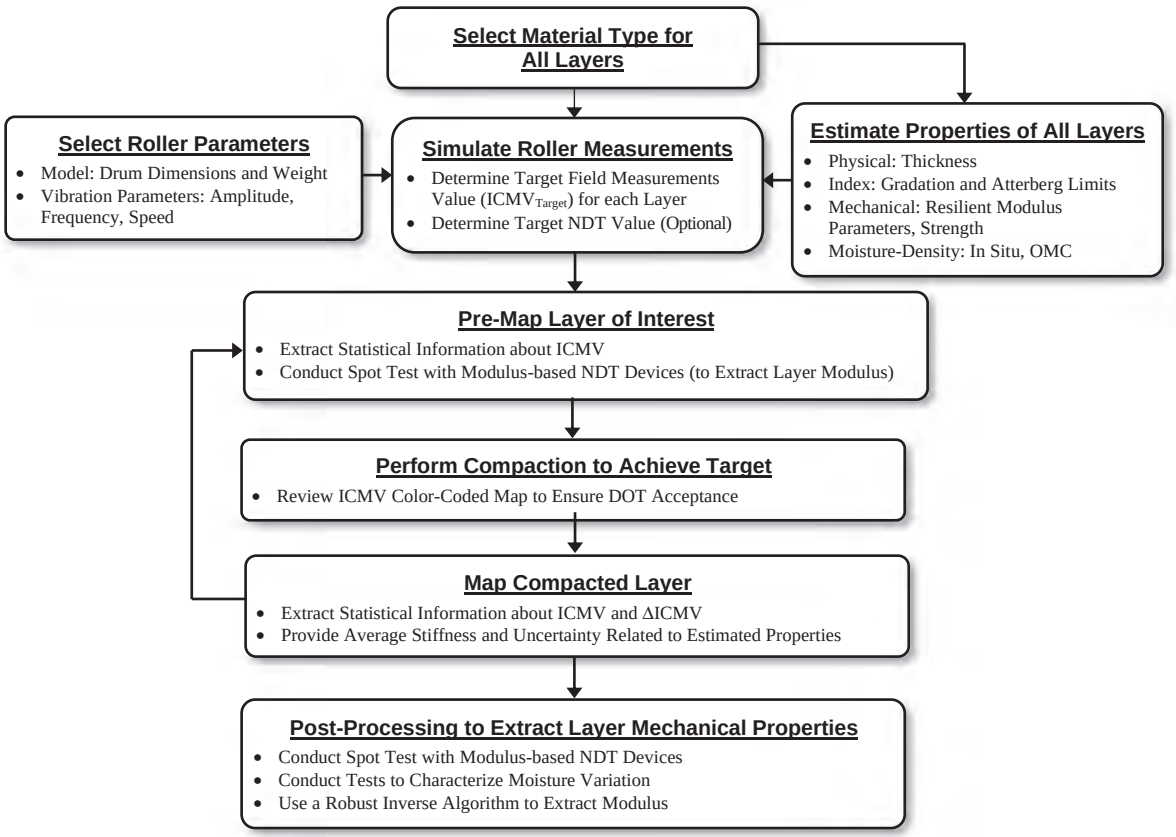


***Figure S-1. Implementing roller IC technology (generic flowchart).***

were used as part of the development of the forward and inverse models and the validation of the proposed approach for extracting the mechanical properties of compacted materials. The sites were instrumented with embedded geophones to investigate the relationship between roller measurements and the developed numerical models for calibration purposes. Relationships between ICMVs and measurements from lightweight deflectometer spot tests were investigated and used for calibrating the numerical models and the inverse solver for extracting layer modulus. The following sections summarize the findings obtained as part of the different tasks completed in this research study.

## Numerical Modeling

Different studies evaluating the experimental data collected with instrumented rollers revealed complex nonlinear roller vibration behaviors, such as loss of contact between the drum and the soil and nonlinear behavior of the materials subjected to compaction. For representative prediction of the responses, it was found necessary to use a three-dimensional (3D) nonlinear finite element (FE) model to simulate the proof-mapping process of single-layer and two-layer geosystems, with an automatic surface-to-surface contact model to account for the soil-drum interaction.

A comprehensive database of cases with different input parameters was assembled for single-layer and two-layer geosystems and various drum dimensions with different operating conditions. Different levels of complexity were introduced into the model to numerically assess the impact of the vibratory conditions and to consider both linear and

4 Evaluating Mechanical Properties of Earth Material During Intelligent Compaction

nonlinear geomaterial constitutive models on the pavement responses. Correlations were established among the responses of the different models and the obtained relationships were evaluated to simplify the modeling.

## Mapping of ICMV

IC measuring systems collect vibration data at discrete points at the edge of the roller drum during IC proof mapping. Commercially available IC systems incorporate various processes to extrapolate the measured ICMV data points over the width of the roller prior to generating the color-coded maps. In this study, the research team developed a system to evaluate the vibration characteristics of the IC rollers and the response of ground layers during the IC operations. The roller vibration data was collected with up to two accelerometers mounted at the drum of a roller while a GPS unit mounted on the roller monitored the roller's location. Another component consisted of 3D geophones embedded at different depths into the earthwork. The geophones were connected to a data acquisition system to measure the responses of the ground layers during mapping operations.

The impacts of the data collection rate and reduction processes on the collected IC measurements were evaluated to set appropriate levels of spatial density and resolution. To make the process more practical, the collected IC data was partitioned into virtual sublots equal to the width of the roller and the length equal the minimum length of the compacted section that was practical to rework. For mapping ICMV, all ICMV measurements falling inside a sublot were averaged to obtain representative ICMVs. This approach can accommodate the inherent uncertainties related to the accuracy of the GPS devices and the precise position of the moving roller in a straightforward and transparent manner.

To ensure uniformity throughout the site, a color-coded map representing the coefficient of variation (COV) of the ICMVs within each sublot should accompany the mapping of ICMVs. Such COV color-coded maps allow the identification of sublots where the representative ICMVs are no longer reliable due to construction- or equipment-related issues. The traditional approach to color coding relies on the standard deviation of the site; however, this approach loses its effectiveness as the site becomes more variable (yields a higher standard deviation).

The research team used an enhanced approach, establishing a color-coded criterion under which any sublot with representative ICMVs greater than the average ICMV of the lot was considered relatively *stiffer* and assigned a color (green). Sublots with average ICMV of less than 75% of the average ICMV of the lot were considered as *less stiff* (not inferior quality) and were represented in a second color (red). Sublots with ICMVs of 75% of the average ICMV of the lot or higher, and lower than the average ICMV of the lot, were considered *moderately stiff* and were represented in a third color (yellow). For any given site, the resulting color-coded map might not contain any red areas as long as the work is uniform enough to yield a COV of less than 25%. Again, sublots with ICMVs less than 75% of the average ICMV of the lot do not necessarily imply that they do not meet stiffness requirements; this threshold implies only that their stiffness is less than that of other sublots.

Using the information acquired with the data acquisition system, additional maps were generated for real-time quality control of collected IC data. The mapping of operating frequency, roller speed, line passes, number of discrete measurements per sublot, and amplitude (i.e., surface displacement) served for conducting quality control of the ICMVs acquired during mapping. This information also was to be used as input into the backcalculation algorithms for the backcalculation of layer moduli.

## Field Evaluation

Four test cells at the MnROAD test track facility were instrumented. Test sections were built with full-scale construction equipment to simulate normal highway construction. Each cell consisted of distinct combinations of subgrade and unbound aggregate base materials. All sections were proof mapped using an IC roller equipped with a data acquisition system consisting of accelerometers mounted at the edge of the drum and a GPS system to measure the location of the roller. This procedure allowed the comparison of the collected IC data with the roller's IC measurements obtained from the Controller Area Network (CAN) bus. Both measurements were found to be in agreement. A second data acquisition system collected soil displacements from the embedded geophones during the roller's mapping operations. This information was used for further comparison and calibration purposes of the numerical model responses. During IC mapping, data acquisition for each cell was conducted on top of the subgrade (single-layer system) and on top of the constructed base layer (two-layer system).

All test sections were evaluated using NDT devices to measure modulus-based properties of the compacted materials. NDT testing consisted of the use of a light weight deflectometer (LWD), falling weight deflectometer (FWD), and dynamic cone penetrometer (DCP) to estimate the modulus/stiffness of compacted base and subgrade sections implemented in equally spaced spots along the length and width of the test sections. Similarly, a nuclear density gauge (NDG) was employed to evaluate the moisture-density properties of compacted geomaterials. Soil samples were transported to the laboratory to measure their in-place moisture content, index properties, and to perform resilient modulus tests. The implementation of dense spot tests along the test section allowed the research team to address the field variability of the material properties and how this affects the measurements collected by the IC roller.

Note: In the literature, the term *resilient modulus* has various abbreviations (e.g., MR, $M_R$, and $m_r$). All three abbreviations may appear in figures or equations in *NCHRP Research Report 933*, reflecting their presentation in the original sources. To minimize confusion, the text typically spells out the term rather than using the abbreviation.

## Calibration of Numerical Models

The developed numerical models were calibrated using field measurements acquired from embedded geophones during IC mapping of test sections at the Minnesota pavement test track (MnROAD) and a construction site in Texas. The pavement properties of the mapped pavement sections were used as input into the FE models used in this project, and the drum was simulated using the dimensions and operating characteristics of the IC roller used in the test sections.

The Texas dataset consisted of a section mapped using IC rollers from various manufacturers vibrating in stationary and moving conditions. The collective field and numerical datasets were used to develop adjustment factors after the comparison of field to numerical pavement responses. Better correlations between the field measurements and their corresponding numerical model responses were observed when local adjustment relationships were obtained as opposed to a single global relationship obtained from field measurements and numerical model responses using only laboratory-obtained properties as inputs. The local calibration approach integrated the LWD test measurements with the resilient modulus test results. This approach incorporated the state of compaction of the layer and to some extent the variation in moisture content in the analysis.

6 Evaluating Mechanical Properties of Earth Material During Intelligent Compaction

## Extraction of Mechanical Properties

A robust backcalculation technique to extract the mechanical properties without excessive processing time during the mapping of the compacted layers was developed. The stiffness (equivalent to a modulus of subgrade reaction) can be extracted directly in the frequency domain by obtaining the ratio of the complex amplitudes of the force imposed by the drum and the roller deflection at that location. This approach was integrated into the almost real-time analysis module that processed the measured datasets in the field as soon as the proof-mapping process was finished. In the case of two-layer geosystems, the roller measurements would provide a composite stiffness because only one piece of information was available at each sublot.

To obtain an optimal predictive function for estimating the moduli of the subgrade and base, two approaches were evaluated for real-time backcalculation: a genetic programming (GP) method that makes use of GAs, and an ANN-based approach. For this purpose, a comprehensive dataset of single-layer and two-layer geosystems with different layer properties and base thicknesses was assembled using a stationary static nonlinear model. After a sensitivity analysis, the parameters that had a more significant impact on the pavement responses were identified and selected as inputs into the proposed GP- and ANN-based inverse solvers. Different inverse solvers, with differing numbers of input variables, were proposed for the various geosystem scenarios. The expectation was that the precision of the predictions would improve with the more complex solvers; however, the more complex inverse solvers would require more laboratory efforts to determine the needed input variables. The inverse solvers were evaluated to select backcalculation scenarios that were best suited for predicting layer moduli for both single-layer and two-layer systems. The predictive power of the inverse solvers improved when local adjustment factors were used. The predictions made using both the GP method and an ANN approach were compared to the results obtained from the FE models, and a decision was made to continue the research by refining and further testing the ANN-based model.

## Findings from Validation Process

Visits were conducted to four additional test construction sites in Minnesota, Ohio, and Texas to evaluate and validate the practicality of the developed forward models and backcalculation algorithms under field conditions. These test sections were also instrumented using embedded geophones at different depths to record soil displacements during the mapping process for further improvement of the inverse solver algorithms. The impact of variability in the measurements toward the extraction of the mechanical properties of the compacted layers was also assessed. The results were used to further evaluate and improve the framework of the specification. In general, the conclusions drawn and lessons learned during the validation phase were reasonably similar to those obtained from the test sections that were evaluated during development.

As part of the dissemination of the proposed specification, the following items should be strongly emphasized to the highway agencies:

- The adoption of a specification to extract the mechanical properties of compacted materials using IC needs to be approached in the context of the levels of uncertainty associated to the uniformity of the compaction.
- The most consistent results are obtained when proof mapping is carried out in conjunction with the modulus-based measurements and when variability in the ICMVs is kept at less than 25%.

- Due to large diversity in construction practices and material types, the implementation of the draft specification requires more localized field studies by DOTs to adopt it to their local materials and construction practices.

Based on this study and interaction with the highway agencies, the following comments and suggestions can be made:

- This research study provides a critical review of the strengths and concerns about the implementation of a specification to extract the mechanical properties of compacted materials using IC technology. The research team attempted to highlight the complexities that could arise and made an effort to address them in a comprehensive manner.
- Even though this report emphasizes both the strengths and concerns with the proposed specification, the proposed specification is a big step toward higher quality highway construction.

## Recommended Specifications

Following AASHTO PP 81-14 as a baseline, two proposed specifications were developed; one for stiffness-based acceptance, entitled "Proposed Standard Specification for Quality Management of Earthwork and Unbound Aggregates using Intelligent Compaction (IC)," and one for extraction of the modulus of compacted layers, entitled "Proposed Standard Specification for Extracting Modulus of Compacted Geomaterials Using Intelligent Compaction (IC)." These specifications are presented in Appendix A of this report. Two test methods that are proposed to accompany the specifications also are provided in Appendix A.

The use of the stiffness-based specification serves as an almost real-time approach for determining mechanistic-based field target values for routine quality management purposes. The modulus-based specification, on the other hand, would be preferred if the goal of the highway agencies is to extract the moduli of the layers. For the implementation of the modulus-based specification, however, the highway agency should be prepared to conduct some laboratory testing up front and institute more rigorous process control during the compaction process. The specifications make use of an approach to partition the lot into virtual sublots for mapping ICMVs. The sublot dimensions equal the width of the roller and the minimum length of the compacted section that is practical to rework, which is set at the discretion of the engineer. ICMVs falling inside a sublot are averaged to obtain representative ICMVs. This approach is proposed to accommodate the inherent uncertainties related to the accuracy of the GPS devices and the precise position of the moving roller. It also facilitates identification of the less stiff areas. The modulus-based specification requires using IC to identify the sublots with more uniform ICMVs for conducting additional spot tests.

CHAPTER 1

# Introduction

## Problem Statement

The primary tool currently used for quality management of earthwork and unbound aggregates is a nuclear density gauge (NDG) to ensure appropriate density and moisture content. With the emphasis on the mechanistic-empirical (ME) pavement design procedures in the last decade, significant research effort has been devoted to understanding and implementing modulus-based quality control of compacted geomaterials (e.g., Von Quintus et al. 2009; Tutumluer 2013; Nazzal 2014). Nazarian et al. (2014) systematically enumerated the technical and institutional complications related to incorporating modulus-based spot-testing devices such as the light weight deflectometer (LWD) and provided practical solutions to some of them. These complications included (1) relating the design parameters to the construction quality control parameters, (2) incorporating the impact of moisture content on the measured modulus, and (3) developing field-calibrated numerical models that can be used in the proper evaluation and acceptance of the compacted geomaterials. Many of those complications are directly applicable to the implementation of the IC systems. If implemented properly, the IC technology can provide quality control over 100% of the compacted geomaterials (a major shortcoming of the spot testing). Furthermore, the uniformity of the compaction process can be assessed realistically with IC measurement values (ICMVs).

Despite the tremendous efforts to investigate the application of the IC technology in the construction quality control, knowledge gaps remain that prevent it from being used for quality acceptance. These gaps include:

- Lack of a robust and practical methodology to determine the lift-specific target ICMV ($ICMV_{Target}$) with the consideration of moisture content, and
- Absence of a rational means of relating the different proprietary ICMVs reported by different roller vendors.

A realistic numerical model for a roller-soil system can be combined with a state-of-the-art inverse algorithm to provide layer-specific ICMVs for quality control and potentially for the quality acceptance.

## Objective

The main objective of this research was to develop procedure(s) to estimate the mechanical properties of the geomaterials using the IC technology. The final process needed to be robust and practice-ready so that departments of transportation (DOTs) and state highway agencies (SHAs) can readily incorporate it in their IC specifications. Figure 1-1 illustrates the process followed by the research team to achieve this objective. During the course of the project,

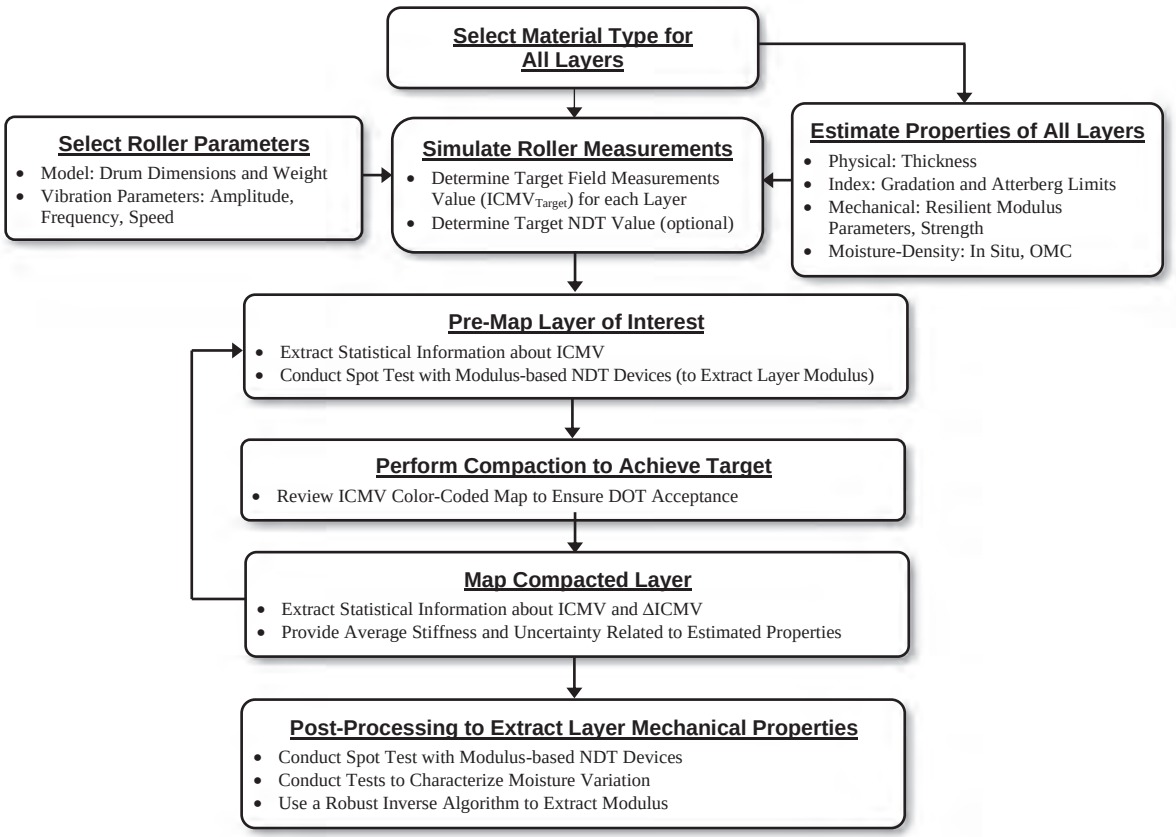


***Figure 1-1. Implementing roller IC technology (generic flowchart).***

the flowchart acted as a living document and was updated as warranted by the results of the experimental and numerical studies.

## Organization of Report

The study has been divided into three phases. Phase 1 (Documentation) covered the following topics:

- Compilation of literature and current IC specifications;
- Documentation of fundamental, technological and practical limitations of IC technology;
- Improvement of numerical models and conduction of sensitivity analyses;
- Development of algorithms to estimate target ICMV that are based on mechanical properties;
- Recommendation of the proper way to incorporate the variations in moisture content in the process;
- Recommendation of the most appropriate QC/QA process; and
- Conduction of field evaluation to calibrate the FE models and to verify the processes for estimating ICMVs and mechanical properties for a wide variety of fine- and coarse-grained geomaterials.

These topics are summarized in Chapter 2. The five primary tasks associated with Phase 2 consisted of:

1. Addressing Practical Issues,
2. Developing a Forward Model,

3. Developing an Inverse Algorithm,
4. Calibrating and Validating Models, and
5. Implementation Plan of Proposed IC.

Phase 2 consisted of a systematic research effort to establish field processes and analysis algorithms considering the following attributes for diverse range of geomaterials:

- The most relevant parameters that should be considered,
- Their practical and desirable tolerances,
- A means of rapidly measuring output parameters, and
- A means of analyzing the field results in a rapid and robust manner that balances the risks of highway agencies and the contractors.

The outcomes of this phase were generic specifications and a work plan to evaluate and validate their different options.

Phase 3 consisted of the evaluation of the practicality of the methods and validation and fine-tuning of the proposed algorithms and test methods that had been developed in Phase 2. Field tests were performed to validate the robustness and practicality of the proposed specifications. Phase 3 also included summarizing the research and field activities into this final report and draft construction specifications for compaction of geomaterials with IC and extracting layer properties. The proposed specifications are presented in Appendix A of this report.

To keep this report as concise as possible, each chapter presents a summary of the relevant information, with more extensive information and analysis presented in the appendices. Depending on familiarity or interest, the reader can review the summary and then proceed to the referred appendices for more in-depth information. Specifically,

- Chapter 2 briefly describes the fundamentals of IC measuring systems and summarizes the state of knowledge in the areas of IC and current IC specifications.
- Chapter 3 summarizes the findings from the numerical modeling of roller compaction of geomaterials and assembly of a comprehensive databases of pavement responses of various pavement structures and layer properties subjected to IC roller compaction during mapping operations.
- Chapter 4 summarizes field test activities conducted at sites in Texas and the MnRoad facility in Minnesota, and features the information collected from both the field measurements and laboratory testing. Data obtained from laboratory and field activities is used to develop appropriate transfer functions.
- Chapter 5 contains information about the evaluation and calibration of the forward models using measured field data.
- Chapter 6 discusses the development, calibration and evaluation of the inverse models for extracting the mechanical properties. This chapter also proposes preliminary adjustment factors that can be used for extraction of mechanical properties of geomaterials.
- Chapter 7 provides the findings of the implementation of the specification for extracting modulus from compacted materials using IC from the field studies conducted at four additional test construction sites in Minnesota, Ohio, and Texas.
- Chapter 8 discusses the framework for an IC specification along with the rationale for incorporating different items in the draft specification. This chapter also contains the limitations of the proposed process and recommendation for smooth implementation of the specification.
- Chapter 9 summarizes the findings and conclusions from this project.

Eight appendices are provided to complement these chapters. Appendix A, titled "Proposed Standard Specifications and Test Methods to Estimate Mechanical Properties of

Geomaterials Using Intelligent Compaction," is printed with this report and contains the following documents:

- Proposed Standard Specification for Extracting Modulus of Compacted Geomaterials Using Intelligent Compaction (IC);
- Proposed Standard Specification for Quality Management and Design Verification of Earthwork and Unbound Aggregates Using Intelligent Compaction (IC);
- Proposed Standard Test Method for Determining Intelligent Compaction Measurement Value (ICMV) Using Intelligent Compaction (IC) Technology; and
- Proposed Standard Test Method for Estimating Modulus of Embankment and Unbound Aggregate Layers with Portable Falling Weight Devices.

The remaining seven appendices are grouped together in a downloadable PDF file which can be obtained from the *NCHRP Research Report 933* webpage at www.trb.org. The PDF file contains:

- Appendix B: Experimental Plan for Phase 3 Field Activities;
- Appendix C: Review of Literature;
- Appendix D: Numerical Modeling of Compaction of Geomaterials;
- Appendix E: Extracting Mechanical Properties from IC Data;
- Appendix F: Field Study for Implementation and Evaluation of NDT and IC for Quality Acceptance and Design Modulus Verification;
- Appendix G: Calibration of Models Using Field Data; and
- Appendix H: Mechanical Property Measurements.

CHAPTER 2

# Construction Quality Management Using Intelligent Compaction

## Introduction

Technological improvement of construction technologies has resulted in the popularity of the IC techniques. Even though the basic concept of IC was developed in the early 1970s (Adam and Pistrol 2016), this technology has been under continuous development and implementation during the past decade. The following sections summarize the current body of research relevant to the performance management methods, including the IC applications. The information gathered from the literature on different methods for estimating the modulus of compacted geomaterials in the field and laboratory, and the various factors that impact the mechanical properties also are summarized. The chapter includes a brief review of the numerical modeling techniques, constitutive and material models, and soil-drum contact mechanics used for simulating roller compaction of geomaterials. It also provides a review of Intelligent Compaction Measurement Values (ICMVs) and current techniques for backcalculation of mechanical properties. Finally, the chapter offers a summary of current specifications for implementing IC technology.

## Estimation of Modulus of Compacted Geomaterials

The stiffness/modulus of the compacted geomaterials can be estimated either from the laboratory or from in-situ tests. The behavior of the unbound materials under repeated loading is quite complex and involves many different factors. Given the complexity and time-consuming nature of the resilient modulus tests, simple methods have been proposed for estimating the modulus of the geomaterials in the laboratory. Strength tests, such as the unconfined compressive strength or laboratory California Bearing Ratio (CBR), also are commonly used to estimate the modulus. Correlations have been developed by various studies in the literature to predict the modulus from the soil index parameters; however, most models exhibit poor predictive power when they are tested on soils not used to develop the relationships (Von Quintus and Killingsworth 1998; Yau and Von Quintus 2002; Wolfe and Butalia 2004; Malla and Joshi 2007). A comprehensive review of the concepts and definitions regarding the response of geomaterials is provided in Appendix C.

### Factors Impacting Modulus of Compacted Geomaterials

Puppala (2008) and Tutumluer (2013), among others, synthesized the body of literature regarding the estimation of the modulus of the unbound geomaterials. The following sections summarize the body of literature regarding the factors influencing the modulus/stiffness of the earthwork and unbound geomaterials:

**State of Stress.** Several material models have evolved in the decades since the 1960s. Different forms of the stress state have been implemented to explain the stress-dependency of the modulus. The representative modulus of a given geomaterial placed in a pavement section is not a unique value and depends on the underlying and/or overlying layers. The state of the stress of a given geomaterial placed in a pavement section can only be estimated if the moduli of all layers are known. The estimation of the modulus must be carried out iteratively using an analytical layered structural model.

**Residual Stresses During Compaction.** The stresses imposed by compaction equipment during the construction process are usually the largest stress states that the compacted unbound geomaterials will experience during their service lives. The particle interlock that is formed during the compaction process, along with the lateral confining pressure, forms a residual stress within the geomaterial layer that could affect the responses of the pavement layers during the repeated traffic loading.

**Moisture Content.** A review of the literature reveals that significant efforts have been dedicated to studying the impact of the moisture variation in terms of the moisture content or matric suction (Gupta et al. 2007). Like those of Cary and Zapata (2010), most of these studies are based on the concepts of the unsaturated soil mechanics. Wolfe and Butalia (2004) acknowledged the significance of unsaturated soil mechanics in characterizing the behavior of pavement subgrades and the influence of suction or moisture content variation on modulus. The soil may be subjected to variation in stiffness due to interaction with the atmosphere, leading to repeated cycles of infiltration and evaporation, referred to as hydraulic hysteresis, which in turn can lead to a change in soil stiffness (McCartney and Khosravi 2013).

As detailed in Appendix C, several research efforts have documented the specific impact of moisture variations and the general impacts of environmental changes on the modulus/stiffness of compacted earthwork and unbound geomaterials. The lack of a correlation between the modulus of the compacted geomaterials and the field moisture content is discussed in Richter (2006). Von Quintus et al. (2010) and Pacheco and Nazarian (2011) also attempted to address that concern. The importance of the difference between the moisture content at the time of compaction and at the time of testing has been suggested by Khoury and Zaman (2004) and by Nazarian et al. (2014).

The Mechanistic-Empirical Design Guide (MEPDG) recommended the following function to consider the effects of the environmental factors, $F_{env}$, on the resilient modulus, $MR$, at any degree of saturation:

$$F_{env} = MR/MR_{opt} \tag{2-1}$$

where $MR_{opt}$ = the resilient modulus at the optimum moisture content (OMC).

That model was further calibrated in terms of degree of saturation using a series of experiments under different moisture conditions in the following form:

$$\log\left(\frac{MR}{MR_{opt}}\right) = a + \frac{b-a}{1+e^{\beta - K_m(S-S_{opt})}} \tag{2-2}$$

where

$S$ = current degree of saturation (decimal),
$S_{opt}$ = degree of saturation at OMC (decimal),
$a$ = minimum of log ($MR/MR_{opt}$),

$b$ = maximum of log ($MR/MR_{opt}$),
$\beta$ = regression parameter = ln ($-b/a$), and
$K_m$ = regression parameter.

Studies about the impact of the moisture content/degree of saturation/suction variation on the stiffness and ICMV of the geomaterials during and shortly after the compaction process are limited. Thompson and White (2007) used test strips constructed at three different moisture contents to evaluate the impact of the moisture content on the ICMVs. They discussed that the inevitable variation in the moisture content of the compacted geomaterials during construction could affect the quality management of earthwork and unbound geomaterials. Siddagangaiah et al. (2014) performed an extensive field evaluation of IC for the quality control of the base and soils in Texas. Even though some weak correlation between the LWD modulus and the moisture content was observed, a reasonable relationship between ICMV and the moisture content could not be reported. They also confirmed that a certain level of uncertainty was associated with the estimation of the in-situ moisture contents using NDG. White and Vennapusa (2015) emphasized the need for the utilization of moisture content sensors in the future development of the IC monitoring of the earthwork and soil layers.

**Density.** The study of the variation in modulus of compacted geomaterials with density has been limited in the literature. Some efforts were aimed at investigating the impact of the density combined with the moisture content in terms of the degree of saturation (Cary and Zapata 2011). Other studies, such as those conducted by Mooney and Rinehart (2009), Von Quintus et al. (2010), Pacheco and Nazarian (2011), and Nazarian et al. (2014), could not establish a direct correlation between the modulus and density. Nazarian et al. (2014) indicated that, considering the uncertainties associated with the estimation of the density by NDG, a reasonable correlation could not be found among any of the in-situ moduli and density.

Floss et al. (1991) reported several correlations between ICMV and density in terms of the percent compaction. The goodness of the fit for their correlations was less than that obtained with the plate load test results. Bräu et al. (2004) reported correlations between ICMV and spot-test results, including density with significant scatter. Mooney et al. (2003 and 2005) correlated ICMV to several spot-test results, including the dry density. They showed that such correlations improved when the lifts were stiff. Peterson (2005) and White and Thompson (2008) reported poor correlations between the ICMV and dry density.

**Gradation and Plasticity.** Many empirical models can estimate the modulus of a geomaterial using index properties such as gradation parameters and Atterberg limits. Navarro et al. (2012) and Nazarian et al. (2014) summarized several such regression models; however, most models are applicable and reasonable only for the specific soil conditions for which the test protocols were developed.

**Long-Term Versus Short-Term Behaviors of Geomaterials.** Significant work has been done to predict the long-term changes in the moisture content/suction and modulus of the compacted geomaterials under the in-service pavement. However, the amount of work related to the short-term behavior of the exposed geomaterials (as related to quality management) has been limited. In a proper field compaction, the geomaterial is placed near the optimum moisture content and the moisture change is due to either evaporation or the introduction of moisture. The moduli obtained from this process can be vastly different from the moduli measured in the laboratory under a constant compaction effort (Khoury and Zaman 2004; Sabnis et al. 2009; Pacheco and Nazarian 2011). During the first few days, a freshly compacted material experiences several phenomena (e.g., thixotropy, moisture loss and equilibrium) that cannot be modeled using most models, which were developed to represent the long-term behavior of the materials in relation to seasonal and other environmental variations.

## Numerical Modeling Techniques of Roller Compaction

Experimental data collected with instrumented roller compactors has revealed complex nonlinear roller vibration behaviors, which include the loss of contact between the drum and the soil, as well as the drum and the frame rocking (Adam and Kopf 2004; Anderegg and Kaufmann 2004; Mooney et al. 2006). Various numerical modeling techniques have been attempted to address some of these concerns.

Numerical models can be either physical-based models or finite element (FE) models. Physical-based models, which include lumped-parameter, boundary-element (BE), and discrete-element (DE) models, have been studied by van Susante and Mooney (2008), Mooney and Facas (2013), and Buechler et al. (2012), among others. Research on FE models has been conducted by Xia and Pan (2010), Mooney and Facas (2013), Erdmann and Adam (2014), and Keneally et al. (2015), among others.

The following summary comments can be made about the implementation of the different models for simulating roller compaction:

- Lumped-parameter models are the simplest but the least realistic models. These models can provide results rapidly, but site-specific calibration may be time-consuming.
- BE models reduce the dimensionality of the problem, resulting in savings of computation time and resources; however, roller dimensions and operation parameters, as well as the plastic response of geomaterials associated with compaction, must be addressed using iterative processes and indirect means to adjust soil responses.
- DE models can provide a wealth of information about the performance of granular materials under the rollers. However, the execution time at realistic scales is prohibitive.
- FE models are the most versatile tools for obtaining the responses of geomaterials under rollers. Simple linear elasto-static models (especially 2D models) are rapid to execute. As the problem is extended to 3D with dynamic loading and with plastic and nonlinear geomaterial behavior, the execution time becomes rather time-consuming for routine use.
- The best numerical model to use is the one that best balances the execution time, the accuracy of the results, and the amount of time a DOT is willing to spend to obtain the necessary material parameters.

Detailed information about the modeling techniques that have been implemented for simulating roller compaction of geomaterials is provided in Appendix D.

### Constitutive/Material Models of Geomaterials

It is essential to incorporate reasonable geomaterial constitutive/material models. A summary of constitutive models of geomaterials is provided in Appendix D. The following statements can be made about them:

- Linear elastic models are the most versatile and recognized constitutive models for geomaterials. Because most of the design algorithms are based on linear elastic models, the harmonization of selecting the target modulus/stiffness for field IC compaction with the design parameter selected for each layer becomes straightforward. However, linear elastic material models may only be applicable to stiffer materials at the end of the compaction process.
- Nonlinear (resilient modulus) models are more realistic than linear elastic models because the highest state of stress that most layers experience is during compaction. However, these models should be implemented with caution. Based on a survey of DOTs conducted during the NCHRP 10-84 study by Nazarian et al. (2014), one of the top two reasons that would

impede the implementation of the modulus-based quality acceptance was the incorporation of the resilient modulus tests in the specifications. If nonlinear models are to be adopted, an indirect means of estimating the nonlinear model parameters should be considered. In addition, the uncertainty of estimating these parameters should be weighed against the benefits gained in terms of the more realistic results.

- Plasticity and hypo-plasticity models have limitations similar to those of resilient modulus models. Though these models offer more realistic responses than the linear elastic models, implementation of plasticity and hypo-plasticity models would require incorporation of laboratory tests such as shear, triaxial, and consolidations tests into the specifications. Inclusion of estimation methods must be developed for parameters used by these models, and their uncertainty must be assessed.

### Soil-Drum Contact Mechanism

Several alternative models, from the classical Hertzian models to the more modern and sophisticated BE models, have been used for addressing the soil-drum contact mechanism. The following statements can be made about the reviewed contact models:

- Hertzian models are easy to implement but are overly simplified, as they overlook the nonlinear response of the geomaterial. Their implementation would require the inclusion of methods to adjust the calculated contact widths in order to address the nonlinear behavior of soils. The use of Hertzian models may, nonetheless, be applicable to stiffer granular materials or at the end of the compaction process.
- BE models better address soil-drum contact width and stress distribution than do Hertzian models. The implementation of BE models would require an iterative approach to adjust the contact width, which is greatly expedited due to faster execution times than common FE approaches.
- DE models have been found to be more realistic in addressing contact widths than Hertzian models, and DE models have been found to better address cohesive soils than do other methods. Further research to investigate the stress fields is still needed, however, and the dynamic analysis required by DE models makes them time prohibitive.
- FE models generally include different contact models depending on the program used. These models address the stress fields and contact widths reasonably well, given the FE software's capacity to consider the soil's nonlinearity, but they require the implementation of dynamic loading, which leads to time-consuming execution analyses that would be unsuitable for routine applications.

More realistic contact widths and stress fields will depend on the chosen numerical model and constitutive material model that better addresses execution time suitable for routine use.

## Intelligent Compaction Measurement Value (ICMV)

Mooney et al. (2010) described the roller measurement values in detail. The various data measurement values used for compaction control are listed in Table 2-1. The ratio between the amplitude of the first harmonic and the amplitude of the excitation frequency was first correlated to the stiffness of the soil as measured by dynamic plate load tests (Thurner and Forsblad 1978). Thurner and Sandström (1980) introduced the compaction meter value (CMV). Since then, various measuring systems have been implemented by the roller manufacturers. In 1982, Bomag introduced the OMEGA value and the Terrameter measuring system, and these systems were followed by the vibration modulus $E_{vib}$, a measure of dynamic soil stiffness (Ferris 1985; Floss et al. 2001; Kröber et al. 2001). In 1999, Ammann introduced the

**Table 2-1. Commercially available roller measurement values (from Mooney et al. 2010).**

| Measurement Value | Manufacturers | Parameters Used | Relations Used |
|---|---|---|---|
| Compaction Meter Value (CMV) | Dynapac, Caterpillar, Hamm, Volvo | Ratio of vertical drum acceleration amplitudes at fundamental vibration frequency and its first harmonic. | $CMV = c\frac{A_{2\Omega}}{A_{\Omega}}$ where $c$ is constant around 300, $A_{2\Omega}$ is the amplitude of second harmonic, and $A_{\Omega}$ is amplitude of fundamental frequency. |
| Compaction Control Value (CCV) | Sakai | Algebraic relationship of multiple vertical drum vibration amplitudes, including fundamental frequency, and multiple harmonics and sub harmonics. | $CCV = \left[\frac{A_1 + A_3 + A_4 + A_5 + A_6}{A_1 + A_2}\right] \times 100$ where $A_i$ are amplitudes at the excitation frequencies. |
| Stiffness, $k_s$ ($k_b$) | Ammann | Vertical drum displacement, drum-soil contact force. | $k_s = \Omega^2\left[m_d + \frac{m_0 e_0 \cos\phi}{z_d}\right]$ where $m_d$ is drum mass, $m_0e_0$ is eccentric mass moment, $\phi$ is phase angle, $z_d$ is drum displacement, and $\Omega$ is frequency. |
| Vibration Modulus, $E_{vib}$ | Bomag | Vertical drum displacement, drum-soil contact force. | $z_d = \frac{2(1-\nu^2)}{\pi \times E_{vib}} \times \frac{F_s}{L} \times \left(1.8864 + \ln\frac{L}{b}\right)$ where $F_s$ is drum soil interaction force, $L$ is the drum length, $b$ is contact width, $\nu$ is Poisson ratio, and $z_d$ is drum displacement. |
| Machine Drive Power (MDP) | Caterpillar | Difference of gross power and the power associated with sloping grade and machine loss. | $MDP = P_g - WV\left[\sin\theta + \frac{a}{g}\right] - (mV + b)$ where $P_g$ is gross power, $W$ is roller weight, $a$ is acceleration, $g$ is acceleration due to gravity, $\theta$ is slope angle, $V$ is roller velocity, and $m$ and $b$ are internal loss coefficients. |

ACE (Ammann Compaction Expert) that calculated the soil stiffness parameter $k_s$ (also called $k_B$) (Anderegg and Kaufmann 2004; Anderegg 1997).

## Mechanistic ICMVs

The introduction of $E_{vib}$ and $k_s$ signaled an important evolution toward the measurement of more mechanistic, performance-related soil properties (e.g., soil stiffness/modulus). These two ICMVs are determined from the force-displacement hysteresis loops. The hysteresis loops are interpreted from the drum acceleration time histories collected by the IC rollers. The force-displacement loops are created by plotting the time-varying contact force, $F_c$, versus time-varying drum displacement, $z_d$, where contact force is calculated from the vertical response of the drum.

The Ammann ACE system calculates the secant soil stiffness, $k_s$, from the gradient of the line passing through the point of zero dynamic displacement (i.e., displacement due to the static weight of the roller) to the point representing the maximum dynamic drum displacement, as shown in Figure 2-1 (Anderegg and Kaufmann 2004; Mooney et al. 2010). To determine these parameters, the system takes advantage of the lumped-parameter model. That model uses a roller and a 2 degrees of freedom (2 DOF) model representing the vertical kinematics of the drum-frame system. The drum/soil contact force, $F_s$, consists of the machine weight, the eccentric force, and the drum and frame inertias, and is described in Appendix C. The Ammann

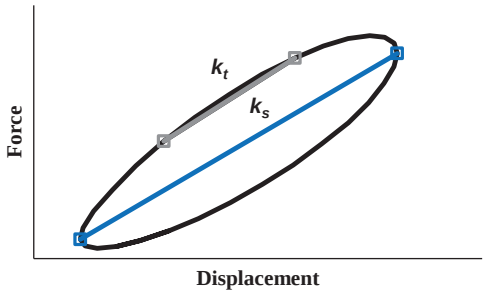


***Figure 2-1. Calculation of secant stiffness, $k_s$, and tangent stiffness, $k_t$.***

system determines the drum inertia and the eccentric force by measuring the vertical drum acceleration and eccentric mass position, whereas the frame inertia is neglected.

The vertical drum displacement amplitude, $z_d$, is determined by the spectral decomposition and integration of the measured peak drum accelerations (Anderegg and Kaufmann 2004). Secant stiffness, $k_s$, is calculated from

$$k_s = \Omega^2 \left[ m_d + \frac{m_0 e_0 \cos\phi}{z_d} \right], \tag{2-3}$$

where

$m_d$ = the drum mass,
$m_0 e_0$ = the eccentric mass moment,
$\Omega$ = the excitation frequency, and
$\phi$ = the phase lag between the eccentric mass and the drum displacement.

Like the Ammann ACE system, the Bomag Variocontrol system makes use of the force-displacement hysteresis curves to determine the tangent stiffness (defined as the slope to the force-displacement loop at locations of 80% and 20% of the difference between the maximum and minimum contact forces in calculating a "vibration modulus," $E_{vib}$ [Mooney et al. 2010]).

## Correlation Analysis Studies

Several studies have evaluated the roller measurement values for the compaction quality management of different pavement layers and embankment soils. Research has also been carried out to correlate the roller measurement values with the in-situ point test measurements. Even though different manufacturers recommend different ICMVs, the vertical, longitudinal, and transverse heterogeneity of the underlying soil strata is the most important factor influencing ICMVs and the modulus-based spot-test results. The correlations developed with ICMVs and the spot tests change whenever there is a change in the underlying condition. The heterogeneity stems from the changes in material type, compaction effort, and moisture contents at the time of compaction and testing (Nazarian et al. 2014). The depth of influence for a regular (11 ton to 15 ton) roller is reported to vary between 2.5 ft. to 4 ft. (Mooney et al. 2010). Hence, the ICMVs measured will reflect the composite stiffness of the geomaterials up to a depth of 2.5 ft. to 4 ft.; however, the spot tests typically reflect the material property up to a depth of 0.5 ft. to 1 ft. (Mooney et al. 2010).

## Current Backcalculation Techniques

Backcalculation (also called system identification or inversion) is an optimization process performed to inverse map a known relation established by discrete or continuous data points. The most commonly known backcalculation process in pavement engineering is related to the interpretation of the results from the FWD. In FWD backcalculation, the measured deflections are "matched" with the calculated deflections from a numerical algorithm. Usually, the matching process between the measured and calculated responses is performed by an iterative process, in which the responses are calculated using different sets of assumed mechanical properties. Göktepe et al. (2006) provided a thorough comparison of the various backcalculation techniques in terms of modeling precision, computational expense, calculation details, and data requirements. Figure 2-2 presents an overview of these backcalculation methods. Their implementation has been possible due to the tremendous advances in computational power, which has significantly minimized the computation time required for the backcalculation processes. In the context of this study, the backcalculation methods can generally be categorized as static, dynamic, or adaptive (Göktepe et al. 2006). Static and dynamic methods are classified by their loading types and utilize the conventional pavement response models. Adaptive methods, such as neural networks and neuro-fuzzy systems, do not directly use a response model; instead, they simulate inverse mapping by learning the target behavior via known input-output data patterns.

A forward model and an inverse algorithm are used in the backcalculation process. In the forward process, the responses are computed based on the loading and pavement structure, typically using a linear elastic procedure. The inverse process can be performed using various optimization (error minimization) processes. Optimization can be performed using a parameter identification algorithm (PIA) such as nonlinear least-squares, database search algorithms (DSA), or genetic algorithms (GAs). GAs are used in genetic programming (GP), which offers a model-free artificial intelligence (AI)-based optimization technique that mimics the theory of evolution.

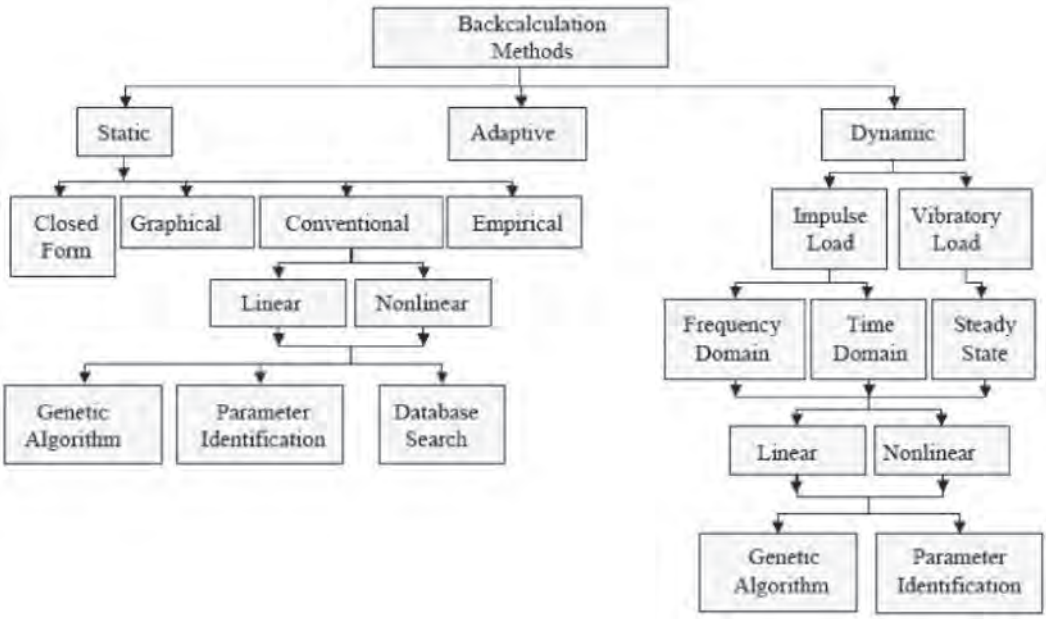


*Source:* Göktepe et al. (2006)

***Figure 2-2. Overview of backcalculation methods.***

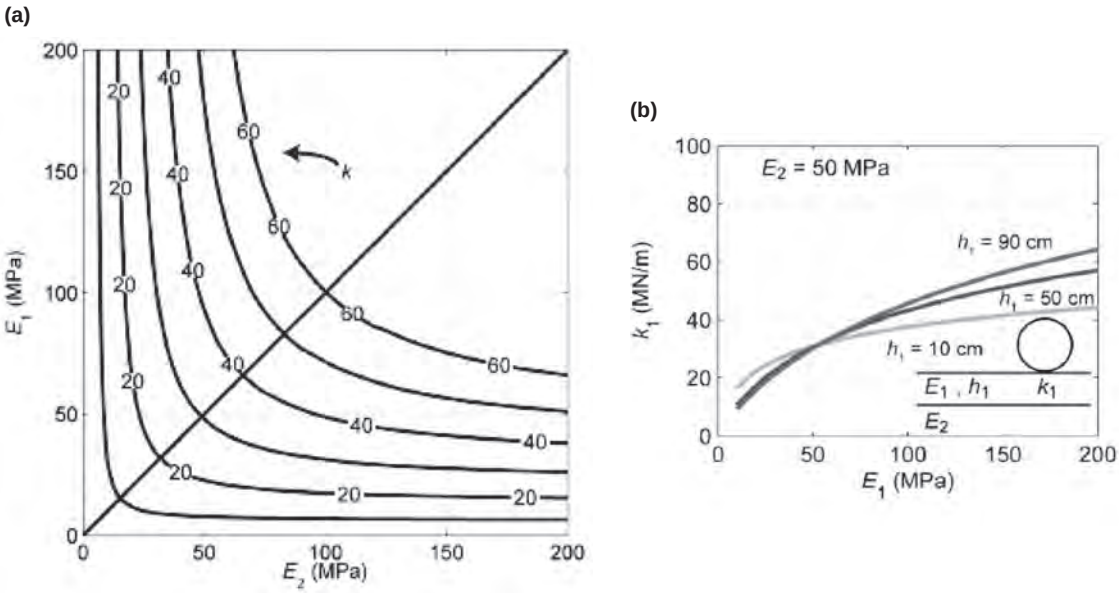


*Source:* Mooney and Facas (2013)

***Figure 2-3. Comparison of simulated stiffness, k, values from BE analysis for a two-layer system with (a) bottom-layer modulus, $E_2$, versus top-layer modulus, $E_1$, and top-layer thickness, $h_1$ = 30 cm; and (b) k versus top-layer modulus, $E_1$, for variable top-layer thickness, $h_1$.***

In the inverse process, the calculated responses are compared to the measured responses so that the new mechanical properties are determined by a parameter identification routine. Optimization is achieved through an iterative process until the differences between the calculated and measured deflections stay under a certain error criterion.

### Backcalculation Methods in IC Technology

Mooney and Facas (2013) evaluated different backcalculation processes for determining layer moduli with a forward process that used a static BE model simulating roller compaction. The forward process predicted the stiffness over a wide range of two-layer pavement structures with different layer moduli and top-layer thicknesses, as shown in Figure 2-3. Based on a sensitivity analysis, the authors suggested that the simple minimization algorithms could be used without the need of more complex techniques. Mooney and Facas found their approach time intensive, as each inversion required 5 to 15 iterations, and each iteration required forward modeling. To increase efficiency in the backcalculation process, they used direct inverse models created through regression analyses to substitute for the simulations in the forward model. The authors found that a local tri-cubic (LTC) interpolation, a ninth-order polynomial fit regression model, and an artificial neural network (ANN) model were able to simulate the responses with acceptable error.

## Approaches to Include IC in Specifications

This section summarizes the approaches to include IC in construction specifications and reviews of the current U.S. and European IC specifications. Mooney et al. (2010) proposed several options to include IC in construction specifications. In Option 1, the IC results are used to identify the weakest areas and test them with the conventional spot-testing devices for acceptance. In Option 2, the acceptance is based on limiting pass-to-pass percentage change in

either mean ICMV (Option 2a) or spatial percentage change in ICMV (Option 2b). In Option 3, the acceptance is based on whether the ICMV has met the requirements of target ICMVs, which can be determined either by relating ICMV to spot-tests (Option 3a), by determining the plateau value of ICMV compaction curve (Option 3b), or by relating ICMV to laboratory tests (Option 3c). Mooney et al. (2010) summarized the challenges to widespread utilization of the IC as a quality acceptance tool in the following manner:

- Heterogeneity in underlying layer support condition;
- High moisture content variation and adjustment of ICMV according to moisture condition;
- Narrow range of spot test measurements and ICMV;
- Machine operation setting variation (e.g., amplitude, frequency, speed) and roller double-jumping;
- Nonuniform drum/soil contact conditions;
- Uncertainty in spatial paring of spot test measurements and ICMV;
- Limited number of spot test measurements;
- Lack of other construction and materials information to help interpreting the IC results; and
- Intrinsic measurement errors associated with ICMV and spot test measurements.

Uniformity is recognized as a key parameter of compaction that relates to performance. Uniformity can be gauged by univariate statistics (e.g., variance) or spatial geostatistics (e.g., semi-variograms), but areas with the same variance may vary in spatial statistics. Another approach is to use the roller coverage as a method-based acceptance process. Most U.S. IC specifications have been using such an approach (e.g., 70% of compacted areas must have the target number of line passes or more). This method does not apply for this project, however, because of the goal of determining mechanical properties of the geomaterials.

## Review of Current Specifications

### *FHWA and AASHTO IC Specifications*

The current FHWA specifications provide generic guidelines to various state and local highway agencies for the implementation of the IC technology. These guidelines can be modified by the agencies to meet the state's specifications and specific project requirements. The current provision, AASHTO PP 81-14, "Standard Practice for Intelligent Compaction Technology for Embankment and Asphalt Pavement Applications," is a combined specification for both soils and hot-mix asphalt applications. The key features of the two specifications are compared in Table 2-2.

### *U.S. States' Specifications*

Figure 2-4 shows the distribution of the current IC specifications across the United States. The "Quality Management Special—Intelligent Compaction (IC) Method" (Minnesota DOT) specifies all the requirements listed by AASHTO PP 81-14. The "Intelligent Compaction for Soils" (Georgia DOT), "Intelligent Compaction Mapping of Subbase and Aggregate Base" (Michigan DOT), and "Intelligent Compaction for Subbase and Reclaimed Stabilized Base (RSB) Applications" (Vermont Agency of Transportation [VTrans]) use a RTK-GPS with a 1.6-in. verification tolerance. The IC rollers to be used on Georgia DOT projects require approval from the DOT and need to be listed in the agency's "Approved Vendor List." The Michigan DOT waives the pre-mapping requirement, and the VTrans waives the training requirement.

The Indiana DOT's "Quality Control/Quality Assurance, QC/QA, Soil Embankment" specification follows the general requirements of the FHWA specification using RTK-GPS with a 6-in. verification tolerance. However, the specification does not require the contractor to perform pre-mapping prior to construction.

**Table 2-2. Comparison of FHWA and AASHTO IC specifications.**

| Reference | FHWA Soils | AASHTO |
|---|---|---|
| GPS verbiage | HPPS[1] | RTK-GPS |
| GPS verification tolerance | 12 inch | 6 inch |
| Temperature verification tolerance (for asphalt) | NO | 5°F |
| Require alignment files | NO | YES[2] |
| Departmental approval of rollers | NO | YES |
| Roller vendors listed | NO | NO |
| Test strip required | YES | YES |
| Pre-construction mapping | YES[3] | NO |
| Veta software required | YES | YES |
| IC training | 4-8 hours[4] | Required[5] |
| IC training includes Veta | YES | NO[6] |
| Data submittal | Daily | Daily |
| IC-based acceptance | NO[7] | NO |
| Basis of payment | Lump sum | Lump sum and partial[8] |

[1]HPPS is intended to include all positioning technologies including GPS, laser, cellular signals, and so forth.

[2]AASHTO requires agencies to provide alignment files.

[3]FHWA only allows pre-mapping on soils and granular subbase.

[4]FHWA recommends project-specific just-in-time training.

[5]AASHTO requires yearly certification.

[6]AASHTO assumes that agencies are trained to use Veta.

[7]FHWA includes "IC Construction Operations criteria" that are based on pass count and ICMV coverage.

[8]AASHTO includes partial payments: 10% based on certification, 10% based on providing IC equipment, and 80% based on roller pass counts coverage.


***Figure 2-4. Current IC specifications for soils application.***

The "Special Note for Intelligent Compaction of Aggregate Bases and Soils" of the Kentucky Transportation Cabinet (KYTC) follows the FHWA guidelines and specifies the use of RTK-GPS. In addition, the KYTC specification includes an approval process for the IC rollers.

The Iowa DOT, North Carolina DOT, Pennsylvania DOT, and Texas DOT use the RTK-GPS but do not require any verification of GPS, and do not require pre-mapping to be performed prior to construction. The North Carolina DOT requires the roller vendor to have prior IC experience (three completed projects). The Texas DOT requires approved rollers from the vendor list only. The Texas DOT also waives the training requirement.

### *European Specifications*

Specifications for roller-integrated measurement systems for quality control and quality assurance have been developed and implemented in Europe as national compaction standards for more than two decades under the term *Continuous Compaction Control* (CCC). Introduced in Austria in 1990 with revisions in 1993 and 1999, these revisions were adopted in Germany in 1994 with revisions in 1997 and 2009 (see ZTVA-StB 97); in Finland in 1994; in Sweden in 1994 with revisions in 2004 (see VVR VÄG 2009); and in Switzerland in 2006. The International Society for Soil Mechanics and Geotechnical Engineering (ISSMGE) developed specifications based primarily on the Austrian specifications (ISSMGE 2005; Adam 2007). Mooney et al. (2010) classified the European specifications under two options:

- **Option 1: Spot Testing in Roller-Identified Weak Areas.** Following these specifications, the CCC roller performs a vibratory proof roll over the earthwork area under evaluation. The quality acceptance inspector uses the roller MV data map to identify the weakest area(s) for spot testing. If the roller-identified weakest areas meet the spot-test requirements, the entire evaluation area meets the threshold for acceptance. In principle, the validity of this option is tied to the existence of a positive correlation between the spot-test measurements and the ICMVs (i.e., high ICMVs correspond to high density and vice versa). Such positive correlations should be verified before quality acceptance testing.
- **Option 2: Calibration of ICMVs to Spot Test Values.** Specifications classified under this option consist of (1) An on-site correlation assessment to relate the ICMV to the selected (or contract specified) spot test measurement; (2) identification of an ICMV target value ($ICMV_{Target}$) consistent with the required spot-test value based on the regression performed in Step 1; and (3) acceptance testing by comparing the ICMV data from the evaluation area with the $ICMV_{Target}$.

Given its relative simplicity, Option 1 is the more common of the two options, and it is the only option permitted in Sweden.

The principal components of the various specifications and planned revisions are described in Ninfa (2013). Spot-testing requirements vary by country. Acceptance of earthwork materials in Europe is based primarily on use of the plate load test (PLT) or the lightweight deflectometer (LWD), whereas in the United States acceptance is primarily based on the dry density measurements using NDG.

## Common Elements of IC Specifications

Common elements of the federal and state IC specifications can be categorized using four sets of characteristics:

- Pre-approval of IC system requirements and quality control plan,
- Field operation requirements,
- Data requirements and submission, and
- Measures and payment.

### *Pre-Approval of IC System Requirements and Quality Control*

**Rollers Types, Vendors and Department Approval.** Agency specifications typically require that contractors submit documentation of the roller supplier, make, and roller model, along with the number of IC rollers to be provided for the project. Application-based instrumented roller types are specified, along with the requirements for their accuracy, GPS, rolling speed, frequency, and amplitude. Agency approval of the instrumented rollers may be required, as may the demonstration of the rollers at agency-approved locations. Some specifications include lists of approved or recommended IC roller brands and models. One key requirement is an "accelerometer-based" measurement system that provides a measure of the vibration amplitude of the roller, preferably in conjunction with measurement of the applied load, which enables an assessment of the compaction quality (generically as an ICMV). The preferred parameters that meet this requirement include kb (Ammann/Case) and Evib (BOMAG and Dynapac). Alternative systems that might be acceptable include CCV (Sakai), CMV (Caterpillar, Trimble, and TOPCON), EDV (VOLVO), and HMV (Hamm).

**GPS Requirements.** The GPS radio and receiver units are required to be mounted on each IC roller to track the roller passes. A handheld GPS also is required for measuring the locations of the spot tests with the density/modulus-based devices for correlation with the ICMV data. General specifications related to the GPS, including the definitions, devices, and networks, are included. GPS is often a loose definition to cover all global navigation satellite systems (GNSS), including GPS from the United States and GLANOSS from Russia. The precision requirements often specify real-time kinematic (RTK) or survey-grade precision. A high precision positioning system (HPPS) is used to cover all positioning technologies such as the GNSS, laser-based, and cellular-based systems.

**Contractor Quality Control Plan.** The contractor is required to prepare and submit a written Quality Control Plan (QCP) for the project. In addition to meeting the requirements of a general construction QCP, the plan should list the person(s) responsible for operating the IC roller(s) and attached IC equipment, and include the training documentation for the roller operator(s).

### *Field Operation Requirements*

**IC Training.** Appropriate IC training is critical to implement the IC procedure successfully because most contractors and DOT staff are not familiar with this technology. The IC vendors' technical support normally provides the IC training.

**GPS Field Validation.** The requirements to check the proper setup and to verify the accuracy of the GPS on the IC rollers against a hand-held rover are common and critical. Without such validation, the GPS offsets may render the IC data useless. The tolerances for the difference between the measurements have been specified as 6 in. to 12 in. The daily field GPS validation is often specified but not always enforced.

**Alignment Files.** An alignment file may be loaded onto the onboard documentation system of the instrumented roller and into the cloud-computing mapping software when used. A requirement for the agency to provide the relevant alignment files is usually included.

**Pre-Paving Mapping.** Performing pre-mapping with an IC roller on the existing support geomaterials is recommended to identify the weak areas and to evaluate the condition of the underlying materials such as soils subgrade, aggregate bases, or similar materials.

**Test Strip.** A test strip to test section construction in order to successfully establish target compaction pass counts and target values for the strength of the materials is specified. Test strips are not always enforced at actual projects, especially for embankment work.

**Conventional Spot Testing.** IC technology is currently used for quality control, but the acceptance is still based on the geomaterial density and sometimes on moisture measurements made with the NDG. A need exists for identification of the standard testing device(s) and frequency for measuring the in-place density and moisture content of the soil.

### *Data Requirements and Submission*

**IC Data Requirement.** An IC roller is both a construction machine and a data collection system. The IC data is the key to leveraging the benefits of the IC technologies. The data header block and data blocks are often required, with the most common data elements including the roller type and size information, GPS system setting, and IC measurements (including the roller passes, vibration amplitudes and frequencies, and ICMV).

**Veta Compatibility.** Currently, most states require that the IC data be compatible with Veta software. Veta (formerly known as Veda) can import data from various IC systems to perform standardized viewing and analysis. Veta is required as a standardized tool in the FHWA and AASHTO IC soils specifications.

**IC Data Submission.** The timely submission of the IC data is normally required. The IC data may include all passes, but including the data from the final coverage is mandatory.

### *Measures and Payment*

**IC-Based Acceptance.** The IC construction operations criteria does not generally affect the standard agencies' acceptance processes for the materials or construction operations since IC is mainly used for quality control.

**Basis of Payment.** The incorporation of the IC process in a project is currently based on a lump-sum price in most DOTs. This item includes all costs related to providing the IC roller(s) including the fuel, roller operator, GPS system, or any other equipment required for the IC process. All quality control procedures, including the IC rollers and GPS systems representatives' support, on-site training, and testing facility, are included in the contract lump-sum price. It is becoming increasingly popular to include payment breakdown to cover the IC equipment provided, training conducted, IC data submitted, and IC coverage (e.g., minimum number of line passes within a certain project boundary).

## Issues with Implementing Current IC Specifications

Given that the intention of the research team was to ensure the practicality and robustness of the specification, it was desirable to consider the current issues related to the implementation of the IC. Based on the experience of the research team, the important issues included:

- **Uniformity Across the Country.** Most state IC specifications are primarily modeled after the FHWA's generic IC specifications, but variations remain. (For more information, see Appendix C in the downloadable "Appendices.pdf" available from the *NCHRP Research Report 933* web page at www.trb.org.) State IC specifications range from 3 pages in length (e.g., the KYTC specifications) to 19 pages (e.g., the Minnesota DOT specifications). The IC vendors often report difficulties communicating with the DOTs and meeting their specifications, though vendors sell the same machines and systems across the country.
- **Lack of Field Qualification/Certification Process for IC Rollers and Operators.** The IC technology is primarily used for quality control. The inclusion of pay items that tie to the IC data is gaining popularity in specifications. As a result, an increasing need is to have a field procedure to qualify and certify the IC systems to ensure valid data is collected for calculating pay items. Currently, only the AASHTO IC specification includes "certification" verbiage in

the appendices regarding contractor personnel and provides a checklist to approve IC rollers. Like the pavement profiler certification, this certification is not trivial, and it may be costly to establish and operate.

- **Qualification of On-Site Training.** The IC training is one of the critical requirements to ensure the success of any IC project. Though most state IC specifications require an on-site or "just-in-time" training, it is difficult to provide qualified trainers to do so. A need may exist to include additional training-related language in the specifications to clarify who would provide the training and who would receive the training.
- **Difficulty of Conducting Daily GPS Validation and Complications of Not Performing Such Tests.** Most of the current problems with smooth implementation of IC technology are GPS-related issues. Most of the issues resulted from failing to perform the GPS validation prior to the fieldwork. Most contractors still do not understand that implementing the IC and GPS is not a turnkey solution, but rather requires rigorous steps to ensure that all elements of the IC technologies, with the GPS as the core, function as they are supposed to function. Among states that do require daily GPS validation, enforcement of this requirement may be neglected because it is time-consuming to perform the necessary tasks.
- **Controversy of Pre-Mapping Requirement.** Pre-mapping can be used to identify less stiff areas and perform corrective actions. Due to the limitations set by the unknown depth of the identified less stiff layer(s) using the current ICMV technologies, the question, "How weak is too weak?" does not yet have a definitive answer. In addition, the roller manufacturers do not recommend pre-mapping of hard surfaces due to concerns with the potential damage to the rollers.
- **Practicality of Conducting Test Strips.** For various reasons, it may not be practical to conduct a test strip for every project. Besides being time consuming, it can be impractical to conduct test strips when variations in moisture content or soil type affect support conditions throughout a project.
- **Difficulty of Determining Target Values from Test Strip Data.** Several DOT IC specifications include the requirements to determine target roller passes and target ICMV from test strip data. The material, production, equipment, and climatic variabilities encountered during construction make it difficult to determine and set target values, not to mention the differences in test mechanism and testing footprint and measurement depths. Therefore, one of the main goals of this research was to provide proven, practical field procedures to determine layer-specific target values for compaction acceptance.
- **Issues with Data and Report Submission (Data Management).** Currently, the IC systems allow either manual data storage or wireless data transmission. Manual data storage makes use of USB drives and is prone to errors or file loss with ill-trained personnel. Wireless transmission relies on a cellular connection for automated submission, and the connection is not always reliable given potential losses of cellular coverage or incorrect project setup. Pitfalls related to both data submission methods are still unresolved. Also, it is still a steep learning curve for the contractors to learn the vendors' software to export the IC data. Although several DOTs have started requiring their contractors to submit both the IC data and the IC analysis reports, the contractors and IC vendors are still struggling to meet such requirements due to a lack of training. Therefore, data management is currently one of the main concerns in the IC implementation.

CHAPTER 3

# Findings from Numerical Model

## Introduction

This chapter presents the development of a 3D FE model simulating the roller compaction of one- and two-layer geosystems. Different levels of complexity were considered in the model, including the use of linear and nonlinear geomaterial approaches and simulations of the roller operation ranging from a static load to a stationary vibratory load to moving vibratory loads. The responses of the model to these various geomaterial properties were numerically assessed, and correlations among the responses were established to study (a) whether the simplified model can account adequately for the behavior of the geomaterials under compaction and (b) whether these relationships can be used to simplify the modeling.

## Development and Limitations of Numerical Simulation of IC

The multi-purpose FE program LS-DYNA, which makes use of explicit and implicit time integration techniques, was used for simulating roller compaction. A 3D mesh was assembled to simulate a roller's drum in the process of proof mapping geomaterials at a given loading amplitude and vibrating frequency (see Figure 3-1). The drum of the roller was simulated as a rigid body containing shell elements with the commercially available regular dimensions of an IC roller (i.e., 2 m [80 in.] wide and 1.5 m [60 in.] diameter). A section of the geomaterial layer, 4 m (160 in.) wide, 4 m (160 in.) long, and 2.5 m (100 in.) deep, was modeled with nonreflective boundaries. A mesh consisting of brick elements was used to represent the geosystem. The mesh was composed of approximately 64,000 elements. Smaller elements with $50 \times 50 \times 50$ mm ($2 \times 2 \times 2$ in.) dimensions were used near the roller up to 0.5 m (20 in.) in depth, 0.6 m (24 in.) longitudinally, and 1.2 m (48 in.) transversally from the center of the drum, beyond which larger elements were used. The interaction between the drum and the geosystem was simulated using an automatic single-surface contact type that allows the decoupling of the drum from the soil surface as it occurs in the field. To that end, about 75,000 shell elements were used to simulate the drum.

The centrifugal force caused by the rotation of the eccentric masses inside the drum induces an excitation force, $F_e$, defined as

$$F_e(t) = m_0 e_0 \Omega^2 \cos(\Omega t), \tag{3-1}$$

where

$t$ = time,
$\Omega$ = the rotational frequency, and
$e_0$ = the eccentricity of the rotating mass, $m_0$.

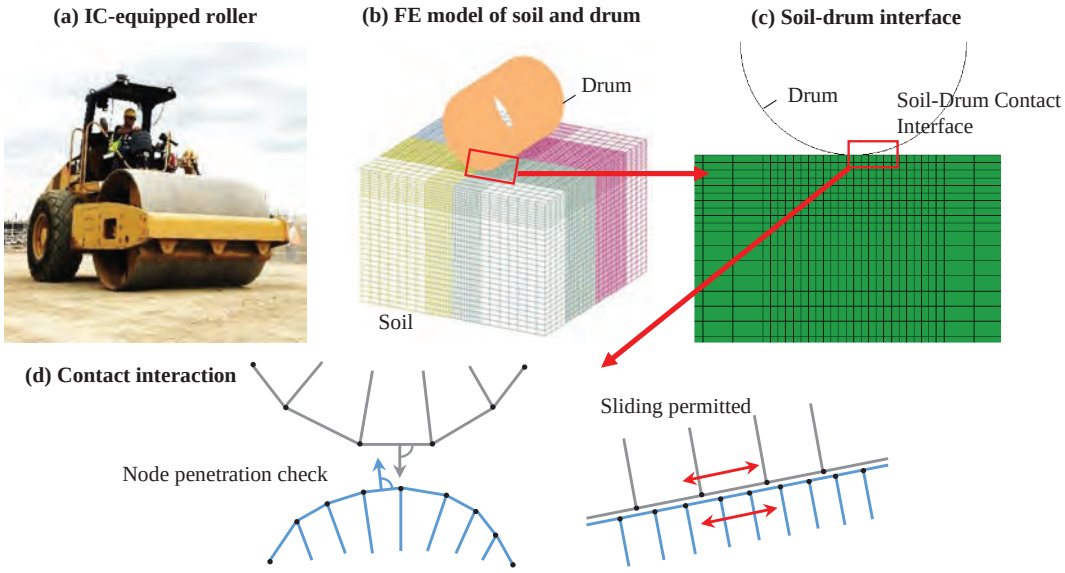


***Figure 3-1. Schematic representation of drum-soil system.***

Typical values used for the simulated drum are shown in Table 3-1. The vibratory motion of the roller was maintained for 200 ms, equivalent to six load cycles. The stress, strain, and displacement time histories were calculated for every time interval of 1 ms underneath the center of the roller. Rayleigh constants were defined as $\alpha = 25$ and $\mu = 0.0002$, as recommended by Mooney and Facas (2013) to minimize the dilatational and shear wave reflections.

Ooi et al. (2004) proposed a resilient modulus material model in which the resilient modulus, *MR*, is defined as

$$MR = k_1' P_a \left( \frac{\theta}{P_a} + 1 \right)^{k_2'} \left( \frac{\tau_{oct}}{P_a} + 1 \right)^{k_3'}, \tag{3-2}$$

where

$\theta$ = bulk stress,
$\tau_{oct}$ = octahedral shear stress,
$P_a$ = atmospheric pressure, and
$k'_{1,2,3}$ = regression constants.

**Table 3-1. Specifications for simulated drum.**

| Operating Parameter | Symbol | Value |
|---|---|---|
| Width of drum (compaction width) | $L$ | 2.0 m (80 in.) |
| Diameter of drum | $d$ | 1.5 m (60 in.) |
| Mass of drum | $m_d$ | 6,000 kg (34.3 lb. × s²/in.) |
| Weight of drum | $m_d g$ | 58,840 N (13,200 lb.) |
| Mass-eccentricity | $m_0 e_0$ | 5.36 kg·m (1.20 lb. × s²) |
| Centrifugal force (Vertical excitation force) | $F_{ev}$ | 170 kN (38 kips) |
| Frequency | $f$ | 28 Hz (1,680 vpm) |
| Frequency | $\Omega$ | 176 rad/s |
| Operating speed | $v$ | 0.9 m/s (3.24 km/h, 2.0 mph) |

This model was incorporated as a user defined material subroutine into LS-DYNA to account for the nonlinear behaviors of geomaterials under loading conditions.

Mazari et al. (2014) found that this model yielded more representative responses of modulus-based devices as compared to the standard material model incorporated in the MEPDG. Considering the practical problems the use of this model may cause for highway agencies that utilize the MEPDG material model, the authors also provided simple relationships for converting the more common MEPDG model parameters into the nonlinear parameters shown in Equation 3-2.

## Development of Comprehensive Database of Pavement Sections

A comprehensive database of linear and nonlinear 3D dynamic cases with different input parameters was assembled for single-layer and two-layer geosystems. The information stored in the database was used to evaluate the sensitivity of the geosystem responses to the various input parameters. That database was also used to develop an optimized model that simulated the response of different geomaterials subjected to a vibratory roller with a variety of levels of sophistication. The database contained the following types of data:

- Roller operating parameters, including drum dimensions, mass of drum, frequency, vertical excitation force, and operating speed.
- Geosystem structure and geomaterial properties, including layer thickness, nonlinear $k'$ parameters of layers, and the *representative* resilient modulus per layer.
- Level of sophistication of the FE model, including the type of analysis (static, quasi-static, or dynamic); geomaterial constitutive model (linear elastic or nonlinear); and contact type (roller load applied directly to the geosystem or by means of a contact model).
- Geosystem responses obtained after simulation of roller compaction, including maximum surface vertical displacement, maximum stress observed under the load, and depth of influence.

Three groups of geosystems were simulated, consisting of one single-layer (subgrade-only) system and two-layer systems with top layer (base) thicknesses of 150 mm (6 in.) and 300 mm (12 in.) on top of the subgrade. Feasible ranges of $k$ nonlinear parameters (proposed by Velasquez et al. [2009]) were used for the coarse- and fine-grained geomaterials, as shown in Table 3-2.

For each geosystem, 200 randomly generated cases were initially selected considering a uniform distribution within the feasible range of values shown in Table 3-2. This prototype database contained information about the distributions of stress, strain, displacement, and modulus (when applicable), and was used to study the feasibility of different concepts. As soon as a concept was deemed feasible, a more expanded strategic database relevant to that concept was developed. The representative resilient modulus of the base was constrained to a range between 70–700 MPa (10–100 ksi), whereas the representative resilient moduli of the subgrade were constrained to a range between 35–350 MPa (5–50 ksi).

**Table 3-2. Feasible range of layer properties.**

| | Nonlinear Parameters | | |
|---|---|---|---|
| **Material Type** | $k_1$ | $k_2$ | $k_3$ |
| Coarse-grained | 400–3,000 | 0.2–1.0 | -0.9 – -0.1 |
| Fine-grained | 1,000–4,000 | 0.01–0.5 | -6.0 – -1.5 |

*Source:* Velasquez et al. (2009)

**Table 3-3. Characteristics of different levels of sophistication of FE model for parametric study.**

| FE Model Characteristics | Label | Load Type | Constitutive Model | Roller Velocity |
|---|---|---|---|---|
| Static Stationary Linear | SSL | Static | Linear Elastic | -- |
| Static Stationary Nonlinear | SSN | Static | Modified MEPDG | -- |
| Vibratory Stationary Linear | VSL | Dynamic | Linear Elastic | -- |
| Vibratory Stationary Nonlinear | VSN | Dynamic | Modified MEPDG | -- |
| Vibratory Moving Linear | VML | Dynamic | Linear Elastic | 0.9 m/s (2 mph) |
| Vibratory Moving Nonlinear | VMN | Dynamic | Modified MEPDG | 0.9 m/s (2 mph) |

The research team considered six levels of sophistication of the FE model, as described in Table 3-3. In terms of the surface displacements and stresses at critical points, the geosystem responses were obtained directly under the drum of single- and two-layer geosystems simulating the drum as static and vibratory. The main levels of sophistication consisted of the following items:

- ***Linear vs. Nonlinear Behavior of Geomaterials:*** The use of the nonlinear material models requires iterative procedures to update the state of stress during the simulation, which leads to longer execution times. For this reason, the linear elastic material models are commonly used. The responses of the linear models were compared with their comparable nonlinear models to explore the possibility of establishing relationships that could estimate the nonlinear response knowing the linear response and the geomaterial $k'$ nonlinear parameters.
- ***Static vs. Vibratory Drum:*** For static loading conditions, a quasi-static analysis was implemented in which the load was applied in 1 ms as a ramp load until the peak excitation force was reached, and then the load was maintained at a constant magnitude for the following 19 ms. In that manner, the impact of inertia was reduced, allowing the contact elements to accommodate the drum. The simulation of a vibratory load consisted of a sinusoidal load with peak vertical force of 170 kN (38 kips) and a frequency of 28 Hz, in addition to the weight of the drum. At that frequency, six load cycles were produced in 200 ms of simulation time.
- ***Stationary vs. Moving/Rolling Drum:*** A prescribed motion to the drum was considered in vibratory moving cases, where velocity, angular velocity, and direction of movement were specified. These assumptions lend to slower executions if the nonlinear behavior of the geomaterials is considered, due to the iterative process required to update the state of the stress. Stationary drums were simulated at a unique position, yet the vibrating load applied to the drum was still incorporated.

Example comparisons of the displacements obtained with the nonlinear (SSN/VSN) and linear (SSL/VSL) models are shown in Figures 3-2 and 3-3 for single- and two-layer geosystems, respectively. These two parameters are correlated with some uncertainty, as judged by the number of cases lying outside the ±20% uncertainty bounds. The stiffer top (base) layer of the two-layer systems reduced the effect of the nonlinear behavior of the subgrade as the stresses attenuated more.

Table 3-4 provides a summary of the slopes, coefficients of determination ($R^2$ values) and normalized standard errors of estimate (SEEs) of the regression lines from single-layer and two-layer 150-mm base on top-of-subgrade scenarios. NSEE is calculated from

$$Normalized\ standard\ error\ of\ estimate\ (SEE) = \sqrt{\frac{\sum_{i=1}^{n}\left(Y_i' - Y_i\right)^2}{\sum_{i=1}^{n}\left(Y_i'\right)^2}}, \quad (3\text{-}3)$$

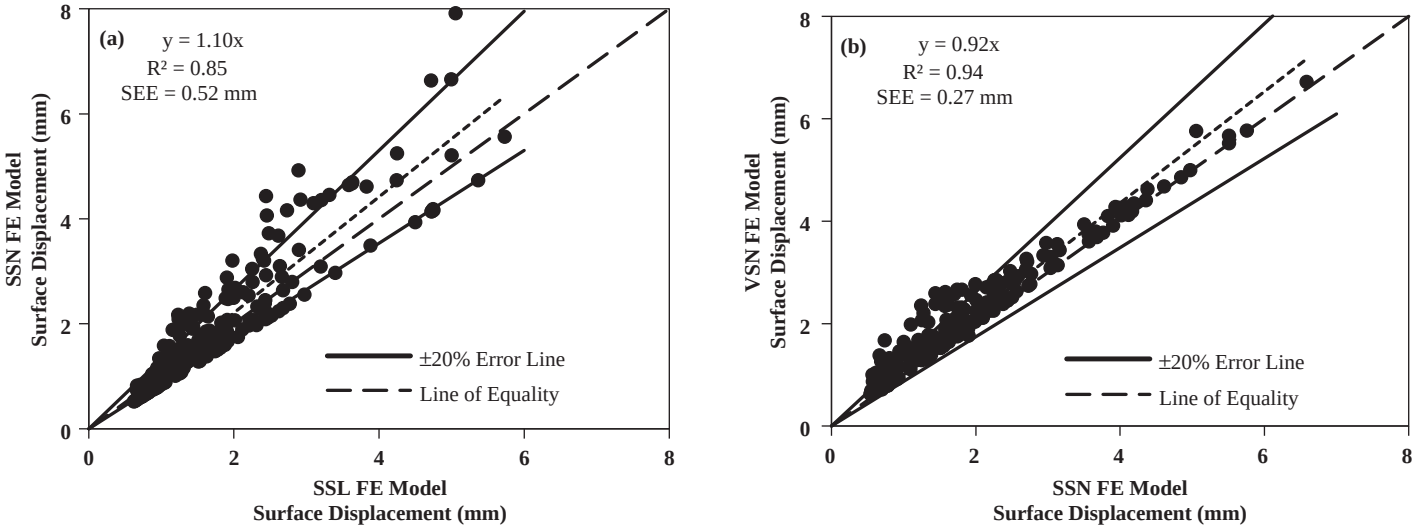


***Figure 3-2. Relationship of surface displacement under roller between (a) linear (SSL) to nonlinear (SSN) static stationary and (b) vibratory (VSN) to static (SSN) stationary nonlinear FE models for a single-layer (subgrade) geosystem.***

where

$Y_i'$ = the estimated displacement obtained from the linear equation of the fitted trend,
$Y_i$ = the displacement from the FE simulation, and
$n$ = the total number of points.

In general, displacement pairs correlated with $R^2$ values greater than 0.85 and typically greater than 0.90, while normalized errors of estimate were typically less than 0.20. These descriptive statistics suggest that the surface deflections as obtained from the more sophisticated FE models may be estimated using relationships that adjust the responses of the less-sophisticated (i.e., less computationally intense) FE models. The level of sophistication impact

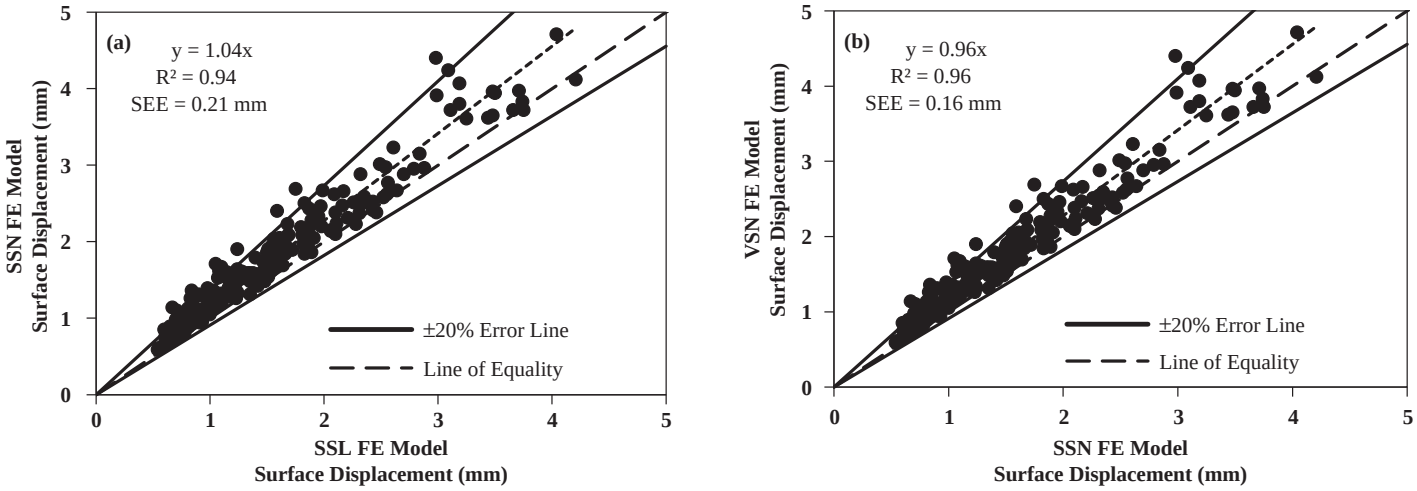


***Figure 3-3. Relationship of surface displacement under roller between (a) linear (SSL) to nonlinear (SSN) static stationary and (b) vibratory (VSN) to static (SSN) stationary nonlinear FE models for two-layer geosystem with 150 mm (6 in.) base layer on top of subgrade.***

**Table 3-4. Descriptive statistics for various levels of sophistication of FE model.**

| | Level of Sophistication of FE Model | | | | | | | | | | | |
|---|---|---|---|---|---|---|---|---|---|---|---|---|
| | Single-Layer System | | | | | | Two-Layer System (150 mm base on top of subgrade) | | | | | |
| | Slope of Fitted Linear Relationship | | | | | | Slope of Fitted Linear Relationship | | | | | |
| Model | SSL | SSN | VSL | VSN | VML | VMN | SSL | SSN | VSL | VSN | VML | VMN |
| SSL | 1 | 1.10 | 0.98 | 1.04 | 1.00 | 1.13 | 1 | 1.04 | 0.97 | 1.01 | 1.01 | 1.15 |
| SSN | | 1 | 0.85 | 0.92 | 0.87 | 1.00 | | 1 | 0.93 | 0.96 | 0.96 | 1.10 |
| VSL | | | 1 | 1.05 | 1.02 | 1.14 | | | 1 | 1.03 | 1.04 | 1.18 |
| VSN | | | | 1 | 0.95 | 1.09 | | | | 1 | 0.99 | 1.14 |
| VML | | | | | 1 | 1.13 | | | | | 1 | 1.14 |
| VMN | | | | | | 1 | | | | | | 1 |
| Model | Coefficient of Determination ($R^2$) | | | | | | Coefficient of Determination ($R^2$) | | | | | |
| | SSL | SSN | VSL | VSN | VML | VMN | SSL | SSN | VSL | VSN | VML | VMN |
| SSL | 1 | 0.85 | 1.00 | 0.92 | 0.99 | 0.93 | 1 | 0.94 | 0.99 | 0.99 | 0.99 | 0.93 |
| SSN | | 1 | 0.83 | 0.95 | 0.79 | 0.90 | | 1 | 0.93 | 0.96 | 0.92 | 0.90 |
| VSL | | | 1 | 0.91 | 0.99 | 0.82 | | | 1 | 0.96 | 0.92 | 0.91 |
| VSN | | | | 1 | 0.90 | 0.93 | | | | 1 | 0.98 | 0.93 |
| VML | | | | | 1 | 0.85 | | | | | 1 | 0.94 |
| VMN | | | | | | 1 | | | | | | 1 |
| Model | Normalized Standard Error of Estimate (SEE) | | | | | | Normalized Standard Error of Estimate (SEE) | | | | | |
| | SSL | SSN | VSL | VSN | VML | VMN | SSL | SSN | VSL | VSN | VML | VMN |
| SSL | -- | 0.22 | 0.03 | 0.15 | 0.04 | 0.19 | -- | 0.11 | 0.04 | 0.04 | 0.03 | 0.11 |
| SSN | | -- | 0.23 | 0.12 | 0.23 | 0.15 | | -- | 012 | 0.09 | 0.13 | 0.14 |
| VSL | | | -- | 0.16 | 0.05 | 0.21 | | | -- | 0.06 | 0.05 | 0.13 |
| VSN | | | | -- | 0.16 | 0.12 | | | | -- | 0.06 | 0.11 |
| VML | | | | | -- | 0.19 | | | | | -- | 0.10 |
| VMN | | | | | | -- | | | | | | -- |

on the analysis time and the relationships between all the models are described in detail in Appendix D, which is available as part of the downloadable "Appendices.pdf" file on the *NCHRP Research Report 933* webpage).

## Establishing Depth of Influence of IC

The depth of influence was defined as the depth at which the geomaterial's response diminishes to 10% of the peak response. Different depths can be obtained based on the response criterion used being either the displacements, stresses, or strains underneath the drum. Table 3-5 presents a summary of the normalized depth of influence with respect to the contact width ($z/B$) calculated using the displacement criterion for all models with different levels of sophistication. The average influence depth slightly increases for the vibratory moving drums as compared to the stationary vibratory or static conditions. Nevertheless, the differences in the mean values among the six different cases is less than 11%. Based on these case studies, for practical purposes one can approximate the depth of influence to about six times the effective contact width (i.e., about 1.8 m [70 in.] in depth).

When material nonlinearity is introduced, the depth of influence increases as $k_2'$ increases (i.e., as the geomaterial becomes more granular) and decreases as the absolute value of $k_3'$ increases (i.e., the geomaterial becomes less cohesive). As shown in Figure 3-4, the effect of the

**Table 3-5. Descriptive statistics of normalized depths of influence with respect to displacement for various levels of sophistication of FE model.**

| | Levels of Sophistication of FE Model | | | | | |
|---|---|---|---|---|---|---|
| | | Two-Layer System | | | Two-Layer System | |
| Normalized Depth of Influence (z/B) | One-Layer System | 150 mm Base | 300 mm Base | One-Layer System | 150 mm Base | 300 mm Base |
| **Static Stationary** | **Linear Geomaterial (SSL)** | | | **Nonlinear Geomaterial (SSN)** | | |
| Mean | 5.89 | 6.12 | 6.29 | 5.82 | 6.01 | 6.18 |
| Median | 5.90 | 6.13 | 6.30 | 5.91 | 6.03 | 6.03 |
| Standard Deviation | 0.03 | 0.17 | 0.26 | 0.58 | 0.37 | 0.37 |
| **Vibratory Stationary** | **Linear Geomaterial (VSL)** | | | **Nonlinear Geomaterial (VSN)** | | |
| Mean | 6.09 | 6.31 | 6.46 | 5.94 | 6.11 | 6.24 |
| Median | 6.11 | 6.30 | 6.46 | 5.99 | 6.13 | 6.30 |
| Standard Deviation | 0.06 | 0.19 | 0.28 | 0.40 | 0.30 | 0.28 |
| **Vibratory Moving** | **Linear Geomaterial (VML)** | | | **Nonlinear Geomaterial (VMN)** | | |
| Mean | 6.12 | 6.33 | 6.49 | 5.91 | 6.08 | 6.24 |
| Median | 6.13 | 6.34 | 6.51 | 5.99 | 6.09 | 6.25 |
| Standard Deviation | 0.05 | 0.17 | 0.27 | 0.43 | 0.32 | 0.28 |

material nonlinearity on the depth of influence was more significant in single-layer geosystems than in two-layer geosystems. This was also reflected in the standard deviation values of the depths of influence shown in Table 3-5, where higher standard deviations occurred in single-layer systems as well.

Detailed analyses for the stress criterion are provided in Appendix D. The depth of influence decreased to four times the drum contact width (i.e., about 1.2 m [48 in.]).

## Impact of Geomaterial Properties on ICMVs

The effect of the nonlinear $k'$ parameters on the roller responses were also quantified. The influence of the nonlinear nature of the geomaterials on the pavement responses was studied using Spearman's correlation (McDonald 2014). Different levels of sophistication of the FE

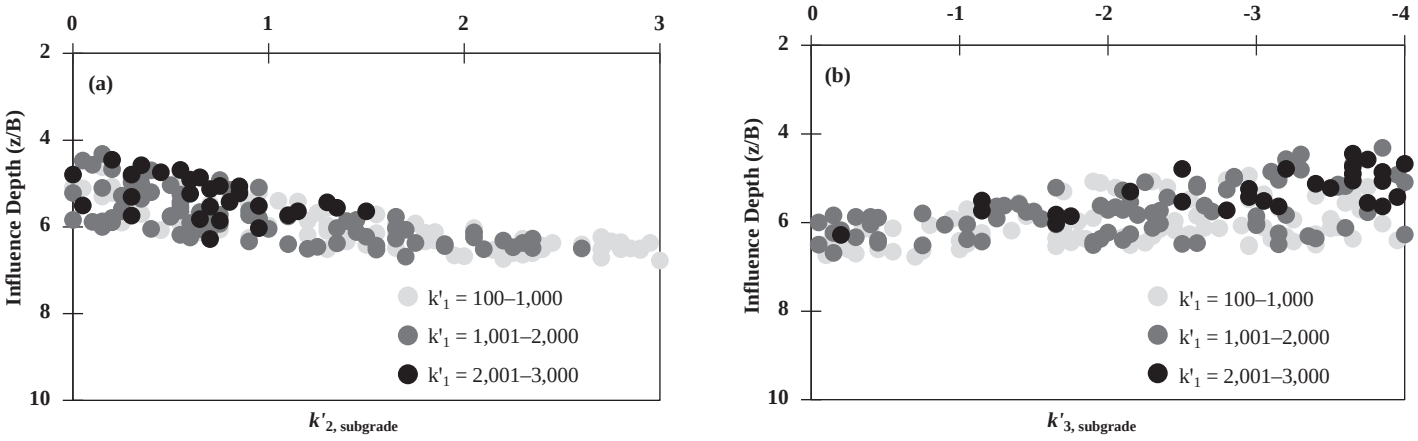


***Figure 3-4. Variation in influence depth with nonlinear k' parameters of subgrade for single-layer systems based on displacement criterion.***

**Table 3-6. Impact of nonlinear material parameters on surface displacement.**

| Level of Sophistication of FE Model | Spearman's Correlation Coefficients | | | | | |
|---|---|---|---|---|---|---|
| | Base Parameters | | | Subgrade Parameters | | |
| | $k'_1$ | $k'_2$ | $k'_3$ | $k'_1$ | $k'_2$ | $k'_3$ |
| **Single-Layer (Subgrade Only)** | | | | | | |
| SSN | -- | -- | -- | -0.37 | -0.42 | -0.18 |
| VSN | -- | -- | -- | -0.42 | -0.35 | -0.15 |
| VMN | -- | -- | -- | -0.32 | -0.37 | -0.30 |
| **150 mm (6 in.) Base Thickness** | | | | | | |
| SSN | -0.08 | -0.14 | -0.19 | -0.45 | -0.36 | -0.15 |
| VSN | -0.12 | -0.10 | -0.18 | -0.56 | -0.24 | -0.06 |
| VMN | -0.17 | 0.07 | -0.29 | -0.49 | -0.30 | -0.13 |
| **300 mm (12 in.) Base Thickness** | | | | | | |
| SSN | -0.12 | -0.19 | -0.28 | -0.49 | -0.20 | -0.08 |
| VSN | -0.21 | -0.06 | -0.23 | -0.55 | -0.22 | -0.03 |
| VMN | -0.24 | 0.03 | -0.31 | -0.54 | -0.23 | -0.05 |

models were also taken into consideration. Table 3-6 shows that subgrade nonlinear parameters $k'_1$ (related to stiffness) and $k'_2$ (granularity causing stress hardening) impact surface displacement the most, even for two-layer systems. In addition, material granularity (i.e., $k'_2$) seemed to have a more significant impact on the surface stress directly under the drum than did other parameters. This greater impact is shown in Table 3-7 for single-layer and two-layer geosystems, respectively. The nonlinear parameters of the subgrade tend to influence the surface stresses less significantly, especially as the base thickness increases.

## Impact of Roller Operating Features on Geomaterials Responses

Roller parameters significantly affect both the roller measurements and the geomaterials' responses during the mapping process. Aside from the pavement structure and mechanical properties of geomaterials (e.g., modulus and nonlinear $k'$ parameters), the impact of the

**Table 3-7. Impact of nonlinear material parameters on surface stress for two-layer system.**

| Level of Sophistication of FE Model | Spearman's Correlation Coefficients | | | | | |
|---|---|---|---|---|---|---|
| | Base Parameters | | | Subgrade Parameters | | |
| | $k'_1$ | $k'_2$ | $k'_3$ | $k'_1$ | $k'_2$ | $k'_3$ |
| **Single Layer (Subgrade Only)** | | | | | | |
| SSN | -- | -- | -- | 0.09 | -0.14 | -0.12 |
| VSN | -- | -- | -- | -0.29 | 0.31 | 0.26 |
| VMN | -- | -- | -- | 0.52 | 0.35 | -0.02 |
| **150 mm (6 in.) Base Thickness** | | | | | | |
| SSN | -0.07 | 0.16 | 0.07 | 0.20 | 0.37 | 0.16 |
| VSN | -0.14 | -0.08 | -0.05 | -0.14 | 0.33 | 0.18 |
| VMN | 0.22 | 0.30 | 0.08 | 0.15 | 0.31 | 0.15 |
| **300 mm (12 in.) Base Thickness** | | | | | | |
| SSN | -0.09 | 0.09 | -0.02 | -0.06 | 0.14 | 0.08 |
| VSN | -0.17 | 0.01 | -0.17 | -0.14 | 0.38 | 0.18 |
| VMN | 0.10 | -0.05 | 0.13 | 0.05 | 0.26 | -0.09 |

**Table 3-8. Simulated rollers with different operating features.**

| Case | Model Code* | Drum Weight (kN) | Centrifugal Force (kN) | Length (m) | Diameter (m) | No. of SSN Cases |
|---|---|---|---|---|---|---|
| 1 | 22.6W_1.00L_0.60D | 7.45 | 15.12 | 1.00 | 0.60 | 600 |
| 2 | 45.1W_1.00L_0.60D | 14.90 | 30.24 | 1.00 | 0.60 | 600 |
| 3 | 38.5W_1.20L_0.70D | 23.93 | 14.60 | 1.20 | 0.70 | 600 |
| 4 | 77.1W_1.20L_0.70D | 47.86 | 29.20 | 1.20 | 0.70 | 600 |
| 5 | 118.7W_1.50L_1.10D | 88.55 | 30.20 | 1.50 | 1.10 | 600 |
| 6 | 118.7W_1.50L_0.55D | 88.55 | 30.20 | 1.50 | 0.55 | 600 |
| 7 | 166.8W_1.50L_1.10D | 88.55 | 78.30 | 1.50 | 1.10 | 600 |
| 8 | 166.8W_1.50L_0.55D | 88.55 | 78.30 | 1.50 | 0.55 | 600 |
| 9 | 113.9W_2.00L_1.50D | 29.42 | 84.50 | 2.00 | 1.50 | 600 |
| 10 | 227.8W_2.00L_1.50D | 58.84 | 169.00 | 2.00 | 1.50 | 600 |
| 11 | 227.8W_2.00L_0.75D | 58.84 | 169.00 | 2.00 | 0.75 | 600 |
| 12 | 227.8W_1.00L_1.50D | 58.84 | 169.00 | 1.00 | 1.50 | 600 |
| | | | | | **Total:** | 7,200 |

* W = operating weight + eccentric force, L = length of drum, D = diameter of drum.

roller's operating features (e.g., operating weight and dimensions of the drum) on the pavement responses should be taken into consideration. To evaluate the effect of the roller operating features on the geomaterials responses, 13 rollers with different operating features were simulated (see Table 3-8). The rollers were identified using a code that summarizes the imparted force plus drum weight, length, and diameter. The soil responses determined under a static load exerted by a stationary drum were evaluated on a set of 200 nonlinear geomaterials systems that were made up of single-layer and two-layer pavement systems, comprising a total of 600 SSN FE models per simulated drum. The conclusions from this study are summarized next. The reader is referred to Appendix D for further details on the analysis presented briefly in this section.

## Impact of Weight

Three rollers with different drum dimensions were considered (Cases 1, 3, and 9, as listed in Table 3-8). As shown in Figure 3-5, increasing the load imposed on the soil by a factor of two

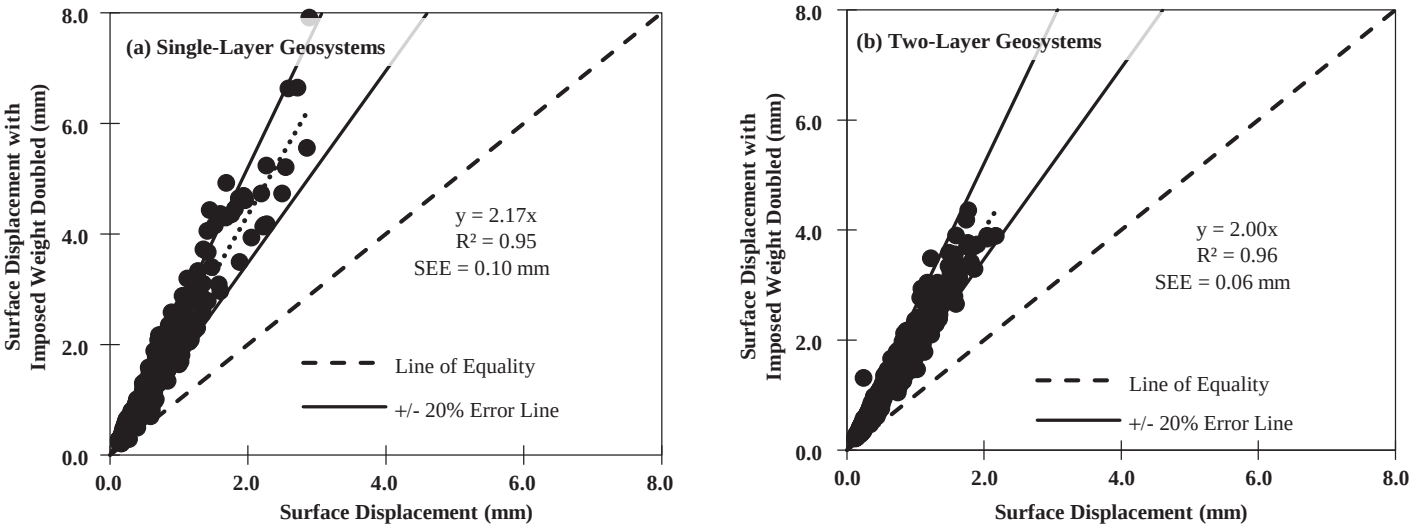


***Figure 3-5. Evaluation of weight impact on surface displacement.***

led to an increase in the surface displacement, with a factor of 2.17 and 2.00 for single-layer and two-layer geosystems, respectively. Like the surface displacements, the surface vertical stresses directly under the drum increased by about a factor of two when the magnitude of the imposed weight increased by a factor of two. More variability was observed in the surface stresses as compared to the surface displacements, however, which may be attributed to the effects that the nonlinear parameters of the top-layer geomaterial have on the contact area.

## Impact of Drum Length

Case 10 had a drum weight plus peak centrifugal force of 228 kN, a drum length of 2.0 m, and a drum diameter of 1.50 m. Case 10 was compared to Case 12, which involved another roller with identical features except that it had half the drum length (1.0 m). As shown in Figure 3-6(a), with the drum length halved, the surface displacement essentially doubled, increasing nearly 2.1 times for single-layer systems and nearly 1.8 times for two-layer systems. Likewise, as shown in Figure 3-6(b), the surface stress increased by about 100% as the drum length was shortened by 50% (increasing by a factor of 2 for single-layer systems and slightly more for two-layer systems). The increase in the contact area with an increase in the drum length results in a reduction in the surface vertical stress.

## Impact of Drum Diameter

Three rollers (Cases 5, 7, and 10) were selected to assess the effect of the drum diameter on soil responses. Their drum diameters were halved while the imposed weight and drum length were kept constant, resulting in the roller conditions described in Cases 6, 8, and 11. No significant change occurred in the surface displacements for both the single-layer and two-layer systems (see Figure 3-6). The surface stress increased when the diameter was halved, ranging from 6% for the smaller and lighter roller (Case 5) to 34% for the heavier and larger roller (Case 11).

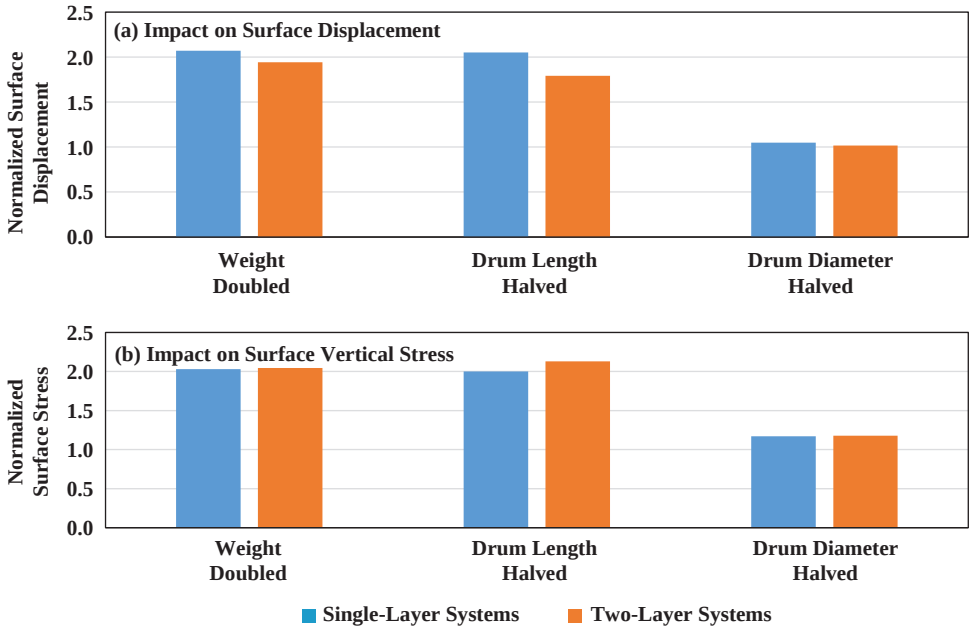


***Figure 3-6. Evaluation of impact of weight, length, and diameter of drum on surface displacement and stress.***

## Evaluation of Approaches for Developing Forward Models

The traditional methods for modeling and optimizing complex drum-soil compaction systems require huge amounts of computational resources. For this reason, a simplified model is necessary to predict the pavement responses with minimal computational effort and reasonable accuracy. Artificial intelligence (AI), with its predictive analytics and machine-learning components, provides powerful predictive capabilities commensurate to traditional methods in modeling the complex behavior of materials without incurring high levels of computing time and effort. Two models were developed using symbolic regression, one using a genetic programming (GP) approach and the other using an artificial neural network (ANN) approach. A database was generated that consisted of 7,200 cases of stationary static nonlinear (SSN) FE models with different operating features as listed in Table 3-8, and geosystems with different properties using the feasible ranges of nonlinear *k'* parameters shown in Table 3-2.

### Displacement

For both single-layer and two-layer systems, the general form of the mathematical model proposed using the GP approach for predicting surface displacement underneath the center of the drum, $d_{SSN}$, consisted of a function, defined as follows:

$$d_{SSN} = f(k_1'^b, k_2'^b, k_3'^b, k_1'^s, k_2'^s, k_3'^s, h, L, D, W), \tag{3-4}$$

where

$W$ = the weight (in kN), which includes the total force due to the drum weight, $F_D$, and the peak eccentric vertical force, $F_{ev}$;
$L$ = the drum length (in m);
$D$ = the drum diameter (in m);
$h$ = the thickness of the base (in mm); and
$k_i'^b$ and $k_i'^s$ = nonlinear parameters of the base and subgrade, respectively.

To predict the maximum surface displacement under ordinary static drums with differing operating features, the $d_{SSN}$ calculation could be adapted by incorporating variables to represent the various operating features along with an operating index, ψ, The operating index, ψ, was defined as follows:

$$\psi = \frac{L}{D} \times W, \tag{3-5}$$

where

$L$ = the drum length (in m), and
$D$ = the drum diameter (in m), and the variables $C_1$ through $C_8$ were used to capture the operating features of the drums.

Equation 3-6 shows the new equation as constructed to predict displacement for two-layer geosystems. To predict displacement for single-layer geosystems, the last term of Equation 3-6 is excluded.

$$d_{SSN} = C_1 + C_2 W + \frac{C_3}{k_1'^s} + C_2 \cos(W) + C_5 W(k_1'^s + k_2'^s + k_3'^s) + C_6 \psi \cdot k_1'^s (W + k_1'^s) + \frac{C_7 W}{\cos\left(\frac{223L}{D}\right)} + \frac{C_8 h \cdot \psi}{k_1'^b \cdot k_2'^b \cdot k_3'^b}, \tag{3-6}$$

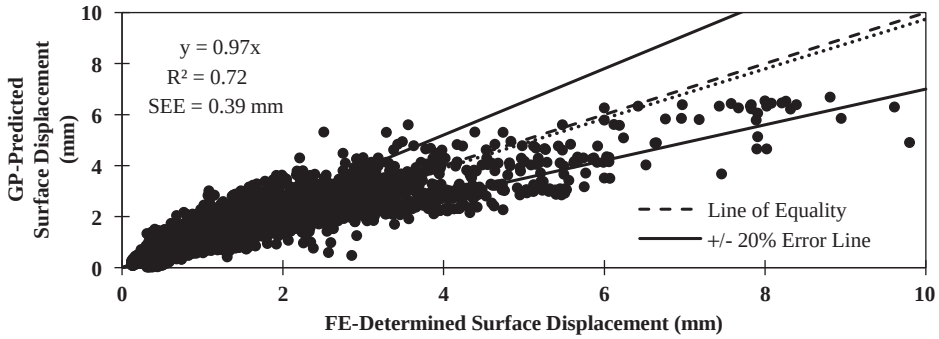


***Figure 3-7. Comparison of GP-predicted surface displacement to FE-determined surface displacement obtained from stationary drums with different operating features.***

where

$C_1 = 0.00425$,
$C_2 = 0.0139$,
$C_3 = 205$,
$C_4 = 0.075$,
$C_5 = 5.58 \times 10^{-6}$,
$C_6 = 2.98 \times 10^{-10}$,
$C_7 = 0.0004$,
$C_8 = 4.65 \times 10^{-5}$, and
$\psi$ = the operating index (as defined in Equation 3-5).

Figure 3-7 compares the GP-predicted surface displacements under the drum to the corresponding surface displacements as determined by FE modeling. The GP approach estimated the peak surface displacement under rollers with different operating features fairly well, as most of the cases fell within the ±20% uncertainty bounds, with an $R^2$ value of 0.73 and standard error of the estimate of 0.39 mm.

To further improve the estimation of the surface displacements directly under the drum, an ANN-based method was developed. As shown in Figure 3-8, the ANN-based method predicted the surface displacements more accurately than the GP method. With the ANN method, the error of the estimate was less than 15% in 85% of the cases. The ANN method predicted surface displacements with an $R^2$ of 0.99 and a SEE of 0.10 mm (see Figure 3-9).

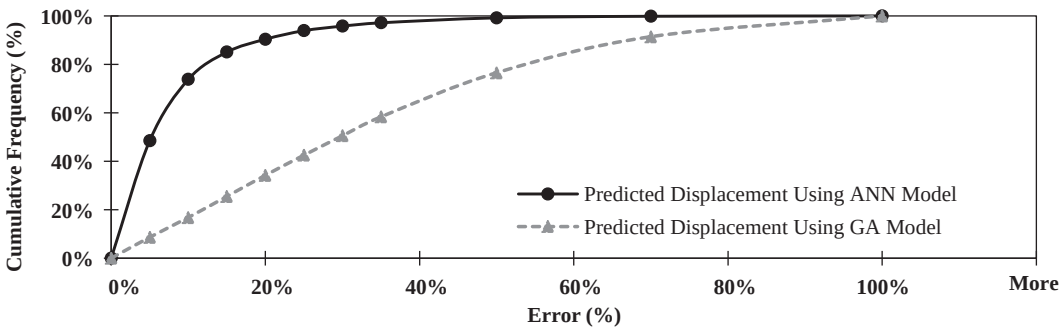


***Figure 3-8. Cumulative distribution of estimation error for the predicted surface displacement using GP- and ANN-based methods.***

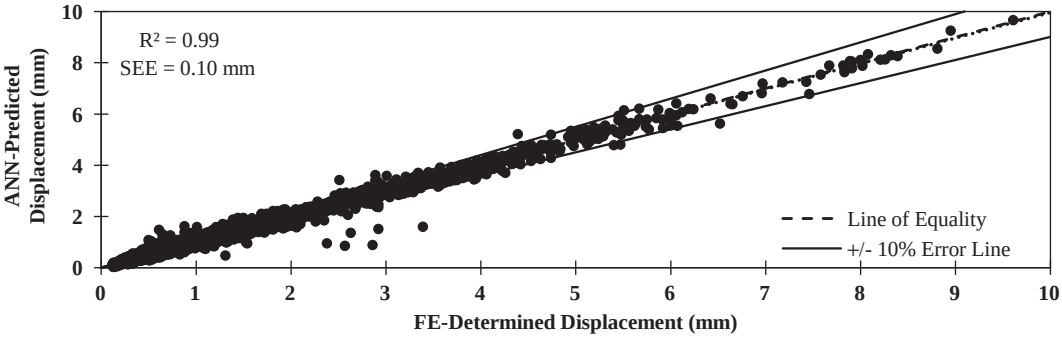


***Figure 3-9. Comparison of predicted surface displacement from ANN method versus FE model.***

## Stiffness

Stiffness is defined as the resistance to deformation of a material under an applied load. As such, stiffness is not a unique material property; rather, it is the response of the pavement system to the load. Roller-measured soil stiffness can normally be derived from the vertical force equilibrium of the vibrating drum. In this study, the soil stiffness during pre-mapping as well as during the mapping process can be determined as the ratio of force over surface displacement ($k = W/d_{SSN}$) for the SSN FE models. The general form of the proposed model for prediction of geomaterials stiffness for single-layer ($k_{s\text{-}SUBG}$) and two-layer ($k_{s\text{-}COMP}$) geosystems is expressed using Equation 3-7.

$$d_{SSN} = f(k_1'^b, k_2'^b, k_3'^b, k_1'^s, k_2'^s, k_3'^s, h, L, D, W), \tag{3-7}$$

where

$k_s$ = the stiffness of geomaterials (in MN/m);
$W$ = weight (in kN), including the total force due to the drum weight, $F_D$, and the peak eccentric vertical force, $F_{ev}$;
$L$ = the drum length (in m);
$D$ = the drum diameter (in m);
$h$ = the thickness of the base (in mm); and
$k_i'^b$ and $k_i'^s$ = nonlinear parameters of the base and subgrade, respectively.

The composite stiffness of compacted geomaterials in two-layer system, $k_s$, can be predicted using the following GP equation:

$$k_s = C_1 k_1'^s + C_2 h k_2'^b + L k_1'^s e^{k_2'^s}(C_3 + C_4 k_3'^s) + C_5 h k_2'^b e^{k_2'^s} + \frac{C_6 h \psi k_2'^b}{k_1'^b}, \tag{3-8}$$

where

$C_1 = 0.0252$,
$C_2 = 0.135$,
$C_3 = 0.0339$,
$C_4 = 0.00616$,
$C_5 = -0.0143$,
$C_6 = -0.0399$, and
$\psi$ = an operating index, as defined in Equation 3-5.

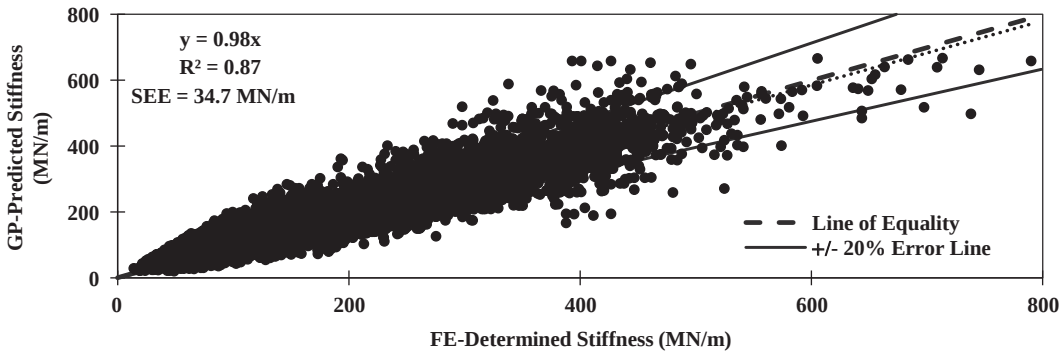


***Figure 3-10. Comparison of GP-predicted stiffness of layered geomaterials to FE-determined stiffness obtained from stationary drums with different operating features.***

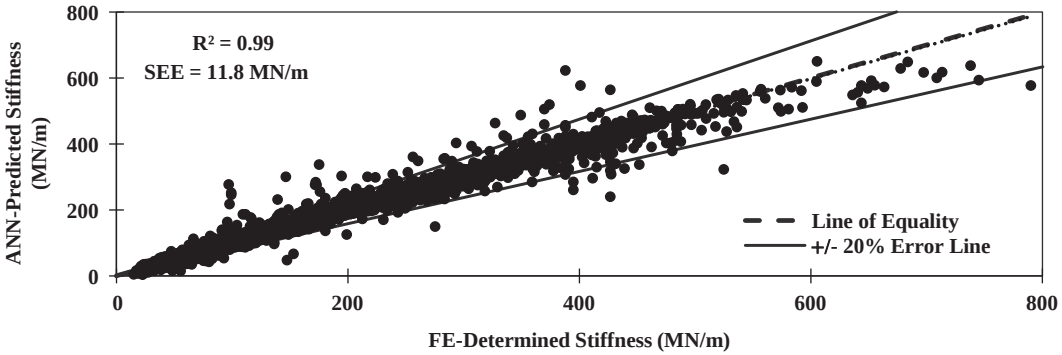


***Figure 3-11. Comparison of ANN-predicted stiffness of layered geomaterials to FE-determined stiffness obtained from stationary drums with different operating features.***

For the prediction of stiffness for single-layer geosystems, Equation 3.8 reduces to:

$$k_s = C_1 k_1'^s + L k_1'^s e^{k_2'^s} (C_3 + C_4 k_3'^s), \tag{3-9}$$

where coefficients $C_1$, $C_3$, and $C_4$ are defined as shown in Equation 3-8.

Figure 3-10 compares the GP-predicted composite stiffness values to the stiffness values as determined from the FE responses. Both single-layer and two-layer systems are evaluated and included in the figure. The figure shows that the proposed GP method can predict the stiffness favorably, as judged by the number of cases falling inside the 20% error lines. The best regression line passing through the results shows an $R^2$ value of 0.87 and a SEE value of 34.7 MN/m.

As an alternative option, an ANN-based method also was developed with the purpose of improving the prediction of stiffness. Figure 3-11 compares the ANN-predicted composite stiffness for both single-layer and two-layer systems with the stiffness determined from the SSN FE models. The ANN method yielded a more favorable prediction of stiffness than the GP method, as shown by the higher $R^2$ value (0.99) and the lower SEE value (11.8 MN/m). Thus, the ANN method proves to be an efficient tool that can reproduce the results provided by FE models in an expedited manner without conceding accuracy, making it suitable for implementation in field operations.

CHAPTER 4

# Field Evaluation

## Introduction

Initial field tests for this research took place at two locations: Cleburne, Texas, and the 9.5 km (6 mi.) MnROAD test track pavement facility located 65 km (40 mi.) northwest of Minneapolis–Saint Paul, Minnesota (Figure 4-1). At the Texas location, testing involved a clayey subgrade on top of an existing embankment. The results of the field tests in Texas are discussed in Chapter 5. Testing at the MnROAD facility involved sandy and clayey subgrades and an unbound aggregate base on top of a subgrade. This chapter summarizes the findings from the field tests performed at the MnROAD facility, where spot tests with NDTs and proof mapping with IC were conducted to evaluate the outcomes of the numerical models. Table 4-1 contains a summary of the activities at each MnROAD site. Each activity is briefly explained.

**Test Strip.** Tests were carried out in cells 185, 186, 188, and 189 on the south side of the MnROAD low-volume road loop, shown in Figure 4-2. (Cell 187 was not constructed or tested). The pavement structures of the four test sections are shown in Figure 4-3. All sections consisted of a 300 mm (12 in.) base over a 90 mm (3.5 in.) intermediate layer of granular material on top of subgrade. Coarse and fine recycled concrete aggregates (RCA) were used for the base layer in cells 185 and 186, respectively. Limestone and recycled aggregate Class 6 were used for the base layers in cells 188 and 189, respectively. The existing subgrade was tens of feet of an imported sandy material for cells 185 and 186, whereas a natural clayey subgrade was used for cells 188 and 189. Geophones were installed at 150 mm (6 in.) and 600 mm (24 in.) within the subgrade and at 150 mm (6 in.) within the base layer, and pressure cells were placed at 300 mm (12 in.) within the base and subgrade, as shown in Figure 4-3. Actual identification of a test strip and preparations for ground instrumentation are shown in Figure 4-4. Instrumentation of the test strip is shown in Figure 4-5.

**Setup of GPS.** The Minnesota DOT's base station was used. Data acquisition of the UTEP system was synchronized with the roller's Controller Area Network (CAN) system.

**Setup of IC Roller.** UTEP personnel, in cooperation with Caterpillar personnel, prepared the setup of the IC roller. A smooth drum IC vibratory soil compactor with an operating weight of 157 kN (35 kip), shown in Figure 4-6, was used for mapping the test sections after compaction. The specifications of the IC roller are shown in Table 4-2. Sensors were mounted on the IC roller to collect vibration data. The IC roller was checked for proper data collection and operating settings, including roller speed, vibration frequency, and amplitude. Instrumentation of roller at the test site is shown in Figure 4-6.

**Construction.** The UTEP team observed the construction processes but was not involved in or interfered with the operation.

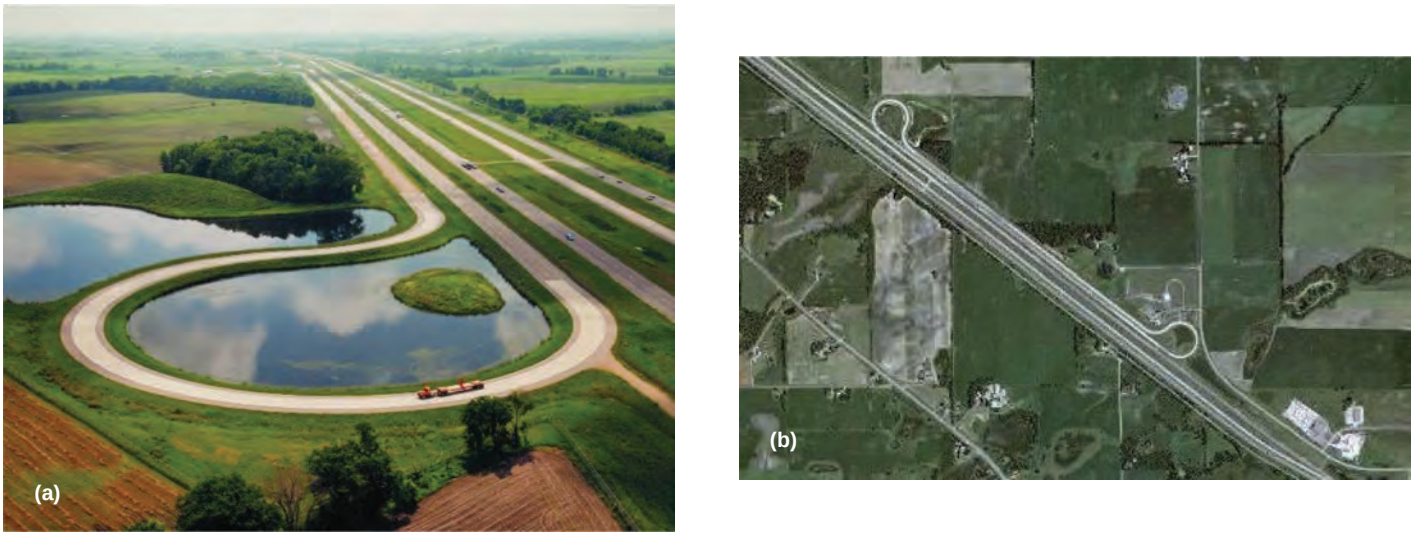


***Figure 4-1. MnROAD test track: (a) Aerial view of MnROAD low-volume road and (b) satellite view of low-volume road, mainline, and bypass I-94.***

**Table 4-1. Test activity and schedule (MnROAD facility).**

| Dates | Tasks | Activities |
|---|---|---|
| July 17–19, 2017 | Coordination and Initial Setup | Construct and compact subgrade layer.<br>Obtain representative sample of subgrade material (Minnesota DOT).<br>Coordinate with IC roller operator regarding how to collect, record, save, download and transfer data for this project (CAT and UTEP). |
| July 20–25, 2017 | Subgrade | Mark the test section and test spots in each cell (UTEP).<br>Arrange for field instrumentation (MnROAD, UTEP).<br>Obtain GPS coordinates for spot test locations (UTEP).<br>Install geophones at a depth of 150 mm (6 in.) and 600 mm (24 in.) from the top of subgrade, and pressure cells at a depth of 300 mm (12 in.) from the top of subgrade (UTEP, MnROAD).<br>Map subgrade with IC roller (CAT and UTEP).<br>Carry out in-situ testing with modulus-based devices and NDG to establish moduli (UTEP, Minnesota DOT). |
| August 1–2, 2017 | Unbounded Aggregate Base (UAB) | Construct and compact base prior to testing.<br>Obtain representative sample from base prior to testing (Minnesota DOT).<br>Install geophone at a depth of 150 mm (6 in.) within the base, and pressure cell at a depth of 300 mm (24 in.) from the top of base (UTEP, MnROAD).<br>Map Aggregate Base with IC roller (CAT and UTEP).<br>Carry out in-situ testing with modulus-based devices and NDG to establish moduli (UTEP, Minnesota DOT). |

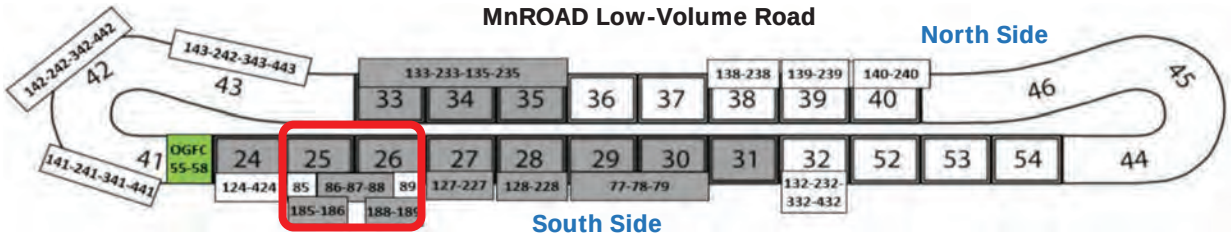


*Figure 4-2. Location of cells used for test sections in MnROAD low-volume road.*

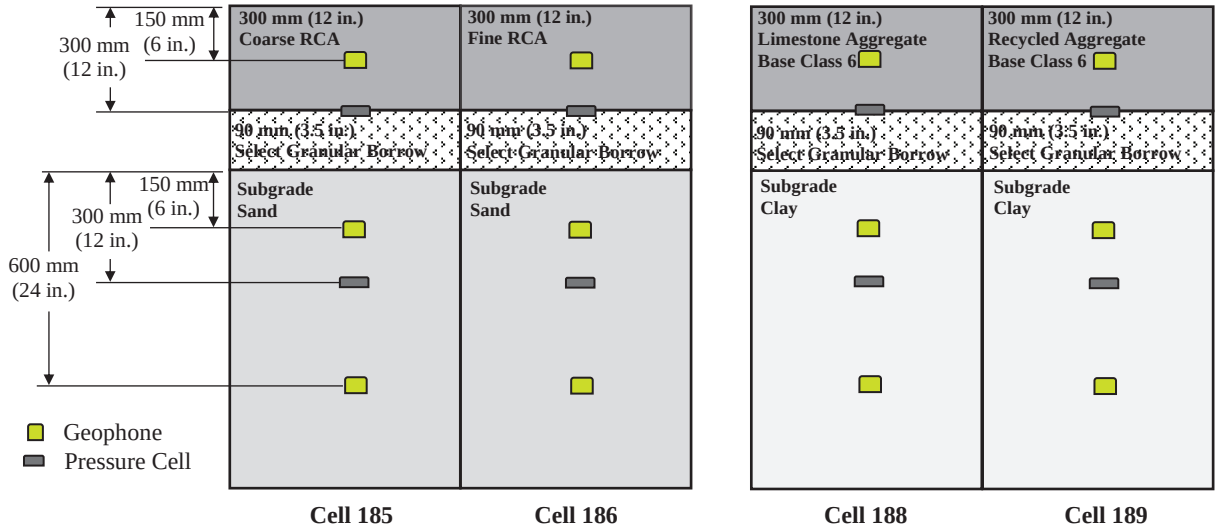


Figure is not to scale.

*Figure 4-3. Pavement structure of test cells and installation of ground sensors.*


*Figure 4-4. The MnROAD test strip: (a) a view of the test strip, and (b) and (c) UTEP and MnROAD personnel preparations for embedding ground instrumentation.*


***Figure 4-5. Installation of ground sensors: (a) preparation of ground sensors, (b) wiring of sensors by UTEP and MnROAD personnel, (c) embedment of geophone, (d) and (e) geophones within geomaterial, and (f) pressure cell within geomaterial.***

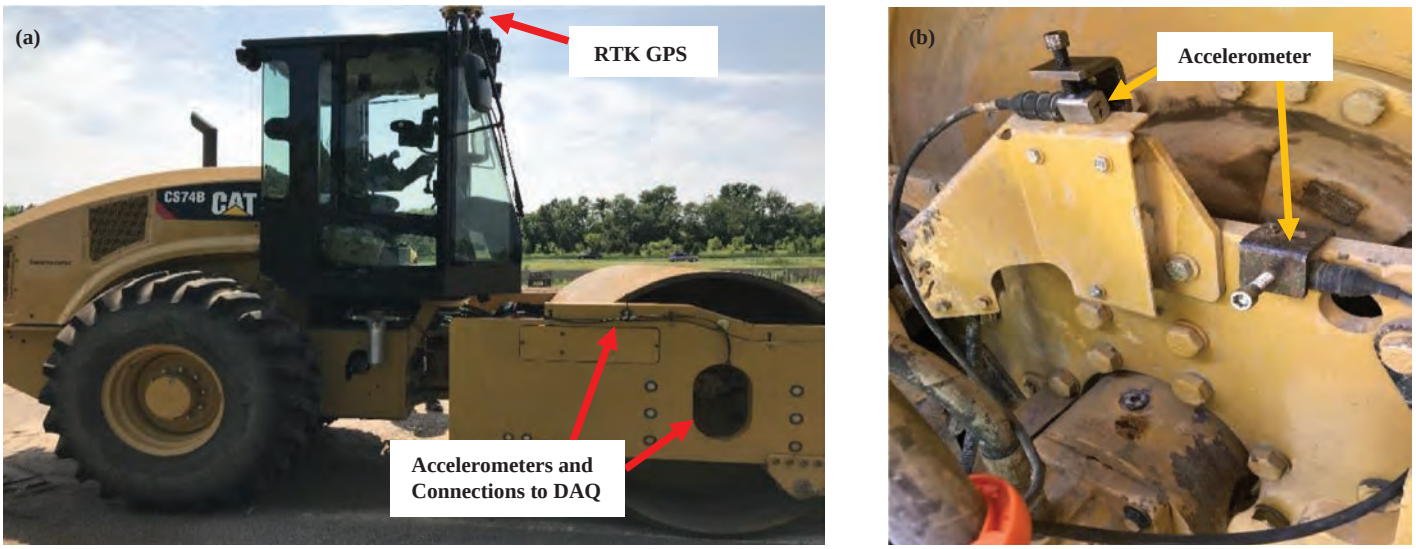


***Figure 4-6. Field site instrumentation of roller compactor: (a) RTK GPS and wiring of accelerometers to data acquisition (DAQ) system and (b) installation of both accelerometers to measure vertical and horizontal vibration on roller compactor drum frame.***

**Proof Mapping.** Minnesota DOT and UTEP personnel coordinated to perform proof mapping of test sections after compaction of the section was finished. Four forward passes were performed to cover the test section width. Embedded ground sensor measurements were monitored and recorded by UTEP personnel as the roller passed along the line passing over the embedded sensors. UTEP researchers monitored the adequate accelerometer's measurements during each of the roller passes, as evidenced in Figure 4-7.

**Post-Mapping Tests.** UTEP and the Minnesota DOT personnel carried out spot tests at 36 points for correlation testing, separated at a spacing of 7.5 m (25 ft.) longitudinally, and 2.1 m (7 ft.) in the transverse direction, as schematically shown in Figure 4-8. The spacing

**Table 4-2. Specifications of IC roller used in test sections.**

| | | |
|---|---|---|
| **Mass/Weights** | | |
| Operating Weight | 157 kN | 35,260 lb. |
| Drum and Frame Weight | 116 kN | 26,110 lb. |
| Mass of Drum | 5,153 kg | 353.1 lb. × $s^2$/ft. |
| Eccentric Mass, $m_0e_0$ | 5.06 kg·m | 1.137 lb. × $s^2$ |
| **Operating Specifications** | | |
| Compaction Width | 2.1 m | 84 in. |
| Static Linear Load | 48.8 kN/m | 278.7 lb./in. |
| **Dimensions** | | |
| Drum Diameter | 1.5 m | 60.4 in. |
| Drum Width | 2.1 m | 84 in. |
| **Vibratory System** | | |
| Centrifugal Force – Maximum | 332 kN | 74,600 lb. |
| Centrifugal Force – Minimum | 166 kN | 37,300 lb. |
| Nominal Amplitude – High | 2.1 mm | 0.083 in. |
| Nominal Amplitude – Low | 1.0 mm | 0.039 in. |
| Vibratory Frequency – Standard | 28 Hz (1,680 vpm) | |

*Figure 4-7. UTEP personnel monitoring proof-mapping process.*

of spot-test measurements was modified for Cell 185 and Cell 186 to accommodate enough representative measurements. The NDT devices used for those tests included:

- Nuclear Density Gauge (NDG), used by the Minnesota DOT;
- Dynamic cone penetrometer (DCP), used by the UTEP and the Minnesota DOT;
- Light weight deflectometer (LWD), used by the UTEP and the Minnesota DOT;
- Falling weight deflectometer (FWD), used by the Minnesota DOT; and
- Moisture sampling for validation of NDG data, used by the UTEP.

**Laboratory Testing.** Samples of geomaterials were collected at the site to determine the variations in moisture content in the laboratory and to conduct laboratory resilient modulus tests at several moisture contents, as well as index tests (gradation and Atterberg limits) and moisture-density tests. The purpose of the laboratory evaluation was to determine the correlation between the extracted mechanical properties of compacted geomaterials under field conditions with those estimated under laboratory conditions.

## Laboratory Test Results

Table 4-3 summarizes the Atterberg limits and Unified Soil Classification System (USCS) classification of the two subgrades. Figure 4-9(a) shows the resilient modulus test results for the sandy subgrade material, and Figure 4-9(b) shows the results for the clayey subgrade material at OMC.

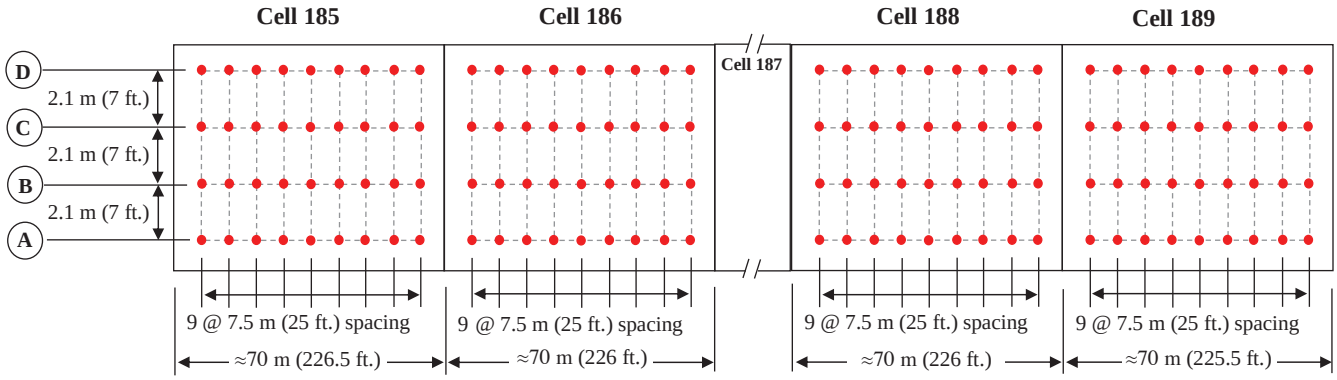


*Figure 4-8. Schematic of the proposed test layout.*

**Table 4-3. Index properties of MnROAD subgrade materials.**

| Cells | | Cell 185 and Cell 186 | Cell 188 and Cell 189 |
|---|---|---|---|
| Material Type | | Sandy Subgrade | Clayey Subgrade |
| USCS Classification | | SP-SM | CL |
| Gradation (%) | Gravel | 30 | 9 |
| | Coarse Sand | 39 | 32 |
| | Fine Sand | 20 | 51 |
| | Fines | 11 | 8 |
| Atterberg Limits (AASHTO T-89 and T-90) | Liquid Limit (LL) | Nonplastic | 31 |
| | Plastic Limit (PL) | | 17 |
| | Plasticity Index (PI) | | 14 |
| Moisture/Density (AASHTO T-99) | Optimum Moisture Content (OMC) | 6.5% | 14.4% |
| | Maximum Dry Density (MDD) | 2,342 kg/m$^3$ (146.2 pcf) | 1,897 kg/m$^3$ (118.4 pcf) |

Table 4-4 summarizes the measured parameters from the resilient modulus tests performed as per AASHTO T-307 for both types of subgrade. Detailed laboratory results are available in Appendix F.

Samples of four distinct base materials, designated as coarse reclaimed concrete aggregate (RCA), fine RCA, limestone aggregate Class 6, and reclaimed asphalt and concrete aggregate (RAP+RCA) Class 6, also were retrieved from the MnROAD facility, from cells 185, 186, 188, and 189, respectively. Table 4-5 summarizes the optimum moisture content (OMC) and maximum dry density (MDD) of the four base materials following AASHTO T 180. Resilient modulus tests also were carried out on duplicate specimens at five different moisture contents. Detailed laboratory results are included in Appendix F. Table 4-6 summarizes the resilient modulus tests of the four different base materials at OMC. For all the materials, the highest resilient modulus occurred at dry conditions (i.e., at moisture contents below the OMC). Resilient moduli decreased gradually as moisture increased.

## Field Testing Results

A data reduction process was implemented to obtain the acceleration time histories necessary for the calculation of the roller-based stiffness. This data reduction process started with the conversion of the accelerometer time-domain voltage output into time-domain acceleration

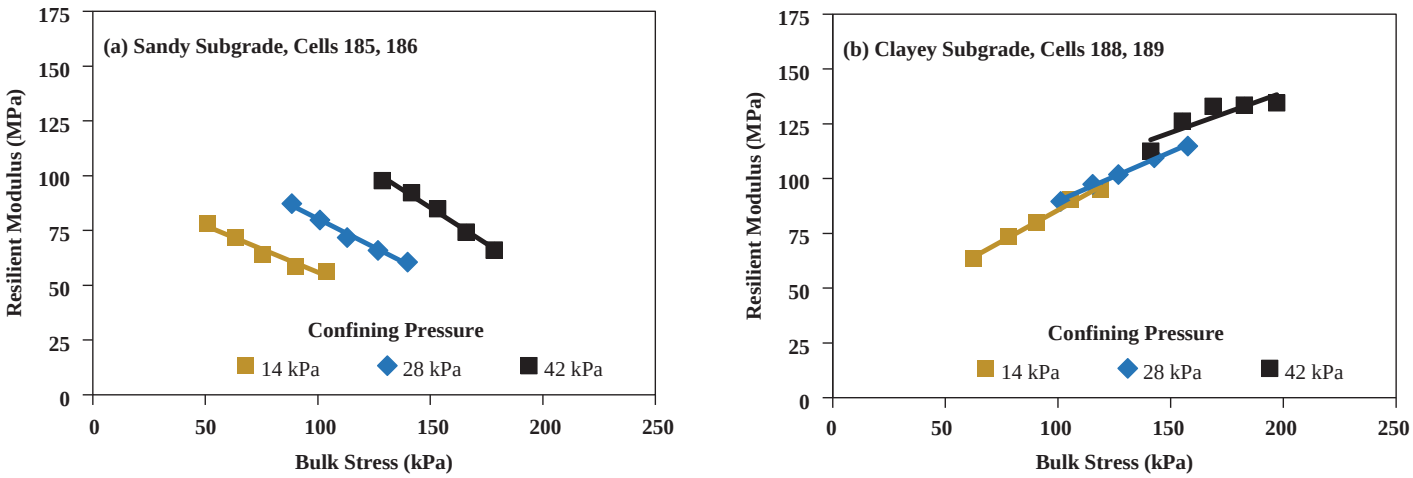


*Figure 4-9. Resilient modulus test results for subgrade materials at OMC.*

**Table 4-4. Resilient modulus results at OMC for subgrade materials.**

| Cells | Moisture Content % | Dry Density kg/m³ | Dry Density pcf | Nonlinear Parameters $k'_1$ | $k'_2$ | $k'_3$ | Representative Resilient Modulus (MR) MPa | ksi |
|---|---|---|---|---|---|---|---|---|
| 185, 186 | 6.5 | 2,342 | 146.2 | 352 | 1.41 | -0.42 | 77.9 | 11.3 |
| 188, 189 | 14.1 | 1,897 | 118.4 | 649 | 0.62 | -2.56 | 59.3 | 8.6 |

Note: $\sigma_c$ = 85.5 kPa (12.4 psi) and $\tau_{oct}$ = 20.7 kPa (3 psi) for subgrade, as recommended by NCHRP Project 1-28A.

measurements. To capture the eccentric mass position and acceleration of the roller precisely, data was sampled at a frequency of 10 kHz using blocks with 6,000 data points, for a resolution of 1.67 Hz in the frequency domain. For analysis purposes, such as the calculation of CMV, the acquired acceleration time histories were decimated and filtered to blocks of 600 data points acquired at a sampling frequency of 1 kHz for a spatial resolution of roller measurements of 0.5 m (1.7 ft.) when the roller speed was 3.2 kph (2 mph).

## Comparison of Data Acquisition Systems for ICMVs

Figure 4-10 compares the raw CMV data as collected by the Controller Area Network (CAN) for the communication between the roller's data acquisition components and the UTEP data acquisition system as measured during proof mapping on top of sandy and clayey subgrades, and on top of base on top of the shown subgrades. CMVs from the CAN and the UTEP data acquisition systems were almost identical. The sandy subgrade exhibited higher CMVs than did the clayey subgrade. Higher CMVs observed at the beginning and ending of the roller operation were attributed to the roller's proof-mapping speed and/or to brief periods (during acceleration or deceleration) when the roller's frequency and speed differed from the preset

**Table 4-5. Index properties of MnROAD base materials.**

| Cells | | 185 | 186 | 188 | 189 |
|---|---|---|---|---|---|
| Material Type | | Coarse RCA | Fine RCA | Limestone Aggregate Class 6 | RAP+RCA, Class 6 |
| USCS Classification | | GW | SP | GW | GP |
| Moisture/Density (AASHTO T 180) | Optimum Moisture Content (OMC) | 10.5% | 10.9% | 6.6% | 10.5% |
| | Maximum Dry Density (MDD) | 1,962 kg/m³ (122.5 pcf) | 1,922 kg/m³ (120.0 pcf) | 2,284 kg/m³ (142.6 pcf) | 1,969 kg/m³ (122.9 pcf) |

**Table 4-6. Resilient modulus results at OMC for base materials.**

| Cells | Moisture Content % | Dry Density kg/m³ | Dry Density pcf | Nonlinear Parameters $k'_1$ | $k'_2$ | $k'_3$ | Representative Resilient Modulus (MR) MPa | ksi |
|---|---|---|---|---|---|---|---|---|
| 185 | 10.5 | 1,962 | 122.5 | 511 | 0.82 | -0.06 | 128.7 | 18.7 |
| 186 | 10.9 | 1,922 | 120.0 | 484 | 0.86 | -0.06 | 126.2 | 18.3 |
| 188 | 6.6 | 2,284 | 142.6 | 500 | 0.60 | -0.05 | 97.9 | 14.2 |
| 189 | 10.5 | 1,969 | 122.9 | 408 | 0.96 | -0.12 | 117.2 | 17.0 |

Note: $\sigma_c$ = 214 kPa (31 psi) and $\tau_{oct}$ = 51.7 kPa (7.5 psi) for subgrade, as recommended by NCHRP Project 1-28A.

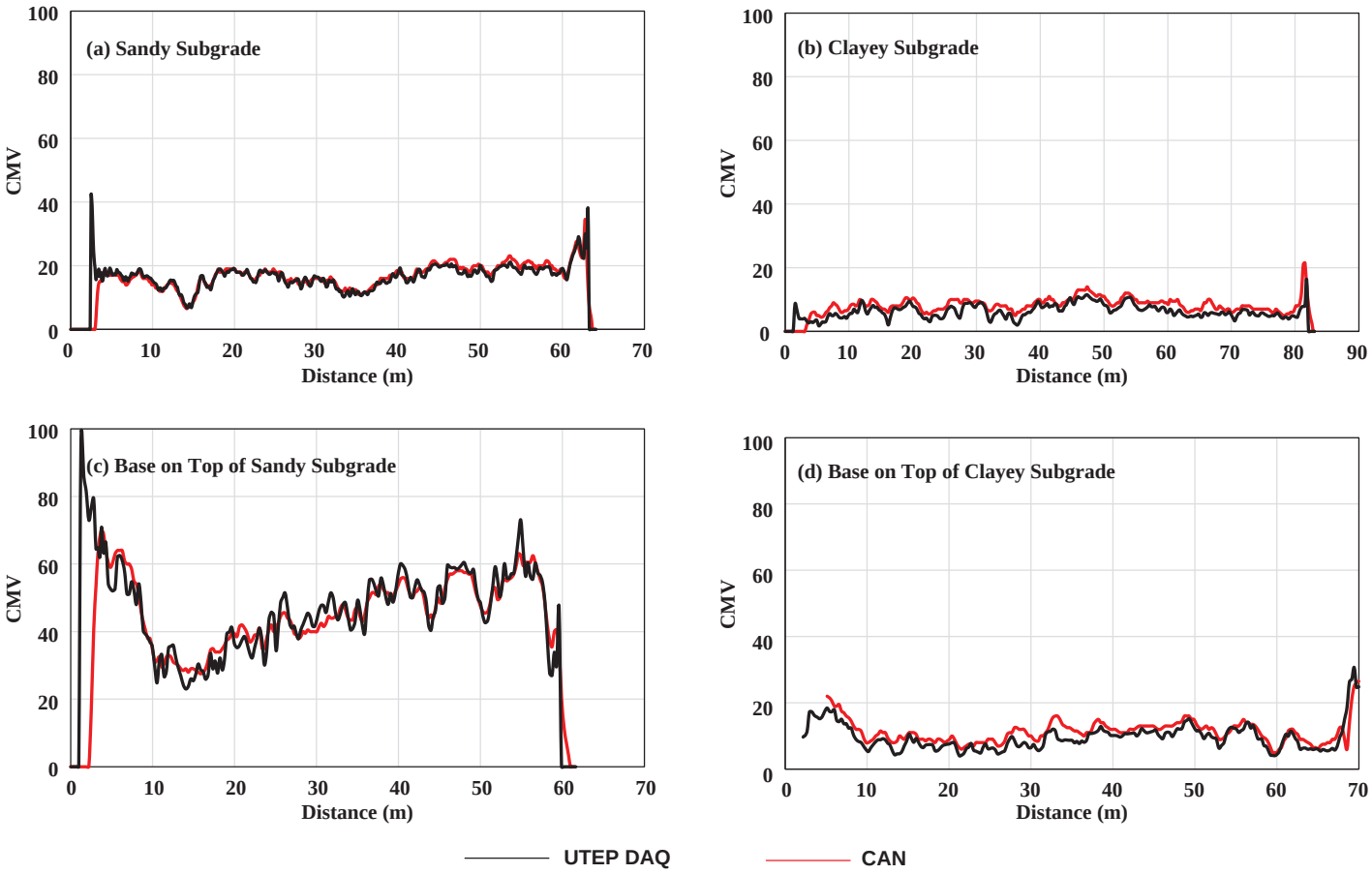


***Figure 4-10. CMVs collected by the UTEP DAQ system and the CAN while proof mapping on top of subgrade and base course materials.***

operating speed and frequency. In addition, the CMVs obtained on top of the flexible bases were greater than those obtained on their respective subgrades. Appendix F (available in the downloadable "Appendices.pdf" file) provides further comparison for all sites.

## Mapping of ICMVs

Because the vibration data is collected at a discrete point at the edge of the roller drum during IC proof mapping, many data analysis programs incorporate various processes to extrapolate that measured ICMV data point over the width of the roller before generating the color-coded map. These extrapolation techniques include Inverse Distance Weighting (IDW) and spline and ordinary kriging (Mazari et al. 2014). These methods enhance the "richness" of the data visualization by smoothing the color-coded contours and filling in gaps in the information; however, using these techniques may affect the "fidelity" of the ICMV data. Kriging (an advanced geostatistical procedure that generates an estimated surface from a set of scattered points) does not pass through any of the measured points, and its use for mapping purposes causes interpolated values to be higher or lower than real values. Spline interpolation does not work well when sample points have extreme differences in magnitude and are close together. It is also impractical to estimate the exact position of the roller for a reported coordinate based on its size, given that (1) the roller must move some distance to collect adequate data to estimate an ICMV, and (2) the accuracy of the reporting GPS devices and satellite coverage have their own inherent uncertainties. For this reason, the research team elected to establish a grid made up of *sublots*.

Each sublot was equal in width to the width of the roller, and the length was equal to the minimum length of the compacted section that was deemed practical to rework, as set by the judgment and discretion of the engineer. In the study performed at MnROAD, a length of 7.5 m (25 ft.) was used. For mapping ICMV measurements, rectangular sublots around feature points defined by the geo-referenced spot test locations were established following the proposed test layout, as illustrated in Figure 4-9. All actual ICMV measurements with the accelerometer falling inside each sublot were averaged to obtain a representative ICMV.

Figure 4-11 shows the roller line as it passes through the superimposed sublots, as well as the number of ICMV measurement points per sublot for subgrade cells. ICMVs found within these sublots were averaged to obtain a representative ICMV for that sublot. This approach for discretizing the continuous collected CMV data facilitated the comparison of the geospatial data obtained with the IC-instrumented roller with supplemental NDT spot-test measurements.

Figure 4-12 shows the sublots' averaged CMVs in a color-coded map as obtained after processing the data acquired by the UTEP data acquisition (DAQ) system on top of the Cell 189 clayey subgrade. The results from the other cells can be found in Appendix F.

The team used color coding and adopted criteria for mapping ICMVs that assumed that a variation of up to 25% was considered acceptable (see Table 4-7). Sublots with a representative ICMV of less than 75% of the average ICMV of all sublots were considered *less stiff* and were shown in red. Sublots with a representative ICMV greater than the average ICMV of the lot were considered *relatively stiffer* and were shown in green. Sublots with a representative ICMV of 75% of the average ICMV of the lot were not judged to have provided an *inadequate* modulus; rather, the modulus for these sublots was simply considered less than the modulus for other areas of the lot. Thus, if the representative ICMVs of all sublots were within ±25% of the average ICMV of the lot, the color-coded map might not contain any red sublots.

COV color-coded maps could be used to determine whether the representative ICMVs can be trusted, a necessary judgment because—reflecting either construction-related or equipment-related issues—any given sublot will not be uniform. Soil characteristics and heterogeneity, as well as the underlying soil, can significantly affect the ICMVs. The higher the variability of the measurements, the less reliable they will be. To assess the variability of the IC measurements and thus address the uniformity of the test section, the research team generated maps representing the COV of the averaged ICMVs for each sublot. Before generating the maps, quality control on the ICMV datasets was performed to remove ICMVs that occurred in sublots that exhibited high variability (COV > 50%) and those calculated at operating frequencies beyond ±5 Hz of the roller nominal operating frequency, which usually leads to erroneous ICMVs.

Figure 4-13 shows a representative map of the COV of CMVs for a clayey subgrade section (Cell 189). Table 4-8 shows the color-coded criteria for mapping the COV.

## Mapping of Displacement

Figure 4-14 shows the color-coded surface displacement map of the Cell 189 clayey subgrade obtained from the measured acceleration (which is explained in detail in Appendix H). This case corresponds to the mapping of surface displacements on top of subgrade. The color-coding criteria from Table 4-7 were applied to color the sublots. Higher surface displacements were observed in sublots that were identified as less stiff.

## Mapping of Total Applied Force

Mapping of the total applied force also was performed as part of the post-processing of the acquired acceleration time histories. The total applied force consists of the machine weight,

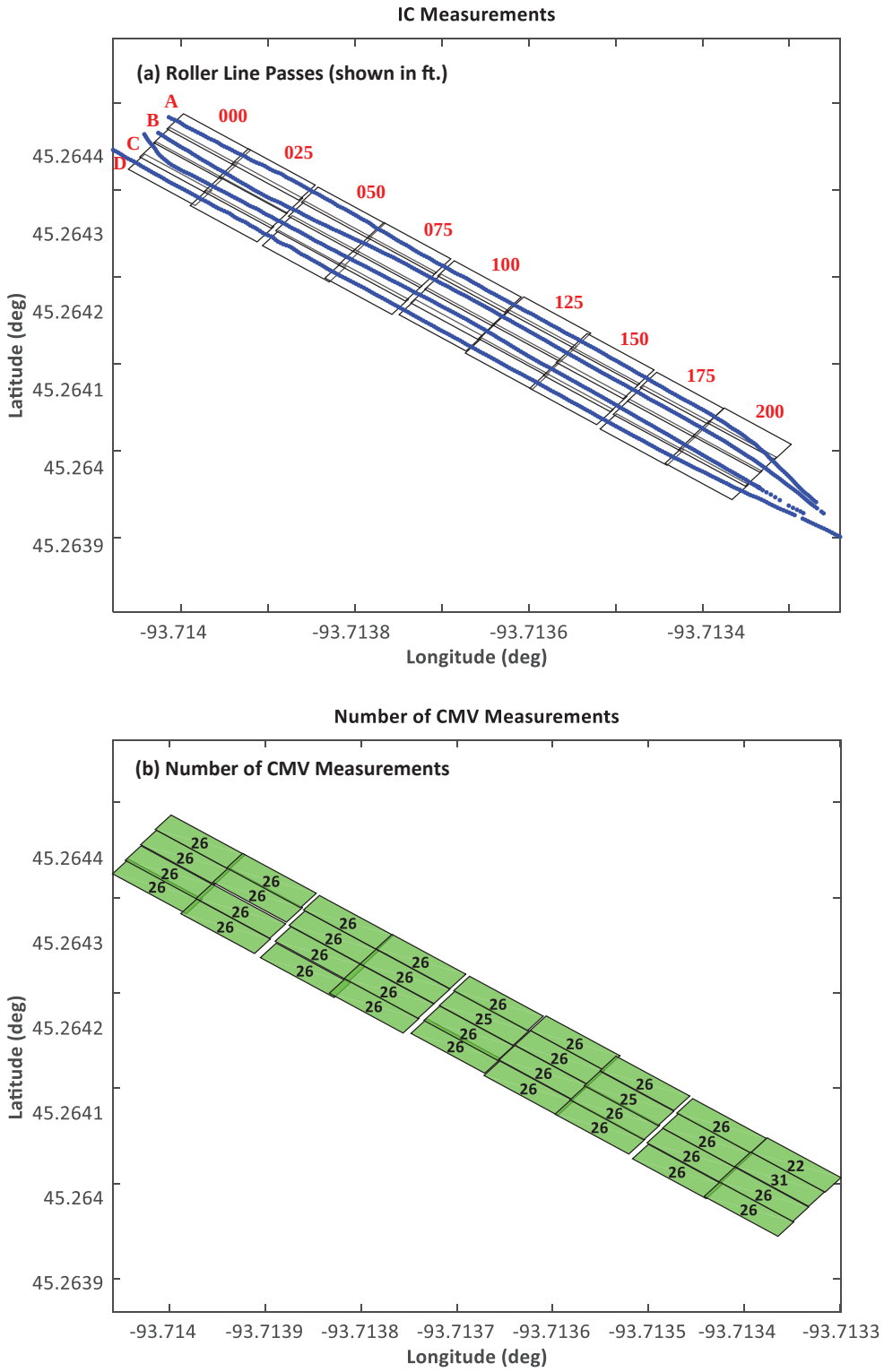


***Figure 4-11. Mapped sublots showing (a) roller line passes and (b) number of CMV measurements.***

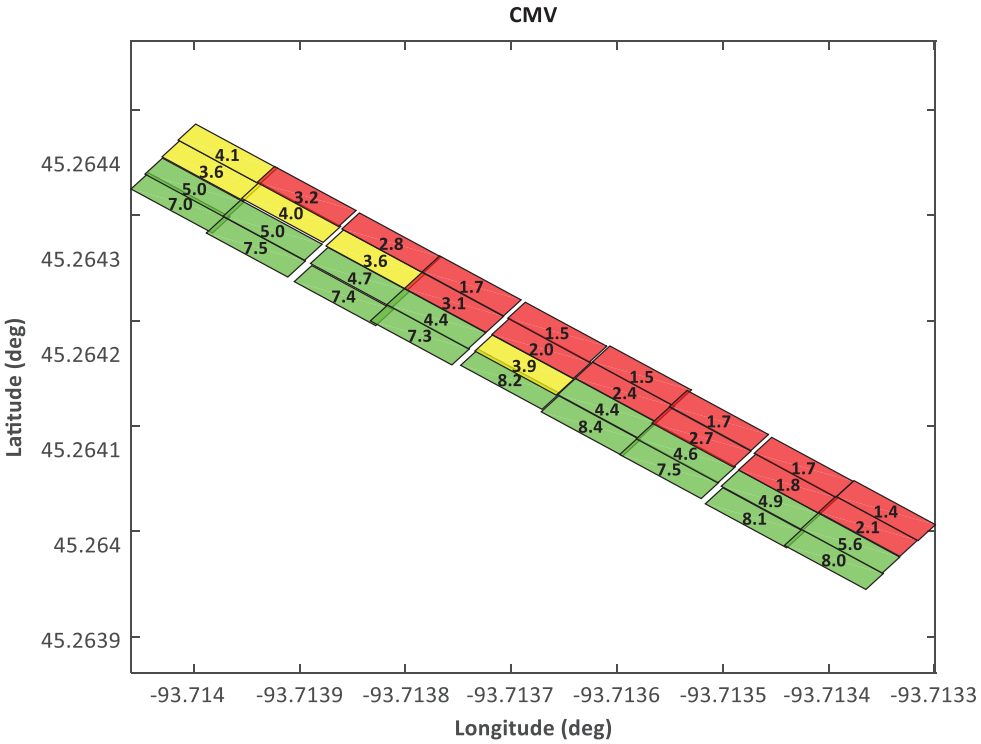


Red = < 75% Mean; Yellow = 75%–100% Mean; Green = > Mean.

***Figure 4-12. Mapped sublots showing color-coded CMV measurements.***

the eccentric force, and the drum and frame inertia. The drum and frame weight, mass-eccentricity, and phase lag are parameters listed among the operating features of the roller used at the site, and are provided in Table 4-2. To calculate the applied force, the eccentric force is calculated by measuring the vertical drum acceleration and eccentric mass position while the frame inertia is neglected. The position of the eccentric mass is identified using a third channel of the DAQ system, which is dedicated to recording a pulse signal that indicates the eccentric mass position. The procedure for acquiring these measurements is further explained in Appendix H.

Figure 4-15 shows the color-coded map of the averaged applied force for Cell 189, which was created using the coding criteria defined in Table 4-7. As seen in Figure 4-15, Line 2 exerted relatively higher loads to the pavement.

## Mapping of Stiffness

Using the force and displacement time histories, the force-displacement hysteresis loops can be developed to obtain the roller-measured stiffness. Figures 4-16 and 4-17 show the

**Table 4-7. Criteria for color-coded maps of measurement values.**

| Color | Criterion for CMV, Force, Frequency, Speed and NDT Spot-Test Measurement | Criterion for Displacement |
|---|---|---|
| Red | < 75% Mean | > 133% Mean |
| Yellow | 75%–100% Mean | 100%–133% Mean |
| Green | > Mean | < Mean |

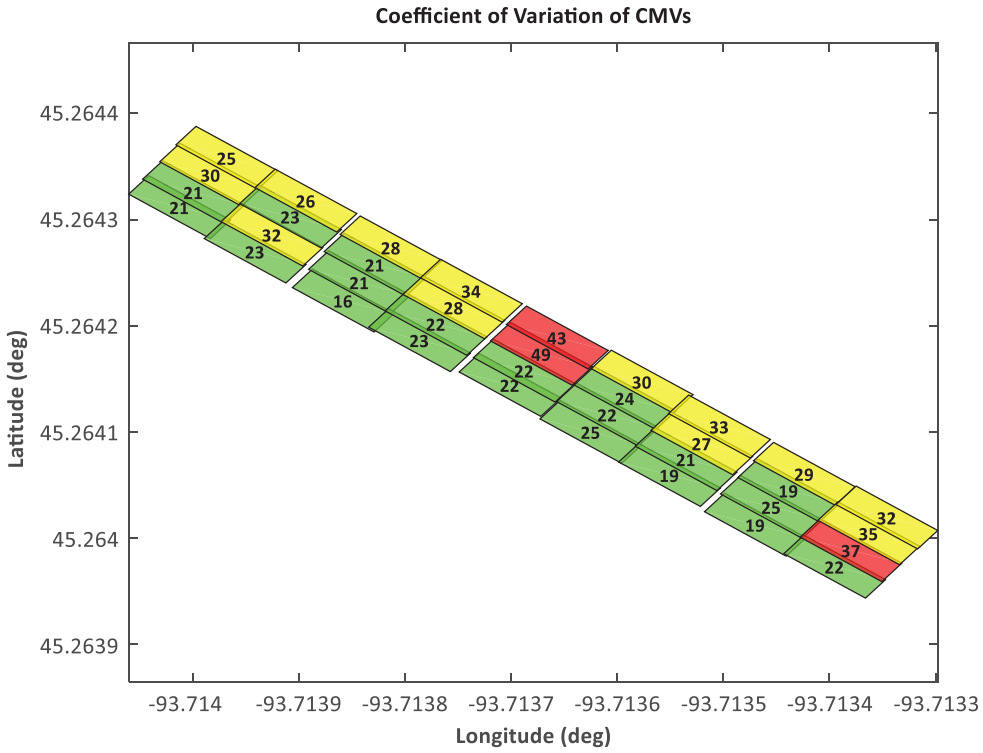


***Figure 4-13. Mapped sublots showing color-coded COVs of CMVs.***

force-displacement hysteresis loops from proof-mapping measurements along one of the line passes on top of the two different subgrade materials and on top of one of the base materials, respectively. Figure 4-16 compares the stiffness between the sandy and clayey subgrade materials.

As expected, higher stiffness values were measured on top of the sandy subgrade. When a 300 mm (12 in.) coarse RCA base material was laid on top of the sandy subgrade, the roller-measured stiffness increased in magnitude when compared to the stiffness obtained on top of the sandy subgrade in the same location, as shown in Figure 4-17.

The calculation of the stiffness was simplified by obtaining the ratio of the complex amplitudes of the force and displacement records in the frequency domain at the roller's operating frequency. This approach, which rapidly and robustly yields a unique stiffness value for each block of data assigned to a GPS coordinate, provides a representative stiffness analogous to the average stiffness calculated from multiple force-displacement hysteresis loops for that block of data points. Integrating this approach into the analysis module that processes the measured proof-mapping datasets acquired by the UTEP DAQ system allowed the generation of maps

**Table 4-8. Criteria for color-coded mapping of COV of IC measurements.**

| Color | Criterion |
|---|---|
| Red | > 35% |
| Yellow | 25%–35% |
| Green | < 25% |

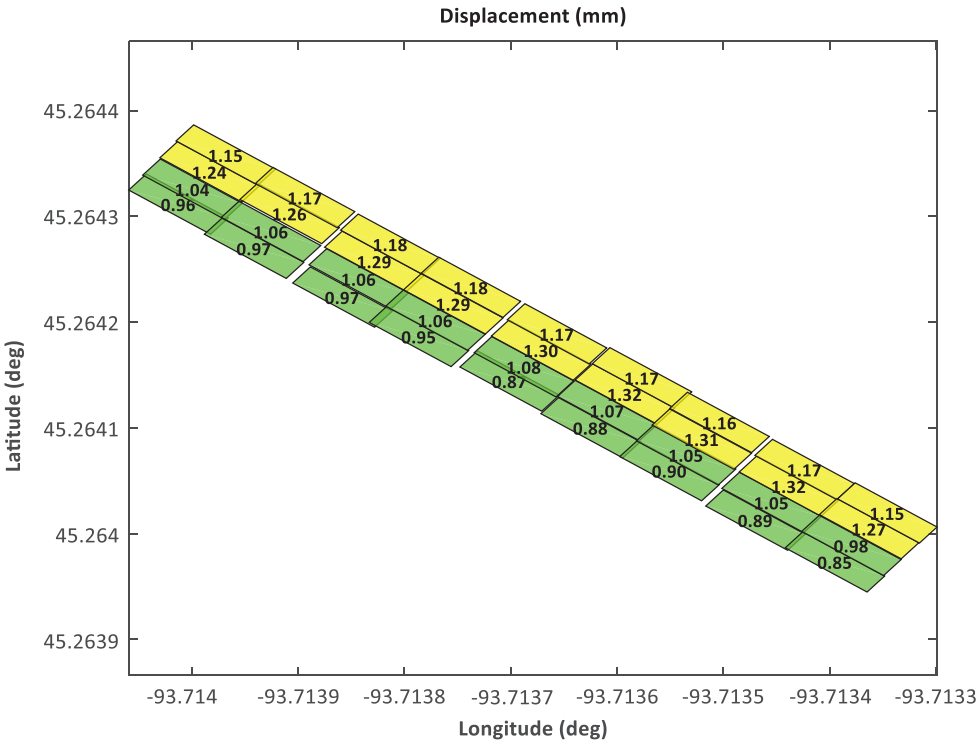


Red = > 133% Mean; Yellow = 100%–133% Mean; Green = < Mean.

***Figure 4-14. Map of surface deflection measurements.***

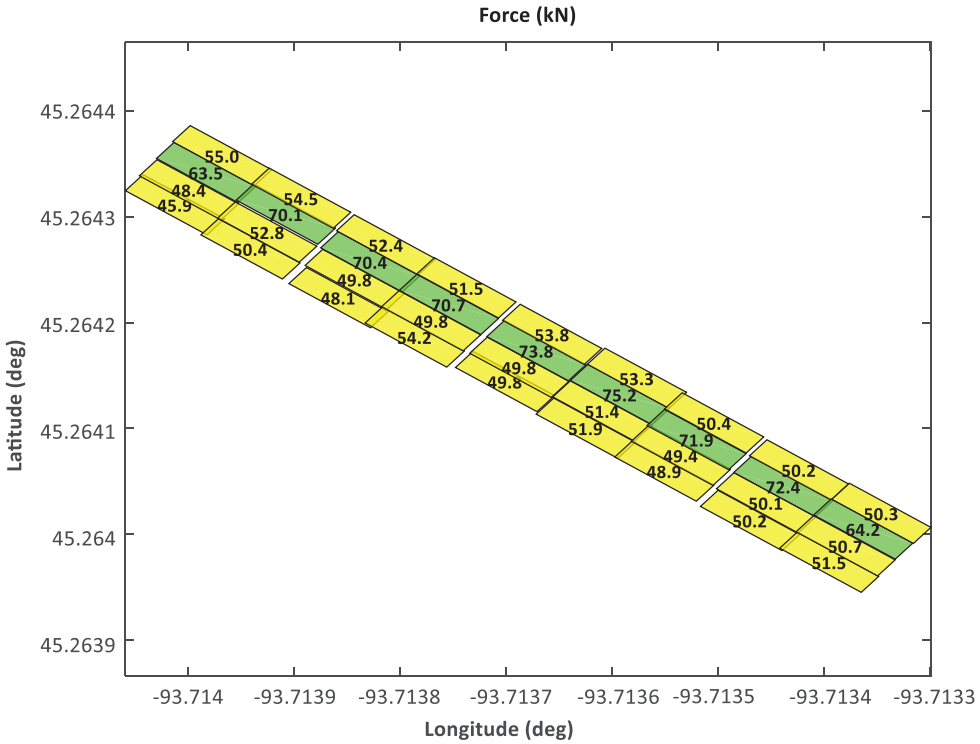


Red = < 75% Mean; Yellow = 75%–100% Mean; Green = > Mean.

***Figure 4-15. Map of average applied forces.***

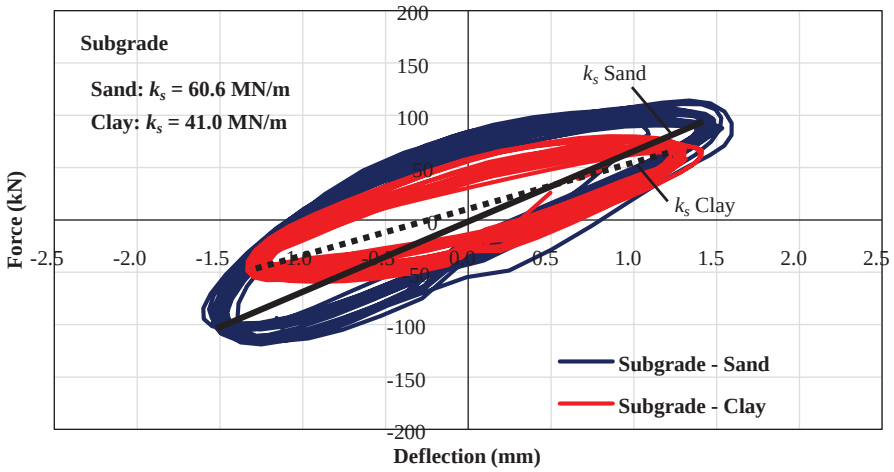


***Figure 4-16. Force-displacement hysteresis loops for the calculation of stiffness, $k_s$, obtained from measurements on sandy subgrade materials (Cell 185) and clayey subgrade materials (Cell 188).***

showing the stiffness of proof-mapped geomaterials using the proposed sublots. Like CMV measurements, stiffness measurements were averaged within each sublot to provide a unique stiffness value that represents an area that is adequate for rework. Figure 4-18 shows the spatial variation in stiffness obtained by the UTEP DAQ system as the roller proof-mapped the site for a clayey subgrade.

## Mapping of NDT Spot-Test Measurements

Supplemental LWD, FWD, and DCP tests were performed along the evaluated test sections. Triplicate LWD tests were carried out every 7.5 m (25 ft.) at every spot corresponding to each sublot, as shown in Figure 4-8. In addition, DCP tests were performed at every spot, and FWD testing was conducted following the roller line passes. Figure 4-19, which maps the average LWD and FWD moduli, as well as the number of DCP blows to penetrate 450 mm (18 in.),

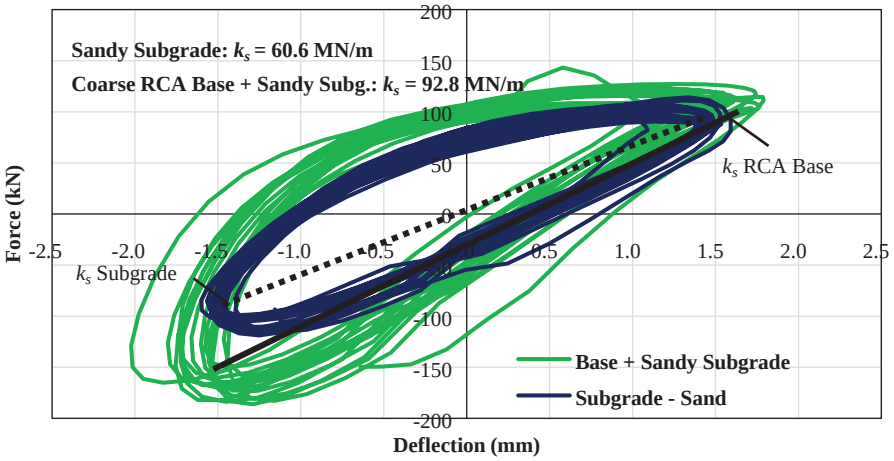


***Figure 4-17. Force-displacement hysteresis loops for the calculation of stiffness, $k_s$, obtained from measurements on sandy subgrade and coarse RCA base material on top of sandy subgrade, both on Cell 185.***

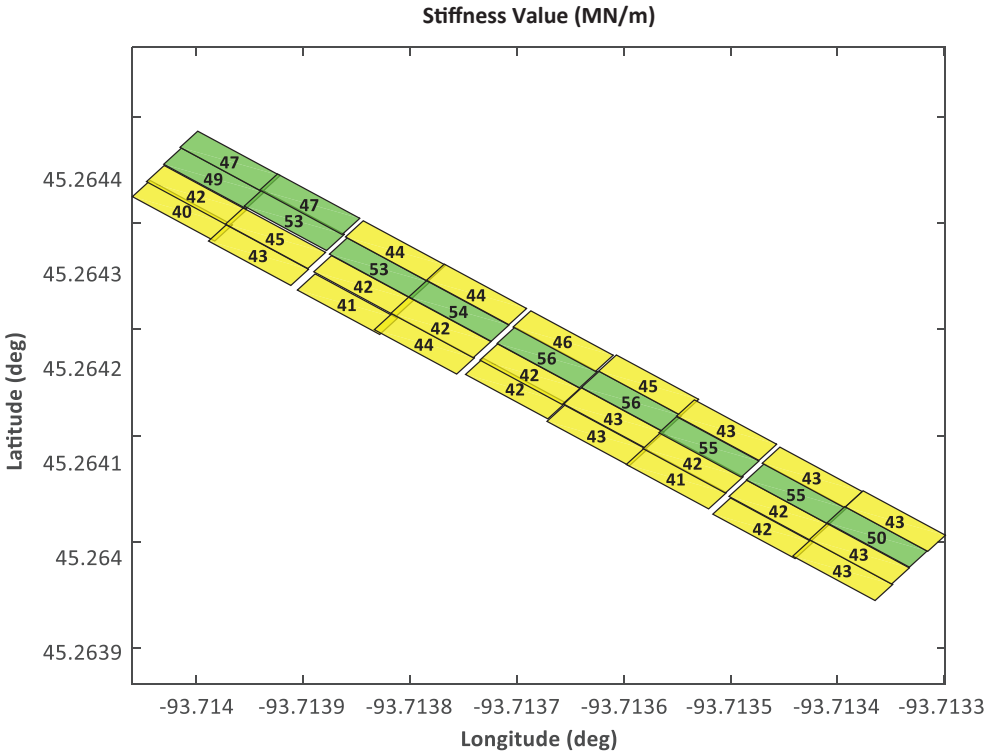


Red < 75% Mean; Yellow = 75%–100% Mean; Green > Mean.

***Figure 4-18. Map of stiffness.***

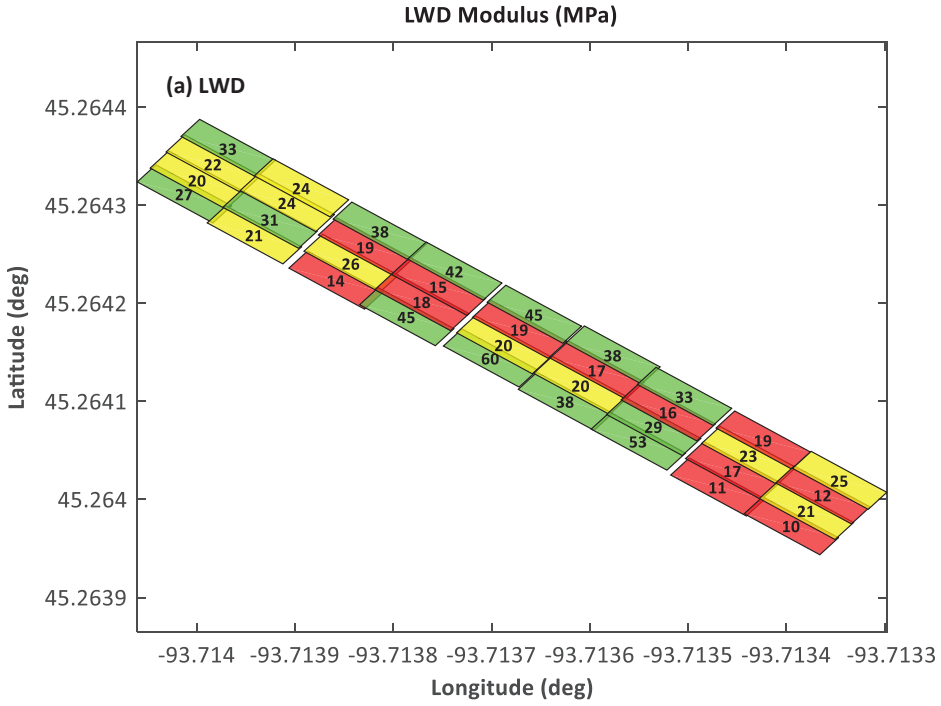


***Figure 4-19. Maps of spot tests: (a) LWD modulus, (b) FWD modulus, and (c) number of blows to penetrate 450 mm (18 in.).***

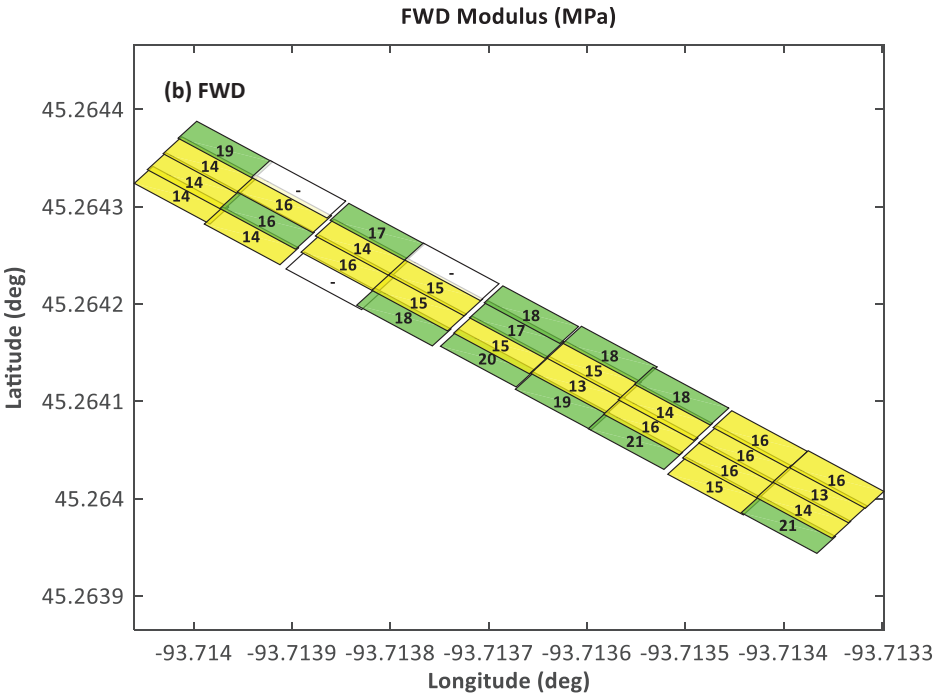


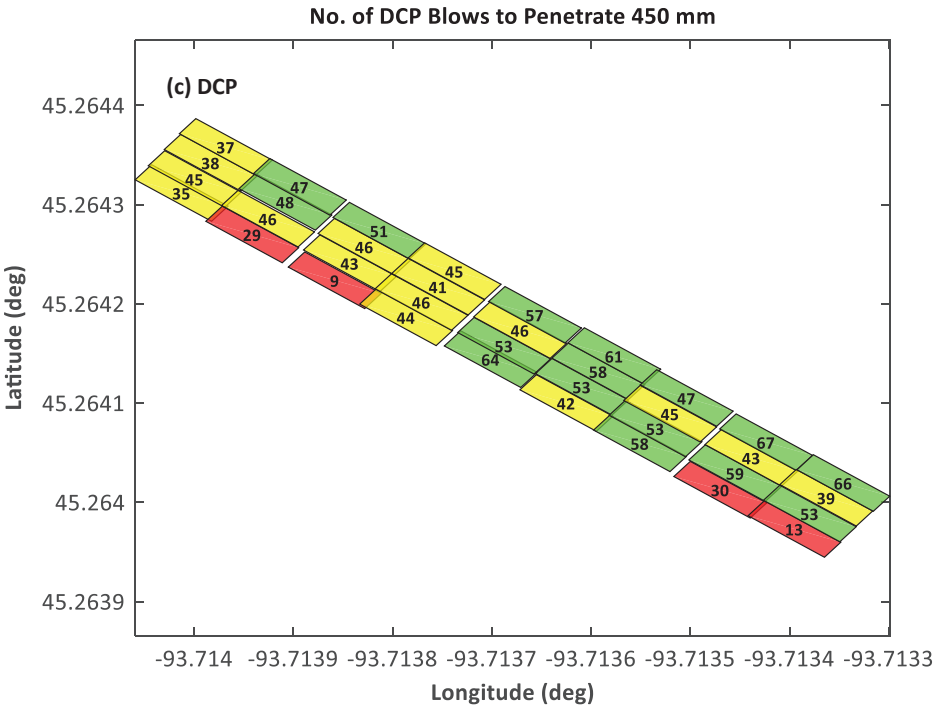


Red = < 75% Mean; Yellow = 75%–100% Mean; Green = > Mean.

***Figure 4-19. (Continued).***

is color coded using the criteria shown in Table 4-7. The FWD moduli were calculated using the same equation for calculating the LWD moduli, by using the deflection directly under the load. Spot-test measurements were collected, and maps were developed with the purpose of evaluating the proposed backcalculation models described in Chapter 5 of this report. These measurements were also used for calibrating the developed forward models. Sublots lacking any measurement were coded as white areas, as shown in Figure 4-19(b).

## Mapping of Additional Roller Operating Parameters

To better assess the variability of the roller measurements, part of the analysis included the mapping of the sublot average operating frequencies and average roller speeds during proof mapping. Operating frequencies were calculated based on the frequency at which the fundamental frequency, $A_0$, occurs after transforming 600 data points of time-history measurements assigned to a GPS coordinate into the frequency domain. Figure 4-20 shows representative maps of the average operating frequencies and the roller speeds for a clayey subgrade test site (Cell 189).

The mapping of the frequency of vibration and the speed of the roller allowed the research team to better understand CMV measurements and their variability. For instance, proof mapping on the subgrade was mostly performed uniformly with an operating frequency of 28 Hz; however, operating frequencies below 28 Hz were observed along some line passes during the proof mapping of the base material. This led to an increase in the variability of the measurements, leading to higher coefficients of variation of the CMV measurements. To reduce variability in the roller measurements, operating conditions must adhere to the roller's recommended settings. The manufacturer's recommended settings for the roller used in this project were an operating frequency of 28 Hz and speed of about 5 km/h (3 mph).

In Figure 4-20, individual sublots are coded green, yellow, or red (not shown). Colors were assigned based on the average value calculated in the code for all the sublots, and the numbers provided in the figure were rounded to one decimal for display purposes. In this figure, green coding indicates that the average frequency or speed was acceptably close to the recommended setting, with only minor variations observed in the individual measurements for that sublot. Yellow coding indicates that the average frequency or speed was acceptably close to the recommended setting, but greater variation was observed in the individual measurements. Red coding would indicate that the average frequency or speed was not acceptably close to the recommended setting and/or that extreme variations were observed among the individual measurements for that sublot; however, no red-coded sublots appear in Figure 4-20. For purposes of this study, "acceptably close" was defined as ±5% for frequency (at 10% starts impacting the variability of CMVs) and as ±15% (no more than ±20%) for speed.

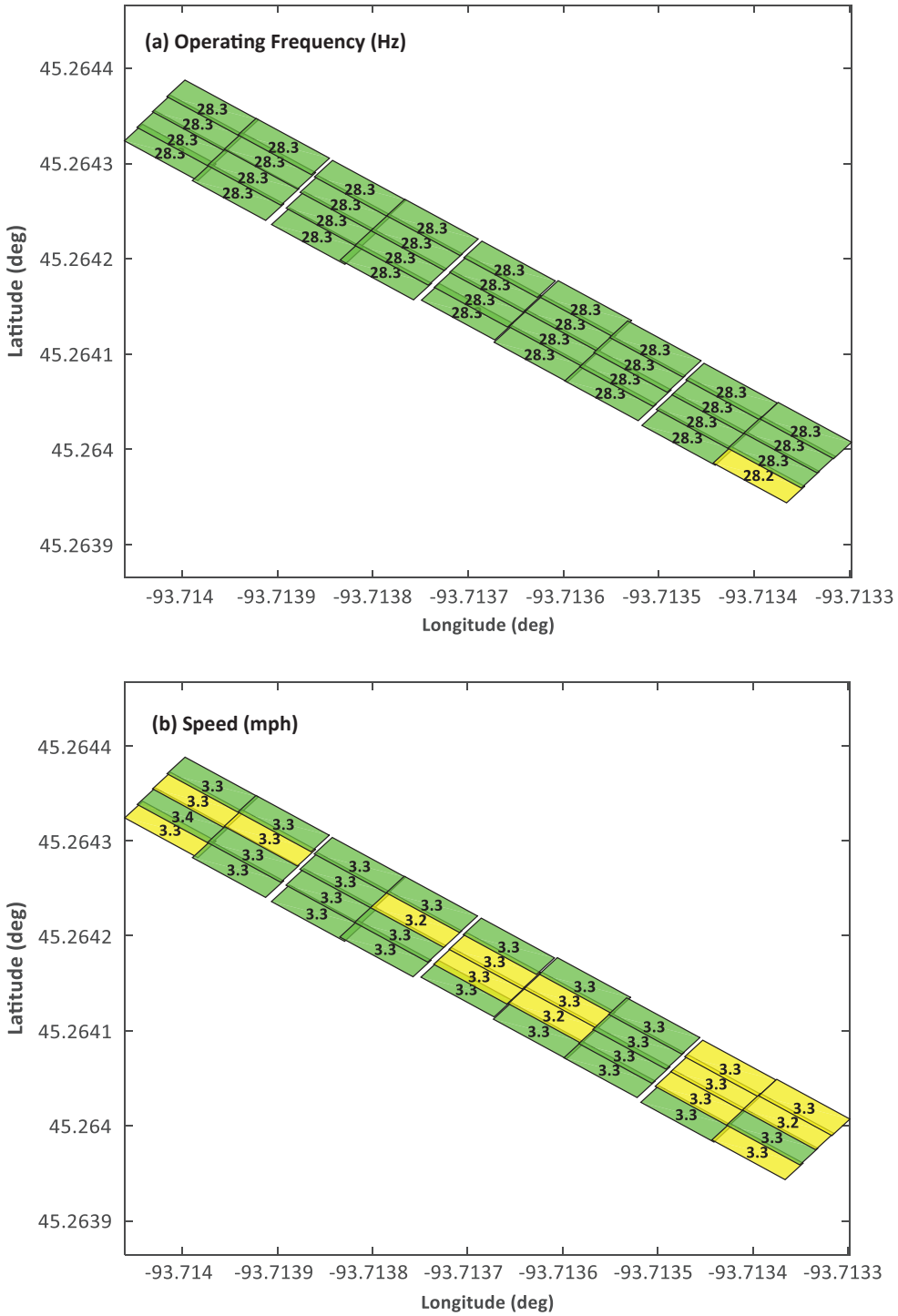


Green = Average sufficiently close to recommended setting with minimal variations observed in measurements; Yellow = Average sufficiently close to recommended setting with some variations observed in measurements; Red (not shown) = Average not sufficiently close to recommended setting and/or unacceptable variations observed in measurements.

***Figure 4-20. Maps of roller operating frequencies and speed.***

CHAPTER 5

# Calibration of Numerical Models

## Introduction

This chapter compares the measured field data with the responses obtained from the forward models with different levels of sophistication. It presents strategies for calibration of the forward models that simulate the pavement responses during mapping and discusses the process of deriving adjustment factors for the forward models to represent the field conditions more realistically.

## Structural Models

Nazarian et al. (2014) indicated that direct estimation of field moduli using deflection-based NDT devices from laboratory-measured moduli was not appropriate, and that the lab and field moduli must be related through calibrated structural models. With that precedent, different response algorithms were developed and calibrated with the experimental results obtained from the laboratory tests and field measurements of the actual pavement sections. These models involved various levels of sophistication, as described in Chapter 3 and listed in Table 3-3.

## Evaluation and Calibration of Forward Models

Table 5-1 presents information about the two construction sites that were used for field testing to support the evaluation of forward models. (Additional details are provided in Appendix G.) The data collected for this purpose consisted of the vertical displacements measured as a roller approached and moved away from embedded geophones (see Figure 5-1). Additional information included the laboratory properties of the geomaterials and field spot-test measurements. The data collected at Site 1 (Cleburne, Texas) was used to evaluate the pavement responses under several rollers with different operating features.

Table 5-2 lists the properties of the layers at these two test sites. Table 5-2 also lists the averaged LWD moduli obtained on top of each layer as part of the spot-testing program conducted at the sites. In the case of the two-layer systems, the LWD moduli correspond to composite moduli of the top and bottom layers. The base moduli in Table 5-2 were backcalculated using the LWD measurements on top of the subgrade and base.

### Calibration of Forward Models under Stationary Vibration

Three different manufacturers furnished rollers for the vibration measurements at Site 1. The specifications of these rollers are summarized in Table 5-3. As part of the analysis, all three

**Table 5-1. Field test sites for development of models.**

| Site | Location | Layer | Length of Test Section or Cell |
|---|---|---|---|
| 1 | Cleburne, TX | Clayey subgrade on top of existing embankment | 150 m (500 ft.) |
| 2 | MnROAD, MN | Sandy (cells 185 and 186) and clayey (cells 188 and 189) subgrade*<br>300 mm (12 in.) thick unbound aggregate base on top of subgrade* | 70 m (225 ft.)* |

*See Figure 4-3 for detailed information.

roller operators were directed to vibrate their rollers in a stationary position under various settings for very short periods.

Figure 5-2(a) shows the vertical displacement time histories that were measured with two geophones embedded at depths of 0.6 m (24 in.) and 1.2 m (48 in.) during the stationary vibration of a roller at low frequency and high amplitude. Figure 5-2(b) shows the corresponding displacement time histories of the roller. The measured displacements in the stable region (after the roller ramped up to the desired setting and before the roller decelerated to no vibration) were averaged to obtain representative displacements for comparison with the FE models' displacements. For simulations using the linear elastic models, the LWD modulus was used as input.

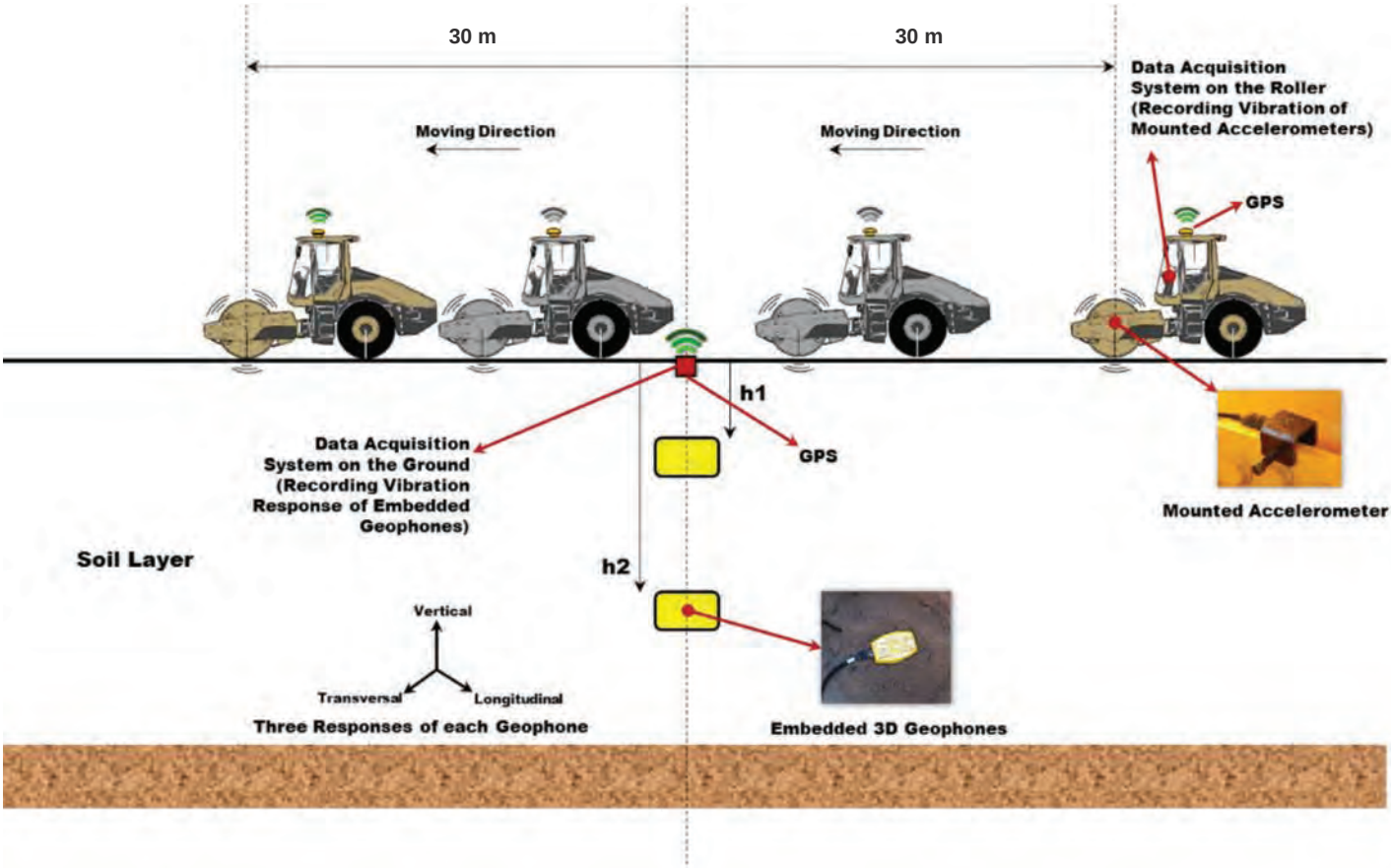


Figure not to scale.

***Figure 5-1. Data collection during vibratory moving condition.***

**Table 5-2. Geomaterial properties of test sections.**

| | | | | Properties of Geomaterial | | | | | |
|---|---|---|---|---|---|---|---|---|---|
| | | | | Resilient Modulus (MR) Results (Modified MEPDG Model) | | | | In Situ Test | |
| Site | Location | | Layer | $k'_1$ | $k'_2$ | $k'_3$ | MR | $E_{LWD}$ | Modulus* |
| 1 | Cleburne, TX | | Subgrade | 269 | 0.54 | -3.0 | 21 MPa (3.1 ksi) | 41.8 MPa (6.1 ksi) | -- |
| 2 | MnROAD | Cell 185 | Subgrade | 335 | 1.6 | -0.6 | 79 MPa (12 ksi) | 29 MPa (4.3 ksi) | -- |
| | | | Base | 512 | 0.8 | -0.1 | 129 MPa (19 ksi) | 63 MPa (9 ksi) | 117 MPa (17 ksi) |
| | | Cell 186 | Subgrade | 335 | 1.6 | -0.6 | 79 MPa (12 ksi) | 36 MPa (5.2 ksi) | -- |
| | | | Base | 484 | 0.9 | -0.1 | 126 MPa (18 ksi) | 99 MPa (14 ksi) | 193 MPa (28 ksi) |
| | | Cell 188 | Subgrade | 649 | 0.6 | -2.6 | 59 MPa (8.6 ksi) | 43 MPa (6.2 ksi) | -- |
| | | | Base | 500 | 0.6 | -0.1 | 98 MPa (14.2 ksi) | 78 MPa (11.3 ksi) | 138 MPa (20 ksi) |
| | | Cell 189 | Subgrade | 649 | 0.6 | -2.6 | 59 MPa (8.6 ksi) | 26.3 MPa (3.8 ksi) | -- |
| | | | Base | 408 | 0.9 | -0.1 | 118 MPa (17.1 ksi) | 67 MPa (9.7 ksi) | 134 MPa (19 ksi) |

*Base modulus backcalculated using LWD moduli measured on top of base and subgrade surface.

**Table 5-3. Specifications of IC rollers used for calibration of forward models.**

| Vendor/Manufacturer | | Model | Width (m) | Operating Weight (kN) | Centrifugal Force (kN) | Frequency (Hz) |
|---|---|---|---|---|---|---|
| Caterpillar |  | CS74B | 2.1 | 157 | 166–332 | 23.3–28 |
| Sakai |  | SV540T | 2.1 | 109 | 172–255 | 28.3–33.3 |
| Hamm |  | HD120 | 2.1 | 110 | 171–246 | 30–40 |

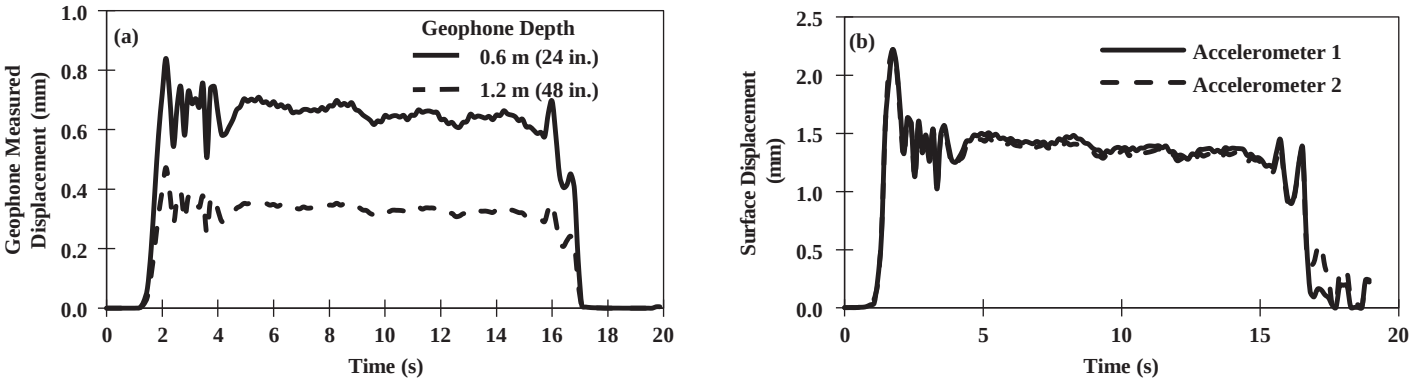


***Figure 5-2. Measured IC data during stationary vibratory test on top of embankment using Sakai roller operating under low frequency and high amplitude: (a) displacement measured by embedded geophones; (b) surface displacement calculated from mounted accelerometers.***

Figure 5-3 compares the measured and simulated displacements under the vibratory roller at low and high amplitude settings. The two displacements show similar trends but with different amplitudes.

Figure 5-4 compares the measured and simulated displacements during stationary tests with all three rollers under five different scenarios. Different roller manufacturers had different definitions for the low and high amplitude vibrations. The closeness of the measured and simulated data for each case is summarized in Table 5-4. The displacements from the SSL FE model are systematically about 2.6 times greater than those measured by geophones in the field, as shown in Figure 5-4(a). By introducing nonlinearity into the static stationary FE model (SSN), a better correlation between the measured field data and computed nonlinear SSN FE model is obtained, as judged by a higher $R^2$ (0.74), and a lower SEE (0.17 mm), as seen in Figure 5-4(b); however, the slope of the regression line indicates a systematic difference of 5.5 times. These systematic differences can be attributed to the differences in the stress states and the compaction efforts achieved in the field and laboratory.

To better represent the state of stress and compaction effort, parameter $k_1'$ in Equation 3-2 was recalculated by replacing the representative resilient modulus with the LWD modulus while maintaining the $k_2'$ and $k_3'$ to their corresponding values obtained from the laboratory resilient modulus tests. As shown in Figure 5-4(c), the simulated displacements are about 2.9 times greater than the measured ones. Figures 5-4(d) and 5-4(e) show that the introduction of vibratory conditions to the simulation only marginally impacted the outcomes.

## Calibration of Forward Models Under Moving Vibration

The dataset consisting of accelerometer and geophone measurements collected under a moving vibratory roller at Site 2 is used as an example of this process. A Caterpillar CS74B roller with low amplitude and high frequency operating settings was used in this site and simulated for calibration purposes. (For additional specifications of the roller, see Table 5-3.)

**Single-Layer Systems.** Figure 5-5(a) shows the measured vertical displacements as recorded by the embedded geophones over 30 m (100 ft.) during mapping of the clayey subgrade of Cell 188. Figure 5-5(b) shows the corresponding surface displacements. Distance zero corresponds to the location of the embedded geophones. As seen in the figure, most of the appreciable vertical geophone deformations are limited to ±2 m (±6 ft.) of the embedded geophones.

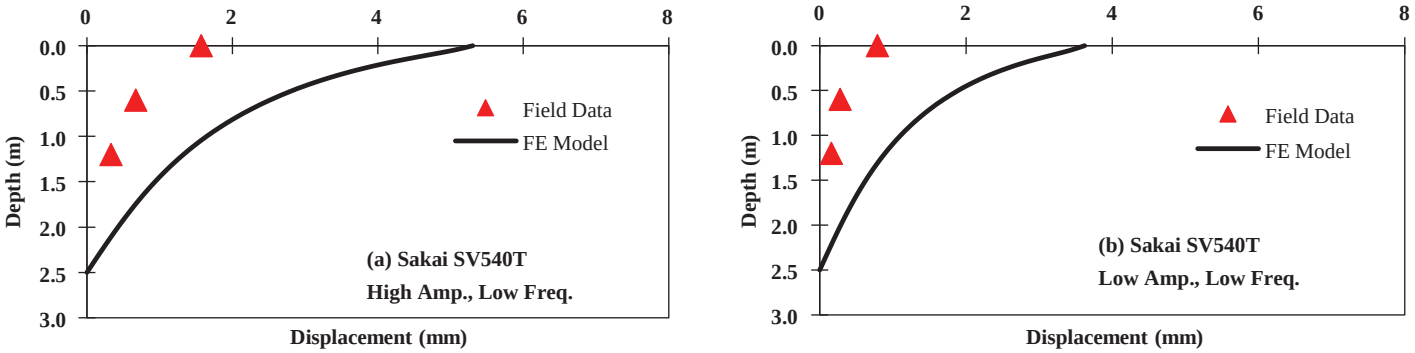


*Figure 5-3. Vertical displacement at different depths as obtained from SSL FE model and field measurements during stationary vibratory tests on top of subgrade.*

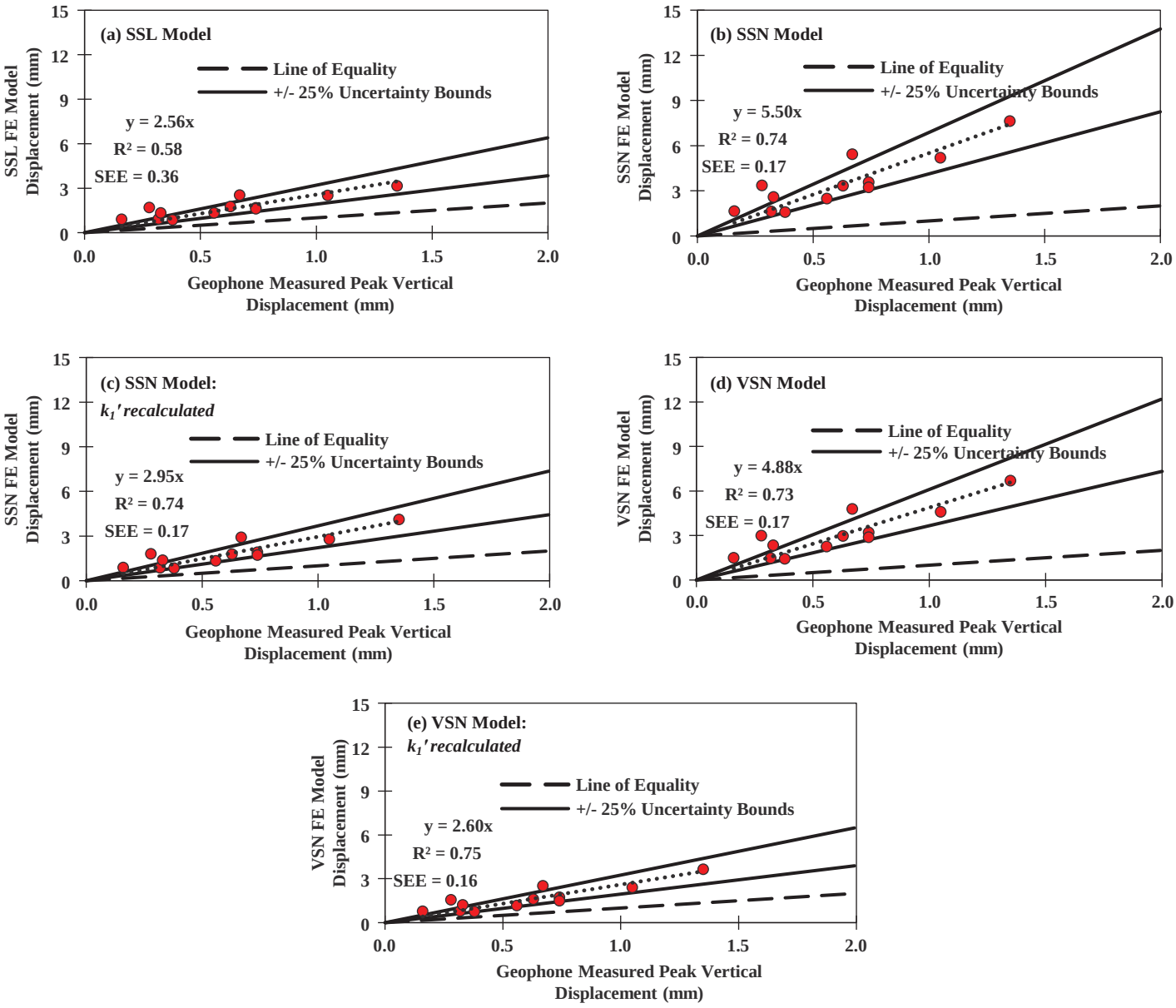


***Figure 5-4. Relationship between geophone measurements during stationary tests for single-layer geosystem at Site 1 to their corresponding FE responses.***

**Table 5-4. Summary of relationships of measured field displacements for single-layer geosystem during stationary tests at Site 1 to FE model responses from various levels of sophistication.**

| Descriptive Correlation | SSL FE Model | SSN FE Model | | VSN FE Model | |
|---|---|---|---|---|---|
| | | *Laboratory* $k'_1$* | *Recalculated* $k'_1$† | *Laboratory* $k'_1$* | *Recalculated* $k'_1$† |
| Adjustment Factor, *S* | 2.56 | 5.50 | 2.95 | 4.88 | 2.60 |
| $R^2$‡ | 0.58 | 0.74 | 0.74 | 0.73 | 0.75 |
| *SEE*‡ | 0.36 | 0.17 | 0.17 | 0.17 | 0.16 |

* Nonlinear $k'_1$ parameter determined from resilient modulus test as per AASHTO T-307.
† Recalculated $k'_1$ parameter using LWD modulus as resilient modulus in Equation (3-2).
‡ Coefficient of determination, $R^2$, and standard error of the estimate, *SEE*.

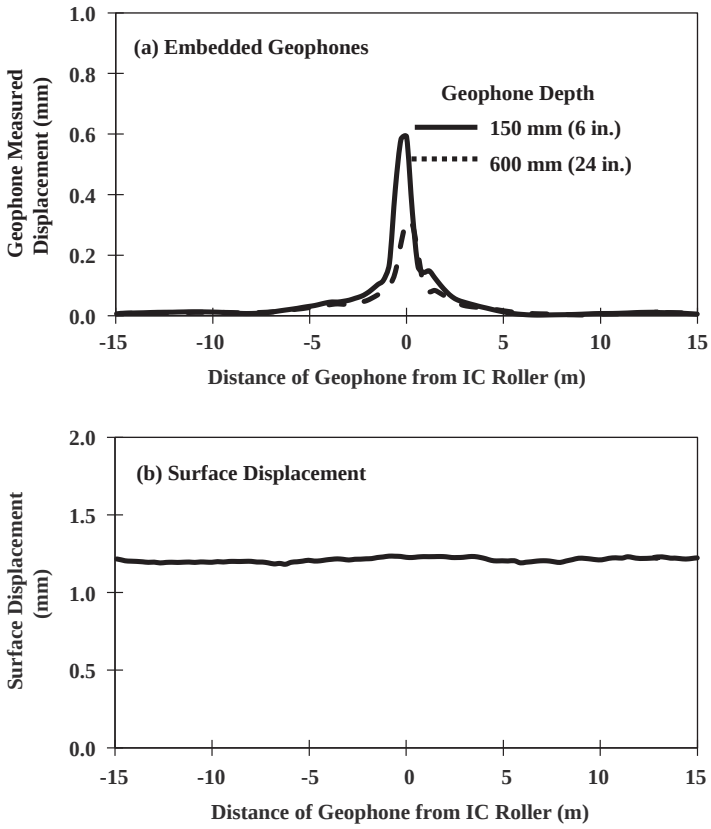


***Figure 5-5. Field measurements during proof mapping on top of clayey subgrade at Site 2.***

The displacements that were measured and simulated using a stationary static linear (SSL) condition are compared in Figure 5-6. The deflection basins resemble one another but show some shift in the magnitude.

Table 5-5 presents the summary of the peak displacement measurements on top of the subgrade for cells 185, 186, 188, and 189 at Site 2. The displacements measured by the geophones embedded in the sandy subgrades are slightly larger than those obtained for the clayey subgrades. The influence depth of cells containing sandy material is thus slightly greater than the penetration depth observed in the clayey subgrade.

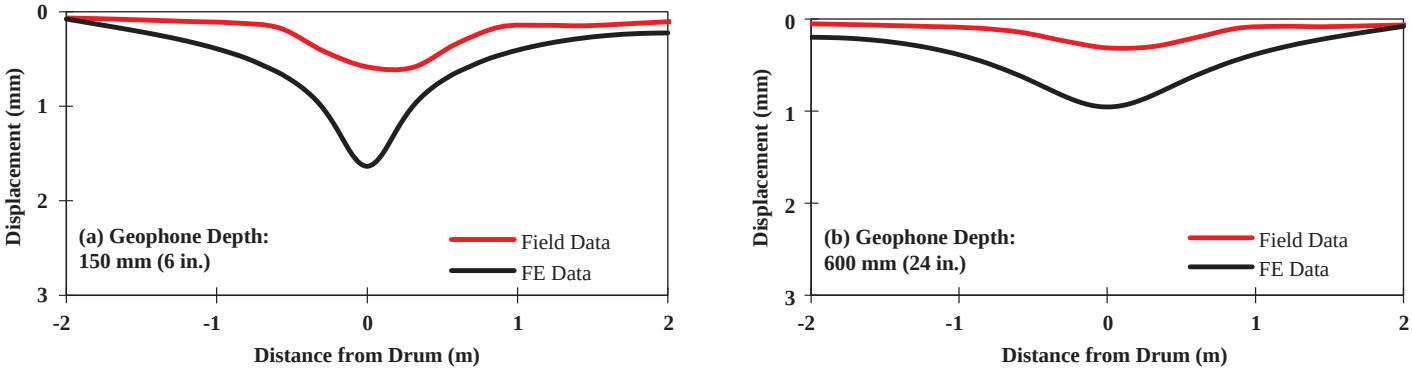


***Figure 5-6. Displacement basin at different depths as obtained from SSL FE model and field measurements during vibratory moving test on top of subgrade for Cell 188.***

**Table 5-5. Vertical displacement at different depths for cells 185, 186, 188, and 189 under moving vibration tests on top of subgrade at Site 2.**

| Embedded Geophone Depth | | Peak Vertical Displacement (mm) | |
|---|---|---|---|
| Sandy Subgrade | | Cell 185 | Cell 186 |
| Depth | Surface | 1.41 | 1.34 |
| | 150 mm (6 in.) | 0.75 | 0.70 |
| | 600 mm (24 in.) | 0.46 | 0.37 |
| Clayey Subgrade | | Cell 188 | Cell 189 |
| Depth | Surface | 1.22 | 1.18 |
| | 150 mm (6 in.) | 0.59 | 0.26 |
| | 600 mm (24 in.) | 0.31 | 0.61 |

Table 5-6 summarizes the transfer functions between the measured and simulated displacements for several levels of sophistication of FE models for all four cells. The SSL FE model displacement responses were about 3.5 times greater than those measured in the field, with a weak correlation coefficient of determination of 0.48. The best relationships between the measured and simulated results were obtained when the vibratory and nonlinear nature of the load was considered.

**Two-Layer Systems.** The approach described in the previous section also was implemented for the two-layer (subgrade and base) systems. Figure 5-7(a) shows the example measurements of the embedded geophones at different depths for a pavement structure consisting of an unbound aggregate base layer on top of a clayey subgrade (Cell 188). The base layer attenuates the measured displacement of the embedded geophones in the subgrade. Figure 5-7(b) shows the surface displacements during the mapping of the base layer (Cell 188). When compared to the measurements on top of the subgrade that were seen in Figure 5-5(b), the measurements in Figure 5-7(b) are more variable, reflecting both the bouncing of the drum due to the stiffer base material and the skill of the operator, who tended to drive the roller faster than instructed.

Figure 5-8 compares the displacement basins measured and simulated with SSL FE at the three different depths for Cell 188. As the roller moves farther away from the geophones, the displacements attenuated at a faster rate for the FE model in comparison to the field data.

As was done for the single-layer systems, different FE scenarios were taken into consideration for the two-layer systems, including linear and nonlinear behaviors for the simulated geomaterials under static and vibratory loading conditions. Table 5-7 summarizes the descriptive

**Table 5-6. Summary of relationships of measured field displacements for single-layer geosystem during moving tests at Site 2 as compared to FE model responses for various levels of sophistication.**

| Descriptive Correlation | SSL FE Model | SSN FE Model | | VSN FE Model | |
|---|---|---|---|---|---|
| | | *Laboratory* $k'_1$* | *Recalculated* $k'_1$† | *Laboratory* $k'_1$* | *Recalculated* $k'_1$† |
| Adjustment Factor, *S* | 3.47 | 1.41 | 2.85 | 1.67 | 4.04 |
| $R^2$‡ | 0.48 | 0.48 | 0.60 | 0.79 | 0.79 |
| SEE‡ | 0.53 | 0.08 | 0.44 | 0.13 | 0.41 |

* Nonlinear $k'_1$ parameter determined from resilient modulus test as per AASHTO T-307.
† Recalculated $k'_1$ parameter using LWD modulus as resilient modulus in Equation (3-2).
‡ Coefficient of determination, $R^2$, and standard error of the estimate (SEE).

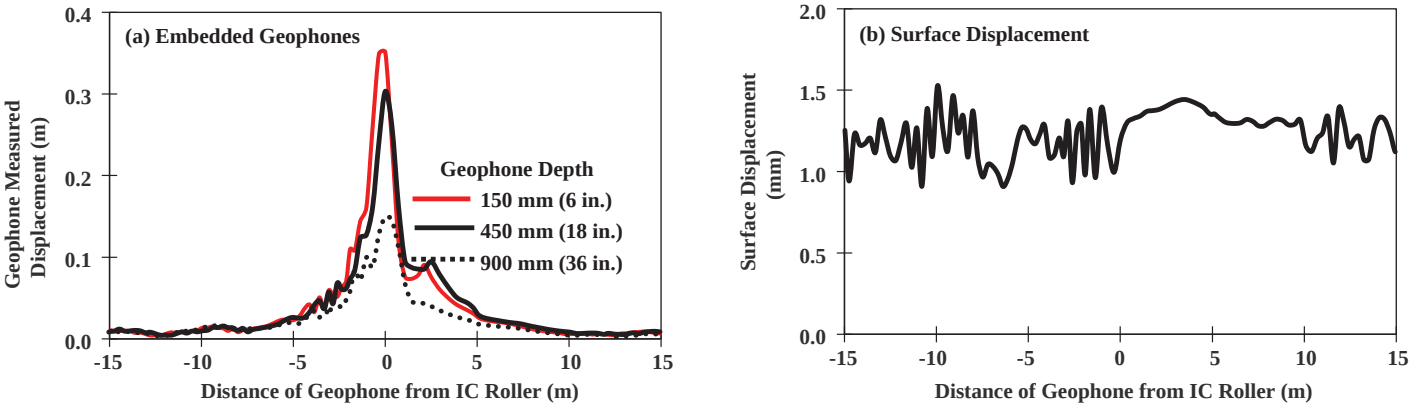


*Figure 5-7. Field measurements during proof mapping of base layer on top of clayey subgrade at Site 2.*

statistics of the relationships for the vibratory moving IC tests that were performed on top of the base layer at Site 2. Considering the nonlinear behavior of the materials yields better relationships among the measured and simulated results.

Detailed analyses and information, including the local relationships between the attempted FE scenarios and measured field data for the stationary and moving test protocols performed on top of single- and two-layer systems at Site 1 and Site 2 are provided in Appendix G.

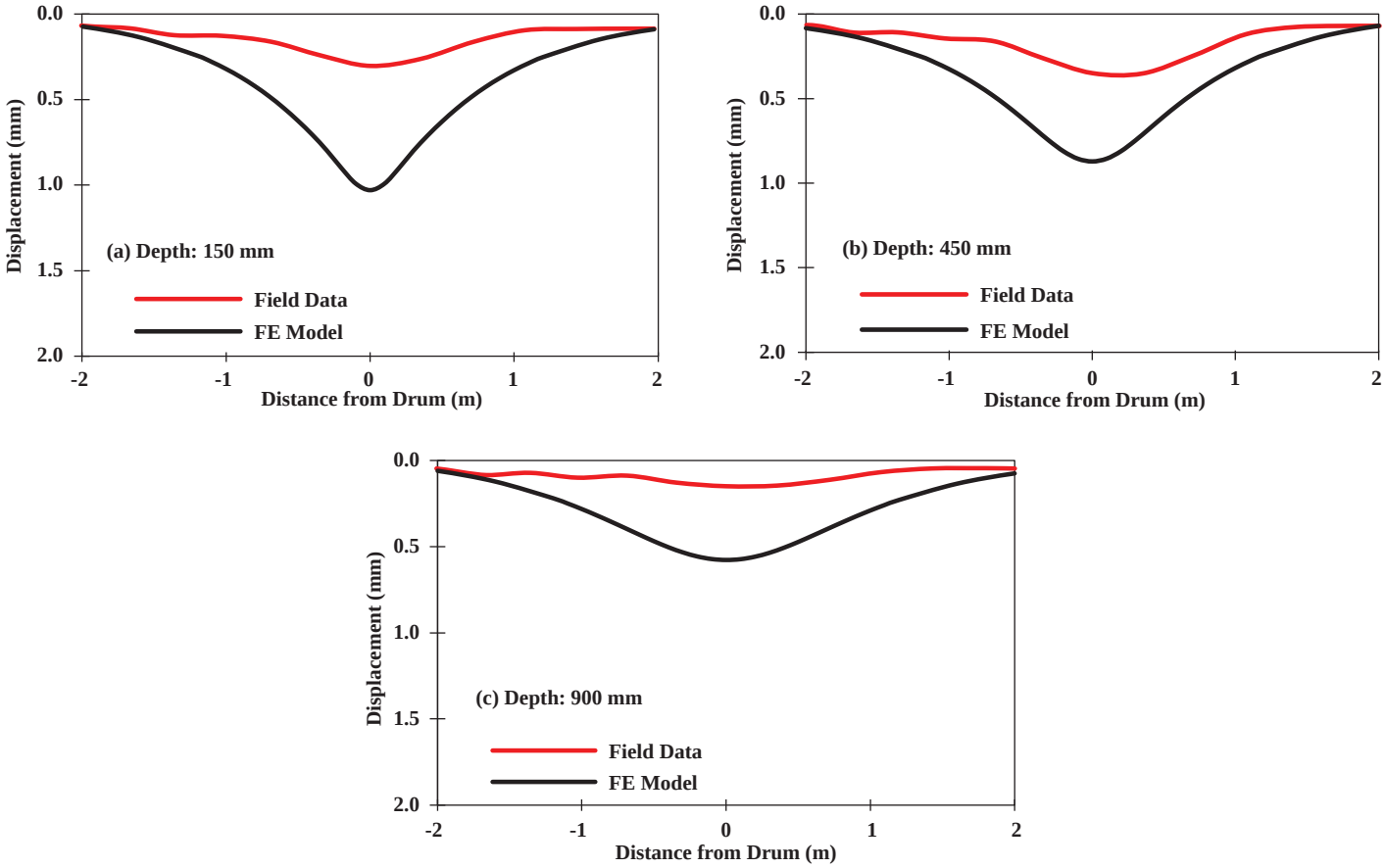


*Figure 5-8. Displacement basin at different depths as obtained from SSL FE model and field measurements during vibratory moving test on top of base for Cell 188 at Site 2 (MnROAD).*

**Table 5-7. Summary of the descriptive relationships of the measured field displacements for two-layer geosystem during moving tests at Site 2 as compared to the FE model responses for various levels of sophistication.**

| Descriptive Correlation | SSL FE Model | SSN FE Model | | VSN FE Model | |
|---|---|---|---|---|---|
| | | Laboratory $k_1'^{*}$ | Recalculated $k_1'^{\dagger}$ | Laboratory $k_1'^{*}$ | Recalculated $k_1'^{\dagger}$ |
| Adjustment Factor, $S$ | 5.11 | 3.19 | 5.06 | 3.55 | 5.84 |
| $R^{2\ddagger}$ | 0.45 | 0.81 | 0.54 | 0.72 | 0.57 |
| SEE$^{\ddagger}$ | 0.26 | 0.08 | 0.36 | 0.16 | 0.58 |

* Nonlinear $k_1'$ parameter determined from resilient modulus test as per AASHTO T-307.
† Recalculated $k_1'$ parameter using LWD modulus as resilient modulus in Equation (3-2).
‡ Coefficient of determination, $R^2$, and standard error of the estimate (SEE).

## Global Relationships

Considering the results obtained from the two test sites on top of single- and two-layer geosystems, this section aims to develop global relationships between the measured field data and the FE responses.

Figure 5-9 compares the measured and simulated peak displacements directly under the roller at different depths, under both the stationary and moving conditions for the evaluated sites. The SSL FE model yields displacements that are globally about 2.85 times greater than the field measurements with significant scatter. These results concur with those found in NCHRP 10-84 (Nazarian et al. 2014) for spot tests. The scatter in the data can be attributed to the variability of the moisture content along the test sections.

Figure 5-10(a) shows the global relationships of the nonlinear SSN FE model and the corresponding field data considering the laboratory-determined nonlinear $k'$ parameters as model inputs. Two trends were observed for the measurements corresponding to Site 1 and Site 2 that can be attributed to the difference in compaction effort resulting in different states of stress. In that respect, resilient modulus tests of clayey subgrade materials yielded a nonlinear $k_1'$ parameter (the parameter associated to stiffness) at Site 1 that was lower in magnitude than the nonlinear $k_1'$ parameters obtained for Site 2. However, a higher averaged LWD modulus was reported for the subgrade at Site 1 compared to Site 2 (see Table 5-2). These differences can be attributed to the resilient modulus test, which cannot properly account for the compaction effort the geomaterials experience in the field, leading to different site-specific adjustment factors as shown in Figure 5-10(a).

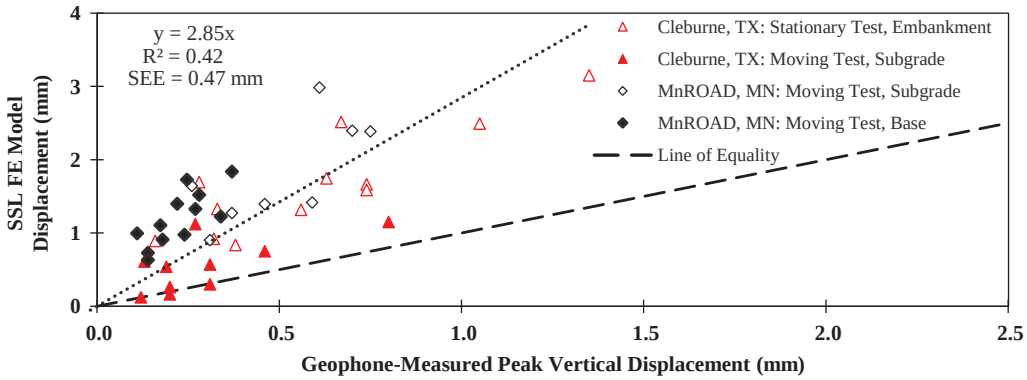


***Figure 5-9. Global relationship between field-measured displacements for vibratory rollers and SSL FE model displacements.***

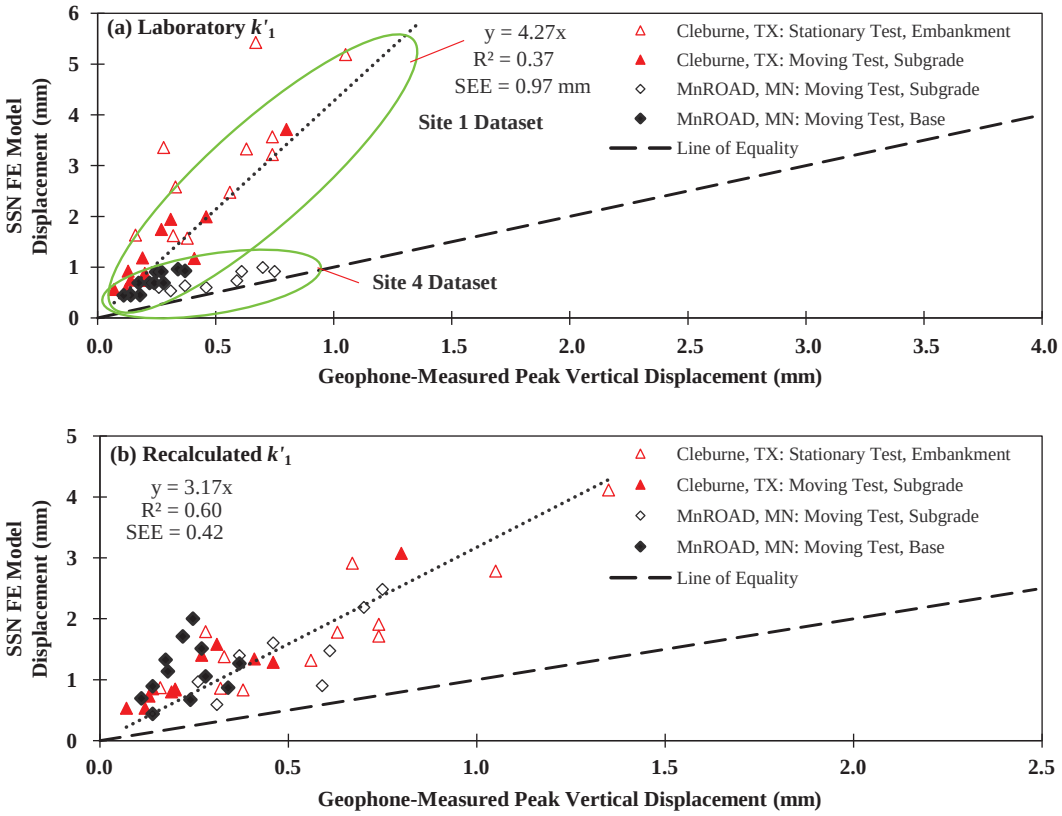


***Figure 5-10. Global relationships between field geophone-measured displacements and their corresponding SSN FE model displacements with different input modeling approaches.***

To minimize this drawback, the LWD and laboratory results can be integrated so that the stress hardening and cohesiveness causing softening behaviors of the geomaterials under the loading can be quantified by nonlinear $k'_2$ and $k'_3$ parameters, respectively. The $k'_1$ parameter (associated with stiffness), on the other hand, can be more representative as compared to field conditions when it is adjusted by LWD measurements. As shown in Figure 5-10(b), this approach yields a more uniform global relationship with a higher $R^2$ value and a lower SEE. The results in this case again confirm the findings of NCHRP 10-84 with spot-test devices.

The developed global adjustment factors are necessary to accommodate the differences between field measurements and numerical analysis. These transfer functions can be incorporated as part of the process to extract the mechanical properties of compacted geomaterials during proof mapping using robust inverse solvers that were developed based on the numerical pavement responses.

CHAPTER 6

# Extraction of Mechanical Properties

## Introduction

To extract mechanical properties in a practical manner, a robust backcalculation technique that does not require excessive processing time is needed. This chapter reports on the research team's efforts to develop procedure(s) to extract the mechanical properties of geomaterials during mapping of the compacted layers on a real-time basis.

## Selecting the Backcalculation Process

The extraction of mechanical properties of layered materials can be performed directly using ICMVs captured during the mapping process or indirectly using a reliable inverse solver that incorporates ICMVs in the estimation of soil properties. The following sections describe each of the two approaches.

### Estimation of Stiffness

As was discussed in Chapter 4, the layer stiffness can be extracted directly from the force imposed by the drum and the deflection at that location. Force-displacement loops are created by plotting the time-varying contact force versus drum displacement (see Figures 4-16 and 4-17). However, the calculation of stiffness can be simplified by obtaining the ratio of the complex amplitudes of the force and displacement records in the frequency domain at the roller's operating frequency. This process allowed the development of maps of the surface deflections and the stiffness of geomaterials (see Figure 4-18).

### Backcalculation of Modulus

Due to the nonlinear behavior of the unbound geomaterials, the modulus of a layer varies spatially and with depth. To gauge the quality of the pavement, it is desirable to use a representative modulus for the layer. The moduli at half-depth of the base and at 300 mm (12 in.) into the subgrade were considered as their representative properties. For the single-layer geosystems (subgrade), the layer stiffness can be extracted directly at each spatial location by dividing the known force of the roller by the corresponding deflection. For a multi-layer geosystem, this process would provide a composite stiffness.

For developing inverse models for the backcalculation of the moduli of the subgrade and base layers, a set of machine-learning techniques was implemented. GP and ANN methods were used for that purpose. A training dataset that consisted of 2,200 single-layer and 4,400 two-layer geosystems with different base thicknesses was used to develop a predictive function using the

GP method for symbolic regression. To arrive at the optimal predictive function using the GP approach, the inputs considered were:

- The nonlinear $k'$ parameters of the subgrade, $k_i'^s$;
- The surface displacement, $d_1$, measured on top of the subgrade;
- The base nonlinear parameters, $k_i'^b$ and layer thickness, $h$; and
- The surface displacements, $d_2$, recorded on top of the base layer.

These inputs yielded relationships for the subgrade, $E_{SUBG}$, and the base modulus, $E_{BASE}$, as follows:

$$E_{SUBG} = f\left(k_i'^s, d_1\right) \tag{6-1}$$

and

$$E_{BASE} = f\left(k_i'^s, k_i'^b, h, d_1, d_2\right). \tag{6-2}$$

To build the models for a roller commonly used in the field (with operating features as shown in Table 3-1), the moduli at their representative locations were obtained from the SSN FE model and used as target values.

The following equation provided the best predictive modulus of subgrade from the GP method:

$$E_{SUBG} = C_1 k_1'^s + \frac{C_2 + C_3 k_2'^s + C_4 k_3'^s + \left(C_5 + C_6 k_2'^s\right) e^{\left(k_3'^s\right)} - C_7 k_2'^{s2}}{d_1}, \tag{6-3}$$

where

$C_1 = 0.0191$,
$C_2 = 136$,
$C_3 = 107$,
$C_4 = 45.9$,
$C_5 = 38.1$,
$C_6 = 40.5$, and
$C_7 = 9.9$.

The GP method was then applied to the training dataset, and the resulting predictions of subgrade moduli were compared to subgrade moduli obtained using the SSN FE model with the same dataset. As seen in Figure 6-1, Equation 6-3 provided a reasonable estimate of the subgrade moduli generated by the SSN FE model.

Following a similar process, the best equation for predicting the base modulus took the following form:

$$E_{BASE} = C_1 k_1'^b + \frac{\left(C_2 - h\right) k_1'^b k_2'^b + C_3 k_1'^b k_3'^b}{d_2\left(h + k_1'^b + k_1'^s - k_1'^b k_3'^b\right) + C_4 h k_1'^b}, \tag{6-4}$$

where

$C_1 = 0.108$,
$C_2 = 2.97 \times 10^3$,
$C_3 = 1.42 \times 10^3$, and
$C_4 = 0.0098$.

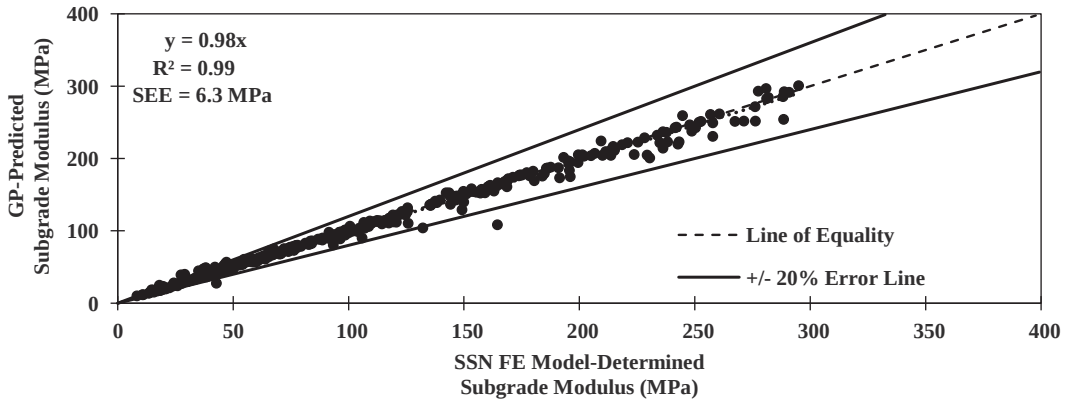


***Figure 6-1. Comparison of GP-predicted subgrade modulus to SSN FE model-determined subgrade modulus using data set aside for validation.***

Applying Equation 6-4 to the training dataset, the resulting base modulus predictions were again compared to those determined using the SSN FE model. As seen in Figure 6-2, the base modulus can be predicted favorably using the proposed equation.

The ANN-based method involved an input layer that, at the most complex level, included nine predictor independent variables: the nonlinear $k'$ parameters of the base and the subgrade; base thickness $h$; surface displacements $d_1$ and $d_2$, corresponding to the top of the subgrade and the base layer, respectively; and an output layer that included the values predicted by the network. When the ANN method was applied to the dataset, the resulting predictions of subgrade moduli were compared to the subgrade moduli determined using the FE model, yielding the results shown in Figure 6-3 and Figure 6-4.

After comparing the results of the GP method with those from the ANN method, a decision was made to continue with the ANN-based method. Using the ANN method, more complex inverse solvers can be developed to predict the output more precisely; however, more complex inverse solvers would require more laboratory efforts to determine the needed input variables. Based on the available input parameters from IC field operation and laboratory test results, two backcalculation scenarios were proposed for predicting $E_{SUBG}$ and five scenarios were proposed for $E_{BASE}$. The scenarios and their corresponding input parameters are listed in Table 6-1.

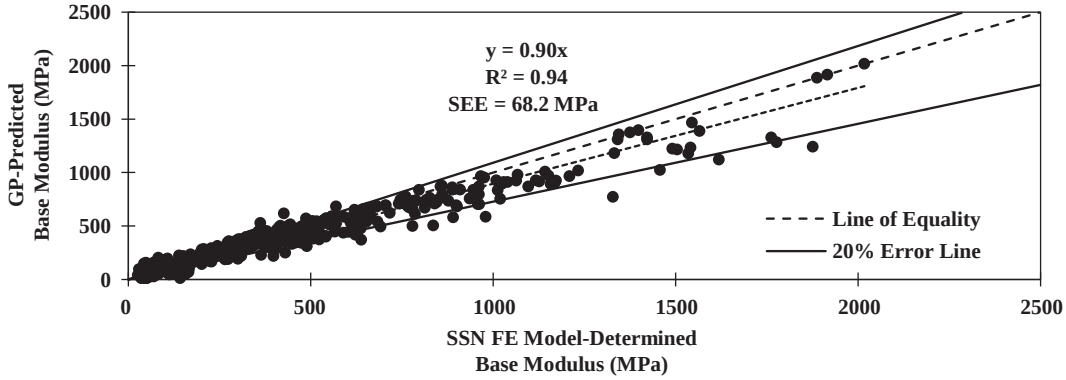


***Figure 6-2. Comparison of GP-predicted base modulus versus SSN FE model-determined base modulus using data set aside for validation.***

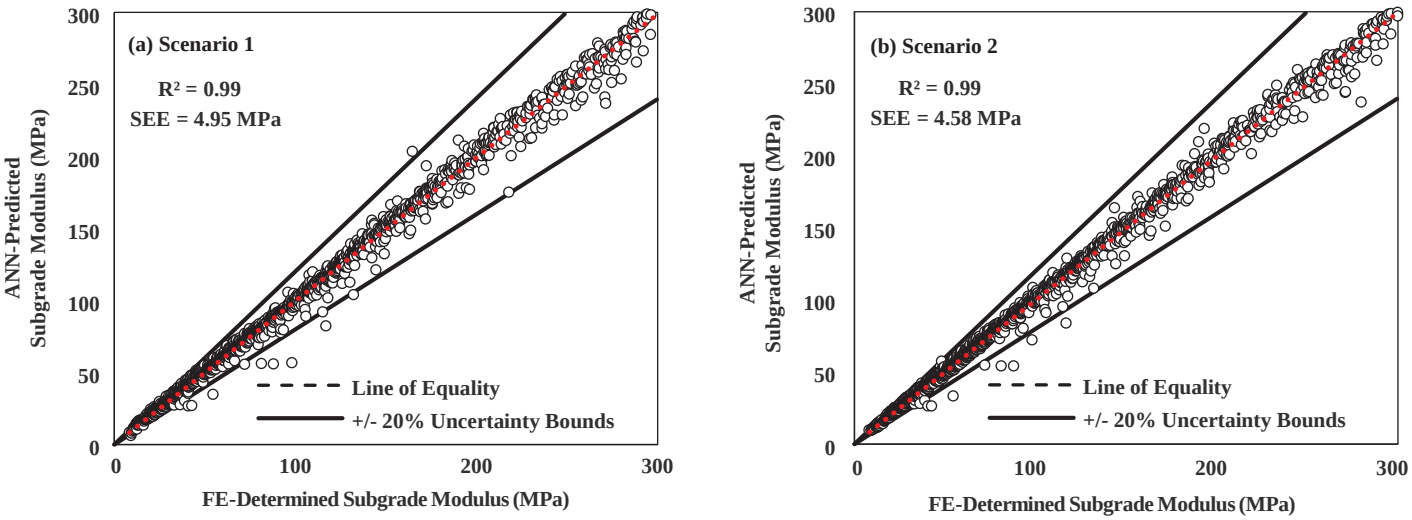


*Figure 6-3. Comparing ANN-predicted versus FE-determined subgrade moduli with different input scenarios.*

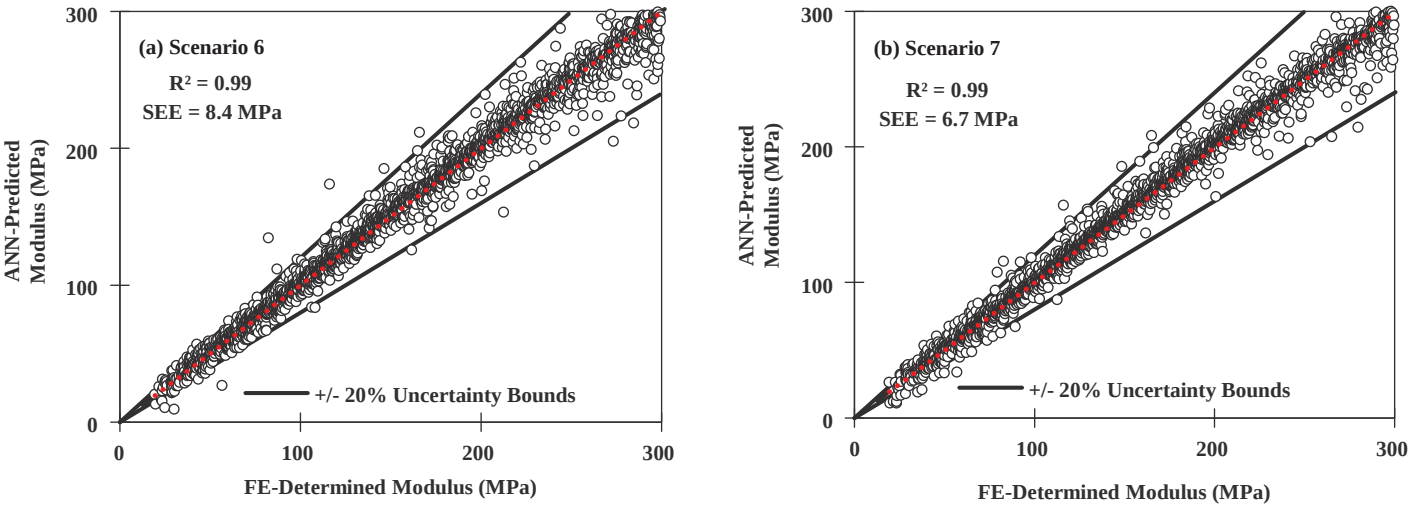


*Figure 6-4. Comparison of ANN-predicted versus FE-determined base modulus using ANN with different input scenarios.*

**Table 6-1. Feasible backcalculation scenarios based on available IC field and laboratory data.**

| Geosystem | Scenario | Input Parameters* | Target |
|---|---|---|---|
| Single-Layer | 1 | $h$, $k'_1{}^s$, $k'_2{}^s$, $k'_3{}^s$, $d_1$ | Subgrade Modulus $E_{SUBG}$ |
| | 2 | $h$, $k'_1{}^s$, $k'_2{}^s$, $k'_3{}^s$, $d_1$, $MR_{SUBG\text{-}Rep}$ | |
| | 3 | $h$, $k'_2{}^b$, $k'_3{}^b$, $d_2$, $d_1$ | |
| | 4 | $h$, $k'_2{}^b$, $k'_3{}^b$, $d_2$, $E_{SUBG}$ | |
| Two-Layer | 5 | $h$, $k'_2{}^b$, $k'_3{}^b$, $d_2$, $MR_{SUBG\text{-}Rep}$ | Base Modulus $E_{BASE}$ |
| | 6 | $h$, $k'_1{}^b{}_{\text{-back}}$, $k'_2{}^b$, $k'_3{}^b$, $d_2$, $d_1$ | |
| | 7 | $h$, $k'_1{}^s{}_{\text{-back}}$, $k'_2{}^s$, $k'_3{}^s$, $k'_1{}^b{}_{\text{-back}}$, $k'_2{}^b$, $k'_3{}^b$, $d_2$, $d_1$ | |

* $E_{SUBG}$ input values in Scenario 4 for two-layer systems is the modulus of subgrade determined at 300 mm (12 in.) from the top of the subgrade as obtained from nonlinear FE analysis; $MR_{SUBG\text{-}Rep}$ is the resilient modulus of subgrade material calculated from NCHRP 1-28A representative stresses; and $k'_{1\text{-}back}$ is the backcalculated $k'_1$ value using the LWD modulus $E_{LWD}$ of the corresponding layer in Equation 3-2, following the model from Ooi et al. (2004).

More detailed information regarding different levels of sophistication of the FE models used during the backcalculation process can be found in Appendix F. Figure 6-3 shows the results obtained from the trained algorithms to backcalculate subgrade modulus for the proposed Scenarios 1 and 2. The results show that both scenarios can predict the subgrade modulus quite accurately. Scenario 1 was preferred because of its simplicity.

In contrast to the single-layer systems, the backcalculation of the modulus of the base layer requires additional input parameters. The results of the trained algorithms for Scenarios 3 through 5 were not as promising, as is discussed in Appendix F. Scenarios 6 and 7 were proven viable, as is shown in Figure 6-4.

## Evaluation and Calibration of Inverse Models

The displacement measurements acquired during the proof mapping of the MnROAD test sections (Site 2) and the nonlinear $k'$ parameters obtained from the resilient modulus test as per AASHTO T-307 were used for evaluating the proposed inverse scenarios/architectures. Table 6-2 lists the inputs used for the evaluation of the inverse solver scenarios using data from the four pavement sections built at MnROAD. Prior to feeding the input displacements $d_1$ and $d_2$ into the inverse solver, the field-measured displacements were calibrated using a global adjustment factor $f = 3.2$, which was obtained for the SSN models using the process discussed in Chapter 5.

The extracted moduli of single- and two-layer systems obtained from the inverse scenarios were compared with the corresponding LWD measurements for cells 185, 186, 188, and 189, as seen in Figure 6-5:

- Scenarios 1 and 2 yielded promising results for the single-layer systems as most of the samples fall within the 20% uncertainty bounds.
- Scenario 1 is optimal for extracting the modulus of subgrade materials because it requires fewer input parameters than Scenario 2.
- Scenarios 6 and 7 both predicted the base modulus with reasonable accuracy.
- Scenario 6 is recommended as the most optimized inverse solver for extracting the base modulus because it is less complicated and requires fewer input parameters and less laboratory efforts than Scenario 7.

As observed in Figures 6-5(c) and 6-5(d), the extracted moduli of the top (base) layer from Scenarios 6 and 7 are about 1.2 and 1.1 times the backcalculated LWD moduli, respectively.

**Table 6-2. Summary of predictor variables measured for Site 2 (MnROAD).**

| MnROAD Cells | Base Thickness $h$ (mm) | Nonlinear Parameters for Subgrade Layer* | | | Nonlinear Parameters for Base Layer* | | | Modulus of Subgrade* | | Surface Displacement on Top of | |
|---|---|---|---|---|---|---|---|---|---|---|---|
| | | $k'^{s}_{1\text{-}back}$ | $k'^{s}_{2}$ | $k'^{s}_{3}$ | $k'^{b}_{1\text{-}back}$ | $k'^{b}_{2}$ | $k'^{b}_{3}$ | $E_{SUBG}$ (MPa) | $MR_{SUBG}$ (MPa) | Base $d_2$ (mm) | Subgrade $d_1$ (mm) |
| 185 | 300 | 123 | 1.60 | -0.60 | 467 | 0.80 | -0.10 | 29 | 79 | 1.36 | 1.41 |
| 186 | 300 | 152 | 1.60 | -0.60 | 722 | 0.90 | -0.10 | 36 | 79 | 1.29 | 1.34 |
| 188 | 300 | 462 | 0.60 | -2.60 | 709 | 0.60 | -0.10 | 43 | 60 | 0.99 | 1.22 |
| 189 | 300 | 283 | 0.60 | -2.60 | 470 | 0.90 | -0.10 | 26 | 60 | 1.25 | 1.18 |

*$E_{SUBG}$ is the subgrade modulus, in this case using the LWD modulus determined on top of subgrade; $MR_{SUBG}$ is the resilient modulus of subgrade material as obtained from resilient modulus test as per AASHTO T-307; and $k'_{1\text{-}back}$ is the backcalculated $k'_1$ value using the LWD modulus $E_{LWD}$ of the corresponding layer in Equation 3-2, following the model from Ooi et al. (2004).

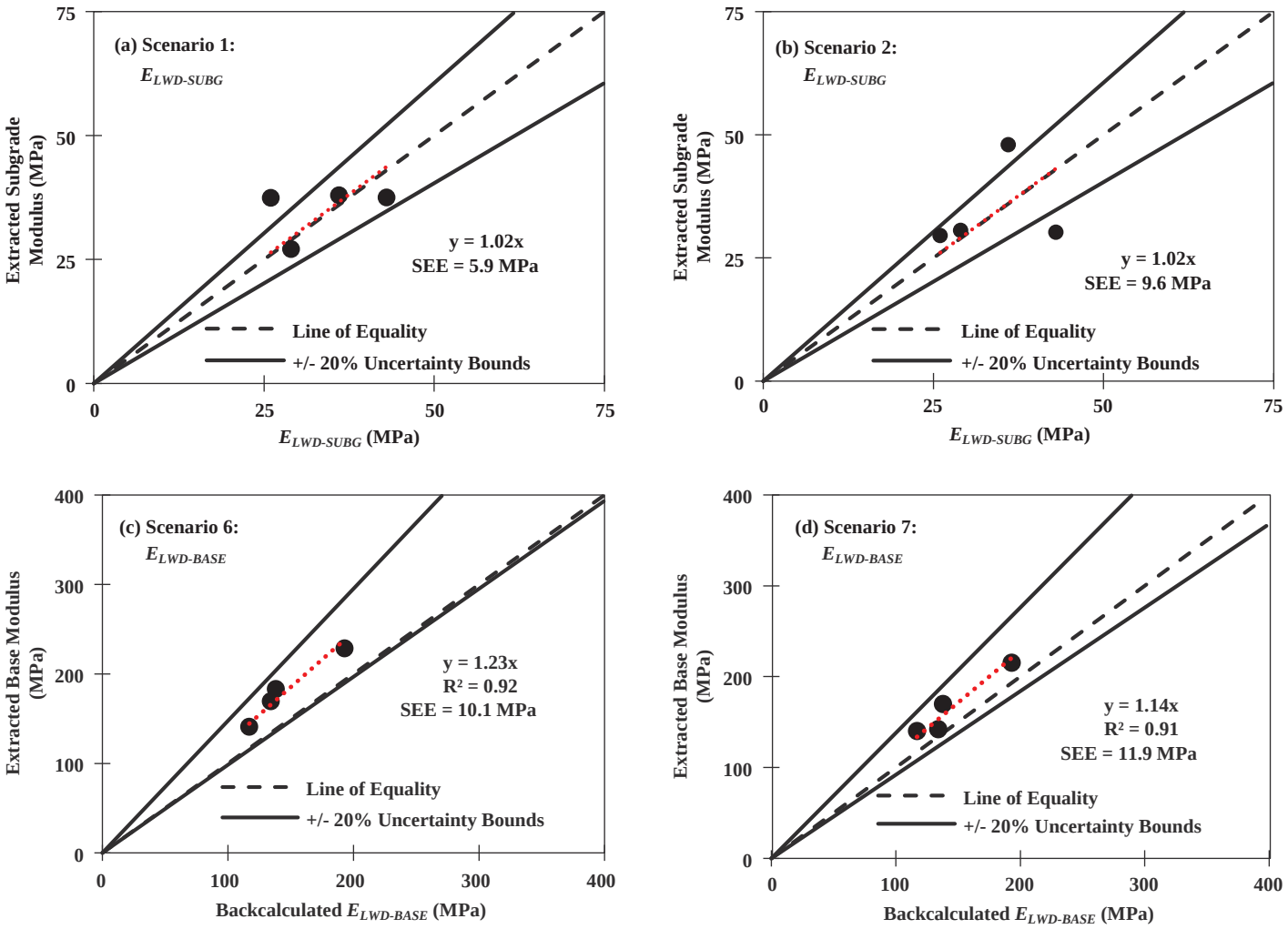


***Figure 6-5. Comparison of extracted subgrade and base modulus obtained from four proposed scenarios with corresponding backcalculated modulus.***

The difference between the field measurements and the extracted values can be attributed to the global adjustment factor acquired during the calibration process that was discussed in Chapter 5. The prediction can be thus improved by developing local adjustment factors for single- and two-layer systems distinctly.

## Extracting Modulus Using ANN Inverse Solvers (Approach 1)

The dataset obtained during the field evaluations conducted at the MnROAD site was used to evaluate the developed inverse solvers for extracting subgrade and base moduli. Figure 6-6 summarizes the steps of the proposed approach. The inputs to the inverse solvers are the material properties (nonlinear parameters and layer thicknesses), drum dimensions and weight, and surface deflection measurements of the drum. The roller-induced surface displacement is obtained from the mapping process using the average drum displacement in each sublot. The nonlinear parameters $k_2'$ and $k_3'$ are obtained from resilient modulus tests conducted in the laboratory at the optimum moisture content. The nonlinear $k_1'$ parameter is adjusted using

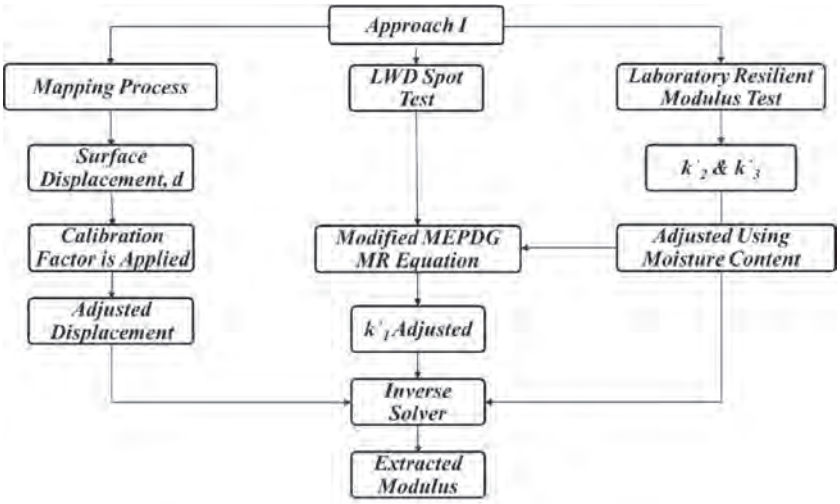


***Figure 6-6. Flowchart for extracting modulus of unbound materials using ANN inverse solvers.***

the LWD modulus after conducting LWD tests at the sublots. The next section describes an evaluation of this process as used for both single-layer and two-layer systems.

## Single-Layer System

Figure 6-7 shows the moisture-adjusted nonlinear parameters $k_2'$ and $k_3'$ at the time of compaction of the clayey subgrade in the sublots corresponding to cells 188 and 189. The nonlinear parameters were estimated using a best-fit regression curve through the variations of the relevant parameters from the resilient modulus tests with moisture content. The adjustment process also was applied to the nonlinear parameters for sandy subgrade samples from cells 185 and 186 (not shown). Nonlinear parameter $k_1'$ was adjusted using the LWD modulus obtained along the test section on each sublot.

Figure 6-8 compares the modulus of each sublot as predicted by the inverse solver and compared to the corresponding sublot's LWD modulus, $E_{LWD}$. Figure 6-8 provides comparisons for both the sandy subgrade materials (cells 185 and 186) and the clayey subgrade materials

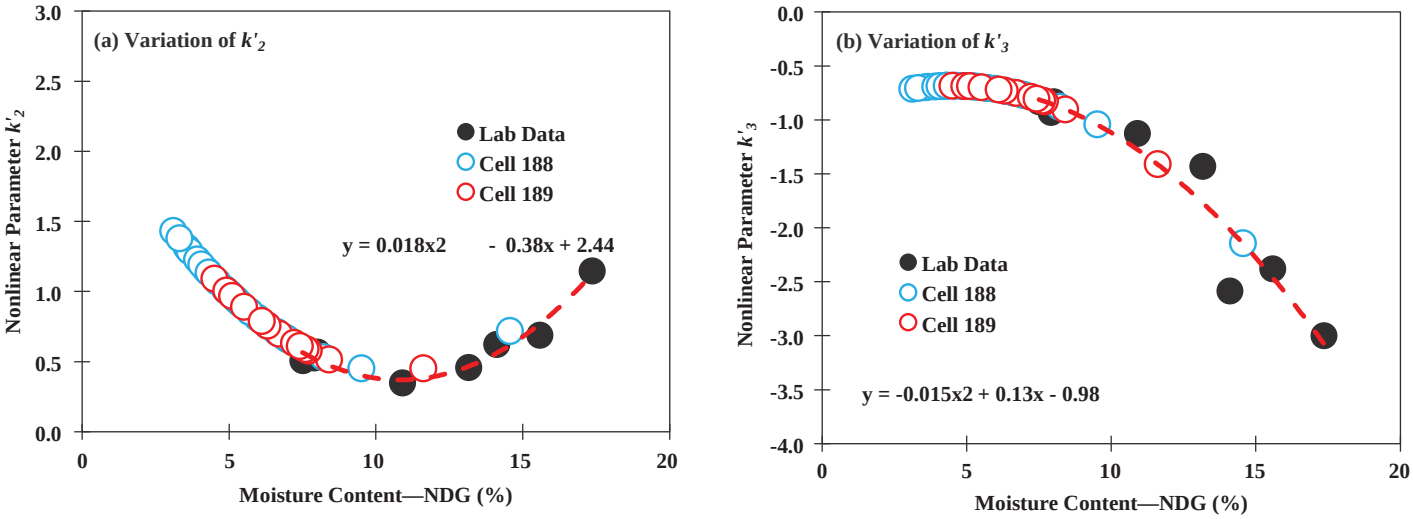


***Figure 6-7. Adjustment of parameters $k_2'$ and $k_3'$ using moisture correction for clayey subgrade (cells 188 and 189).***

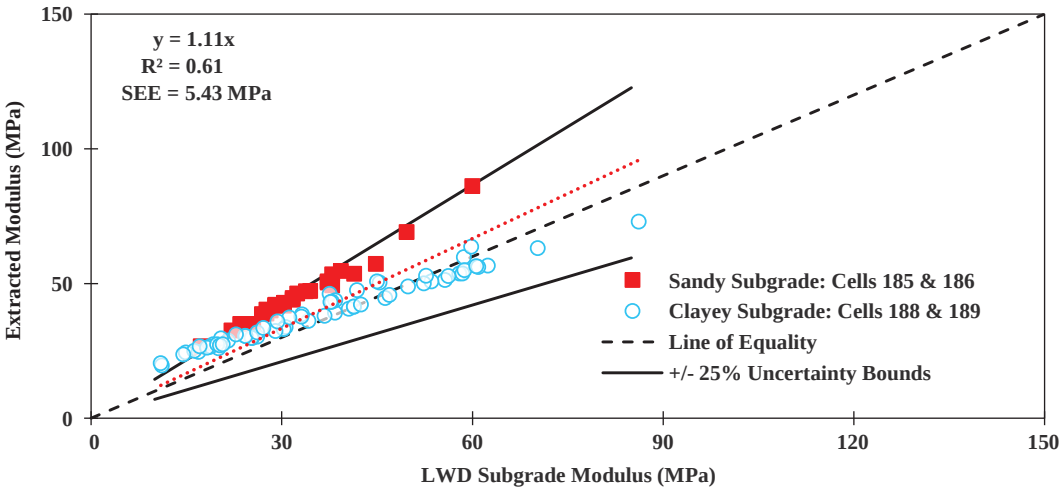


***Figure 6-8. Comparison of extracted subgrade moduli obtained from inverse solver with corresponding measured moduli for each of the sublots (cells 185, 186, 188, and 189).***

(cells 188 and 189). As shown by Figure 6-8, the inverse solver can predict the modulus of subgrade with reasonable accuracy.

## Two-Layer System

Similar to the subgrade, the nonlinear parameters of the base layers were adjusted for moisture for each sublot. The nonlinear parameters were interpolated and, in some cases, extrapolated using regression lines similar to those shown in Figure 6-7.

The base moduli were backcalculated using the LWD measurements on top of the base and corresponding measurements on top of the subgrade using a layered-elastic program through an iterative process. The nonlinear parameters, in conjunction with the roller-surface deflections on top of the subgrade and base layers, were used as inputs to the inverse solver for extracting the base modulus. The extracted base moduli compared well with the corresponding LWD base moduli, as judged by the number of cases that fall within the ±25% uncertainty bounds (see Figure 6-9).

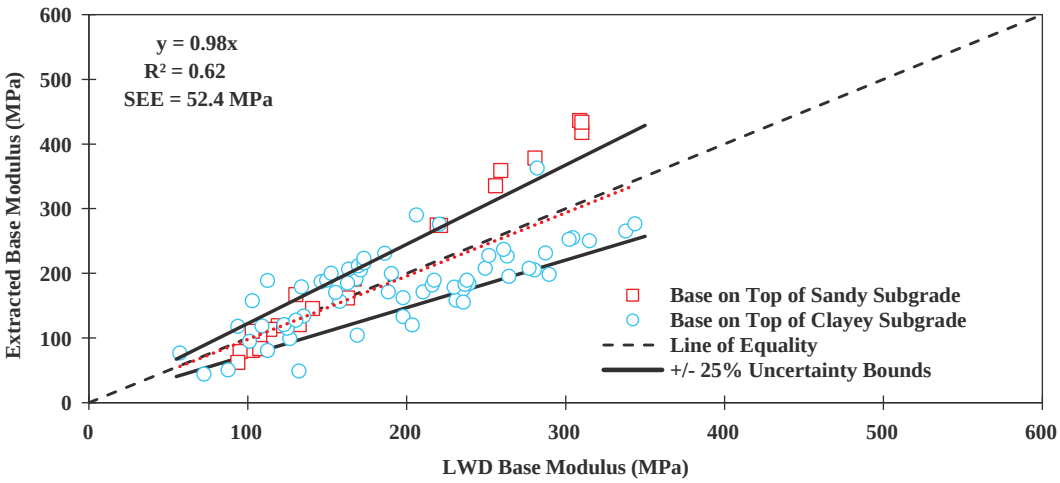


***Figure 6-9. Comparison of extracted subgrade moduli obtained from inverse solver with corresponding measured moduli for each of the sublots.***

The extracted base moduli compared well with the corresponding LWD base moduli as judged by the number of cases that fall within the ±25% uncertainty bounds.

## Retrieving Modulus Using Dynamic Drum Force (Approach 2)

A more practical approach for determining the modulus of single-layer and two-layer systems was developed using the drum force, $F_d$, determined from the accelerometers measuring the drum's inertia. Using the dynamic drum force does not require laboratory resilient modulus and field LWD testing. The expectation was that the impact of the variability of the compacted geomaterial properties would be less significant toward the calculation of the geomaterial's modulus if the more uniform areas of the lot were identified and considered for the local calibration process. Illustrated in Figure 6-10, the dynamic drum force approach consisted of four steps:

1. Upon completion of the mapping process, generate color-coded maps of (a) the dynamic drum force, (b) CMVs, and (c) coefficient of variation (COV) of the CMVs.
2. To obtain optimal results, choose at least five sublots with a COV of CMV less than or equal to 25%.
3. Obtain a site-specific local calibration factor between the LWD modulus and the drum force of the sublots selected in Step 2.
4. Estimate the moduli using the measured dynamic forces adjusted with the established site-specific calibration factor.

### Evaluation of Approach to Determine Modulus Using the Drum Force

Figure 6-11 illustrates the process used to retrieve the moduli of the sandy subgrade of MnROAD Cell 186. Figure 6-11(a) shows the mapping of the sublot's representative CMVs,

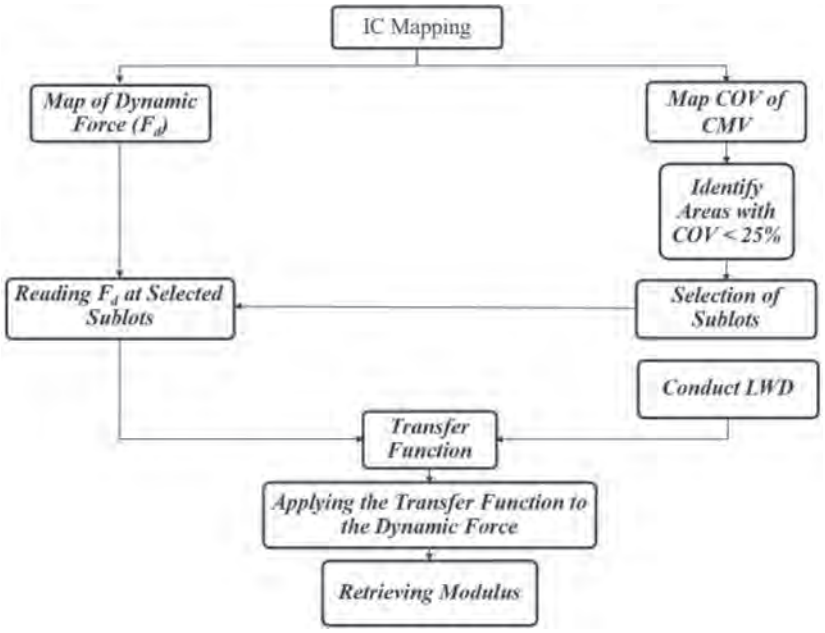


***Figure 6-10. Flowchart for estimation of moduli of unbound materials using dynamic drum force.***

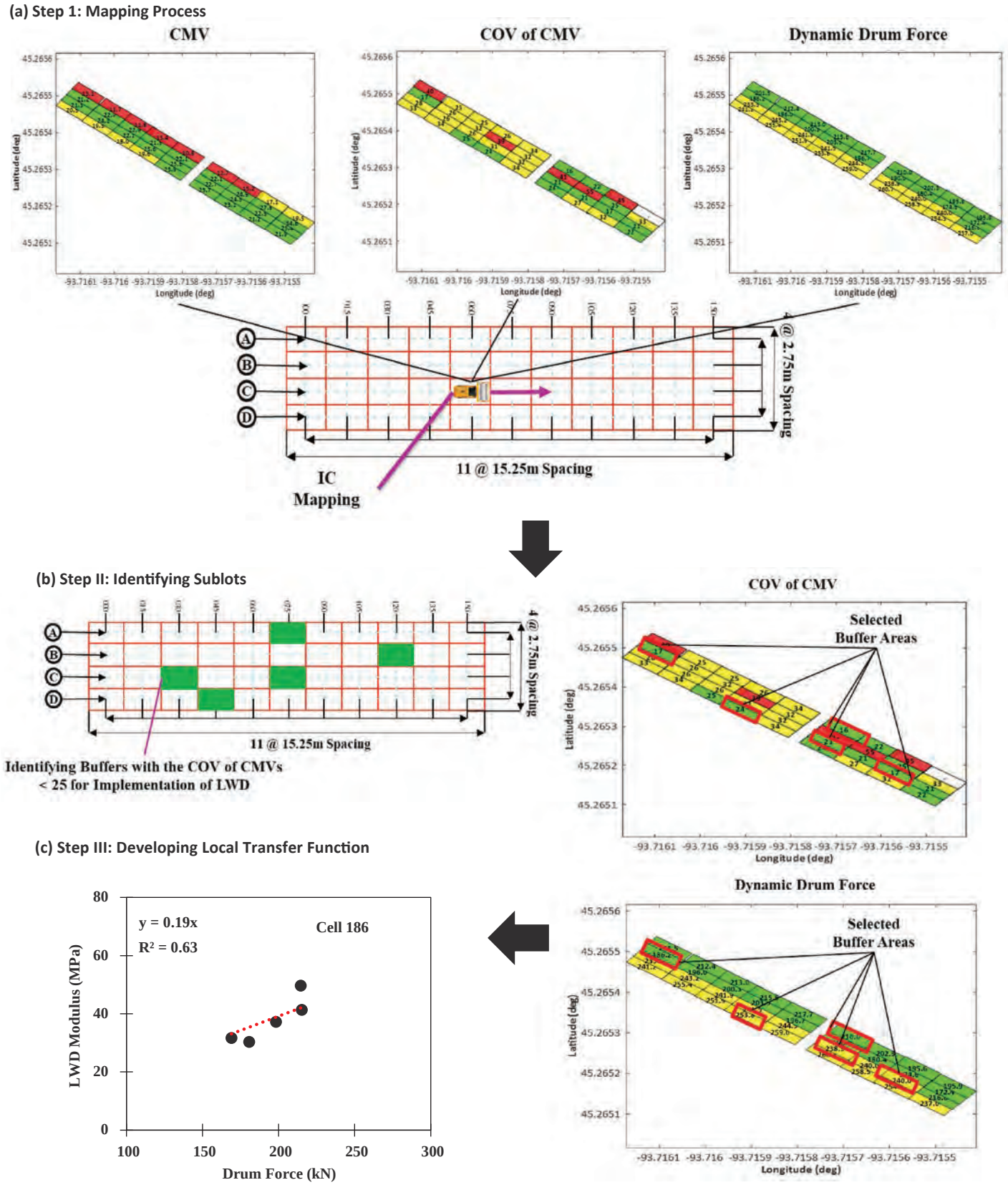


*Figure 6-11. Process of retrieving modulus using dynamic force for sandy subgrade at MnRoad (Cell 186).*

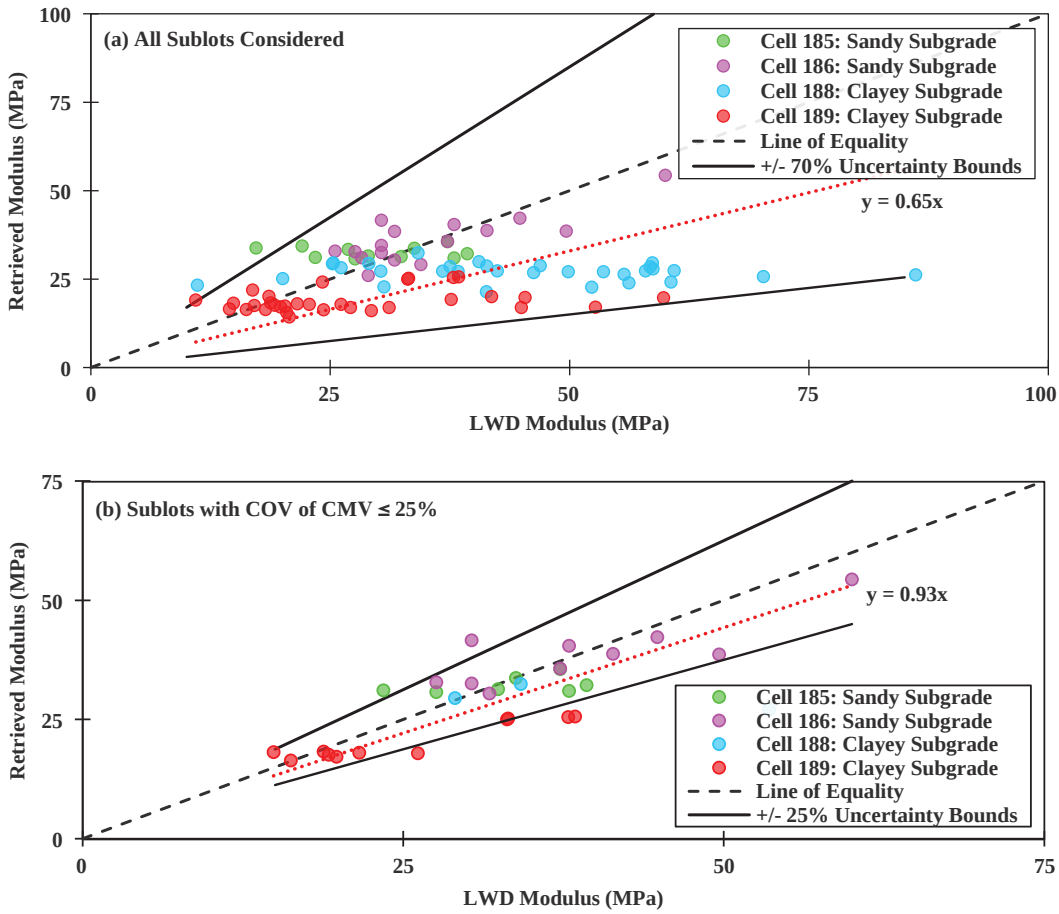


***Figure 6-12. Relationship between retrieved modulus and LWD modulus for sandy and clayey subgrade sections at MnROAD using (a) all sublots and (b) sublots with COV of CMVs less than or equal to 25%.***

COV of CMV, and drum force. Five sublots with COV of the CMVs less than or equal to 25% were selected for conducting LWD tests, as seen in Figure 6-11(b). The drum forces and LWD moduli from the selected sublots were used to develop a local calibration factor, as shown in Figure 6-11(c). The moduli of all sublots were then calculated by multiplying the adjustment factor by the corresponding drum forces.

Figure 6-12 compares the retrieved and LWD moduli for all sublots of the subgrade sections evaluated at MnROAD (cells 185, 186, 188, and 189). Figure 6-12(a) shows the results of this approach, excluding the condition imposed to the variability of CMV measurements (i.e., uniformity of the proof-mapped section) discussed above. Figure 6-12(b) compares the LWD and retrieved moduli by considering the condition of selecting the sublots with COV of the CMVs less than or equal to 25% to develop the adjustment factor.

Identifying sublots exhibiting more uniformity in their CMV measurements significantly reduces the uncertainty of the calculated moduli as obtained from the drum force. As seen in Figure 6-12(b), data points tend to fall closer to the line of equality.

CHAPTER 7

# Observations from Implementation of Specification

## Introduction

To evaluate and validate the practicality of the developed forward models and backcalculation algorithms under field conditions, four additional test construction sites were visited for actual field implementation of IC. The evaluation and validation processes at these sites were aimed to help understand the variabilities associated with the construction and compaction phases under field conditions. The four sites were located in Minnesota, Ohio, and Texas. Detailed information about the test sites and the rollers used appears in Table 7-1, and the pavement structures of each test section are shown in Figure 7-1. Actual test sections showing representative line passes during proof-mapping and sublots are illustrated in Figures 7-2 through 7-5.

## Field Testing Program and Test Layout

The following activities were undertaken at the construction sites:

1. **Identification of Test Section.** The research team, along with the contractor and DOT personnel, identified a test section that at least spanned 60 m (200 ft.) in length and had a minimum width of 7.5 m (24 ft.).
2. **Setup of GPS.** The research team set up a base station or connected to the DOT or contractor's base station.
3. **Setup of IC Roller.** The research team set up the IC roller using the data acquisition system described in Chapter 4. The IC roller was checked for proper data collection, including vibration frequency, amplitude, and roller speed.
4. **Installation of Instrumentation.** Geophones were embedded into the soil at different depths and were connected to a second data acquisition system to monitor the propagation of roller vibration. Figure 7-1 shows the depths of the geophones for each test section.
5. **Setup of Grid.** At each test section, the team set up a grid of points to define sublots and fine-tune the models. A total of 44 points were marked and latitude/longitude coordinates were measured using a GPS rover at each of the marked points. Four rows of 11 points spanning the test section length were marked. Each row of points was placed under the line pass path to be traversed by the IC roller during mapping operations. Rows were spaced equidistantly based on the roller's drum length along the test section width, as shown in the field test layout in Figure 7-6.
6. **Proof Mapping (following Compaction).** An IC roller was used for proof mapping the layer after the completion of compaction. Test section was mapped using one forward pass of the IC roller.
7. **Field Testing.** Field testing was carried out using LWD and NDG equipment on the compacted surface as soon as proof mapping was completed at each of the marked

**Table 7-1. Validation field test sites.**

| Site | Location | Length | Section | Layer | Roller * | Drum Mass (Weight) |
|---|---|---|---|---|---|---|
| 1 | El Paso, TX | 66 m (220 ft.) | Lomaland Park | Embankment<br>300 mm (12 in.) Subgrade | Hamm H11 ix | 5,890 kg (12,985 lb.) |
| 2 | Burnsville, MN | 75 m (250 ft.) | I-35W, North-bound Ramp | Subgrade<br>300 mm (12 in.) Subbase | Caterpillar CS74B | 5,153 kg (11,360 lb.) |
| 3 | Springfield, OH | 75 m (250 ft.) | I-70 West-bound Lane | Cement-Treated Subgrade (4% Cement)<br>150 mm (6 in.) Aggregate Base | Caterpillar CS74B | 5,153 kg (11,360 lb.) |
| 4 | El Paso, TX | 66 m (200 ft.) | US-62/180, Westbound Lane | Embankment<br>300 mm (12 in.) Subgrade | Volvo SD75 | 3,610 kg (8,025 lb.) |

* These tests were conducted at existing worksites using the contractors' rollers. One model (the Caterpillar SC74B) matched equipment that had been used in the developmental field tests, but three models (the Hamm H11 ix, Caterpillar CS74B, and Volvo SD75) differed from those used in the earlier tests.

44 points. Moisture samples also were collected at each of the spot tests for validation of the NDG data.

8. **Collect Sample Material.** Samples of the materials used to make up the pavement layers were collected for resilient modulus testing in the laboratory. Nonlinear material parameters were obtained for input into the backcalculation of modulus algorithms.

The research team did not interfere with the construction operation, and the IC mapping and spot testing were conducted at a time that was least disruptive to the contractor (Figures 7-7 and 7-8). A Caterpillar CS74B smooth-drum IC roller, similar to the one used at the MnROAD facility, was used at Site 2 and Site 3, whereas a Hamm H 11ix smooth-drum roller was operated at Site 1 and a Volvo SD75 at Site 4. All of the rollers were operated under low-amplitude and low-frequency conditions, as listed in Table 7-2. Data was collected using embedded geophones, starting at least 35 m before and ending 35 m after the geophone locations by synchronizing the roller-mounted GPS units with units located next to the embedded geophones.

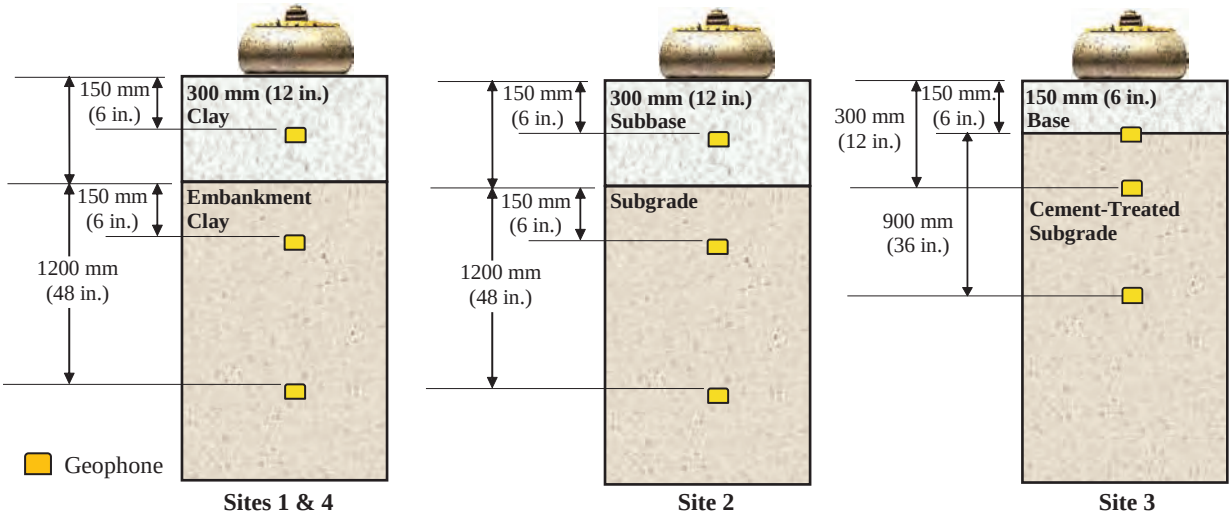


***Figure 7-1. Pavement structure of test sections and locations of embedded geophones.***


*Figure 7-2. Overview of Lomaland Recreational Center construction in El Paso, Texas, showing (a) location of test site, (b) line passes during proof mapping of embankment, (c) test section with sublots, and (d) IC roller used at this location.*

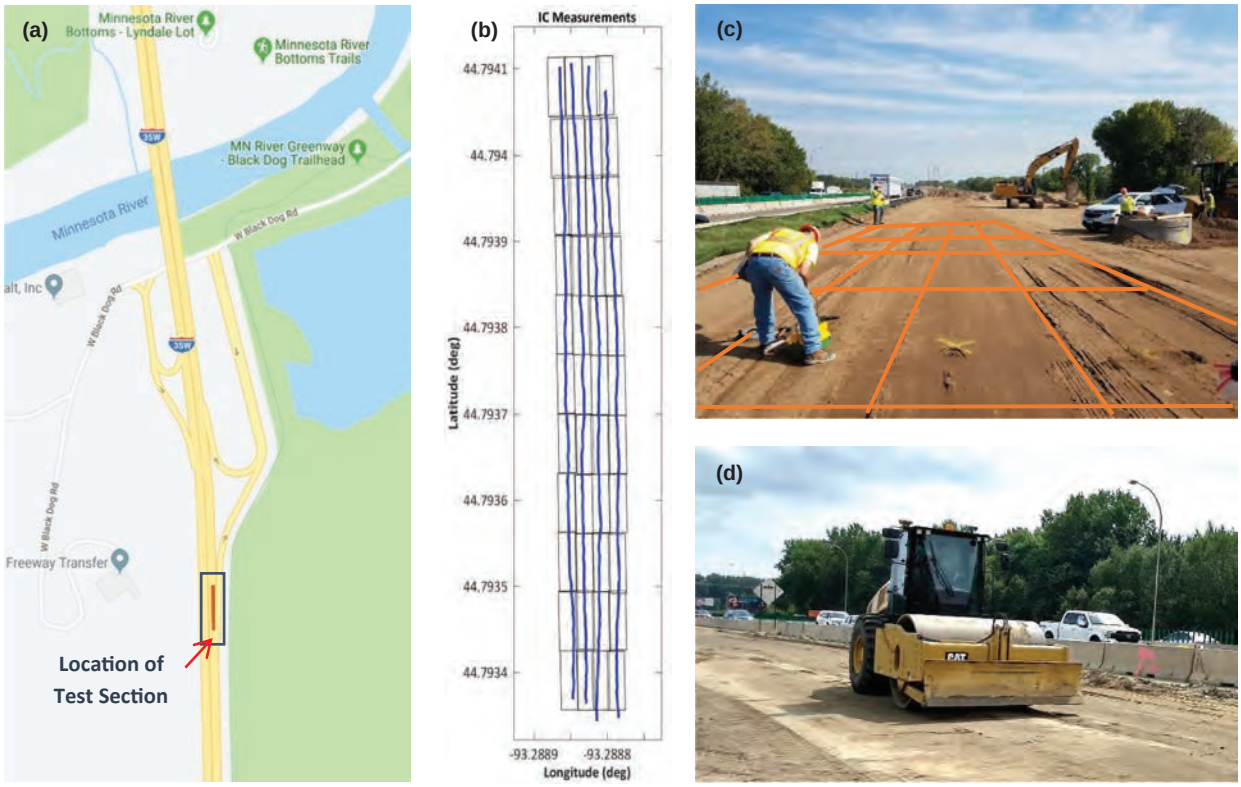


*Figure 7-3. Overview of I-35W northbound reconstruction in Burnsville, Minnesota, showing (a) location of test site, (b) line passes during proof mapping of subgrade, (c) test section with sublots, and (d) roller during proof-mapping of subgrade.*


***Figure 7-4. Overview of I-70 westbound reconstruction in Springfield, Ohio, showing (a) location of test site, (b) line passes during proof mapping of subgrade, (c) test section with sublots, and (d) roller during proof mapping of subgrade.***

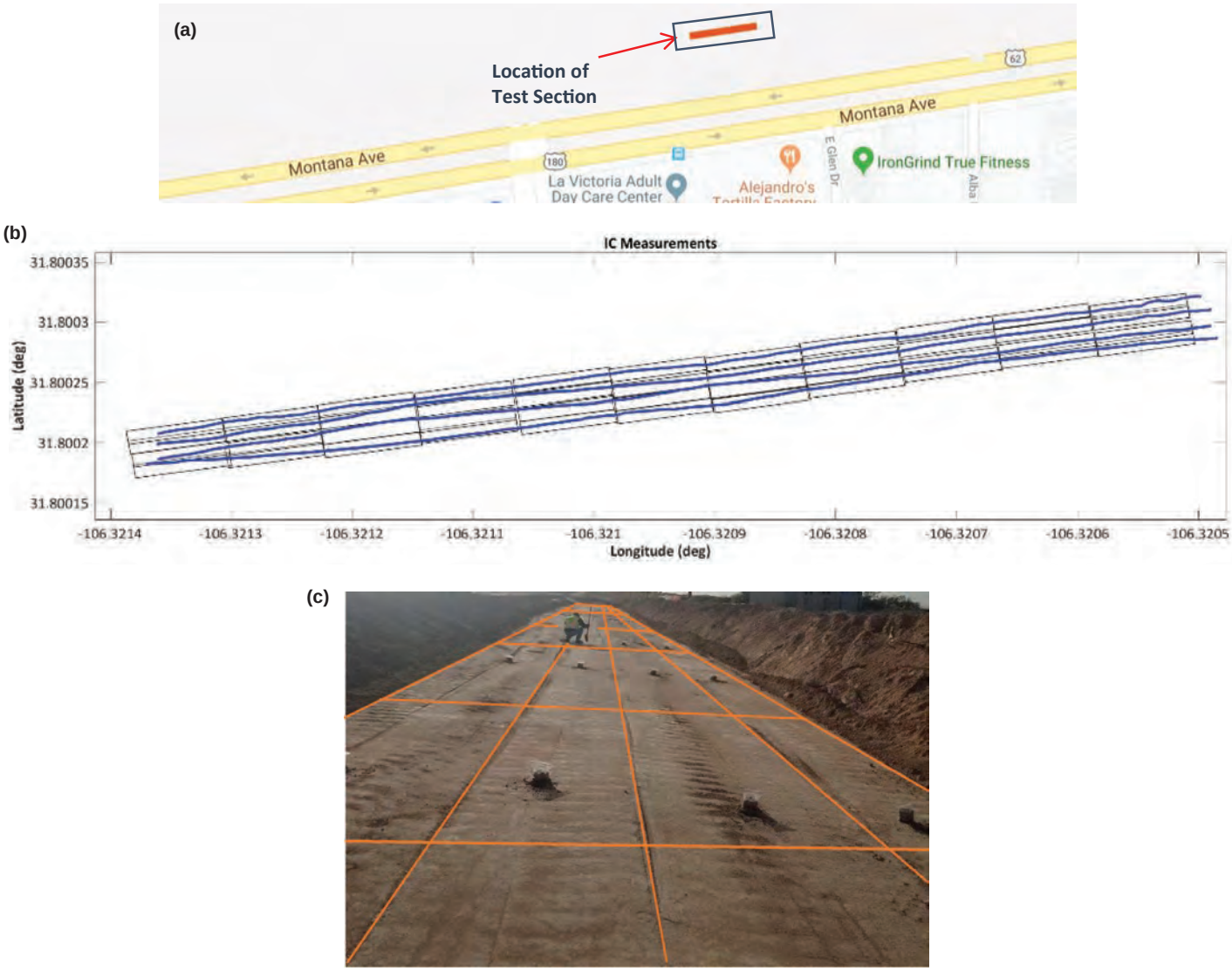


*Figure 7-5. Overview of US-62/180 westbound construction of Montana Expressway in El Paso, Texas, showing (a) location of test site, (b) line passes during proof mapping of subgrade, and (c) test section with sublots.*


*Figure 7-6. Installation process of embedded geophones: (a) GPS localization, (b) drilling with auger, (c) embedding ground sensors, and (d) wiring of geophones to data acquisition system.*

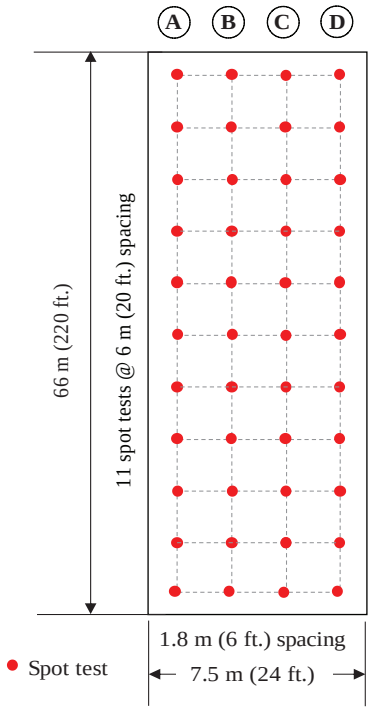


***Figure 7-7. Schematic of spot-test layout.***

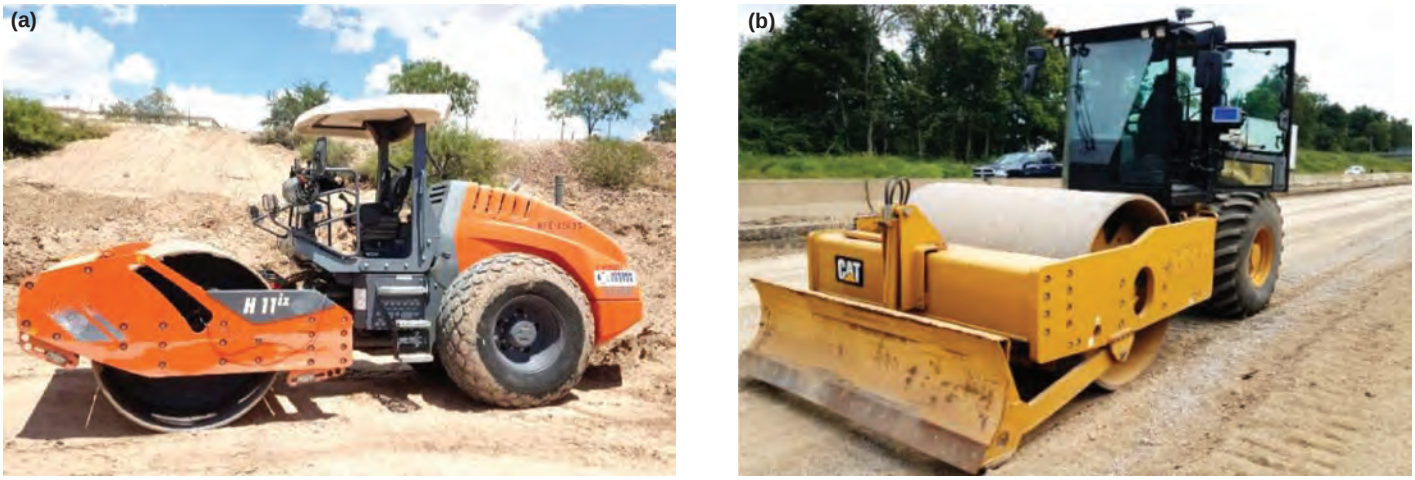


***Figure 7-8. Smooth-drum IC rollers used for mapping: (a) Hamm H 11ix, used at Site 1, and (b) Caterpillar CS74B, used at Site 2 and Site 3.***

**Table 7-2. Specifications of instrumented IC rollers.**

| Vendor/Manufacturer | Model | Width (m) | Drum Mass (kg) | Centrifugal Force (kN) | Frequency (Hz) | Where Used |
|---|---|---|---|---|---|---|
| HAMM | H 11ix | 2.1 | 5,890 | 136 | 30 | Site 1 |
| Caterpillar | CS74B | 2.1 | 5,153 | 166 | 23 | Sites 2 and 3 |
| Volvo | SD75 | 1.7 | 3,610 | 121 | 30 | Site 4 |

## Laboratory Testing

Table 7-3 summarizes the index properties of all sampled materials, including the classification of each geomaterial, as per the Unified Soil Classification System (USCS). The optimum moisture contents and maximum dry unit weights, obtained as per standard Proctor tests (AASHTO T99) for the subgrades and as per modified Proctor tests (AASHTO T180) for base materials, also are reported in the table.

Resilient modulus tests were performed in the laboratory as per AASHTO T307-03 to determine the resilient modulus and nonlinear parameters of geomaterials sampled at the test sections. Representative specimens prepared for resilient modulus testing are shown in Figure 7-9. The results of resilient modulus tests are summarized in Table 7-4 at the optimum moisture content (OMC).

## Validation of Approaches to Extract Modulus

The outcomes of the field test implementation of the two approaches discussed in Chapter 6 are presented in the balance of this chapter.

### Extracting Modulus Using ANN Inverse Solvers (Approach 1)

The inverse solvers make use of the input variables containing the nonlinear parameters obtained from the combination of both laboratory and field measurements, layer thickness of the top layer, and surface deflection from the accelerometer measurements. Using the geophone displacements obtained from the test sites, the inverse solvers were further fine-tuned to

**Table 7-3. Summary of index properties of construction site materials.**

| Site | | 1 | 1 | 2 | 2 | 3 | 4 |
|---|---|---|---|---|---|---|---|
| Layer | | Embankment | Subgrade | Subgrade | Subbase | Base | Embankment Subgrade |
| Material Type | | Sand | Sand/Clay | Poorly Graded Sand | Poorly Graded Sand | Well-Graded Gravel | Sand/Clay |
| USCS Classification | | CL | CL | SP | SP | GW | CL |
| Gradation (%) | Gravel | 0.0 | 0.0 | 16.1 | 16.1 | 42.8 | 0.0 |
| | Coarse Sand | 4.0 | 4.8 | 62.2 | 62.2 | 35.3 | 3.8 |
| | Fine Sand | 46.0 | 45.2 | 17.4 | 17.4 | 12.0 | 48.2 |
| | Fines | 50.0 | 50.0 | 2.4 | 2.4 | 1.2 | 48.0 |
| Atterberg Limits (AASHTO T-89 and T-90) | Liquid Limit (LL) | 20 | 25 | Non-Plastic | Non-Plastic | Non-Plastic | 22 |
| | Plastic Limit (PL) | 12 | 15 | | | | 13 |
| | Plasticity Index (PI) | 8 | 10 | | | | 8 |
| Moisture/Density (AASHTO T-99) | Optimum Moisture Content (%) | 13.8 | 17.1 | 7.1 | 7.1 | -- | 13.8 |
| | Maximum Dry Density | 1,853 kg/m$^3$ (115.7 pcf) | 1,802 kg/m$^3$ (112.5 pcf) | 2,142 kg/m$^3$ (133.7 pcf) | 2,142 kg/m$^3$ (133.7 pcf) | -- | 1,899 kg/m$^3$ (118.5 pcf) |
| Moisture/Density (AASHTO T-188) | Optimum Moisture Content (%) | -- | -- | -- | -- | 6.5 | -- |
| | Maximum Dry Density (MDD) | -- | -- | -- | -- | 2,289 kg/m$^3$ (142.9 pcf) | -- |


***Figure 7-9. Preparation of soil for testing: (a) soil mixture based on the sieving analysis, (b) prepared samples for resilient modulus test, and (c) MTS® Load Unit System.***

improve the predictive accuracy following the process described in Chapter 6 and illustrated in Figure 6-6. The surface displacement data obtained for each sublot during the proof-mapping process was input into the appropriate ANN inverse solver. Also input were the nonlinear $k'_2$ and $k'_3$ parameters obtained from the resilient modulus tests, along with the nonlinear $k'_1$ parameter adjusted using the LWD modulus at representative sublots.

The comparison of the measured and extracted moduli for each sublot obtained from the ANN inverse solver for the single-layer systems of the three test sites is shown in Figure 7-10. The inverse solver can predict the modulus of the subgrade with a variability of up to 25%. This level of variability was deemed acceptable given the variability of the earthwork in each sublot.

Similarly, the top-layer moduli for the two-layer systems were extracted using the appropriate ANN inverse solver. In addition to the nonlinear parameters obtained from the laboratory resilient modulus tests, the surface displacements measured on top of both the single-layer and

**Table 7-4. Geomaterial properties of test sections used for validation of inverse models.**

| Sites | Layer Two Thickness $h$ (mm) | Nonlinear Parameters for Layer One* | | | Nonlinear Parameters for Layer Two* | | | Modulus* (MPa) | | | | Surface Displacement on Top of | |
|---|---|---|---|---|---|---|---|---|---|---|---|---|---|
| | | | | | | | | $E_{LWD}$ | | $MR$ | | Layer 1 | Layer 2 |
| | | $k'_{1\text{-}back}$ | $k'_2$ | $k'_3$ | $k'_{1\text{-}back}$ | $k'_2$ | $k'_3$ | Layer 1 | Layer 2 | Layer 1 | Layer 2 | $d_1$ (mm) | $d_2$ (mm) |
| 1 | 300 | 217 | 1.57 | -2.04 | 313 | 1.24 | -3.00 | 39 | 40 | 40 | 39 | 1.07 | 1.11 |
| 2 | 300 | 598 | 1.69 | -2.16 | 267 | 1.69 | -2.16 | 130 | 58 | 115 | 51 | 1.26 | 1.52 |
| 3 | 150 | 1581 | 0.61 | -0.05 | 329 | 0.57 | -0.05 | 231 | 91 | 230 | 103 | 1.08 | 1.05 |
| 4 | 300 | 213 | 1.76 | -2.6 | 214 | 1.76 | -2.6 | 40 | 29 | 37 | 37 | 1.07 | 1.11 |

*$E_{SUBG}$ is the subgrade modulus, in this case using the LWD modulus determined on top of subgrade. $MR_{SUBG}$ is the resilient modulus of subgrade material as obtained from the resilient modulus test as per AASHTO T-307, and $k'_{1\text{-}back}$ is the backcalculated $k'_1$ value using the LWD modulus $E_{LWD}$ of the corresponding layer in Equation 3-2 following the model from Ooi et al. (2004).

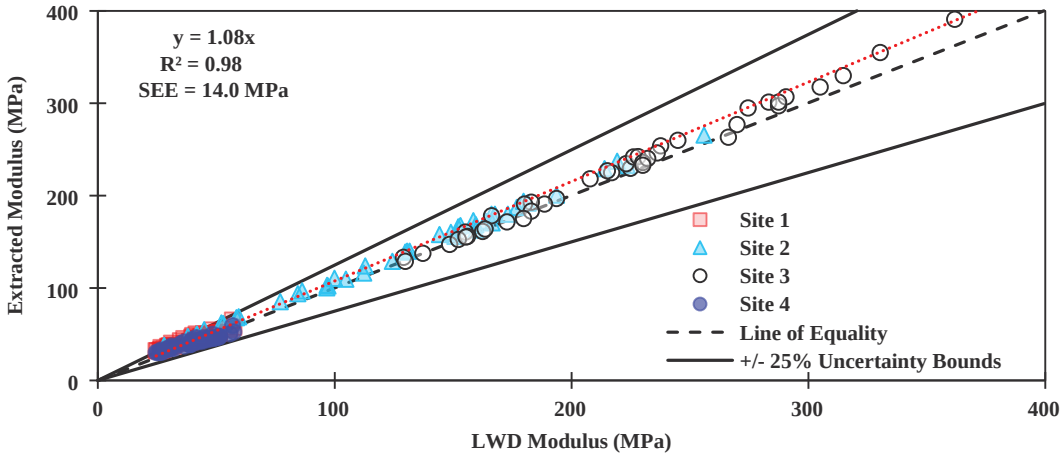


***Figure 7-10. Comparison of LWD and extracted moduli for single-layer systems for Sites 1–4.***

two-layer systems of each sublot were used as inputs. Figure 7-11 compares the extracted moduli of the top layer with the corresponding backcalculated LWD moduli. Comparing Figure 7-10 with Figure 7-11, the two-layer inverse model extracts the moduli with less accuracy than the single-layer inverse model but still falls within the ±25% uncertainty bounds (a variability of up to 25%).

### *Variability of Extracted Modulus Due to Number of Spot Tests*

Given that an extensive testing program is impractical in day-to-day operations, the research team also assessed the minimum number of spot tests with LWD. The sublots exhibiting considerable nonuniformity were first excluded because they introduced significant uncertainty in the process. Based on a substantial field database, Tirado et al. (2019) defined sublots with COV of CMVs 25% and less as "uniform."

Figure 7-12 compares the extracted moduli and the LWD moduli averaged per station for the subgrade layers of Site 1 through Site 4. The error bars represent one standard deviation of moduli at each station. The extracted moduli shown in the figures exhibit little variability

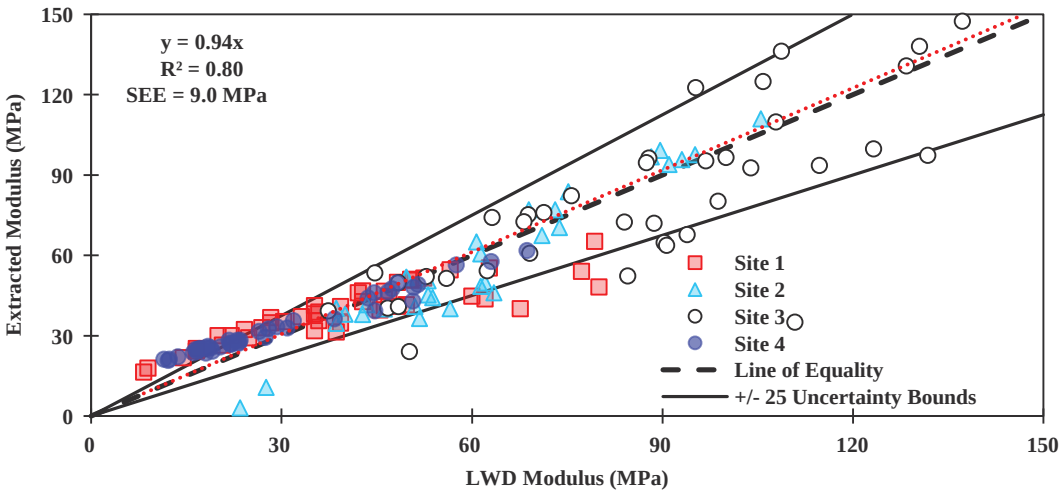


***Figure 7-11. Comparison of LWD and extracted moduli for two-layer systems for Sites 1–4.***

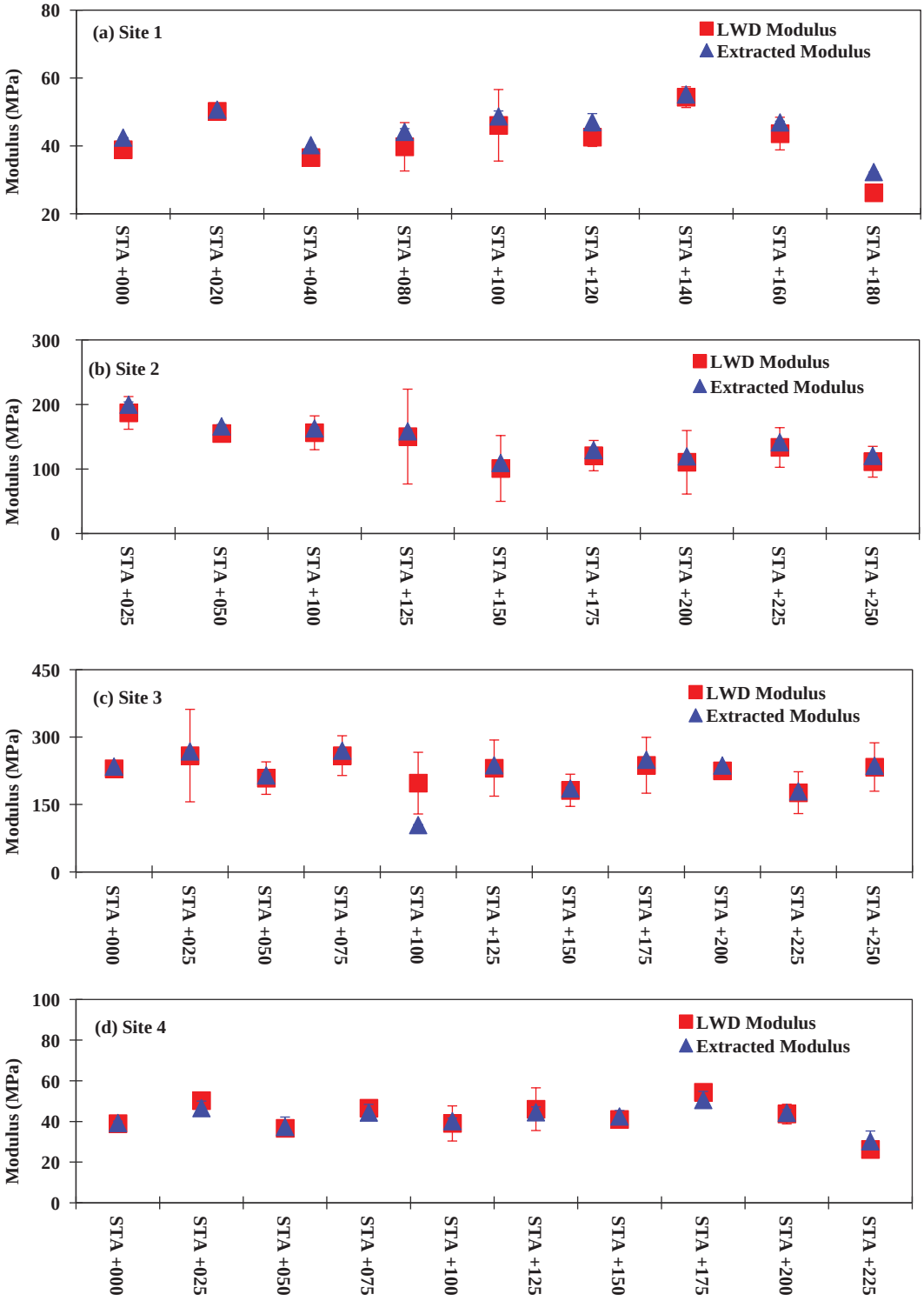


***Figure 7-12. Relationship between LWD measured and extracted moduli per station for single-layer systems in Sites 1–4.***

because each point was calculated using an average of up to 50 surface displacement values measured in each sublot, and also because the single $k_1'$ value has been adjusted and assigned to represent a station. The LWD and extracted moduli exhibit similar trends along the length of the lot for all four sites. Similarly, for two-layer systems, the backcalculated LWD moduli and extracted top layer moduli using the inverse solver exhibited similar trends along the lots, as shown in Figure 7-13.

Figures 7-14 and 7-15 compare the color-coded maps of the LWD moduli and the moduli extracted from the inverse solvers for single-layer and two-layer systems at Site 1, respectively, after implementing this procedure. The LWD modulus and backcalculated modulus maps show some resemblance. Blank sublots in the extracted modulus map correspond to sublots with considerable variability in their ICMVs (COVs greater than 35%), and thus were removed from the verification process.

Figure 7-16 shows the percent difference between the extracted and the LWD moduli per site. A mean percent error (MPE) of 10% exists when using 11 spot-test measurements. Maps of the estimated moduli for the single-layer and two-layer systems, calibrated with five LWD tests, are also shown in Figures 7-14 and 7-15, respectively. Reducing the number of LWD tests to five in sublots with COV of CMVs of less than 25% results in an increase in MPE to 23%. Thus, using five spot tests still provides extracted moduli within ±25% accuracy, which is appropriate given the inherent variability of soils.

## Using Drum Force to Extract Modulus (Approach 2)

The second approach for the extraction of modulus, described in Chapter 6, employs an inverse model that uses the roller's drum force and LWD spot measurements at selected locations with COVs of CMV of 25% and less. Figure 7-17 shows the COVs of CMV for the drum force and LWD modulus at every sublot of the embankment of Site 1. Sublots with COVs of 25% and less are shown in green. Selected sublots for conducting LWD testing are highlighted in the maps. The same process was applied to the 300 mm (12 in.) layer of clay material laid on top of the embankment for identifying potential sublots for conducting LWD. Values within these sublots were used to develop a localized calibration factor between the drum force and LWD modulus (see Figure 7-18).

Figure 7-19 compares the estimated moduli from the drum force with the LWD-measured moduli on top of the embankment and the additional 300 mm (12 in.) layer in areas with COVs of CMV of 25% and less. The extracted moduli are in general agreement with the LWD moduli for both layers as judged by the number of cases falling within the ±25% uncertainty bounds. The uncertainty in the estimation of modulus using the drum inertial force can be closely related to the level of uniformity achieved for the compacted section. In other words, the more uniform the section is, the more certain the modulus estimation will be.

### *Validation of Approach 2 Using Expanded Database*

To further validate the proposed approach, a database assembled from an extensive IC testing program that was acquired as part of a Texas Department of Transportation research project (FHWA/TX-19/0-6903-1) was used. Table 7-5 summarizes the general information about the test sites. The data consisted of CMV, surface deflection, and drum force measurements. LWD testing was conducted as part of the field evaluation of the single-layer and two-layer systems at a 7.5 m (25 ft.) spacing along the roller line passes at the center of each sublot.

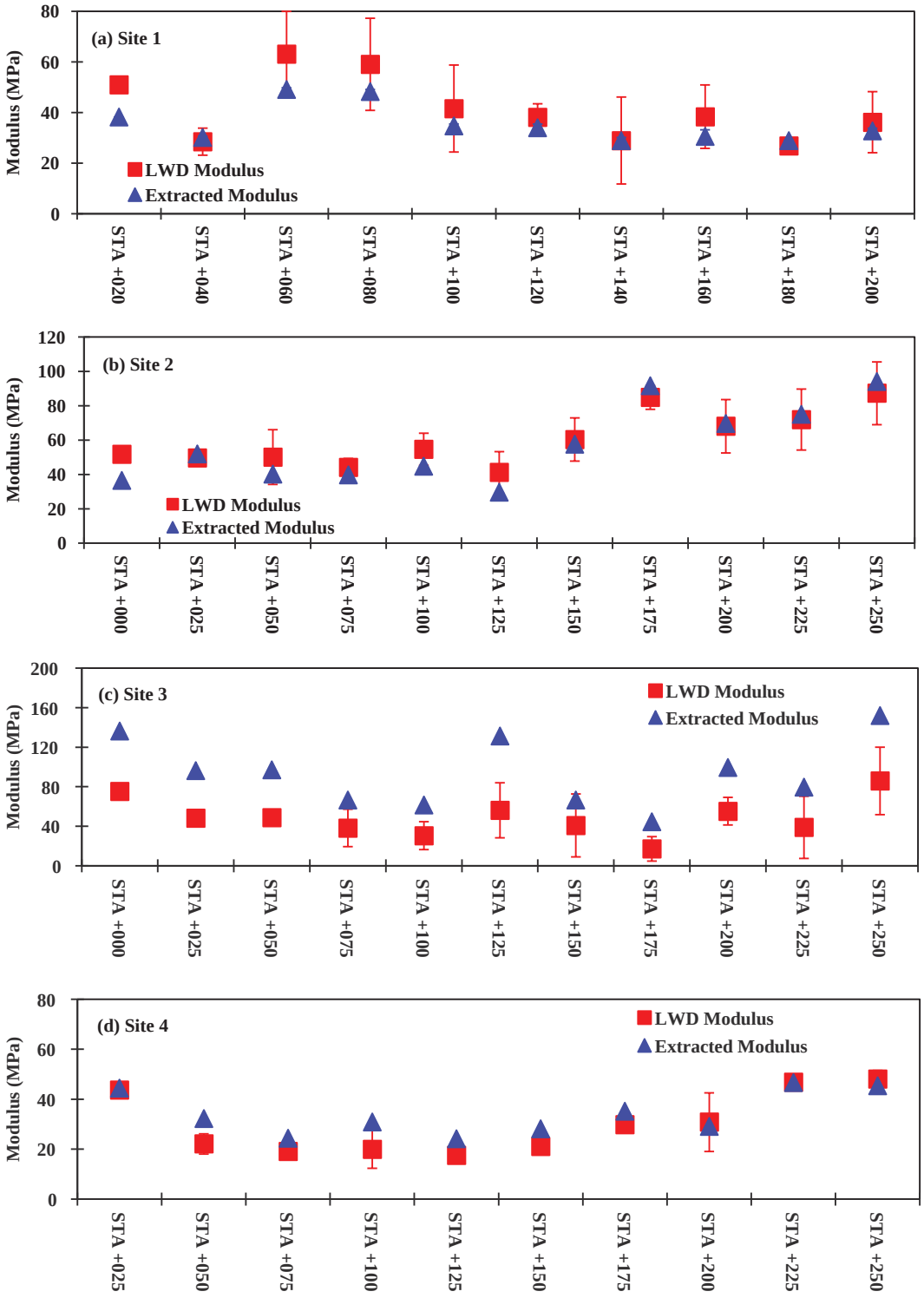


*Figure 7-13. Relationship between averaged rectangular buffered areas measured and extracted moduli for two-layer systems in Sites 1–4.*

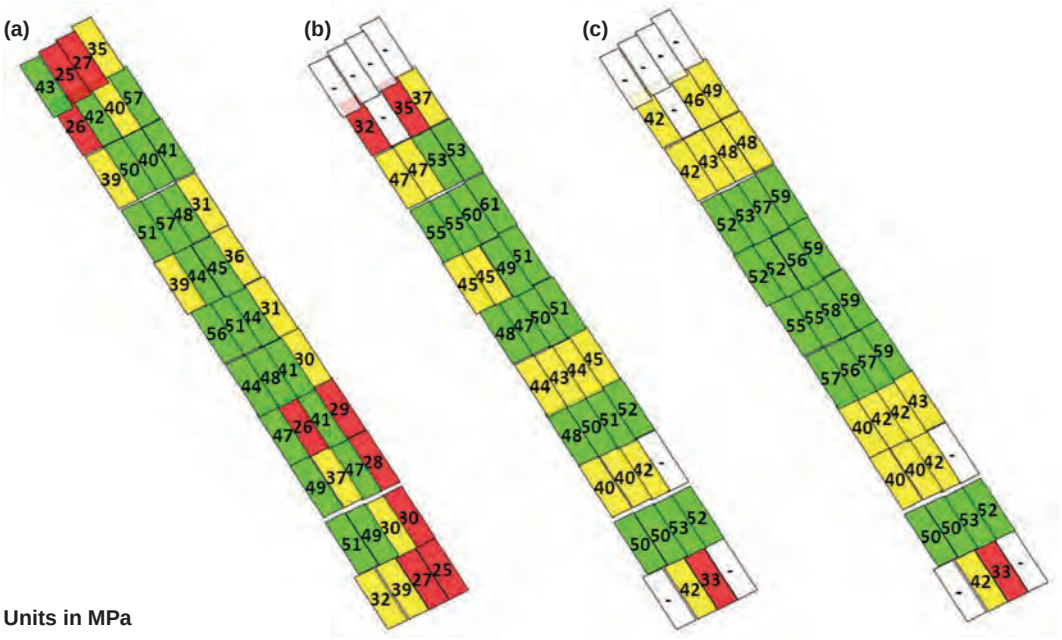


*Figure 7-14. Comparison of mapping of (a) LWD modulus and extracted modulus for a single layer in Site 1, calculated using (b) 11 spot tests and (c) 5 spot tests.*

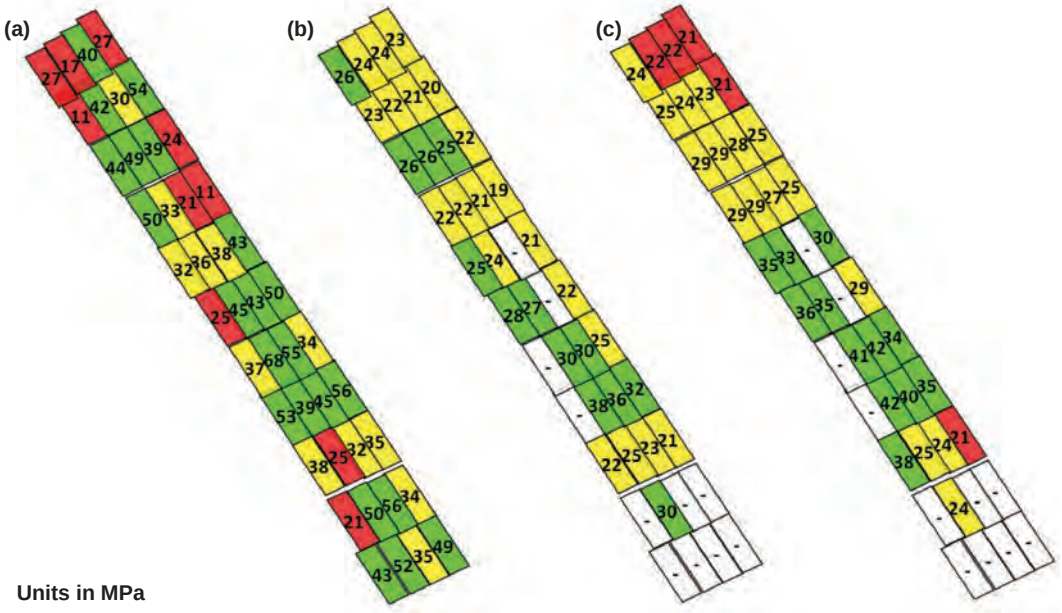


*Figure 7-15. Comparison of mapping of (a) LWD modulus and extracted modulus for two-layer system in Site 1, calculated using (b) 11 spot tests and (c) 5 spot tests.*

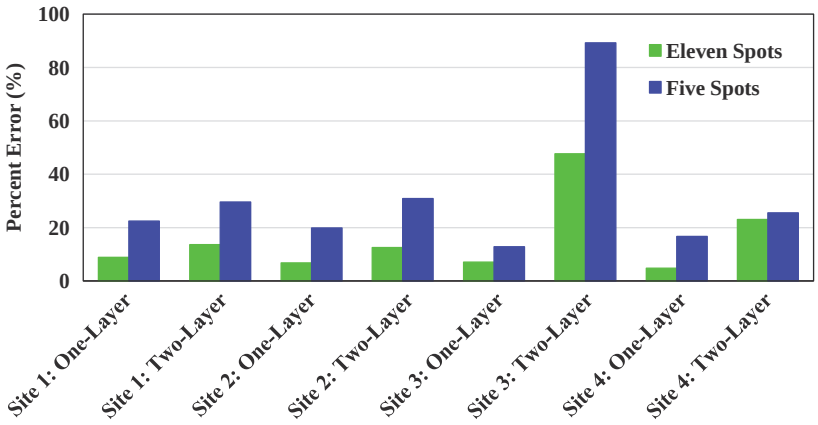


*Figure 7-16. Comparison of variability of inverse solver extracted modulus with respect to LWD modulus for all sites and for single-layer and two-layer systems.*

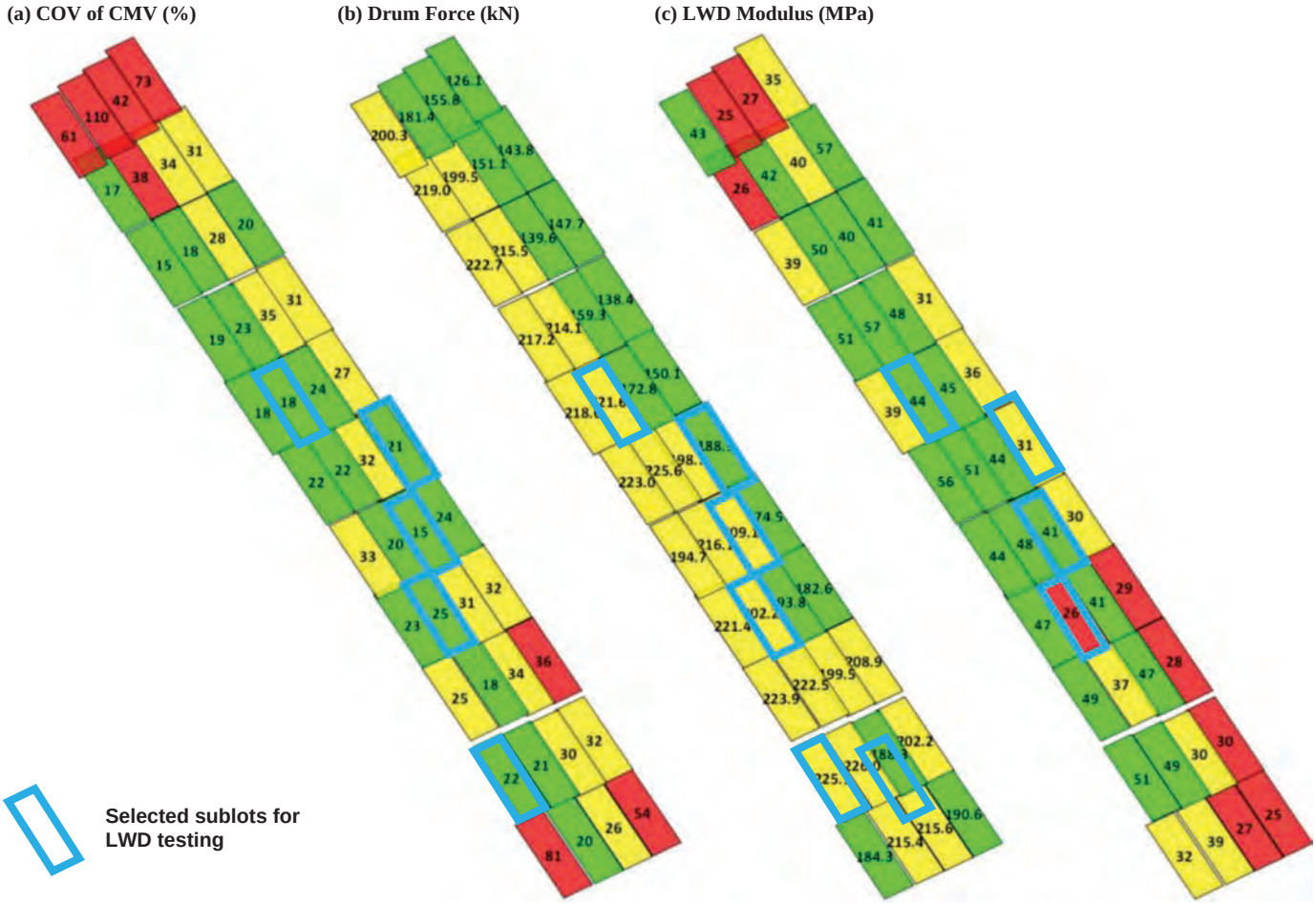


*Figure 7-17. Mapping after compaction of embankment showing (a) COV of CMV, (b) drum force, and (c) LWD modulus.*

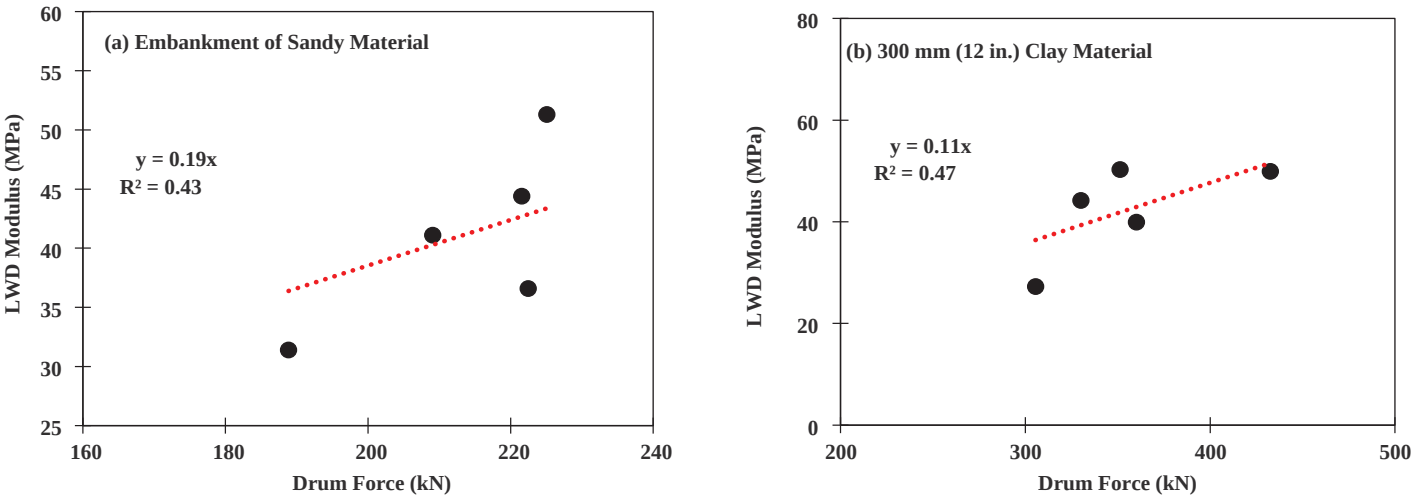


*Figure 7-18. Development of local transfer functions at Site 1 for (a) embankment of sandy material and (b) 300 mm (12 in.) clayey material.*

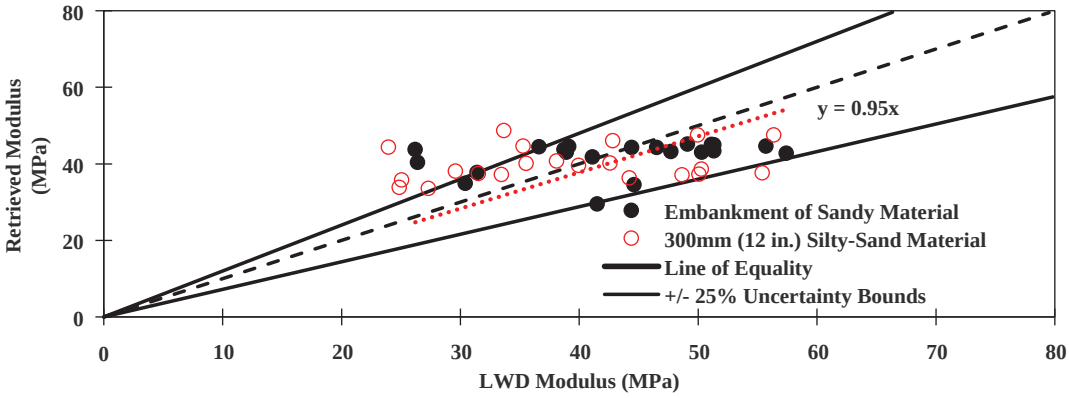


*Figure 7-19. Relationship between retrieved modulus and LWD modulus of sublots with COV of CMV less than or equal to 25% for embankment of sandy material and 300 mm (12 in.) silty-sand material.*

**Table 7-5. Validation field test sites.**

| Site | Length | Layer* | Roller | Drum Mass (Weight) |
|---|---|---|---|---|
| 5 | 75 m (250 ft.) | 150 mm (6 in.) Cement-Treated Subgrade (CTS)<br>150 mm (6 in.) Cement-Treated Base (CTB) on Top of CTS | Bomag BW 211 D-40 | 5,750 kg (12,677 lb.) |
| 6 | 75 m (250 ft.) | 300 mm (12 in.) Lime-Treated Subgrade (LTS) | CAT CS87B | 12,960 kg (28,572 lb.) |
| 7 | 75 m (250 ft.) | 450 mm (18 in.) Reclaimed Asphalt (RAP) and Base Material as Subgrade<br>150 mm (6 in.) Flexible Base on Top of RAP/Base Material Subgrade | Ingersoll Rand DD-110 | 6,075 kg (13,393 lb.) |
| 8 | 75 m (250 ft.) | 300 mm (12 in.) Cement-Treated Subgrade (CTS)<br>300 mm (12 in.) Cement-Treated Base on Top of CTS | CASE SV 212 | 7,354 kg (16,213 lb.) |

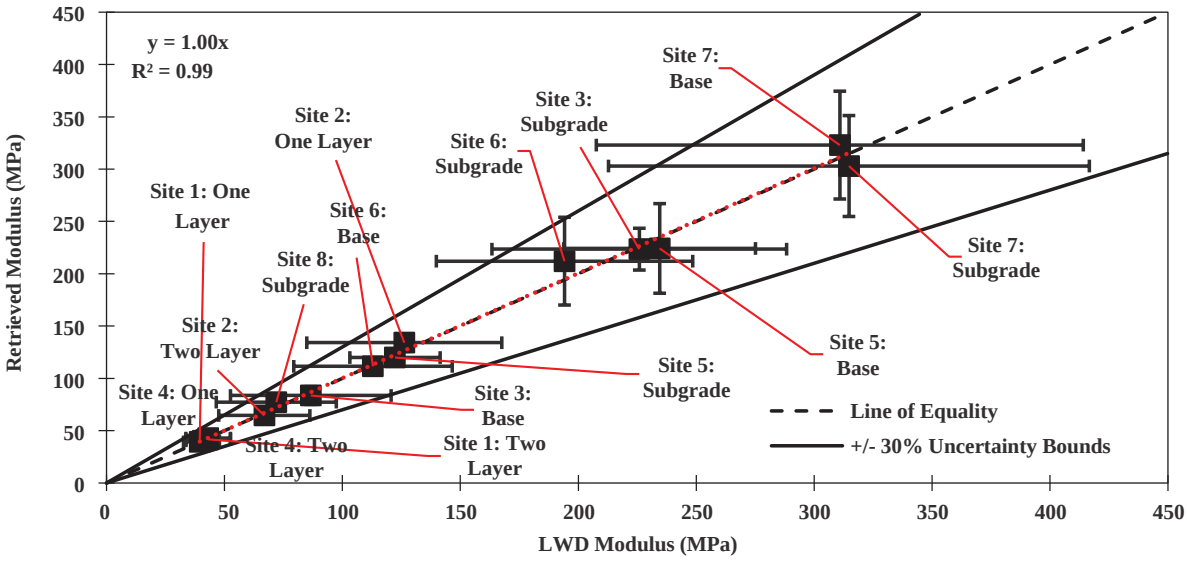


***Figure 7-20. Relationship between averaged retrieved modulus and LWD modulus.***

Figure 7-20 compares the retrieved layer moduli with their corresponding LWD moduli after implementing the proposed approach for subgrade and base materials at those test sections. Data points represent average of extracted layer moduli of the sublots with the COV of CMV less than or equal to 25% and LWD moduli as obtained for each of the evaluated test sites. The error bars show the bound between the first and third quartiles of the measurements per test site. Some extracted moduli shown in the figures exhibit little variability because each point was calculated using an average of up to 50 drum force values measured in each sublot and because these sites were more uniform in terms of ICMVs as compared to LWD moduli.

The layer modulus can be predicted using the drum force within a level of uncertainty of less than 30%. These analyses show that the modulus retrieved using the dynamic drum force can be more representative and reliable when compaction uniformity is achieved. The compaction uniformity plays a key role on retrieving the modulus of geomaterials with certainty. In other words, when the uniformity in compaction is not achieved, an LWD spot test cannot appropriately represent the quality of compaction for a sublot with approximate size of 45 $m^2$ (500 $ft.^2$).

Two approaches to using inverse solvers with differing numbers of input variables were evaluated. The first approach used an inverse solver that was developed using an extensive database that had been assembled from responses of a wide range of pavement properties and layer thicknesses using a calibrated FE model. The use of this approach required a laboratory effort to determine the needed input variables. The second approach needed fewer inputs than the first approach because it made use of the dynamic drum force. Given that compaction uniformity affects the extraction of modulus, it was found that both approaches benefit from the use of sublots exhibiting uniform compaction. This observation points toward the usefulness of developing a local calibration to reduce the variability of the model output.

## Determining Target Field Values for Quality Acceptance

For a robust acceptance process, the target field values should be set. The target value can be the stiffness for the vibratory IC rollers. Most of the deflection-based devices measure the stiffness of the pavement system, and the reported stiffness is based on an elastic half space

Boussinesq theory. This limitation is particularly critical for a multi-layered system being tested with deflection. For this study, however, an inverse model was used to determine the target stiffness (as described in Chapter 3). Table 7-6 provides the target stiffness values that were determined from the inverse model constructed for single-layer and two-layer systems for Sites 1 through 4. The target stiffness was set using the operating features of the roller (see Table 7-2), the layer thicknesses (see Table 7-1), and the nonlinear parameters obtained from the resilient modulus test.

A fair and equitable acceptance process requires appropriate tolerances based on the uncertainties in establishing the target modulus and the measuring device (in this case, the IC roller). In this study, 75% of the target stiffness served as the boundary for marginal acceptance. Figure 7-21 compares the averaged measured stiffness per station with the target stiffness obtained from the inverse solver for single-layer systems for all four sites. The error bars show the bounds between the first and third quantiles of the stiffness measurements per station. Site 3 was the only site for which the testing of the subgrade yielded stiffness measurements that marginally passed. Likewise, Figure 7-22 shows the comparison of the measured stiffness with the corresponding target stiffness obtained from the inverse solver for the two-layered systems for Site 1 through Site 4. For the two-layer systems, the measured stiffness marginally passed for all the visited sites except Site 4, where roller measurements indicated that this site did not meet the design stiffness.

With all of these steps taken into account, the vibratory IC rollers can be considered as rigorous stiffness-based devices for quality acceptance of the compacted geomaterials to replace density-measured approaches, as stiffness parameters are more relevant to and employed in pavement design even though the use of IC for quality control and acceptance might be challenging. Whenever high variability exists in the underlying ground strata, the methodology developed in this study can overcome the limitations mentioned in the literature and is capable of more realistically representing the quality and uniformity of compaction in a continuous manner.

**Table 7-6. Target stiffness values.**

| | Target Stiffness, $k_{s\text{-}Target}$ (MN/m) | |
|---|---|---|
| Site | Single-Layer | Two-Layer |
| 1 | 38 | 30 |
| 2 | 61 | 47 |
| 3 | 198 | 171 |
| 4 | 37 | 37 |

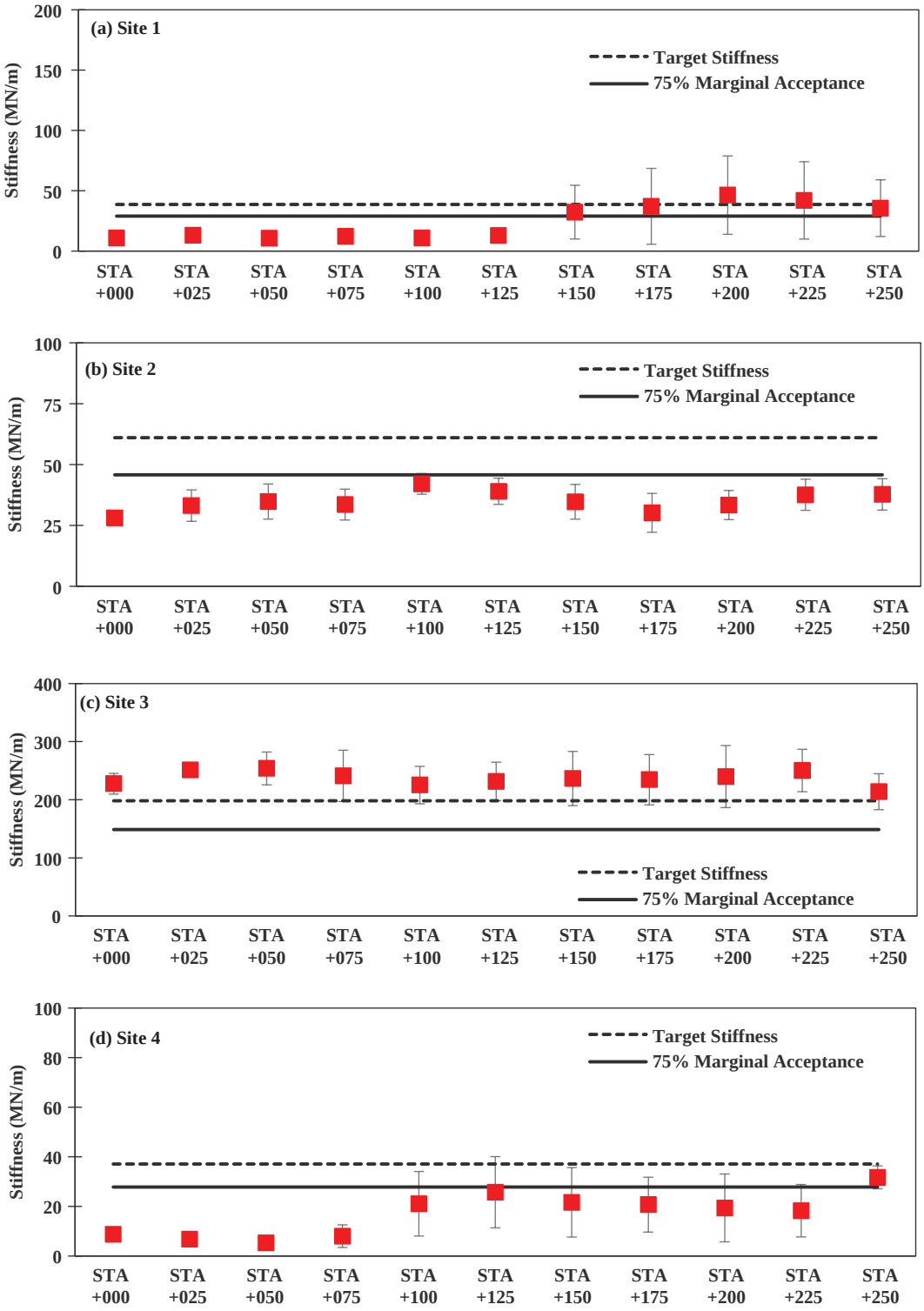


***Figure 7-21. Averaged stiffness per station, with corresponding target stiffness for single-layer systems at Sites 1–4.***

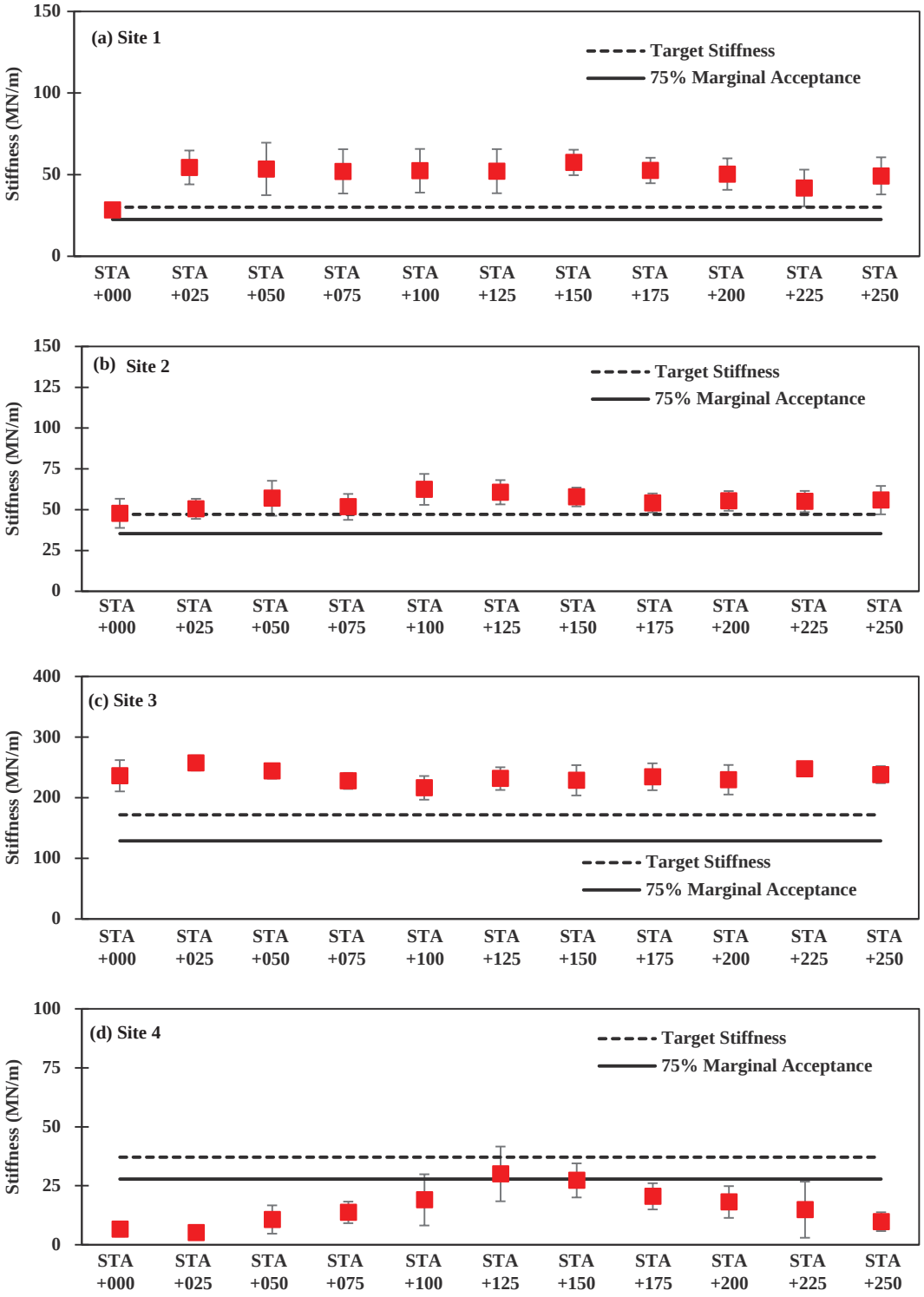


***Figure 7-22. Averaged stiffness per station, with corresponding target stiffness for two-layered systems at Sites 1–4.***

CHAPTER 8

# Framework of IC Specification

The goal of this project was to develop and propose an expanded IC specification that goes further than any existing specification. For this project, success involved ensuring balance and harmony among the technical rigors of the specification, the feasibility and level of effort to obtain the necessary input parameters, the sophistication of the forward model, and the robustness of the backcalculation process. All these elements would have been moot, however, if the roller manufacturers could not provide the necessary input parameters.

Appendix A contains two proposed specifications:

1. The "Proposed Standard Specification for Extracting Modulus of Compacted Geomaterials Using Intelligent Compaction (IC)," and
2. The "Proposed Standard Specification for Quality Management and Design Verification of Earthwork and Unbound Aggregates Using Intelligent Compaction (IC)."

The research team perceives the two specifications as complementary. The use of the second (stiffness-based) specification is adequate and practical if the goal of the SHA is routine quality management, because this approach is robust, almost real-time, and provides mechanistic-based field-target values. If the goal is to extract the moduli of the layers, however, the modulus-based approach will be more desirable. For the implementation of the modulus-based specification, the SHA should be prepared to conduct some laboratory testing up front and institute more rigorous process controls during the compaction process.

Appendix A also presents two proposed test methods that complement the proposed specifications and provide device-specific protocols. One test method addresses determining the mechanical properties of geomaterials using IC Technology, and the other addresses determining the modulus of geomaterials using LWD.

Development of the proposed specifications and test methods included the following constraints:

- The specification(s) were to be based on field measurement of the mechanical ICMVs of compacted geomaterials;
- Acceptance criteria were to be correlated with design moduli;
- The specification(s) were to provide a practical, coherent, user-friendly and well-defined method for determining mechanical properties that would be compatible with a variety of compacted geomaterials;
- Variations in the modulus of compacted geomaterials with different levels of moisture content needed to be accounted for in establishing the specification criteria and limits for compaction; and
- Available models, devices, and methods were to be incorporated in the proposed specifications.

AASHTO PP 81-14 was used as a baseline to provide continuity in the development of the specifications. The research team envisions that the SHAs may implement both earthwork specifications, following these major steps:

**Step 1: Estimating Properties of All Layers.** Geomaterials can be either in place or imported from quarries. The main properties of the geomaterials required in the proposed IC specifications are:

- Geometrical properties, such as thickness of layers, including base/subgrade/embankment;
- Index properties, including gradation parameters and Atterberg limits;
- Mechanical properties that may include the materials' resilient/elastic properties; and
- Moisture-density characteristics.

Parameters $k'_1$ through $k'_3$ should preferably be determined from laboratory tests on the geomaterial sampled from the site. Understanding the constraints that this activity may bring to the operations of highway agencies, the proposed specifications also provide an option for estimating these parameters from index properties of the geomaterial.

Different resilient modulus laboratory test protocols (e.g., AASHTO T-307 and NCHRP 1-28A) may yield different nonlinear parameters $k'_1$ through $k'_3$. The relationships provided in this report are based on the AASHTO T-307. The proposed relationships in the proposed specifications and test methods should be recalibrated by highway agencies that use other test protocols.

Equation 8-1 presents the MEPDG nonlinear material model from Ooi et al. (2004):

$$MR = k_1 P_a \left( \frac{\theta}{P_a} \right)^{k_2} \left( \frac{\tau_{oct}}{P_a} + 1 \right)^{k_3}. \tag{8-1}$$

Equation 8-2 modifies the MEPDG nonlinear material model in a way that seems to yield more representative responses of the modulus-based devices:

$$MR = k'_1 P_a \left( \frac{\theta}{P_a} + 1 \right)^{k'_2} \left( \frac{\tau_{oct}}{P_a} + 1 \right)^{k'_3}. \tag{8-2}$$

Understanding the practical problems that this change may cause for highway agencies that utilize the MEPDG material model, relationships developed in NCHRP Project 10-84, "Modulus-Based Construction Specification for Compaction of Earthwork and Unbound Aggregate," have been provided to convert parameters $k_1$ through $k_3$ (as recommended by the MEPDG) to $k'_1$ through $k'_3$ (as used in this study) in the test procedure for determining LWD modulus.

**Step 2: Simulating Roller Measurements.** The structural response algorithms are described in Chapter 3 and evaluated in Chapter 5 of this report. As discussed under the heading "Evaluation and Calibration of Forward Models," the nonlinear FE algorithm seems more appropriate for estimating the behavior of compacted geomaterials under roller-induced loads. However, the traditional FE model for simulating roller compaction of soil systems requires intensive computational resources and long simulation times, making it prohibitive for the estimation of target field measurement values during field operations. A simplified model to predict pavement responses/target measurement values with minimal computational effort and reasonable accuracy was proposed and developed using soft computing techniques. For this purpose, a comprehensive database generated by simulating a wide range of pavement structures subjected to roller compaction using a nonlinear structural model was used to develop the model

to predict pavement responses/measurement values. These responses have been calibrated using field measurements. The database, development, and calibration of these models are discussed in Chapter 3 under "Evaluation of Approaches for Developing Forward Models" and Chapter 5 under "Evaluation and Calibration of Forward Models."

The roller parameters significantly affect both the roller measurements and the behavior of geomaterials during compaction. The following roller parameters should be defined prior to the numerical simulations and field evaluations:

- Geomaterial nonlinear properties,
- Layer thickness (for two-layer systems), and
- Weight and dimensions of the drum.

Once the material properties (Step 1) and roller parameters (Step 2) are defined, the proposed simulation tool is employed to estimate a stiffness value representative of the composite response of the comprising layers down to the roller's depth of influence that will be used as a target field-measurement value. This task can be integrated with the pavement design, if desired. The process might be accompanied by estimation of discrete NDT device target values to further ensure the credibility of the established target values.

**Step 3: Pre-Mapping of Layer of Interest.** Given the depths of influence of the IC rollers, the variability in the stiffness of the existing layers propagates to the next layer. IC measurements can be performed on an existing layer to extract information about the uniformity of that layer before placing the next layer. This process is called pre-mapping. The vibration frequency and amplitude, as well as the roller direction and speed, should be nominally identical to the values specified for the mapping of the layer after the completion of compaction. The statistical information of the collected ICMVs will be determined in terms of the distribution of the ICMVs to identify the range, mean, and standard deviation. If the variability of the existing layer is significant according to either the engineer or the specification, it may be prudent to rework the existing ground to improve its uniformity before placing the next layer.

The results from the pre-mapping can also be used in the subsequent backcalculation scheme. Without pre-mapping, only one input data point is available per location. As such, only one stiffness parameter (the global stiffness) can be extracted from the IC measurement. Pre-mapping provides a second piece of information as an input to the backcalculation. Spot testing during pre-mapping is necessary for the implementation of a more robust inverse algorithm for the extraction of the layer moduli.

**Step 4: Performing Compaction to Achieve Target Stiffness.** The optimal goal of the compaction process is to achieve a uniform pavement that provides mechanical parameters that meet the design moduli. This step is conceptually straightforward but practically complex. For the contractors, one major source of frustration with the implementation of the IC is this step. For earthwork, the roller type and roller setting that are needed to achieve optimal compaction can differ considerably from the roller type and roller setting necessary for proper mapping. For example, on clayey soils, the padfoot rollers are by far more effective than the smooth drum rollers. Most current specifications require a smooth drum roller set at a low vibration setting and a slow roller speed for IC mapping. These settings are quite reasonable for mapping, but they are not always reasonable for compaction of the layer. The contractor may also need to utilize several different compactors to expedite compaction. Currently, it is marginally possible to utilize the IC data to establish the number of line passes from several rollers simultaneously; however, it is not yet feasible to extract and harmonize the ICMVs. Even when the technology becomes available, the integration of the ICMVs from more than one IC roller may need regular

harmonization (i.e., the contractors must be able to ensure that the different rollers yield similar ICMVs on the same section).

The opinion of the research team is that the use of the IC technology will accelerate when the contractors are convinced that using the IC measurements during compaction is essentially a process control that benefits their production rate and the uniformity of the final project. A contractor representative and/or the roller operator can review the real-time map of the collected IC data during compaction as a process control tool to ensure uniformity. The proposed process also can positively affect the data management issues experienced by many DOTs. DOT staff can focus on the results of the mapping, as discussed in the next step for quality control and eventually perhaps for quality assurance.

**Step 5: Mapping Compacted Layer.** After compaction is completed, the mapping of the compacted layer is performed with an IC roller. The vibration parameters, in terms of the frequency, amplitude, roller speed, and roller direction, should be identified for the mapping process. The statistical parameters of the collected ICMVs, along with the differences between the mapping and pre-mapping values, should be identified.

Mapping and pre-mapping imply the use of geospatial coordinates extracted from a Global Navigation Satellite System (GNSS). Ideally, the planar coordinates can be used to locate the position of the roller and the altitude coordinates can be used to extract the thickness of the layer being mapped. In practice, the accuracy and precision of GNSS readouts and the frequency of IC measurements will dictate the certainty of these values.

In addition to the typical mapping of ICMVs, maps allow the identification of areas that lack uniformity. As was discussed in Chapter 4, a color-coded map showing the COV of the ICMV can be used for that purpose. Maps of other operating features also can be provided as a quick check of the appropriateness of the mapping process.

**Step 6: Post-Processing to Extract Layer Mechanical Properties.** Once the mapping of the compacted layer has been completed, the post-processing is performed to extract the modulus of the compacted layer. This process has been documented as part of a second proposed specification. Ideally, one should be able to extract the layer-specific mechanical properties of the last layer and the combination of the previous layers if both pre-mapping and mapping data are available. For this purpose, soft computing techniques were used to develop inverse models to determine the layer modulus. The two approaches to developing the inverse models are documented in Chapter 6. The inputs used for feeding the models strongly affect the level of accuracy and sophistication of selected forward and inverse models, as well as the accepted tolerance in prediction of modulus. The use of more robust inverse algorithms to extract the layer properties would require additional modulus/stiffness-based nondestructive spot tests.

The unsaturated soil mechanics concepts in the extraction of stiffness parameters of the geomaterials is conceptually desirable and beneficial. To consider this concept properly in the analyses, almost-continuous measurement of the suction of the geomaterial is required. Given the current state of instrumentation, near-continuous measurement may not be possible. Alternatively, the continuous estimation of the variation in the degree of saturation (perhaps through precise measurements of the moisture content and density) is desirable. Currently, this is possible only through the use of NDG in the field. As developed in NCHRP Project 10-84, moisture content-based relationships can be used as a surrogate for the degree of saturation. The moisture content of the compacted layer can be ideally determined using either a well-calibrated NDG or a microwave oven in the field or using the oven-dry approach in the laboratory.

104 Evaluating Mechanical Properties of Earth Material During Intelligent Compaction

The research team believes that a balanced approach must be devised to develop a practical tool. Until a device that can continuously measure the moisture content and density (or, better yet, the suction) of the material, it might be more feasible and practical to use less-advanced parameters for this purpose.

The uncertainties associated with the extracted mechanical properties relate directly to the uncertainties in the measured ICMVs and to the accuracy and precision of the geospatial coordinates. The uncertainties in the ICMV measurements relate not only to the characteristics and installation and capture of the sensors but also to the analysis technique.

CHAPTER 9

# Conclusions and Recommendations

## Summary of Activities

This study started with a thorough literature review of national and international states of practice and implementation of quality control with IC technology. Reviews of the different approaches to simulate the IC roller compaction process during the mapping operation and of machine learning algorithms to extract mechanical properties of compacted geomaterials also were synthesized.

A realistic 3D nonlinear FE model to simulate the mapping process of single-layer and two-layer geosystems was developed for predicting the representative responses of the geomaterials. The FE model considered a contact model to account for the complex soil-drum interaction, permitting the loss of contact between the drum and the soil. A comprehensive database of cases with different input parameters was assembled for single-layer and two-layer geosystems and various drum dimensions with different operating conditions. Various levels of complexity in the model were evaluated to assess the impact of the vibratory conditions and to consider both linear and nonlinear geomaterial constitutive models on the pavement responses. Relationships were developed among the responses of the models with different levels of complexity to simplify the modeling.

Laboratory and field-testing activities were conducted to validate the responses from the models. To that end, the research team developed a system to evaluate the vibration characteristics of the IC rollers as well as the responses of ground layers during the mapping process. The IC data collected were partitioned into virtual sublots equal to the width of the roller and lengths equal the minimum length of the compacted section that was practical to rework. For mapping purposes, all ICMV measurements falling inside a sublot were averaged to obtain representative ICMVs. This approach allowed the researchers to accommodate the inherent uncertainty related to the accuracy of the GPS devices and the precise position of the moving roller. For practical purposes, a three color-coded scheme was used to map the representative ICMVs. To ensure uniformity throughout the site, another color-coded map was developed to assess the variability of compaction. Mapping the COV of the ICMVs within each sublot allowed the identification of sublots where the representative ICMVs were no longer reliable due to construction- or equipment-related issues.

The researchers also developed a series of inverse algorithms to provide reliable, layer-specific ICMVs for construction quality control. To achieve this, the research team assembled a comprehensive database consisting of pavement response data for single-layer and two-layer geosystems with widespread layer properties and base thicknesses. To select the parameters that had a more significant impact on the pavement responses, a sensitivity analysis was conducted to identify those variables best suited as inputs into the proposed inverse solvers. Various inverse

solvers with differing levels of complexity were proposed with the expectation that greater complexity would improve precision but also would require additional laboratory effort. The inverse solvers were evaluated, and those best suited for predicting layer moduli for both single-layer and two-layer systems were selected for validation purposes. The predictive power of the inverse solvers improved when local adjustment factors were used.

Based on the activities discussed, draft specifications were proposed and evaluated using field tests. These field tests were conducted in four tests cells constructed at the MnROAD test track facility with different subgrade and unbound aggregate base materials. Additional NDT testing, conducted along the test section at each sublot in all four cells, measured modulus-based properties of the compacted materials. The implementation of the spot tests along the test section allowed the research team to address the variability of the material in the field and its impact on the mapped ICMVs.

Samples of the materials used in the construction of the test sections were collected and transported to the laboratory to measure their in-place moisture content, index properties, and perform resilient modulus tests. The collected dataset, made up of ICMVs, roller operating settings, field test measurements using NDT, and the properties obtained from the laboratory tests, was used to calibrate the numerical models and to develop machine-learning algorithms to extract the mechanical properties of compacted geomaterials. Based on those results, the specifications were modified.

To identify any practical restrictions, fine-tune the proposed models and approaches for the extraction of the mechanical properties, and improve the proposed quality control process, the modified specifications were applied and evaluated at three new sites involving actual construction projects. The results of this evaluation were also used to improve the specification's framework.

## General Conclusions

The general conclusions based on the evaluation of the proposed specification for the extraction of mechanical properties of compacted geomaterials using IC are the following:

- The adoption of the specification needs to be approached in the context of the levels uniformity of the compaction.
- The most consistent results are obtained when proof mapping using IC is carried out in conjunction with the modulus-based measurements, and when variability in the ICMVs is kept within (less than or equal to) 25%.
- Given the large diversity in construction practices and material types, the implementation of the draft specification requires more localized field studies by DOTs to adopt it to their local materials and construction practices.

Based on this study and interaction with the highway agencies, the following comments and suggestions can be made:

- This research study provides a critical review of the strengths and concerns about the implementation of a specification to extract the mechanical properties of compacted materials using IC technology. The research team attempted to highlight the complexities that could arise and made an effort to address them in a comprehensive manner.
- Even though this report emphasizes both the strengths and concerns with the proposed specification, the proposed specification is a large step toward higher-quality highway construction.

## Recommendations Related to the Proposed Specifications

Two specifications were developed: one for stiffness-based acceptance, titled "Proposed Standard Specification for Quality Management and Design Verification of Earthwork and Unbound Aggregates Using Intelligent Compaction (IC)," and a second for extraction of modulus of compacted layers, titled "Proposed Standard Specification for Extracting Modulus of Compacted Geomaterials Using Intelligent Compaction (IC)." The proposed specifications and test methods are presented in Appendix A of this report, and contain suggestions about the areas that the state highway agencies (SHAs) should modify to match them to their needs and institutional cultures.

The use of the proposed stiffness-based specification could serve as an almost real-time approach for determining mechanistic-based field-target values for routine quality management purposes. On the other hand, the proposed modulus-based specification would be preferred if the goal of the highway agencies is to extract the moduli of the layers.

For the implementation of the modulus-based specification, highway agencies should be prepared to conduct laboratory testing up front and institute more rigorous process control during the compaction process. The proposed specifications make use of an approach for the mapping of ICMVs that consists of partitioning the lot into virtual sublots, each of them with dimensions equal to the width of the roller and the length equal to the minimum length of the compacted section that is practical to rework as set at the discretion of the engineer. ICMVs falling inside a sublot are averaged to obtain representative ICMVs. This approach is proposed to accommodate the inherent uncertainties related to the accuracy of the GPS devices and the precise position of the moving roller. The approach also facilitates identifying the less stiff areas. The proposed modulus-based specification requires using IC to identify the more uniform sublots in terms of ICMVs for conducting additional spot tests.

## Future Activities

This study demonstrates the technical benefits and challenges related to the implementation of the proposed specification for the extraction of the mechanical properties of compacted geomaterials using IC. Even though all aspects of the development of the protocols were evaluated, the number of test sections and compacted geomaterials where the algorithms and specification were evaluated, fine-tuned, and validated was limited. The current specifications for quality management of compaction of geomaterials vary significantly among the different SHAs. Because the testing conducted for this study involved a selected set of protocols and procedures that were uniformly implemented, the research team recommends a follow-on implementation project to assist SHAs as they implement and adjust the proposed protocols and specifications to local practices. The additional data gathered from such implementation projects also could contribute to a better understanding of the limitations of the process.

The findings of this research should be disseminated in a balanced way to the transportation community. The presentations should not only emphasize the benefits of the specifications but should enumerate the changes in day-to-day operations of the SHAs and means of adapting them in their operations in a gradual manner.

# References


Adam, D., and F. Kopf (2004). "Operational Devices for Compaction Optimization and Quality Control (Continuous Compaction Control & Light Falling Weight Device)." *International Seminar on Geotechnic Pavement and Railway Design and Construction* (Athens, Greece, December 16–17, 2004). Millpress, Rotterdam, The Netherlands, pp. 97–106.

Adam, D., and J. Pistrol (2016). Dynamic Roller Compaction for Earthworks and Roller-Integrated Continuous Compaction Control: State of the Art Overview and Recent Developments. *Proc. Conferenze di Geotecnica di Torino*, XXIV Ciclio, 1–41.

Anderegg, R. (1997). "Nichtlineare Schwingungen bei dynamischen Bodenverdichtern (Nonlinear Vibrations with Dynamic Soil Compactors)." Eidgenössische Technishe Hochschule ETH Zürich, Zürich, Switzerland.

Anderegg, R., and K. Kaufmann (2004). "Intelligent Compaction with Vibratory Rollers: Feedback Control Systems in Automatic Compaction and Compaction Control." *Transportation Research Record: Journal of the Transportation Research Board*, No. 1868, pp. 124–134. http://dx.doi.org/10.3141/1868-13.

Bräu, G., K. Hartman, and G. Pelz. (2004). "Flächendeckende Prufung der Verdichtung (FDVK)-Baupraktische Umsetzung und verfahrens-bezogene Verdichtungsanforderungen (CCC Testing of Compaction-Implementation in Construction Practice and Procedure-Related Compaction Specifications)." Lehrstuhl und Prüfamt für Grundbau, Bodenmechanik und Felsmechanik der Technischen Universitat München, Heft 897, München, Germany.

Buechler, S. R., G. G. W. Mustoe, J. R. Berger, and M. A. Mooney (2012). "Understanding the Soil Contact Problem for the LWD and Static Drum Roller by Using the DEM." *Journal of Engineering Mechanics*, American Society of Civil Engineers, 138(1), 124–132.

Carrasco, C., C. Tirado, and H. Wang (2014). *Numerical Simulation of Intelligent Compaction Technology for Construction Quality Control. CAIT-UTC 029 Report*, El Paso, TX.

Cary, C. E., and C. E. Zapata (2010). "Enhanced Model for Resilient Response of Soils Resulting from Seasonal Changes as Implemented in Mechanistic-Empirical Pavement Design Guide," *Transportation Research Record: Journal of the Transportation Research Board*, No. 2170, pp. 36–44. http://dx.doi.org/10.3141/2170-05.

Cary, C. E., and C. E. Zapata (2011). "Resilient Modulus for Unsaturated Unbound Materials." *Road Materials Pavement Design*, 12 (3), pp. 615–638.

Erdmann, P., and D. Adam (2014). "Numerical Simulation of Dynamic Soil Compaction with Vibratory Compaction Equipment." *XV Danube—European Conference on Geotechnical Engineering (DECGE 2014)*, H. B. & D. Adam, ed., Vienna, Austria, 243–248.

Ferris, A. J. (1985). "Developments in Compaction Control Systems." *Highways & Transportation*, 32(7), pp. 2–5.

Floss, R., G. Bräu, M. Gahbauer, N. Gruber, and J. Obermayer. (1991). "Dynamische Verdichtungsprüfung bei Erd-und Straßenbauten (Dynamic Compaction Testing in Earth and Road Construction)." Prüfamt für Grundbau, Boden-und Felsmechanik Technische Universität München, Heft 612. München, Germany.

Floss, R., W. Kröber, and W. Wallrath (2001). "Dynamische Bodensteifigkeit als Qualitätskriterium für die Bodenverdichtung (Dynamic Soil Stiffness as a Quality Criterion for Soil Compaction)." *4. Internationales Symposium Technik und Technologie des Verkehrswegebaus (4th International Symposium and Technology Series of Transportation Infrastructures)*, BAUMA, München, Germany.

Göktepe, A. B., E. Ağar, and A. H. Lav (2006). "Advances in Backcalculating the Mechanical Properties of Flexible Pavements." *Advances in Engineering Software*, 37(7), pp. 421–431.

Gupta, S., A. Ranaivoson, T. Edil, C. Benson, and A. Sawangsuriya (2007). *Pavement Design Using Unsaturated Soil Technology*, Report No. MN/RC-2007-11, Final Research Report submitted to Minnesota Department of Transportation, University of Minnesota, Minneapolis, MN.

Kenneally, B., O. M. Musimbi, J. Wang, and M. A. Mooney (2015). "Finite Element Analysis of Vibratory Roller Response on Layered Soil Systems." *Computers and Geotechnics*, 67, pp. 73–82.

Khoury, N. N., and M. M. Zaman (2004). "Correlation Between Resilient Modulus, Moisture Variation, and Soil Suction for Subgrade Soils," *Transportation Research Record: Journal of Transportation Research Board*, No. 1874, pp. 99-107. https://doi.org/10.3141/1874-11.

Kröber, W., R. Floss, and W. Wallrath (2001). "Dynamic Soil Stiffness as Quality Criterion for Soil Compaction." *Geotechnics for Roads, Rail Tracks and Earth Structures*, A.A.Balkema Publishers, Tokyo, Japan, pp. 189–199.

Malla, R., and S. Joshi (2007). "Resilient Modulus Prediction Models Based on Analysis of LTPP Data for Subgrade Soils and Experimental Verification." *Journal of Transportation Engineering*, Vol. 133, No. 9, 491–500.

Mazari, M., E. Navarro, I. Abdallah, and S. Nazarian (2014). Comparison of Numerical and Experimental Responses of Pavement Systems Using Various Resilient Modulus Models. *Soils and Foundations*, 54(1), 36–44.

McCartney, J., and A. Khosravi (2013). "Field-Monitoring System for Suction and Temperature Profiles under Pavements." *Journal of Performance of Constructed Facilities*, Vol. 27, Issue 6, pp. 818–825.

Mooney, M. A., and N. W. Facas (2013). *Extraction of Layer Properties from Intelligent Compaction Data: Final Report for NCHRP Highway IDEA Project 145*, Transportation Research Board of the National Academies, Washington, D.C.

Mooney, M. A., and R. V. Rinehart (2009). "In Situ Soil Response to Vibratory Loading and Its Relationship to Roller-Measured Soil Stiffness." *Journal of Geotechnical and Geoenvironmental Engineering*, American Society of Civil Engineers, 135(8), pp. 1022–1031.

Mooney, M. A., P. B. Gorman, E. Farouk, J. N. Gonzalez, and A. S. Akanda (2003). "Exploring Vibration-Based Intelligent Soil Compaction." Final Report, Project No. 2146. Oklahoma Department of Transportation, Oklahoma City, OK.

Mooney, M. A., P. B. Gorman, and J. N. Gonzalez (2005). "Vibration-Based Health Monitoring During Earthwork Construction." *Journal of Structural Health Monitoring*, Vol. 2, No. 4, pp. 137–152.

Mooney, M. A., R. V. Rinehart, and P. J. van Susante (2006). "The Influence of Heterogeneity on Vibratory Roller Compactor Response," in D. J. DeGroot, J.T. DeJong, D. Frost, and L.G. Baise, eds., *GeoCongress 2006: Geotechnical Engineering in the Information Technology Age.* American Society of Civil Engineers, Atlanta, GA, 1–6.

Mooney, M. A., R. V. Rinehart, N. W. Facas, O. M. Musimbi, and D. J. White (2010). *NCHRP Report 676: Intelligent Soil Compaction Systems*. Transportation Research Board of the National Academies, Washington, D.C.

Navarro, E., J. Garibay, I. Abdallah, and S. Nazarian (2012). "Development of Models to Estimate Modulus and Permanent Deformation of Texas Bases," Technical Memorandum: 0-6622-4a. Subtask 4.1: MR and PD Model Developments for Granular Base Materials. Center for Transportation Infrastructure Systems, The University of Texas at El Paso, El Paso, TX.

Nazarian, S., M. Mazari, I. Abdallah, A. J. Puppala, L. N. Mohammad, and M. Y. Abu-Farsakh (2014). *NCHRP Research Results Digest 391: Modulus-Based Construction Specification for Compaction of Earthwork and Unbound Aggregate*. Transportation Research Board of the National Academies, Washington, D.C.

Nazzal, M. (2014). *NCHRP Synthesis 456: Non-Nuclear Methods for Compaction Control of Unbound Materials.* Transportation Research Board, Washington, D.C.

Ninfa, A. (2013). *Experimental Analysis on the Use of CCC Systems to Analyze the In-Situ Bearing Capacity of C&D Materials*. Doctoral dissertation. Università di Bologna, Bologna, Italy.

Ooi, P. S. K., A. R. Archilla, and K. G. Sandefur (2004). "Resilient Modulus Models for Compacted Cohesive Soils," *Transportation Research Record: Journal of the Transportation Research Board*, No. 1874, pp. 115–124. https://doi.org/10.3141/1874-13.

Pacheco, L.G., and S. Nazarian (2011). "Impact of Moisture Content and Density on Stiffness-Based Acceptance of Geomaterials," *Transportation Research Record: Journal of the Transportation Research Board*, No. 2212, pp. 1-13. https://doi.org/10.3141/2212-01.

Petersen, L. (2005), Continuous Compaction Control: MnROAD Demonstration. Final Report No. MN/RC-2005-07, Minnesota Department of Transportation, St. Paul, MN.

Puppala, A. J. (2008). *NCHRP Synthesis 382: Estimating Stiffness of Subgrade and Unbound Materials for Pavement Design.* Transportation Research Board of the National Academies, Washington, D.C.

Richter, C. (2006). *Seasonal Variations in the Moduli of Unbound Pavement Layers.* FHWA-HRT-04-079, Turner-Fairbanks Highway Research Center, McLean, VA.

Sabnis, A. K., I. N. Abdallah, S. Nazarian, and A. J. Puppala (2009). "Development of Shrinkage Model Based on Index Properties for Clays." In *Proceedings of the 88th Annual Meeting of the Transportation Research Board* (No. 09-2153), Washington, D.C.

Siddagangaiah, A. K., R. Aldouri, S. Nazarian, C. M. Chang, and A. Puppala. (2014). "Improvement of Base and Soil Construction Quality by Using Intelligent Compaction Technology." Report FHWA/TX-13/0-6740-1, prepared for the Texas Department of Transportation and the Federal Highway Administration by the Center for Transportation Infrastructure Systems, The University of Texas at El Paso, El Paso, TX.

Thompson, M., and D. White (2007). "Field Calibration and Spatial Analysis of Compaction-Monitoring Technology Measurements." *Transportation Research Record: Journal of the Transportation Research Board*, No. 2004, pp. 69–79. https://doi.org/10.3141/2004-08.

Thurner, H. F., and L. Forsblad (1978). *Compaction Meter on Vibrating Rollers*. Research Bulletin No. 8022, Solna, Sweden.

Thurner, H. F., and Å. Sandström (1980). "A New Device for Instant Compaction Control." *Proceedings of the International Conference on Compaction*, Paris, France, pp. 611–614.

Tirado, C., S. Rocha, A. Fathi, M. Mazari, and S. Nazarian (2019). *Deflection-Based Field Testing for Quality Management of Earthwork.* Technical Report No. 0-6903-1, prepared for the Texas Department of Transportation and the Federal Highway Administration by the Center for Transportation Infrastructure Systems, The University of Texas at El Paso, El Paso, TX.

Tutumluer, E. (2013). *NCHRP Synthesis of Highway Practice 445: Practices for Unbound Aggregate Pavement Layers*. Transportation Research Board of the National Academies, Washington, D.C.

van Susante, P. J., and M. A. Mooney (2008). "Capturing Nonlinear Vibratory Roller Compactor Behavior through Lumped Parameter Modeling." *Journal of Engineering Mechanics*, 134(8), 684–693.

Velasquez, R., K. Hoegh, I. Yut, N. Funk, G. Cochran, M. Marasteanu, and L. Khazanovich (2009). *Implementation of the MEPDG for New and Rehabilitated Pavement Structures for Design of Concrete and Asphalt Pavements in Minnesota.* Research Report MN/RC 2009-06, prepared for the Minnesota DOT by the University of Minnesota, Minneapolis, MN.

Von Quintus, H. L., and B. Killingsworth (1998). Analyses Relating to Pavement Material Characterizations and Their Effects on Pavement Performance. FHWA-RD-97-085, Federal Highway Administration, U.S. Department of Transportation, McLean, VA.

Von Quintus, H. L., C. Rao, R. E. Minchin, S. Nazarian, K. R. Maser, and B. Prowell (2009). *NCHRP Report 626: NDT Technology for Quality Assurance of HMA Pavement Construction.* Transportation Research Board of the National Academies, Washington, D.C.

Von Quintus, H. L., C. Rao, B. Bhattacharya, H. Titi, and R. English (2010). "Evaluation of Intelligent Compaction Technology for Densification of Roadway Subgrades and Structural Layers," Draft Final Report, WHRP Study No. 00092-08-07, submitted to the Wisconsin Highway Research Program by Applied Research Associates, Inc., University of Wisconsin at Milwaukee, Milwaukee, WI.

White, D. J., and M. J. Thompson (2008). "Relationships Between in Situ and Roller-Integrated Compaction Measurements for Granular Soils." *Journal of Geotechnical and Geoenvironmental Engineering*, American Society of Civil Engineers, 134(12), pp. 1763–1770.

White, D. J., and P. K. R. Vennapusa (2015). *Report of the 3rd Workshop for Intelligent Compaction Consortium*. Intrans Project 10-395, Center for Transportation Research and Education (CTRE), Iowa State University, Ames, IA.

Wolfe, W., and T. Butalia (2004). *Continued Monitoring of SHRP Pavement Instrumentation Including Soil Suction and Relationship with Resilient Modulus.* Report No. FHWA/OH-2004/007. Federal Highway Administration, U.S. Department of Transportation, Washington, D.C.

Xia, K., and T. Pan (2010). "Understanding Vibratory Asphalt Compaction by Numerical Simulation." *International Journal of Pavement Research and Technology*, 4(3), pp. 185–194.

Yau, A., and H. Von Quintus (2002). "Study of LTPP Laboratory Resilient Modulus Test Data and Response Characteristics." Final Report FHWA-RD-02-051. Federal Highway Administration, U.S. Department of Transportation, Washington, D.C.

APPENDIX A

# Proposed Standard Specifications and Test Methods to Estimate Mechanical Properties of Geomaterials Using Intelligent Compaction

This appendix contains the proposed specifications developed during NCHRP Project 24-45, which was conducted to develop procedures to estimate mechanical properties of geomaterials using Intelligent Compaction (IC). These proposed specifications have been developed based on the findings obtained from the Phase 1 and Phase 3 activities. The framework for the IC specifications and the rationale for incorporating different items in the proposed specifications are discussed in Chapter 8 of the final report.

Using AASHTO PP 81-14 as a baseline, two proposed specifications have been developed; one addresses backcalculation of layer modulus and the other addresses quality management and design verification using IC:

- Proposed Standard Specification for Extracting Modulus of Compacted Geomaterials Using Intelligent Compaction (IC), and
- Proposed Standard Specification for Quality Management and Design Verification of Earthwork and Unbound Aggregates Using Intelligent Compaction (IC).

Two proposed test methods that supplement these specifications with device-specific protocols also are provided:

- Proposed Standard Test Method for Determining Intelligent Compaction Measurement Value (ICMV) Using Intelligent Compaction (IC) Technology, and
- Proposed Standard Test Method for Estimating Modulus of Embankment and Unbound Aggregate Layers with Portable Falling Weight Devices.

Given the diversity of requirements and practices across differing state highway administrations (SHAs), the values and guidelines provided represent the research team's best effort to provide a set of consensus values and procedures.

The language of the proposed specifications has been maintained as general as possible so that individual SHAs can customize the documents to their requirements. Comments have been incorporated to explain the researchers' thought process and to describe means of adapting the specification to local practices. Reflecting how the proposed specifications and test method documents will be used, the numbering of sections, tables, and figures is specific to each document rather than continuous throughout the appendix.

## PROPOSED STANDARD SPECIFICATION FOR EXTRACTING MODULUS OF COMPACTED GEOMATERIALS USING INTELLIGENT COMPACTION (IC)

### AASHTO Designation: PP YY-XX[1]

### 1. SCOPE

1.1 The primary objective of this document is to develop a procedure to extract the modulus of compacted geomaterials employing Intelligent Compaction (IC) rollers in conjunction with modulus/deflection-based devices.

1.2 IC is defined as a process that uses rollers equipped with a measurement-documentation system that automatically records compaction parameters (e.g., spatial location, pass count, vibration amplitude, and frequency) in real time during the compaction process. IC rollers equipped with accelerometers use roller vibration measurements to estimate stiffness and uniformity through continuous monitoring of operations.

1.3 The Contractor shall supply sufficient numbers of rollers, and other associated equipment, necessary to complete the compaction requirements for the specific materials.

1.4 All tasks are the Contractor's responsibility, unless designated otherwise within this provision.

### 2. REFERENCED DOCUMENTS

2.1 *AASHTO Standards:*

- M 57, Materials for Embankments and Subgrades
- M 147, Materials for Aggregate and Soil-Aggregate Subbase, Base, and Surface Courses
- T 2, Sampling of Aggregates
- T 307, Resilient Modulus of Soils and Aggregate Material
- T 310, In-Place Density and Moisture Content of Soil and Soil-Aggregate by Nuclear Methods

2.2 *ASTM Standards:*

- E 2835, Measuring Deflections using a Portable Impulse Plate Load Test Device
- E 2583, Measuring Deflections with a Light Weight Deflectometer (LWD)

### 3. DEFINITIONS

3.1 ***Intelligent Compaction (IC)***—A system that provides continuous assessment of compaction through roller vibration monitoring and integrates a global positioning system.

3.2 ***Intelligent Compaction Measurement Value (ICMV)***—A generic term that refers to a set of IC data used for measurements of resistance of deformation of underlying material and to assess uniformity based on the responses of the roller drum vibration measurements in units specific to the roller manufacturer.

3.3 ***Intelligent Compaction Retrofit Kit (a.k.a. Aftermarket Kit)***—A set of stand-alone IC instrumentation that could be mounted on almost any dynamic vibratory roller to collect ICMV data.

---

[1] AASHTO PP YY-XX is a generic designation for this proposed specification.

3.4 ***Vibration Amplitude***—The height of a roller drum's lift from the pavement surface during vibratory compaction.

3.5 ***Mapping***—Collecting IC data at a specific vibration setting and roller speed after completion of the compaction process.

3.6 ***Pre-Mapping***—Collecting IC data at a specific vibration setting and roller speed before placement of a new geomaterial layer.

3.7 ***Proof Mapping***—The process of using an IC roller to map the entire section upon completion of compaction for purposes of assessing the uniformity and consistency of compaction.

3.8 ***Light Weight Deflectometer (LWD)***—A nondestructive deflection-based device to evaluate the stiffness of compacted layers by applying an impulse load through dropping a weight from a specified height on a loading plate on top of a compacted geomaterial layer.

## 4. MATERIALS[2]

4.1 Unless waived or altered by the Engineer, materials shall conform to the requirements of the relevant specifications listed in Table 1.

**Table 1. Material specifications.**

| Material | Specification |
|---|---|
| Embankment | AASHTO M 57 |
| Subgrade | AASHTO M 57 |
| Subbase | AASHTO M 147 |
| Base | AASHTO M 147 |

4.2 The Contractor shall produce, deliver, and stockpile materials at the designated sites as directed by the Engineer that conforms to the requirements in Table 1.

4.3 The Contractor shall be responsible for maintaining a gradation process control program in accordance with random sampling procedures in AASHTO T 2.

4.4 A change in material source without permission of the engineer is prohibited.

4.5 The Contractor shall assume full responsibility for the production and placement of acceptable materials.

## 5. EQUIPMENT

5.1 ***Intelligent Compaction (IC) Roller Compactor***—A vibratory roller equipped with a data acquisition (DAQ) system that processes compaction data in real time for the roller operator. The DAQ can be either a factory-installed/Original Equipment Manufacturer (OEM) system or a retrofit system.

5.1.1 ***IC Rollers***—Rollers shall be equipped with accelerometers and mounted in or on the side of the drum to measure the interactions between the roller and compacted materials to evaluate the applied compaction effort.

[2] SHAs can replace the AASHTO specifications and/or test methods with their own specifications and methods.

5.1.2 ***GPS Radio and Receiver Units***—GPS units shall be mounted on each IC roller to monitor the drum locations and track the number of passes of the rollers. The mounted GPS units connect with hand-held survey-grade GPS rover(s) and with a local/virtual base station to transmit and record GPS data. The recorded GPS data, whether from the IC rollers or hand-held GPS rovers, shall include the date (in yyyymmdd format); time (in hh:mm:ss.xx format with a precision of 0.01 seconds required to differentiate sequence of IC data points during post-processing); latitude and longitude (in decimal degrees, dd.dddddddd, with longitudes recorded as negative values when measuring westward from the Prime Meridian); and elevation (in ft.).

5.1.3 ***On-Board Computer Display***—The display unit will show the location of the roller, number of passes, and amplitude and frequency for vibratory rollers, and provides real-time, color-coded maps of the ICMV. The display unit shall be capable of transferring the data by means of a USB port or by automatic wireless uploading to a cloud-based computer storage system. The on-board computer should have the capability to measure, record, and export compaction parameters in Comma Delimited Separated Values (*.csv) format data files.

5.2 ***Light Weight Deflectometer* (LWD)**—The LWD shall conform to ASTM E 2835 or E 2583.

## 6. EXTRACTION OF MODULUS

6.1 The schematic of the implementation of the proposed IC process is illustrated in Figure 1.

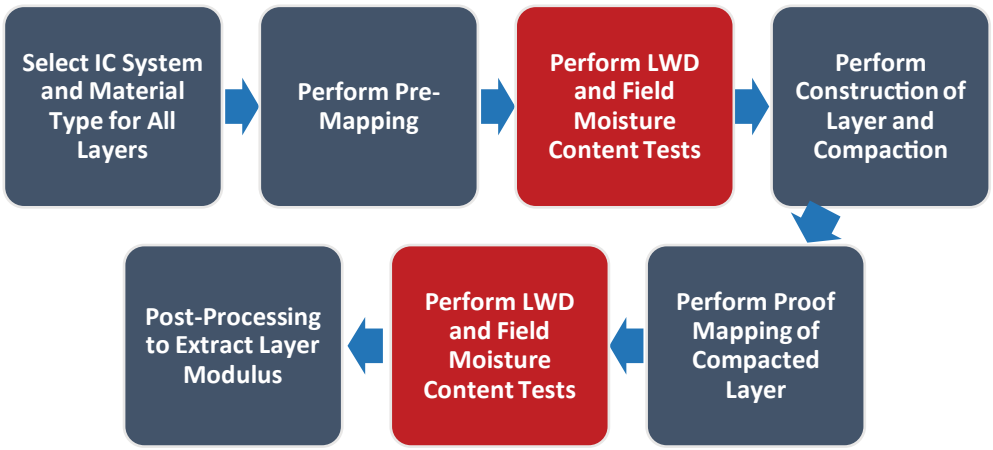


***Figure 1. Field implementation process.***

6.2 ***Select IC System and Material Type for All Layers***—Specify the type of IC roller for use prior to the beginning of the compaction process to include the accuracy of the GPS unit. The specifications of the IC system must be approved by the Engineer. The installation of the retrofit kit on conventional rollers needs special configuration and installation processes that should be planned in advance of their use. Furnish the roller model and serial number prior to installation of the retrofit kit to accommodate any special equipment needed during the installation process. Furnish material conforming to the requirements of Section 4.

6.3 ***Perform Pre-Mapping***—Follow AASHTO T XXX[3] to pre-map the existing layer prior to placement and compaction of the layer of interest. Perform the pre-mapping process at low amplitude and low frequency vibration settings with forward passes of the IC roller over the section at a uniform speed of no more than 3 mph (5 km/h).

Follow the AASHTO PP XX-XX[4] specification to ensure uniformity of the existing layer is achieved.

6.3.1 The mapping of the vibration amplitude (i.e., surface deformation of the existing layer under the drum) should be provided using a rectangular grid. An average value, $d_1$, for the entire mapped section should be provided in the descriptive statistics or should be determined from the mapping of surface deformation.

6.3.2 The mapping of the forces imposed by the drum should be provided using a rectangular grid. An average value, $F_d$, for the entire mapped section should be provided in the descriptive statistics or should be determined from the mapping of drum forces.

6.4 ***Perform LWD and Field Moisture Content Tests***—Perform tests for modulus and moisture at randomly selected locations, at the minimum frequency required (see Table 2). Follow the steps in AASHTO T YYY[5] to perform the LWD test to obtain modulus $E_{LWD\text{-}1}$ of existing layer. The modulus should be adjusted for the moisture content at the time of spot testing ($E_{eff}$) as required by AASHTO T YYY in accordance with AASHTO T 310.

**Table 2. Minimum schedule of modulus-based tests.[6]**

| Material | Maximum Lot Size | No. of Sublots | No. of Tests per Sublot |
|---|---|---|---|
| Embankment | 4,000 yd$^2$ (3,400 m$^2$) | 2 | 5 |
| Subgrade | 3,000 yd$^2$ (2,500 m$^2$) | 2 | 5 |
| Subbase | 2,400 yd$^2$ (2,000 m$^2$) | 2 | 5 |
| Base | 2,000 yd$^2$ (1,700 m$^2$) | 2 | 5 |

6.5 ***Perform Construction of Layer and Compaction***—Construct each layer uniformly, free of loose or segregated areas, in accordance with the plans and the applicable specification items listed in Section 4, "Materials." Provide a smooth surface that conforms to the typical sections, lines, and grades shown on the plans or as directed.

---

[3] AASHTO T XXX is a generic designation for the "Proposed Standard Test Method for Determining Intelligent Compaction Measurement Value (ICMV) Using Intelligent Compaction (IC) Technology." The proposed test method was developed as part of NCHRP 24-45 and is included in this appendix.

[4] AASHTO PP XX-XX is a generic designation for a proposed specification, "Proposed Standard Specification for Quality Management and Design Verification of Earthwork and Unbound Aggregates Using Intelligent Compaction (IC)." The proposed specification was developed as part of NCHRP 24-45 and is included in this appendix.

[5] AASHTO T YYY is a generic designation for the "Proposed Standard Test Method for Estimating Modulus of Embankment and Unbound Aggregate Layers with Portable Falling Weight Devices." The proposed test method was developed as part of NCHRP 24-45 and is included in this appendix.

[6] SHAs can replace the values in Table 2 with their own values. The number of tests per sublot is listed as recommended by Nazarian et al. (2014), *Modulus-Based Construction Specification for Compaction of Earthwork and Unbound Aggregate*. *NCHRP Project 10-84*, El Paso, TX.

6.6 ***Perform Proof Mapping of Compacted Layer***—Upon completion of the compaction process, map the section using the IC roller with the same vibration settings as in Section 6.3, "Pre-Mapping," to generate color-coded maps of the vibration amplitude (surface deformation) using a rectangular grid.

6.6.1 Follow the AASHTO PP XX-XX specification to ensure uniformity and quality management of compacted geomaterials.

6.6.2 Review the variability (coefficient of variation, or COV) of the ICMV color-coded map of the compacted section and identify the more uniformly compacted areas. Identify the more uniform areas, shown as areas marked in green (COV of ICMV ≤ 25%).

6.7 ***Perform LWD and Field Moisture Content Spot Tests***—Perform the spot tests as soon as possible and before the material loses 2% of its placement moisture content, at locations identified as more uniform areas in Section 6.6.2.

Follow the steps in AASHTO T YYY to perform the LWD test to obtain the LWD modulus, $E_{LWD\text{-}2}$. The modulus should be adjusted for the moisture content at the time of spot testing ($E_{eff}$) as required by AASHTO T YYY following AASHTO T 310. The density and moisture measurements shall be taken by the Engineer in the same locations where the spot tests were performed.

Unless altered by the Engineer, compliance shall be documented in accordance with the minimum frequency of testing for modulus and moisture content reflected in Table 2. This frequency can be reduced as justified by the use of continuous compaction control during the Contractor's process control.

6.8 ***Perform Post-Processing to Extract Layer Modulus***—To extract the modulus of the proof-mapped compacted layer, use the inverse models of either of the two options below:

6.8.1 ***Option 1***—Use inverse model by inputting:

- $d_2$ and $d_1$, blocked roller displacements (vibration amplitude) obtained after proof-mapping top (base) layer and underlying (subgrade) layer, respectively,
- $k'_i{}^b$ and $k'_i{}^s$, regression parameters of top and underlying layers, respectively, as obtained from resilient modulus (see Section 7.1.1),
- $E_{LWD\text{-}2}$, the averaged effective LWD modulus ($E_{eff}$) as obtained from the spot tests on the top (base) layer,
- $E_{LWD\text{-}1}$, the averaged effective LWD modulus ($E_{eff}$) as obtained from the spot tests on top of the underlying layer (subgrade),
- $h$, top layer (base) thickness,
- $D$, diameter of drum,
- $L$, length of drum, and
- $W$, weight of drum in addition to centrifugal force as set during proof-mapping.

For single-layer systems, use the corresponding model and the parameters corresponding to subgrade only.

6.8.2 ***Option 2***—Use transfer function by means of the drum force by inputting:

- $F_{d2}$ and $F_{d1}$, blocked drum forces obtained after proof-mapping top (base) layer and underlying (subgrade) layer, respectively,
- $E_{LWD\text{-}2}$, the averaged effective LWD modulus ($E_{eff}$) as obtained from the spot tests on the top (base) layer, and

- $E_{LWD\text{-}1}$, the averaged effective LWD modulus ($E_{eff}$) as obtained from the spot tests on top of the underlying layer (subgrade).

For single-layer systems, use the parameters corresponding to subgrade only.

## 7. DETERMINE NONLINEAR INPUT PARAMETERS FOR INVERSE MODEL

7.1 The following steps shall be used to determine the nonlinear $k'_i$ input parameters for the inverse model.

7.1.1 Determine the resilient modulus (MR) parameters of the layer being tested and the underlying layer(s). In the order of preference, these values should be obtained from one of three options:

7.1.1.1 ***Option 1***—Measure the resilient modulus of the geomaterial over the range of stress states in accordance with AASHTO T 307 on specimens prepared from the stockpile. Prepare specimens at their corresponding optimum moisture contents (OMC) and maximum dry densities (MDD). Obtain regression parameters $k'_1$ through $k'_3$ that best describe the following relationship for each material.

$$MR_{opt} = k_1' P_a \left[\frac{\theta}{P_a} + 1\right]^{k_2'} \left[\frac{\tau_{oct}}{P_a} + 1\right]^{k_3'} \tag{7.1}$$

where $\theta$ = bulk stress, $\tau_{oct}$ = octahedral shear stress, $P_a$ = atmospheric pressure (101.3 MPa, 14.7 psi) and $k'_i$ = nonlinear regression parameters.

7.1.1.2 ***Option 2***—Estimate $k_1$ through $k_3$ related to Equation 7.2 for the OMC and MDD from a catalog of materials tested locally (often in conjunction with the implementation of the mechanistic-empirical design algorithms) and convert them to $k'_1$ through $k'_3$ according to the process discussed in Section 7.1.2.

$$MR_{opt} = k_1 P_a \left[\frac{\theta}{P_a}\right]^{k_2} \left[\frac{\tau_{oct}}{P_a} + 1\right]^{k_3} \tag{7.2}$$

7.1.1.3 ***Option 3***—Estimate regression parameters $k_1$ through $k_3$ related to Equation 7.2 for the optimum moisture content and maximum dry density from relationships established in the literature. The relationships developed from the FHWA Long-Term Pavement Performance (LTPP) program are shown in Appendix I.

7.1.2 Convert the regression parameters $k_1$ through $k_3$ from Equation 7.2 (as determined in Section 7.1.1.2 or Section 7.1.1.3) to $k'_1$ through $k'_3$ for Equation 7.1 using the following relationships

$$k_1' = k_1 e^{-1.32 k_2} \tag{7.3}$$

$$k_2' = 1.88 k_2 \tag{7.4}$$

$$k_3' = k_3 \tag{7.5}$$

## 8. MEASUREMENT AND PAYMENT

8.1 The work performed, materials furnished, equipment, labor, tools, and incidentals will not be measured or paid for directly but will be subsidiary to the pertinent items.

## Appendix I – Estimating Resilient Modulus Constitutive Model Coefficients (as per FHWA-LTPP)

**Crushed Stone Base Materials:**

$$k_1 = 0.7632 + 0.008(P_{3/8}) + 0.0088(LL) – 0.00371(w_{opt}) -0.0001(\gamma_{opt}) \quad \text{(I.1)}$$

$$k_2 = 2.2159 – 0.0016\ (P_{3/8}) + 0.0008\ (LL) – 0.038(w_{opt}) – 0.006(\gamma_{opt}) + 0.00000024(\gamma^2_{opt} / P_{\#40}) \quad \text{(I.2)}$$

$$k_3 = –1.1720 – 0.0082(LL) – 0.0014(w_{opt}) + 0.0005\ (\gamma_{opt}) \quad \text{(III.3)}$$

**Embankments, Soil – Aggregate Mixture, Coarse-Grained:**

$$k_1 = – 0.5856 + 0.0130(P_{3/8}) – 0.0174(P_{\#4}) + 0.0027(P_{\#200}) + 0.0149(PI) + 0.0000016(\gamma_{opt}) – 0.0426(w_s) + 1.6456[\gamma_s / \gamma_{opt}] + 0.3932[w_s / w_{opt}] – 0.00000082[\gamma^2_{opt} / P_{\#40}] \quad \text{(I.4)}$$

$$k_2 = 0.7833 – 0.0060\ (P_{\#200}) – 0.0081(PI) + 0.0001(\gamma_{opt}) – 0.1483[w_s / w_{opt}] + 0.000000027[\gamma^2_{opt}/ P_{\#40}] \quad \text{(I.5)}$$

$$k_3 = – 0.1906 – 0.0026(P_{\#200}) + 0.00000081[\gamma^2_{opt} / P_{\#40}] \quad \text{(I.6)}$$

**Embankments, Soil – Aggregate, Fine-Grained:**

$$k_1 = – 0.7668 + 0.0051(P_{\#4}) + 0.0128\ (P_{\#200}) + 0.0030(LL) – 0.051(w_{opt}) + 1.179[\gamma_s / \gamma_{opt}] \quad \text{(I.7)}$$

$$k_2 = 0.4951 – 0.0141(P_{\#4}) – 0.0061(P_{\#200}) + 1.3941[\gamma_s / \gamma_{opt}] \quad \text{(I.8)}$$

$$k_3 = 0.9303 + 0.293(P_{3/8}) + 0.0036(LL) – 3.8903[\ \gamma_s / \gamma_{opt}] \quad \text{(I.9)}$$

**Fine-Grained Clay Soil:**

$$k_1 = 1.3577 + 0.0106(Clay) – 0.0437(w_s) \quad \text{(I.10)}$$

$$k_2 = 0.5193 – 0.0073(P_{\#4}) + 0.0095(P_{\#40}) – 0.0027(P_{\#200}) – 0.0030(LL) – 0.0049(w_{opt}) \quad \text{(I.11)}$$

$$k_3 = 1.4258 – 0.0288(P_{\#4}) + 0.0303(P_{\#40}) – 0.0521(P_{\#200}) + 0.025(Silt) + 0.0535(LL) – 0.0672(w_{opt}) – 0.0026(\gamma_{opt}) + 0.0025(\gamma_s) – 0.6055\ [w_s / w_{opt}] \quad \text{(I.12)}$$

where:

$LL$ = Liquid limit
$PI$ = Plasticity index of soil
$w_s$ = Water content of the test specimen (%)
$\gamma_s$ = Dry density of the test specimen
$w_{opt}$ = Optimum water content (%)
$\gamma_{opt}$ = Maximum dry unit weight of soil
$P_{3/8}$ = Percentage passing sieve #3/8 sieve
$P_{\#4}$= Percentage passing #4 sieve
$P_{\#40}$= Percentage passing #40 sieve
$P_{\#200}$ = Percent passing #200 sieve
$Clay$ = Percentage of clay (%)
$Silt$ = Percentage of silt (%)

## PROPOSED STANDARD SPECIFICATION FOR QUALITY MANAGEMENT AND DESIGN VERIFICATION OF EARTHWORK AND UNBOUND AGGREGATES USING INTELLIGENT COMPACTION (IC)

**AASHTO Designation: PP XX-XX [1]**

### 1. SCOPE

1.1 The primary objective of this document is to develop specifications and procedures that can be used for quality management and design verification of compacted geomaterials employing Intelligent Compaction (IC) rollers.

1.2 This work shall consist of compaction of roadway embankment, subgrade or other unbound geomaterials without stabilizing agents such as lime or cement using Intelligent Compaction (IC) rollers within the limits of the work described in the plans or provisions.

1.3 IC is defined as a process that uses rollers equipped with a measurement-documentation system that automatically records compaction parameters (e.g., spatial location, pass count, vibration amplitude and frequency) in real time during the compaction process. IC rollers equipped with accelerometers use roller vibration measurements to estimate stiffness and uniformity through continuous monitoring of operations.

1.4 The contractor shall supply sufficient numbers of rollers, and other associated equipment, necessary to complete the compaction requirements for the specific materials.

1.5 This specification is to be applied during the contractor's quality control.

1.6 All tasks are the contractor's responsibility, unless designated otherwise within this provision.

### 2. REFERENCED DOCUMENTS

2.1 *AASHTO Standards:*

- M 57, Materials for Embankments and Subgrades
- M 147, Materials for Aggregate and Soil-Aggregate Subbase, Base, and Surface Courses
- T 307, Resilient Modulus of Soils and Aggregate Material
- T 2, Sampling of Aggregates

### 3. DEFINITIONS

3.1 ***Intelligent Compaction (IC)***—A system that provides continuous assessment of compaction through roller vibration monitoring and integrates a global positioning system.

3.2 ***Intelligent Compaction Measurement Value (ICMV)***—A generic term that refers to a set of IC data for measurements of resistance of deformation of underlying material and to assess uniformity based on the responses of the roller drum vibration measurements in units specific to the roller manufacturer.

3.3 ***Intelligent Compaction Retrofit Kit (a.k.a. Aftermarket Kit)***—A set of stand-alone IC instrumentation that could be mounted on almost any dynamic vibratory roller to collect ICMV data.

---

[1] AASHTO PP XX-XX is a generic designation for this proposed specification.

3.4 ***Vibration Amplitude***—The height of a roller drum's lift from the pavement surface during vibratory compaction.

3.5 ***Mapping***—Collecting IC data at a specific vibration setting and roller speed after completion of the compaction process.

3.6 ***Pre-Mapping***—Collecting IC data at a specific vibration setting and roller speed before placement of a new geomaterial layer.

3.7 ***Proof Mapping***—The process of using an IC roller to map the entire section upon completion of compaction for assessing the uniformity and consistency of compaction.

3.8 ***Stiffness***—A measurement value defined as the resistance to deformation of a material under an applied load, in this case the load imposed by the drum centrifugal force and its weight.

## 4. MATERIALS[2]

4.1 Unless waived or altered by the Engineer, materials shall conform to the requirements of the relevant specifications listed in Table 1.

**Table 1. Material specifications.**

| Material | Specification |
|---|---|
| Embankment | AASHTO M 57 |
| Subgrade | AASHTO M 57 |
| Subbase | AASHTO M 147 |
| Base | AASHTO M 147 |

4.2 The Contractor shall produce, deliver, and stockpile materials that conform to the requirements in Table 1 at the designated sites as directed by the Engineer.

4.3 The Contractor shall be responsible for maintaining a gradation process control program in accordance with random sampling procedures in AASHTO T 2.

4.4 A change in material source without permission of the engineer is prohibited.

4.5 The Contractor shall assume full responsibility for the production and placement of acceptable materials.

## 5. EQUIPMENT

5.1 ***Intelligent Compaction (IC) Roller Compactor***—A vibratory roller equipped with a data acquisition (DAQ) system that processes compaction data in real time for the roller operator. The DAQ can be either a factory-installed/Original Equipment Manufacturer (OEM) system or a retrofit system.

5.1.1 **IC Rollers**—Rollers shall be equipped with accelerometers mounted in or on the side of the drum to measure the interactions between the roller and compacted materials to evaluate the applied compaction effort.

5.1.2 ***GPS Radio and Receiver Units***—GPS units shall be mounted on each IC roller to monitor the drum locations and track the number of passes of the rollers. The mounted GPS units connect with hand-held survey-grade GPS rover(s) and with a local/virtual base station to

[2] SHAs can replace the AASHTO specifications and/or test methods with their own specifications and methods.

transmit and record GPS data. The recorded GPS data, whether from the IC rollers or hand-held GPS rovers, shall include the date (in yyyymmdd format); time (in hh:mm:ss.xx format with a precision of 0.01 seconds required to differentiate sequence of IC data points during post-processing); latitude and longitude (in decimal degrees, dd.dddddddd, with longitudes recorded as negative values when measuring westward from the Prime Meridian); and elevation (in ft.).

5.1.3 ***On-Board Computer Display***—The display unit will show the location of the roller, number of passes, and amplitude and frequency for vibratory rollers, and provides real-time, color-coded maps of the ICMV. The display unit shall be capable of transferring the data by means of a USB port or by automatic wireless uploading to a cloud computer storage system. The on-board computer should have the capability to measure, record, and export compaction parameters in the Comma Delimited Separated Values (*.csv) format data files.

## 6. FIELD IMPLEMENTATION

6.1 The schematic of the implementation of the proposed IC process is illustrated in Figure 1.

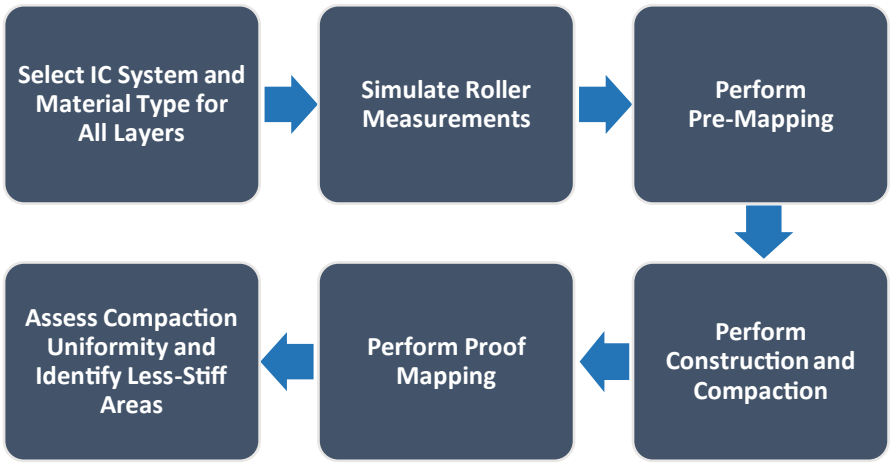


***Figure 1. Field implementation process.***

6.2 ***Select IC System and Material Type for All Layers***—Specify the type of IC roller for use prior to the beginning of the compaction process to include the accuracy of the GPS unit. The specifications of the IC system must be approved by the Engineer. The installation of the retrofit kit on conventional rollers needs special configuration and installation processes that should be planned in advance of their use. Furnish the roller model and serial number prior to installation of the retrofit kit to accommodate the need for any special equipment and installation process. Furnish materials conforming to the requirements of Section 4.

6.3 ***Simulate Roller Measurements***—Using the design pavement structure and properties and drum dimensions and weight, predict target stiffness, $k_{s\text{-}target}$, of single-layer or two-layer system using forward prediction model following the steps provided in Section 7.

6.4 ***Perform Pre-Mapping***—Follow AASHTO T XXX[3] to pre-map the existing layer to generate color-coded maps of the ICMV and COV of ICMV and to assess the uniformity of the existing layer prior to placement and compaction of the layer of interest. Perform the pre-mapping process at low amplitude and low frequency vibration settings with forward passes of the IC roller over the section at a uniform speed of no more than 3 mph (5 km/h). Mapping of the coefficient of variation (COV) of the ICMV should be provided using a rectangular grid based on areas practical for rework. Areas in the map with a high COV of ICMV (COV > 50%) indicate that uniformity was not achieved.

6.5 ***Perform Construction and Compaction***—Construct each layer uniformly, free of loose or segregated areas, in accordance with the plans and the applicable specification items listed in Section 4, "Materials." Provide a smooth surface that conforms to the typical sections, lines, and grades shown on the plans or as directed.

6.6 ***Perform Proof Mapping of Compacted Layer***—Upon completion of the compaction process, map the section using the IC roller with the same vibration settings as in Section 6.4, "Perform Pre-Mapping," to generate color-coded maps of stiffness, $k_s$, in addition to ICMV and COV of ICMV. The mapping of stiffness and/or ICMVs and their respective COVs should be provided using a rectangular grid based on areas practical for rework.

6.7 ***Assess Compaction Uniformity and Identify Less-Stiff Areas***—The following steps should be performed to insure uniformity and to identify the less-stiff areas.

6.7.1 Maps with cells with a high COV of the ICMV (COV > 50%) indicate that uniformity was not achieved and the compacted layer must be subject to rework.

6.7.2 Evaluate the stiffness color-coded map of the compacted section provided after proof mapping to identify the relatively less-stiff areas (marked in red) and compare to target stiffness, $k_{s\text{-}target}$, obtained in Section 7.2 Rework areas that do not meet the established target values.

## 7. ESTABLISHING TARGET STIFFNESS

7.1 The following steps shall be used to set the target stiffness values:

7.1.1 Determine the resilient modulus parameters of the layer under test and the underlying layer(s). In the order of preference, these values should be obtained from one of the options below:

7.1.1.1 ***Option 1***—Measure the resilient modulus of the geomaterial over the range of stress states in accordance with AASHTO T 307 on specimens prepared from the stockpile. Prepare specimens at their corresponding optimum moisture contents (OMC) and maximum dry densities (MDD). Obtain regression parameters $k'_1$ through $k'_3$ that best describe the following relationship for each material.

$$MR_{opt} = k_1' P_a \left[ \frac{\theta}{P_a} + 1 \right]^{k_2'} \left[ \frac{\tau_{oct}}{P_a} + 1 \right]^{k_3'} \tag{7.1}$$

where $\theta$ = bulk stress, $\tau_{oct}$ = octahedral shear stress, $P_a$ = atmospheric pressure (101.3 MPa, 14.7 psi) and $k'_i$ = nonlinear regression parameters.

[3] AASHTO T XXX is a generic designation for a proposed specification, "Determining Intelligent Compaction Measurement Value (ICMV) Using Intelligent Compaction (IC) Technology," which was developed as part of NCHRP Project 24-45 and is included in this appendix.

7.1.1.2 ***Option 2***—Estimate $k_1$ through $k_3$ related to Equation 7.2 for the OMC and MDD from a catalog of materials tested locally, often in conjunction with the implementation of the mechanistic-empirical design algorithms and convert them to $k'_1$ through $k'_3$ according to the process discussed in Section 7.1.2.

$$MR_{opt} = k_1 P_a \left[\frac{\theta}{P_a}\right]^{k_2} \left[\frac{\tau_{oct}}{P_a} + 1\right]^{k_3} \quad (7.2)$$

7.1.1.3 ***Option 3***—Estimate regression parameters $k_1$ through $k_3$ related to Equation 7.2 for the optimum moisture content and maximum dry density from relationships established in the literature. The relationships developed from the FHWA Long-Term Pavement Performance (LTPP) program are shown in Appendix I.

7.1.2 Convert the regression parameters $k_1$ through $k_3$ from Equation 7.2 determined in Section 7.1.1.2 or 7.1.1.3 to $k'_1$ through $k'_3$ for Equation 7.1, using the following relationships

$$k_1' = k_1 e^{-1.32 k_2} \quad (7.3)$$

$$k_2' = 1.88 k_2 \quad (7.4)$$

$$k_3' = k_3 \quad (7.5)$$

7.2 Estimate target stiffness, $k_{s\text{-}target}$, of two-layer systems using a forward prediction model by inputting regression parameters $k'_i$ of top and underlying layers, drum dimensions, and weight, including centrifugal force of selected vibratory setting and top layer thickness. For single-layer systems, use the regression parameters corresponding to subgrade only.

## 8. MEASUREMENT AND PAYMENT

8.1 The work performed, materials furnished, equipment, labor, tools, and incidentals will not be measured or paid for directly but will be subsidiary to the pertinent items.

## Appendix I – Estimating Resilient Modulus Constitutive Model Coefficients (as per FHWA-LTPP)

**Crushed Stone Base Materials:**

$$k_1 = 0.7632 + 0.008(P_{3/8}) + 0.0088(LL) - 0.00371(w_{opt}) - 0.0001(\gamma_{opt}) \quad \text{(I.1)}$$

$$k_2 = 2.2159 - 0.0016\,(P_{3/8}) + 0.0008\,(LL) - 0.038(w_{opt}) - 0.006(\gamma_{opt}) + 0.00000024(\gamma^2_{opt} / P_{\#40}) \quad \text{(I.2)}$$

$$k_3 = -1.1720 - 0.0082(LL) - 0.0014(w_{opt}) + 0.0005\,(\gamma_{opt}) \quad \text{(III.3)}$$

**Embankments, Soil – Aggregate Mixture, Coarse-Grained:**

$$k_1 = -0.5856 + 0.0130(P_{3/8}) - 0.0174(P_{\#4}) + 0.0027(P_{\#200}) + 0.0149(PI) + 0.0000016(\gamma_{opt}) - 0.0426(w_s) + 1.6456[\gamma_s / \gamma_{opt}] + 0.3932[w_s / w_{opt}] - 0.00000082[\gamma^2_{opt} / P_{\#40}] \quad \text{(I.4)}$$

$$k_2 = 0.7833 - 0.0060\,(P_{\#200}) - 0.0081(PI) + 0.0001(\gamma_{opt}) - 0.1483[w_s / w_{opt}] + 0.000000027[\gamma^2_{opt} / P_{\#40}] \quad \text{(I.5)}$$

$$k_3 = -0.1906 - 0.0026(P_{\#200}) + 0.00000081[\gamma^2_{opt} / P_{\#40}] \quad \text{(I.6)}$$

**Embankments, Soil – Aggregate, Fine-Grained:**

$$k_1 = -0.7668 + 0.0051(P_{\#4}) + 0.0128\,(P_{\#200}) + 0.0030(LL) - 0.051(w_{opt}) + 1.179[\gamma_s / \gamma_{opt}] \quad \text{(I.7)}$$

$$k_2 = 0.4951 - 0.0141(P_{\#4}) - 0.0061(P_{\#200}) + 1.3941[\gamma_s / \gamma_{opt}] \quad \text{(I.8)}$$

$$k_3 = 0.9303 + 0.293(P_{3/8}) + 0.0036(LL) - 3.8903[\,\gamma_s / \gamma_{opt}] \quad \text{(I.9)}$$

**Fine-Grained Clay Soil:**

$$k_1 = 1.3577 + 0.0106(Clay) - 0.0437(w_s) \quad \text{(I.10)}$$

$$k_2 = 0.5193 - 0.0073(P_{\#4}) + 0.0095(P_{\#40}) - 0.0027(P_{\#200}) - 0.0030(LL) - 0.0049(w_{opt}) \quad \text{(I.11)}$$

$$k_3 = 1.4258 - 0.0288(P_{\#4}) + 0.0303(P_{\#40}) - 0.0521(P_{\#200}) + 0.025(Silt) + 0.0535(LL) - 0.0672(w_{opt}) - 0.0026(\gamma_{opt}) + 0.0025(\gamma_s) - 0.6055\,[w_s / w_{opt}] \quad \text{(I.12)}$$

where:

$LL$ = Liquid limit
$PI$ = Plasticity index of soil
$w_s$ = Water content of the test specimen (%)
$\gamma_s$ = Dry density of the test specimen
$w_{opt}$ = Optimum water content (%)
$\gamma_{opt}$ = Maximum dry unit weight of soil
$P_{3/8}$ = Percentage passing sieve #3/8 sieve
$P_{\#4}$= Percentage passing #4 sieve
$P_{\#40}$= Percentage passing #40 sieve
$P_{\#200}$ = Percent passing #200 sieve
$Clay$ = Percentage of clay (%)
$Silt$ = Percentage of silt (%)

## PROPOSED STANDARD TEST METHOD FOR DETERMINING INTELLIGENT COMPACTION MEASUREMENT VALUE (ICMV) USING INTELLIGENT COMPACTION (IC) TECHNOLOGY

**AASHTO Designation: T XXX** [1]

### 1. SCOPE

1.1 This test method describes the procedure for determining the Intelligent Compaction Measurement Value (ICMV) using Intelligent Compaction technology on compacted geomaterials used in embankments, subgrade and base layers. The test method is used for quality control testing of compacted geomaterials during construction.

1.2 The values given in Customary Units are to be regarded as the standard; however, some units are provided in SI. The values given in parentheses are not standard and may not be exact mathematical conversions. Use each system of units separately. Combining values from the two systems may result in nonconformance with the standard.

### 2. DEFINITIONS

2.1 ***Intelligent Compaction (IC)***—A system that provides continuous assessment of compaction through roller vibration monitoring and integrates a global positioning system.

2.2 ***Intelligent Compaction Measurement Value (ICMV)***—A generic term that refers to a set of IC data for measurements of resistance of deformation of underlying material and to assess uniformity based on the responses of the roller drum vibration measurements in units specific to the roller manufacturer.

2.3 ***Vibration Frequency***—The rotational speed of the roller drum's lifting off and compaction on pavement surface.

2.4 ***Vibration Amplitude***—The height of a roller drum's lift from the pavement surface during vibratory compaction.

2.5 ***Roller Pass***—The area covered by the width of the roller in a single direction. Roller pass number is the count of roller machine passes within a given mesh for a construction lift.

2.6 ***Proof Mapping***—The process of using an IC roller to map the entire section upon completion of compaction for assessing the uniformity and consistency of compaction.

### 3. EQUIPMENT

3.1 ***Intelligent Compaction (IC) Roller Compactor***—A vibratory roller equipped with a data acquisition (DAQ) system that processes compaction data in real time for the roller operator. The DAQ can be either a factory-installed/Original Equipment Manufacturer (OEM) system or a retrofit system. The IC roller shall be in accordance with the rollers shown on the Department's Approved Product List, "Intelligent Compaction Rollers," and shall comply with the following requirements:

3.1.1 IC rollers shall be equipped with accelerometers mounted in or on the side of the drum to measure the interactions between the roller and compacted materials to evaluate the applied compaction effort.

---

[1] AASHTO T XXX is a generic designation for this proposed test method.

3.1.2 IC rollers shall be equipped with GPS radio and receiver units mounted on each roller to monitor the drum locations and track the number of passes of the roller. The mounted GPS units connect with hand-held survey-grade GPS rover(s) and with a local/virtual base station to transmit and record GPS data. Whether from the IC rollers or hand-held GPS rovers, the recorded GPS data shall be in the following formats:

- *Date*: The date stamp shall be in yyyymmdd format.
- *Time*: The time stamp shall be in hh:mm:ss.xx format, with a precision of 0.01 seconds required to differentiate sequence of IC data points during post-processing.
- *Latitude and longitude*: shall be in decimal degrees, dd.dddddddd. Longitudes are negative values when measuring westward from the Prime Meridian.
- *Elevation*: shall be in ft.

Essential GPS data elements for each data point are shown in Table 1.

**Table 1. GPS data elements for each data point.**

| Item No. | Data Field Name | Example of Data |
|---|---|---|
| 1 | Date Stamp (yyyymmdd) | 20150205 |
| 2 | Time Stamp (hh:mm:ss.xx) | 16:49:31.18 |
| 3 | Longitude (decimal degrees) | -101.87905175 |
| 4 | Latitude (decimal degrees) | 35.11711655 |
| 5 | Elevation (ft.) | 737.092 |

3.1.3 ***On-Board Computer Display***—The display unit will show the location of the roller, number of passes, amplitude, and frequency for vibratory rollers, and provide real-time, color-coded maps of the ICMVs. The display unit shall be capable of transferring the data by means of a USB port or by automatic wireless uploading to a cloud computer storage system. The on-board computer should have the capability to measure, record, and export compaction parameters in Comma Delimited Separated Values (*.csv) format data files.

## 4. PROCEDURE

4.1 **Close off the entire testing area from any vehicular or construction equipment for the entire testing period.** Clear out any other safety concerns that would impact the testing procedure and safety of the testers prior to testing.

4.2 **Calibrate the GPS System on the IC roller.** Perform the GPS calibration process prior to any IC data collection. Verify that the hand-held survey-grade GPS rover(s) and IC roller are connected with the local/virtual base station.

4.3 **Move the IC roller slowly to a designated position to allow the GPS header computation to be stabilized to obtain accurate GPS location.** Once the roller stops, record the last reading, which is associated with the center of the drum. Record the coordinates of both sides of the drum (Figure 1) using the hand-held survey-grade GPS rover that was previously synchronized with the base station. The coordinates of the drum center shall be interpolated from the coordinates of the two sides of the drum. Compare the coordinates reported by the IC roller with the interpolated coordinates from the GPS rover. Adjust the IC roller coordinates to match the interpolated numbers. The tolerance of the differences is 12 in. (300 mm) in the northing and easting directions.

4.4 **Identify the layer IDs using project-typical sections.** The operator must input (or select) the header information using the on-board display prior to compacting the given material and enter a file name to store the IC data.

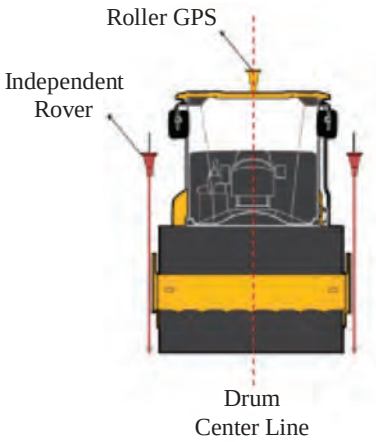


***Figure 1. GPS calibration process.***

4.4.1 ***IC Data File Name***—The operator should name the data file using the following convention: data (yyymmdd); material (see Table 2); traffic direction (NB, SB, WB, EB); lane type (ML, FR, RAMP); Stations (to nearest foot, xxxx+xx to xxxx+xx); PM (proof mapping); and smooth drum (SD) or padfoot roller (PF).

Example: 20160517-SG-NBML-194015TO196045-PM-SD

4.4.2 ***Required Fields in Header***—Each file should contain information about site, material and roller type (see Table 3 for sample header information):

- Design Name, Project ID or Section Title that identifies site. Additional information such as Location Description, Starting Station, Operator, may be added.
- Material Type (see Table 2).
- Roller Model—If provided, additional roller characteristics (roller type and weight and drum dimensions) may be excluded.
- Roller Type—May be excluded if Roller Model provided.
- Roller Drum Width (in.)—May be excluded if Roller Model provided.
- Roller Drum Diameter (in.)—May be excluded if Roller Model provided.
- Roller Weight (lbs.)—May be excluded if Roller Model provided.
- GPS Mode.
- GPS Tolerance.
- Name Index of ICMV Type.
- ICMV Type Unit Index (1: CCV; 2: CMV; 3: $E_{vib}$; 4: HMV; 5: $K_b$; 6: MDP; 7: Other), when ICMV Type name not included.

4.5 **Collect the IC data when the compaction of the entire layer is completed.** Start each pass at least 25 ft. (7.5 m) to 50 ft. (15 m) from test section to allow the IC roller to reach the desired frequency and speed. For this purpose, make each pass continuously, regardless of length, by operating the IC roller according to manufacturer's recommendations to provide reliable and repeatable measurements during proof mapping, on each lift, using consistent operating settings for the following:

- Low Amplitude and Low Frequency (when in vibration mode)
- Speed = 3 mph (5 km/h)

**Table 2. Material type designation acronyms.**

| Item No. | Material Type | Acronym |
|---|---|---|
| 1 | Untreated Subgrade Soil | SG |
| 2 | Lime Treated Subgrade | LTS |
| 3 | Cement Treated Subgrade | CTS |
| 4 | Untreated Flexible Base | FB |
| 5 | Lime Treated Flexible Base | LTB |
| 6 | Cement Treated Flexible Base | CTB |
| 7 | Asphalt Treated Base | ATB |
| 8 | Embankment | EMB |
| 9 | Other material not listed above | Specify |

**Table 3. IC data information.**

| Item No. | Data Field Name | Example of Data |
|---|---|---|
| 1 | Design Name | 20150205-LTS-NBML-1715+15 to 1745+45-PM |
| 2 | Material Type | LTS |
| 3 | Roller Model | HAMM3412 |
| 4 | GPS Mode | RTK Fixed |
| 5 | GPS Tolerance (in.) | Medium (2.0 in.) |
| 6 | ICMV type | CMV |
| 7 | ICMV index | 3 |

The output from the roller is designated as the Intelligent Compaction Measurement Value (ICMV), which represents the stiffness of the materials based on the rolling resistance or vibration of the roller drums and the resulting response from the underlying materials.

IC data files must include at least the following information:

- Roller Pass Number
- Roller Travel Direction (forward or reverse)
- Roller Travel Speed
- Vibration Setting (on or off)
- Vibration Frequency (Hz)
- Vibration Amplitude (mm)
- Intelligent Compaction Measurement Values (ICMVs)

Sample information is available in Table 4.

**Table 4. IC data elements for each data point.**

| Item No. | Data Field Name | Example of Data |
|---|---|---|
| 1 | Roller Pass Number | 1 |
| 2 | Direction | Forward, Reverse or index |
| 3 | Roller Speed (mph) | 3 |
| 4 | Vibration On | Yes, No, On, Off or index |
| 5 | Vibration Frequency (Hz) | 28.4 |
| 6 | Vibration Amplitude (mm) | 1.95 |
| 7 | Intelligent Compaction Measurement Value (ICMV) | 30.5 |

4.6 **Deliver the electronic IC data files and a hard copy of the color-coded map to the Engineer.** The IC data will be color-coded using green, yellow, and red colors as shown in Table 5 and Figure 2.

**Table 5. Color-coded map requirements.**

| Color | Criteria* |
|---|---|
| Red | Area less than 75% of Average ICMV Data |
| Yellow | Area in the range of Average to 75% of Average ICMV Data |
| Green | Area greater than 75% of Average ICMV Data |

* The criteria listed in this table are for producing color-coded maps using Veta software only. The color sequence is listed from lowest to highest stiffness.

Submit compaction information and data elements using Veta. Operator may combine roller data for multiple rollers operating in echelon into a section file.

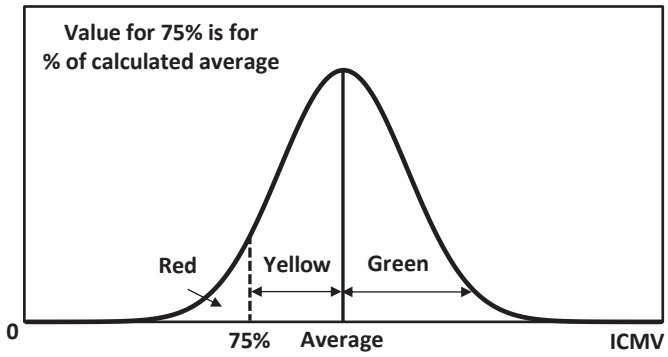


***Figure 2. Criteria for color-coded map of ICMV data.***

4.7 Provide displayed results to the Engineer for review upon request.

## 5. PROCEDURE

5.1 **Close off the entire testing area from any vehicular or construction equipment for the entire testing period.** Clear out any other safety concerns that would impact the testing *IC Data Quality Control Report.* Report the collected IC data in the desired format upon completion of daily IC operations (see Figures 3 and 4). The descriptive statistics of the collected ICMVs, as well as the vibration amplitude and frequency, shall be controlled for any discontinuity or irregular trend in the data. Plots must be scaled to be legible.

Inspector Name: Date:

Project Location: Coordinate System:

County: Roller Type:

Material Type: Roller Model:

Layer Type:

**Intelligent Compaction Data Report Worksheet**


***Figure 3. IC data report worksheet (page 1).***

| | |
|---|---|
| Inspector Name: | Date: |
| Project Location: | Coordinate System: |
| County: | Roller Type: |
| Material Type: | Roller Model: |
| Layer Type: | |

**Intelligent Compaction Data Report Worksheet**

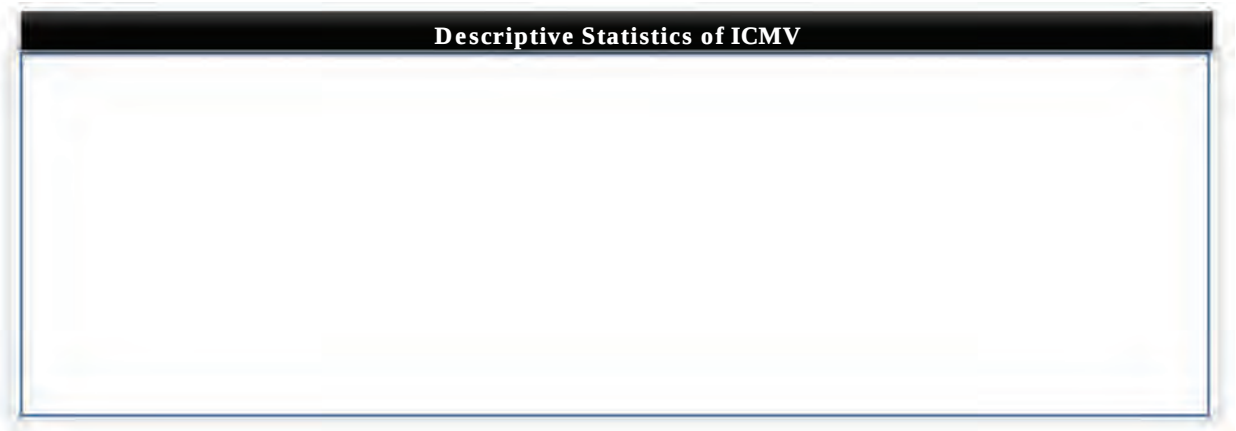


***Figure 4. IC data report worksheet (page 2).***

## PROPOSED STANDARD TEST METHOD FOR ESTIMATING MODULUS OF EMBANKMENT AND UNBOUND AGGREGATE LAYERS WITH PORTABLE FALLING WEIGHT DEVICES

**AASHTO Designation: T YYY** [1]

### 1. SCOPE

1.1 This test method describes the procedure for measuring the deflection with a Light Weight Deflectometer (LWD) and for determining the in-place modulus of compacted geomaterials used in embankments, subgrades, and base layers (without stabilizing agents), and establishing the target modulus for comparison with the measured values.

1.2 The LWD test relates surface deflection with the modulus and is defined as the maximum axial stress of a material divided by the maximum axial strain during that loading.

1.3 The measurements are made with a device that conforms to ASTM E 2835 or E 2583.

1.4 The values given in Customary Units are to be regarded as the standard; however, some units are provided in the International System of Units (SI). The values given in parentheses are not standard and may not be exact mathematical conversions. Use each system of units separately. Combining values from the two systems may result in nonconformance with the standard.

### 2. REFERENCED DOCUMENTS

2.1 *ASTM Standards:*

- E 2835, Standard Test Method for Measuring Deflections using a Portable Impulse Plate Load Test Device
- E 2583, Standard Test Method for Measuring Deflections with Light Weight Deflectometer (LWD)

### 3. DEFINITIONS

3.1 ***Deflection***—The amount of downward vertical movement due to the application of an external load to the material surface.

3.2 ***LWD Effective Modulus***—A composite surface modulus obtained based on a Boussinesq elastic solution obtained from the peak surface deflection response of a layered system of geomaterials to an impact loading.

3.3 ***LWD Adjusted Modulus***—The adjusted composite surface modulus after accounting for difference in the lab and field moduli at the same moisture conditions and density.

### 4. EQUIPMENT

4.1 ***LWD***—The LWD shall conform to either ASTM E 2835 or ASTM E 2583 (see Figure 1). The LWD apparatus include the following features:

4.1.1 A loading device that consists of a falling weight with a guide system, lock pin, and spring assembly. The fixed drop height shall be in accordance with the manufacturer's recommendation. The load is a force pulse, typically 1,000 lb. to 2,000 lb. (4.5 kN to 9 kN), generated by a falling mass dropped onto a spring or buffer assembly that transmits the load pulse to a plate resting on the material under test.

---

[1] AASHTO T YYY is a generic designation for this proposed test method.

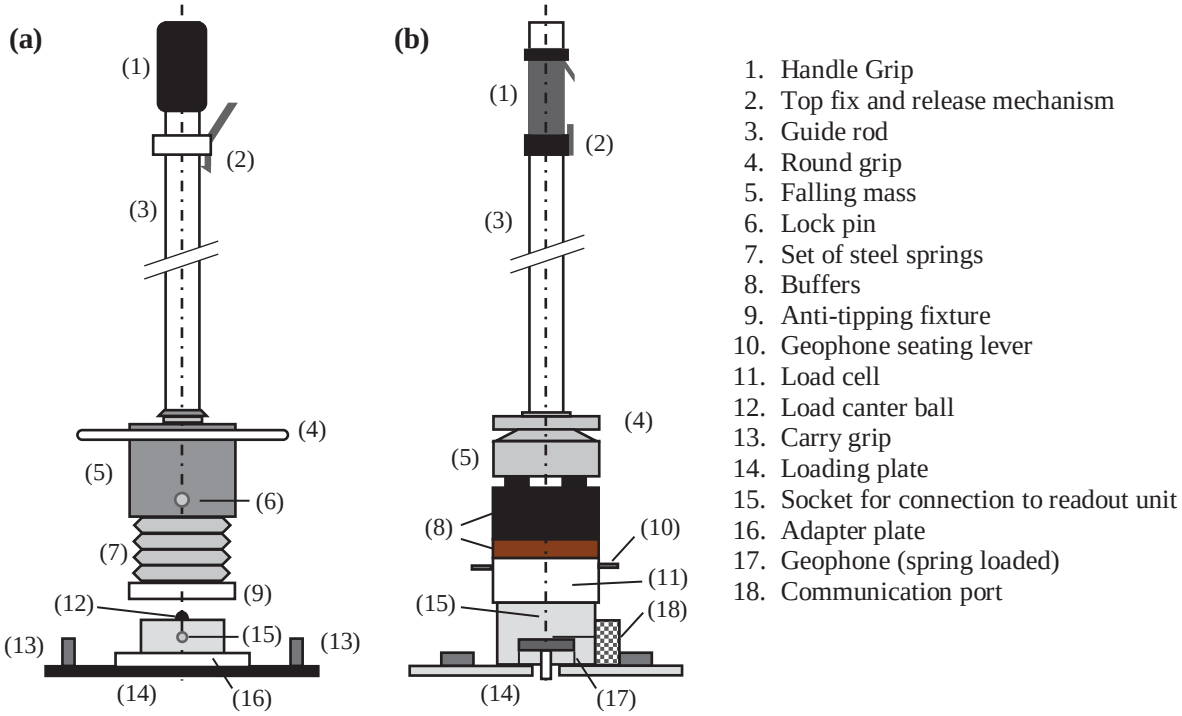


***Figure 1. Components of light weight deflectometer (LWD) that comply with (a) ASTM E 2835 and (b) ASTM E 2583.***

4.1.2 A handle grip, located at the top of the device, that is used to hold the LWD guide rod plumb and to limit the upward movement of the falling weight.

4.1.3 A top fix and release mechanism that holds the falling weight at a constant height.

4.1.4 A guide rod that allows the falling mass to drop freely.

4.1.5 A lock pin that has two positions—locked and unlocked—to release the falling weight for use.

4.1.6 A buffer system (damping system) that provides a controlled transient pulse length to the impact force, typically in the range of 16 ms to 30 ms, and which can be composed of a spring or a set of steel bearing plates that transmits the load pulse to the plate resting on the material to be tested. The spring element is typically a series of rubber cones/buffers or a cylindrical pad system.

4.1.7 A loading plate, consisting of a bearing plate whose diameter typically varies from 8 in. to 12 in. (200 mm to 300 mm) and which provides an approximate uniform distribution of the impulse load to the surface.

4.1.8 A load cell that measures the applied load of each impact (available only on devices that conform to ASTM E 2583).

4.1.9 A deflection sensor that measures maximum vertical movement with an accelerometer or geophone. The location of the deflection sensor may vary depending on the manufacturer's design.

4.2 ***Miscellaneous Equipment***—A spade, broom, trowel, and cotton gloves for operation of the LWD.

## 5. PROCEDURE

5.1 Close off the entire testing area from any vehicular or construction equipment for the entire testing period. Clear out any other safety concerns that would impact the testing procedure and safety of the testers prior to testing.

5.2 For surface preparation, the test area shall be leveled so that the entire undersurface of the load plate is in contact with the material being tested. Loose particles on the surface and protruding material shall be removed. If required, any unevenness shall be filled with fine sand. The test shall not be conducted if the temperature is below freezing. The test area shall be at least 1.5 times larger than the loading plate.

5.3 Select the 8 in. (200 mm) or 12 in. (300 mm) diameter loading plate. Position the loading plate on a properly prepared test site. Set the loading plate parallel to the testing surface on a thin (not to exceed ¼-in. thickness) layer of uniform fine sand using the least quantity for uniform loading. Twisting or working the loading plate back and forth is permitted to help provide uniform seating of the plate.

5.4 After surface preparation and after the loading plate is positioned on the surface, center the loading device on the top of the loading plate and connect the data processing and storage system to the deflection sensor using the cable provided. (The specific components of the loading device will vary depending on the LWD manufacturer and model.) Turn on the readout unit system to be ready for testing.

5.5 Use the following procedure for each drop:

5.5.1 Raise the falling mass to the preset drop height and snap into the release mechanism.

5.5.2 Adjust the guide rod to vertical by either observing the level or visually estimate by others in two perpendicular directions to the rod and itself.

5.5.3 Drop the falling mass by releasing the lock pin.

5.5.4 Catch the falling mass after rebound from striking the plate as recommended by the manufacturer. A test is considered invalid if the operator does not catch the falling weight after the weight rebounds from the load plate or the load plate moves laterally. When the test is invalid, a new test area is required to be performed at least 2 ft. away from the original area of testing.

5.5.5 Raise and snap the load mass into the release mechanism after each rebound.

5.6 Conduct three seating drops by repeating steps 5.5.1 to 5.5.5.

5.7 Following the three seating drops, conduct three drops of the falling mass by repeating steps 5.5.1 to 5.5.5 for analysis and record the deflection and applied load (if applicable) for each drop.

5.8 Record supporting information such as location, material type, and other identification information as needed.

5.9 Measure the in situ moisture content of the material as per AASHTO T 310, “Standard Method of Test for In-Place Density and Moisture Content of Soil and Soil-Aggregate by Nuclear Methods,” or using another method specified by the Engineer right after the modulus/deflection-based measurements are made.

5.10 Follow the process described in steps 6.1 to 6.4 to calculate the LWD effective modulus if desired.

## 6. ADJUSTMENT OF MEASUREMENTS [2]

6.1 Alternatively, the measured LWD deflection, $d_{eff}$, can be converted to adjusted deflection, $d_{adj}$, from:

$$d_{adj} = d_{eff} / K_{adj} \quad (6.1)$$

where $K_{adj}$ is calculated as discussed in Section 6.2.

6.2 To establish the LWD adjustment factor, $K_{adj}$, obtain $K_{adj}$ from:

$$K_{adj} = K_{lab\text{-}field}\, K_{moist} \quad (6.2)$$

where $K_{lab\text{-}field}$ is an adjustment factor that accounts for differences in lab and field moduli at the same moisture content and density, and $K_{moist}$ is an adjustment factor for differences in the compaction and testing moisture contents.

6.3 Estimate $K_{lab\text{-}field}$ from the following relationship:

$$K_{lab\text{-}field} = (F_{env})^{\lambda} \quad (6.3)$$

where $\lambda$ = -0.36 and $F_{env}$ is calculated from:

$$\log F_{env} = \left[ -0.40535 + \frac{1.20693}{1 + e^{\left[0.68184 + 1.33194 \times \left(\frac{S - S_{opt}}{100}\right)\right]}} \right] \quad (6.4)$$

where $S_{opt}$ = degree of saturation at optimum moisture content and $S$ = degree of saturation at compaction moisture content.[3]

6.4 Estimate $K_{moist}$ in the following manner:

$$K_{moist} = e^{\eta(\omega_C - \omega_T)} \quad (6.5)$$

where $\eta$ = 0.18 for fine-grained soils and 1.19 for unbound aggregates, $\omega_T$ = moisture content at time of testing (in percent), and $\omega_C$ = moisture content at time of compaction (in percent).

## 7. CALCULATION OF LWD EFFECTIVE MODULUS

7.1 **Calculate the average of the three deflection measurements obtained in step 5.7. Report the average deflection in inches (or mm).**

7.2 **Estimate the peak load, *F*, as per ASTM E 2835 or ASTM E 2583, based on the LWD model used, following the below equation:**

$$F = \sqrt{2mghC} \quad (7.1)$$

where $h$ = drop height, $m$ = falling mass, $g$ = gravitational force, and $C$ = buffer constant provided by the manufacturer.

---

[2] Please see *NCHRP Research Results Digest 391: Modulus-Based Construction Specification for Compaction of Earthwork and Unbound Aggregate* for the rationale of this approach.

[3] The relationship $\lambda$ = -0.36 is essentially the relationship proposed by Cary and Zapata (2010) simplified by replacing *wPI* with zero. See *NCHRP Research Results Digest 391* for further discussion.

7.3 **Estimate the Poisson's ratio, *ν*, of the geomaterial using recommended values shown in Table 1.**

**Table 1. Typical Poisson's Ratio values for unbound granular and subgrade materials.**

| Material Description | Poisson's Ratio | |
|---|---|---|
| | Range | Typical |
| Clay (Saturated) | 0.4 – 0.5 | 0.45 |
| Clay (Unsaturated) | 0.1 – 0.3 | 0.20 |
| Sandy Clay | 0.2 – 0.3 | 0.25 |
| Silt | 0.3 – 0.35 | 0.32 |
| Dense Sand | 0.2 – 0.4 | 0.30 |
| Coarse-grained Sand | 0.15 | 0.15 |
| Fine-grained Sand | 0.25 | 0.25 |
| Bedrock | 0.1 – 0.4 | 0.25 |

7.4 **Estimate the shape factor, *f*, based on the soil type and plate rigidity. See Table 2 for recommended values.**

**Table 2. Recommended shape factors (*f*) for LWD effective modulus estimation.**

| Soil Type | Plate Type | Shape Factor, *f* |
|---|---|---|
| Clay (elastic material) | Rigid | π/2 |
| Cohesionless Sand | Rigid | 8/3 |
| Material with Intermediate Characteristics | Rigid | π/2 to 2 |
| Clay (elastic material) | Flexible | 2 |
| Cohesionless Sand | Flexible | 8/3 |

7.5 **Calculate the effective modulus of the geomaterials, $E_{eff}$, from:**

$$E_{eff} = \left[\frac{\left(1-\nu^2\right)\times F}{\pi \times a \times d_{eff}}\right] f \tag{7.2}$$

where $F$ = LWD peak load, $a$ = radius of load plate, $d_{eff}$ = peak deflection on top of the compacted layer, $\nu$ = Poisson's ratio of the geomaterials, and $f$ = plate rigidity factor.

7.6 **Follow the process described in steps 5.1 to 5.5 to adjust the LWD effective deflection to account for the differences between laboratory and field conditions as well as the differences in the moisture content of geomaterials at the time of compaction and time of quality management testing.**

## 8. REPORT

8.1 Prepare a one-page report that consists of the following information.

- Date and time of test
- Any unusual observations made during the test

- Layer(s) tested and base layer thickness (if applicable)
- Lift type and thickness (if applicable)
- Nearest station
- Load applied
- Deflection readings for each drop
- Average measured deflection
- Adjusted deflection
- Moisture content of soil at the time of testing
- Estimated effective LWD modulus
- Adjusted effective LWD modulus

# Appendices B–H

*NCHRP Research Report 933* is accompanied by eight appendices. Appendix A, which provides the proposed specifications and test methods, has been included with the printed report. Seven additional appendices accompany the report and are presented in a downloadable PDF file titled "Appendices," which can be accessed from www.trb.org by searching "NCHRP Research Report 933".

The following appendices are included in the downloadable file:

- Appendix B: Experimental Plan for Phase 3 Field Activities
- Appendix C: Review of Literature
- Appendix D: Numerical Modeling of Compaction of Geomaterials
- Appendix E: Extracting Mechanical Properties from IC Data
- Appendix F: Field Study for Implementation and Evaluation of NDT and IC for Quality Acceptance and Design Modulus Verification
- Appendix G: Calibration of Models Using Field Data
- Appendix H: Mechanical Property Measurements

*Abbreviations and acronyms used without definitions in TRB publications:*

| | |
|---|---|
| A4A | Airlines for America |
| AAAE | American Association of Airport Executives |
| AASHO | American Association of State Highway Officials |
| AASHTO | American Association of State Highway and Transportation Officials |
| ACI–NA | Airports Council International–North America |
| ACRP | Airport Cooperative Research Program |
| ADA | Americans with Disabilities Act |
| APTA | American Public Transportation Association |
| ASCE | American Society of Civil Engineers |
| ASME | American Society of Mechanical Engineers |
| ASTM | American Society for Testing and Materials |
| ATA | American Trucking Associations |
| CTAA | Community Transportation Association of America |
| CTBSSP | Commercial Truck and Bus Safety Synthesis Program |
| DHS | Department of Homeland Security |
| DOE | Department of Energy |
| EPA | Environmental Protection Agency |
| FAA | Federal Aviation Administration |
| FAST | Fixing America's Surface Transportation Act (2015) |
| FHWA | Federal Highway Administration |
| FMCSA | Federal Motor Carrier Safety Administration |
| FRA | Federal Railroad Administration |
| FTA | Federal Transit Administration |
| HMCRP | Hazardous Materials Cooperative Research Program |
| IEEE | Institute of Electrical and Electronics Engineers |
| ISTEA | Intermodal Surface Transportation Efficiency Act of 1991 |
| ITE | Institute of Transportation Engineers |
| MAP-21 | Moving Ahead for Progress in the 21st Century Act (2012) |
| NASA | National Aeronautics and Space Administration |
| NASAO | National Association of State Aviation Officials |
| NCFRP | National Cooperative Freight Research Program |
| NCHRP | National Cooperative Highway Research Program |
| NHTSA | National Highway Traffic Safety Administration |
| NTSB | National Transportation Safety Board |
| PHMSA | Pipeline and Hazardous Materials Safety Administration |
| RITA | Research and Innovative Technology Administration |
| SAE | Society of Automotive Engineers |
| SAFETEA-LU | Safe, Accountable, Flexible, Efficient Transportation Equity Act: A Legacy for Users (2005) |
| TCRP | Transit Cooperative Research Program |
| TDC | Transit Development Corporation |
| TEA-21 | Transportation Equity Act for the 21st Century (1998) |
| TRB | Transportation Research Board |
| TSA | Transportation Security Administration |
| U.S. DOT | United States Department of Transportation |

TRANSPORTATION RESEARCH BOARD
500 Fifth Street, NW
Washington, DC 20001

ADDRESS SERVICE REQUESTED

NON-PROFIT ORG.
U.S. POSTAGE
**PAID**
COLUMBIA, MD
PERMIT NO. 88

*The National Academies of*
SCIENCES • ENGINEERING • MEDICINE

The nation turns to the National Academies of Sciences, Engineering, and Medicine for independent, objective advice on issues that affect people's lives worldwide.
**www.nationalacademies.org**

ISBN 978-0-309-67339-6
9 780309 673396 90000